DISSERTATION

CHARACTERIZATION OF THE ENZYMES INVOLVED IN THE METHYLERYTHRITOL PHOSPHATE PATHWAY WITH A VIEW TO DEVELOPMENT OF BROAD–SPECTRUM ANTIBIOTICS INCLUDING ANTI–TUBERCULOSIS DRUGS

Submitted by

Hyung–Jin Eoh

Department of Microbiology, Immunology, and Pathology

In partial fulfillment of the requirements

For the Degree of Doctor of Philosophy

Colorado State University

Fort Collins, Colorado

Fall, 2007

Colorado State University

Oct 24th 2007

WE HEREBY RECOMMEND THAT THE THESIS PREPARED UNDER OUR SUPERVISION BY HYUNG-JIN EOH ENTITLED CHARACTERIZATION OF THE ENZYMES INVOLVED IN THE METHYLERYTHRITOL PHOSPHATE PATHWAY WITH A VIEW TO DEVELOPMENT OF BROAD-SPECTRUM ANTIBIOTICS INCLUDING ANTI-TUBERCULOSIS DRUGS BE ACCEPTED AS FULFILLING IN PART REQUIREMENTS FOR THE DEGREE OF DOCTOR OF PHILOSOPHY.

Committee on Graduate Work

Co-Advisor

Advisor

Department Head

ABSTRACT OF DISSERTATION

CHARACTERIZATION OF THE ENZYMES INVOLVED IN THE METHYLERYTHRITOL PHOSPHATE PATHWAY WITH A VIEW TO DEVELOPMENT OF BROAD–SPECTRUM ANTIBIOTICS INCLUDING ANTI–TUBERCULOSIS DRUGS

Isopentenyl diphosphate (IPP) and dimethylallyl diphosphate (DMAPP) are precursors of all isoprenoids, many of which constitute a large number of natural products and play an essential role for the survival of organisms. To date, two separate pathways have been revealed for the biosynthesis of IPP and DMAPP. The mevalonate (MVA) pathway was discovered in the early 1950's and is utilized by eukaryotes, algae, archaea–bacteria and some Gram–positive bacteria. Besides the well–known MVA pathway, an alternative route (the methylerythritol phosphate pathway; MEP pathway) for the synthesis of IPP and DMAPP through 2–C–methyl–D–erythritol 4–phosphate has been discovered relatively recently. The MEP pathway is utilized exclusively by Gram–negative bacteria, plants and some Gram–positive bacteria. The enzymes in the MEP pathway are considered as potential drug targets for novel broad–spectrum antibacterial drugs, since they are absent in humans and the disruption of any genes encoding the enzymes in this pathway in *E. coli* and some other eubacteria showed lethal phenotypes.

The Centers for Disease Control and Prevention (CDC) and the National Institute of Allergy and Infectious Diseases (NIAID) have categorized lists of biological diseases/ agents based on their potential lethality. The severity of bioterrorist threats has been increased by the emergence of antibiotic–resistant bacilli, including multidrug–resistant *Mycobacterium tuberculosis* (MDR–TB), a major public health problem in controlling

tuberculosis. An ideal state of preparedness for pending bioterrorist attacks would best be achieved by continuous development of novel antibiotics. Three of the six entities designated as of the highest priority (Category A agents) utilize, or appear to utilize, the MEP pathway. Among the twelve second highest priority agents (Category B) listed, eight organisms appear to utilize the pathway. In addition, *M. tuberculosis*, the causative agent of MDR–TB, classified as a Category C agent by the NIAID, also has been proved to utilize the MEP pathway. Thus, the enzymes in the MEP pathway can provide potential drug targets to overcome drug resistant bacilli.

In an attempt to set up a strategy for bioterrorism preparedness and improve the quality of Direct Observed Therapy and Short–course programs for tuberculosis control, we have identified and characterized the enzymes in the MEP pathway of the human pathogens; *Salmonella typhi*, *Vibrio cholerae*, *Burkholderia mallei*, and *M. tuberculosis*. In addition, we developed *in vitro* high throughput screening (HTS) assays to find specific inhibitors. The four pathogens were selected based on the relative phylogenetic distances from the *E. coli* enzymes. In the present dissertation, the two open reading frames encoding the third and fourth steps of the MEP pathway [4–(cytidine 5'–diphosphate)–2–C–methyl–D–erythritol synthase (chapter I–3 and chapter II–2) and 4–(cytidine 5'–diphosphate)–2–C–methyl–D–erythritol kinase (chapter I–4 and chapter II–3)] were cloned, overexpressed, and purified in *E. coli* for the purpose of characterizing the enzymes and developing *in vitro* HTS assays. In addition, previously established *in vitro* enzyme assay of *M. tuberculosis* 1–deoxy–D–xylulose 5–phosphate synthase (chapter I–5) was optimized and applied to help find specific inhibitors from the small compound libraries designed and generated in Dr. Scott Flanzblau's laboratory,

University of Illinois at Chicago. Newly developed *in vitro* HTS assays in this dissertation are facile, direct, and relatively inexpensive compared to NMR spectroscopy or the HPLC based assays which were previously employed for characterizing the orthologs of other organisms. We also proved that the *in vitro* 4–(cytidine 5'–diphosphate)–2–C–methyl–D–erythritol synthase HTS assays are reliable to apply to screen for specific inhibitors by determining Z'–factor values. We expect inhibitors screened through the *in vitro* HTS assays to show broad–spectrum activity. To date, only one compound, fosmidomycin, has been reported that specifically blocks the MEP pathway and is being investigated clinically. Fosmidomycin, whose target is the second enzyme in the MEP pathway, 1–deoxy–D–xylulose 5–phosphate reductoisomerase, has been shown to be effective in treating malaria. Therefore, we anticipate the enzymes in other steps of the MEP pathway presented in this dissertation also are potential targets for developing novel broad–spectrum antibiotics and it would open up an entirely new class of antibiotics.

Hyung–Jin Eoh
Department of Microbiology,
Immunology, and Pathology
Colorado State University
Fort Collins, CO 80523
Fall 2007

ACKNLOWLEDGEMENTS

This work would not be possible without the help of many people. Throughout the years of this program, I have received much support from family, teachers, and friends.

First of all, I would like to express my largest gratitude to my supervisor, Dr. Patrick Brennan for his continuous encouragement, guidance, never ending assistance throughout these researches. Next, I wish to express my sincere appreciation to my co–advisor, Dr. Dean Crick for advising and introducing me to this wonderful project. He always encouraged me with a lot of patience and enthusiasm.

I am also grateful to my committee members, Drs. Varalakshmi Vissa, Richard Slayden, and Norman Curthoys for their valuable comments, advice, stimulating discussion, and patience. Many thanks also go to all members of the laboratory of Drs. Brennan and Crick for their expertise.

Many thanks to Dr. Ray (Sang–Nae) Cho for encouraging me.

Deserving great thanks is my wife, Young–Mi Kim who was always there when I needed advice and comments to bounce ideas off; she put more time into my projects than I would ever expect. I am forever indebted to her for endless support, sacrifice, patience, understanding, encouragement and for standing by me always even on the rainy days. My daughter, Yun–Sun Eoh, always makes me be happy and forget the stress.

DEDICATION

This dissertation is dedicated to my wife, Young–Mi Kim and my daughter, Yun–Sun Eoh, who have supported me in many ways and made many sacrifices that made this dissertation and degree possible.

This work is also dedicated to my parents (Jung–Hyuck Eoh and Dae–Ryun Park) and parents in law (Hee–Su Kim and Jong–Hee Park) for their never ending beliefs.

The whole of my accomplishment and degree is also dedicated to my best friends, Young–Gi Park and Hwi–Bok Choi, for their unchangeable love and encouragement from my country, South Korea.

TABLE OF CONTENTS

LIST OF TABLES

LIST OF FIGURES

LIST OF ABBREVIATIONS

AFB	Acid–fast bacilli
ATCC	American Type Culture Collection
BCA	Bicinchoninic acid
BCG	Bacillus Calmette–Guérin
CDC	Centers for Disease Control and Prevention
CDP–ME	4–(Cytidine 5'–diphosphate)–2–C–methyl–D–erythritol
CDP–ME2P	2–Phospho–4–(cytidine 5'–diphospho)–2–C–methyl–D–erythritol
CFP–10	Culture filtrate protein–10
CMP	Cytidine 5'–monophosphate
CTP	Cytidine 5'–triphosphate
DMAPP	Dimethylallyl diphosphate
DMSO	Dimethyl sulfoxide
DOT	Directly observed therapy
DOTS	Directly observed therapy, short–course
DX	1–Deoxy–D–xylulose
DXP	1–Deoxy–D–xylulose 5–phosphate
DXS	1–Deoxy–D–xylulose 5–phosphate synthase
ELISA	Enzyme–linked immunosorbent assay
EMBnet	European Molecular Biology Network
ESAT–6	Early secretory antigen target–6
ETH	Ethambutol
FAD	Flavin–adenine dinucleotide
FDA	Food and Drug Administration
GAP	Glyceraldehyde 3–phosphate
GHMP	Galactose, homoserine, mevalonate, phosphomevalonate
HAART	Highly active antiretroviral therapy
HIV	Human immunodeficiency virus
HMBPP	1–Hydroxy–2–methyl–2–(E)–butenyl 4–diphosphate
HMG–CoA	3–Hydroxy–3–methylglutaryl–CoA
HMGR	3–Hydroxy–3–methylglutaryl–CoA reductase
HTS	High throughput screening
IFN–γ	Interferon–γ
IMAC	Immobilized metal affinity chromatography
INH	Isoniazid
IPP	Isopentenyl diphosphate
IPTG	Isopropyl–β–D–thiogalactopyranoside
IspC	DXP reductoisomerase
IspD	4–(Cytidine 5'–diphosphate)–2–C–methyl–D–erythritol synthetase
IspE	4–(Cytidine 5'–diphosphate)–2–C–methyl–D–erythritol kinase
IspF	2–C–Methyl–D–erythritol 2,4–cyclodiphosphate synthase

IspG	1–Hydroxy–2–methyl–2–(E)–butenyl 4–diphosphate synthase
IspH	1–Hydroxy–2–methyl–2–(E)–butenyl 4–diphosphate reductase
IUATLD	International union against tuberculosis and lung disease
KEGG	Kyoto encyclopedia of genes and genomes
LAM	Lipoarabinomannan
LB	Luria Bertani broth
MDR–TB	Multidrug–resistant tuberculosis
ME	2–C–Methyl–D–erythritol derivatives
MECDP	2–C–Methyl–D–erythritol 2,4–cyclodiphosphate
MEP	2–C–Methyl–D–erythritol 4–phosphate
MESG	2–Amino–6–mercapto–7–methylpurine ribonucleoside
MOPS	4–Morpholine propane sulfonic acid
MVA	Mevalonate
MVK	Mevalonate kinase
NADH	Nicotinamide adenine dinucleotide
NADPH	Nicotinamide adenine dinucleotide phosphate
NCBI	National Center for Biotechnology Information
NIAID	National Institute of Allergy and Infectious Diseases
NIH	National Institutes of Health
NMR	Nuclear magnetic resonance
NSRB	National screening laboratory for the regional centers of excellence in biodefense and emerging infectious diseases
NTCP	National tuberculosis control program
NTP	Nucleotide 5'–triphosphate
PAS	Para–amino salicylic acid
PCR	Polymerase chain reaction
PDH	Pyruvate dehydrogenase
PEI	Polyethyleneimine
Pol–P	Polyprenyl phosphate
PPD	Purified protein derivative
PPD–S1	Standard PPD
PZA	Pyrazinamide
RD	Region of differentiation
RIF	Rifampin
SDS–PAGE	SDS polyacrylamide gel electrophoresis
TB	Tuberculosis
TLC	Thin layer chromatography
TK	Transketolase
TPP	Thiamine diphosphate
UIC	University of Illinois Chicago
WHO	World Health Organization

Chapter I.

The methylerythritol phosphate pathway of *Mycobacterium tuberculosis:* potential for a drug target

Chapter I–1.

Literature Review on *Mycobacterium tuberculosis*

I.1.A. The epidemiology of tuberculosis

Tuberculosis (TB) has been called a variety of names such as Consumption, King's Evil, Lupus vulgaris, and phthisis in the last several centuries. The landmark discovery of the infectious agent, *Mycobacterium tuberculosis* by Dr. Robert Koch in 1882 (33, 34, 37), introduced the possibility of combating this disease with antimicrobial agents. Despite the availability of effective anti–tuberculosis drugs for over 50 years, TB continues to be a major cause of disability and death, globally (80). The World Health Organization (WHO) has recently estimated that one third of the global community, 1.86 billion people, is infected with the causative organism, *M. tuberculosis* (48). In detail, there were around 8 to 9 million new incident cases and 1.6 million people died of TB in the single year 2005 including 195,000 patients infected with HIV/acquired immunodeficiency syndrome (AIDS) according to recent epidemiological statistics (8). In 2005, the TB incidence rate was stable or in decline, worldwide. However, the total number of new TB cases is still rising slowly, because the case–load continues to grow in the African, Eastern Mediterranean and South–East Asia regions (8). Moreover, approximately 10% of the infected 2 billion people will live with active TB at some point during their lives. Therefore, the WHO declared TB to be a global emergency in 1993, the first classified disease to be so designated in the history of WHO (120, 129).

The prevalence of human immunodeficiency virus (HIV)/AIDS makes TB be the second most dangerous cause of human death by an infectious disease, and if the trends continue, many reports have anticipated that TB will be among the ten leading causes of global disease in the year 2020 (88). Especially, the impact of TB has been elevated with

the spread of HIV infection in endemic areas. Although the prevalence and incidence of TB are similar for both HIV–seropositive and HIV–seronegative TB patients, the risk of proceeding to active TB is elevated dramatically for HIV–seropositive TB patients. People co–infected with HIV and latent TB are at risk of developing active TB at a rate of 7 to 10% per year, compared to approximately 10% per lifetime for HIV–negative individuals (110, 111). The reactivation of TB of HIV–seropositive TB patients may occur at a rate of 37% within the first 6 months, compared to 2 – 5% in the first 2 years among HIV–negative patients (32). Therefore, latent TB and HIV co–infected patients have shown a much higher probability to develop active TB because HIV weakens their immune system. The role of $CD4^+$ T cells and antigen presenting capability in host defense mechanisms are diminished by the marked susceptibility to TB in patients with advanced HIV–induced $CD4^+$ T cell depletion. Mycobacteria are also endowed with mechanisms through which they can evade the host defense response (32, 45, 110).

Along with HIV co–infection, multidrug–resistant TB (MDR–TB), defined as an isolate that is resistant to at least isoniazid (INH) and rifampin (RIF), the two most potent anti–tuberculosis drugs (122, 128), is a phenomenon that is threatening to destabilize global TB control. It has been reported that it did not take a long time for the emergence of drug resistant isolates of *M. tuberculosis* after introducing the first anti–tuberculosis drugs to patients (59, 82, 125, 134). *In vitro* studies showed that MDR–TB arises as a consequence of sequential accumulation of spontaneous genetic mutations conferring resistance to single therapeutic agents (40, 41, 89). Therefore, combination therapy using more than one antibiotic had been recommended to treat patients harboring *M. tuberculosis* to reduce the emergence of drug resistance (83, 131). The major factors for

occurrence of drug resistant mutants in patients are as follows: patients are treated inappropriately, they are exposed to subtherapeutic drug levels, environmental conditions provide adequate positive selection pressure for the emergence of genetic mutation which confers drug–resistance, and patients obtain drug resistant organisms *de novo*. The acquisition of drug resistant strains also can occur from poor patients' compliance to drug regimens due to the large quantity of drugs and prolonged curing duration (42). Therefore, developing new anti–tuberculosis drugs and shortening the length of chemotherapy are important, as this would greatly impact clinical management and the emergence of drug resistance.

After the decline of TB incidence rates during over 20 years, since the early 1990s, an alarming and growing concern of public health has been focused on the emergence of MDR–TB (122, 128). 424,203 MDR–TB cases are estimated to have occurred worldwide in 2004 or 4.3% of all new and previously treated TB cases. There is a great deal of heterogeneity worldwide in MDR–TB distribution (51). Three countries, China, India, and the Russian Federation, accounted for 62% of the estimated global burden (47, 137). Localized high incidence rates of MDR–TB have been found only in particular regions, the "hot zones"; for example, Estonia (14%), Latvia (9%), the Russian oblasts of Ivanova (9%) and Tomsk (7%), and Zhejiang (5%) and Henan (11%) provinces in China (51). The figures in these areas suggest that MDR–TB prevalence may be two to three times higher than incidence (20).

The National Tuberculosis Control Programs (NTCPs) in industrial countries are organized to set the policy and ensure the prevention and proper management of TB cases. One of the aims of the NTCPs is to minimize the development of drug resistant cases.

Combination drug therapy and directly observed uptake were adopted as pillars of the Direct Observed Treatment Short–Course (DOTS) programs, largely to prevent the emergence of drug resistance. However, DOTS programs are generally difficult to manage and have been associated with very high morbidity, prolonged treatment to cure, and an increased risk of spreading drug resistant isolates in the populations (16, 19, 49, 122). Therefore, surveillance of anti–tuberculosis drug resistance is an essential strategy for monitoring the effectiveness of TB control programs and, through policy development, for improving national and global TB control.

Generally, TB control is highly cost–effective and only 0.2% of investment in poor countries has been spent on TB services in recent years. The neglect of TB is a major scandal that has gone for decades and is only now beginning to be addressed. It is estimated that each case of TB costs $25,000 to treat, with each case of MDR–TB costing ten times more (24). An estimate of the current cost of TB control in the United States ranges from $700 million to $1 billion per year (23).

I.1.B. The historical perspectives of tuberculosis

TB has been present in humans since antiquity. One proposed hypothesis is that the genus *Mycobacterium* originated more than 150 million years ago, during the Jurassic period (61). Advanced techniques such as molecular genetics and the genome sequence, support a more rigorous estimation of the time of origin of mycobacteria. An early progenitor of *M. tuberculosis* is believed to have been present in East Africa around three million years ago (60). However, today's variable strains of the major *Mycobacterium*

spp. (*M. africanum, M. canettii, M. microti, and M. bovis*) seem to have expanded from a common ancestor about 35,000 years ago (22, 60, 69). The modern members of *M. tuberculosis* complex seem to have diverged from the common progenitor about 15,000 – 35,000 years ago (60, 116). Although, those five strains may have originated from a single ancestor, the global distributions of mycobacterial lineages are more likely to have been dependent upon human populations (53). Phylogenetic analysis indicates that the present diversity of current strains of mycobacterial lineages occurred around 250 – 1,000 years ago (62, 127).

TB in Egypt was documented more than 5,000 years ago. Recent DNA based typing methods were employed to confirm that typical spinal column abnormalities from Egyptian mummies, including the characteristic Pott's deformities, are definite pathological evidences of tubercular decay and are clearly described in Egyptian art (31, 87, 90, 138, 139). However, the exact strain of *Mycobacterium* was not discovered. Although there are few written records about ancient TB cases, the disease is clearly noted in the Biblical records of Deuteronomy and Leviticus using ancient Hebrew word, schachepheth (current word, schachefet, tuberculosis), which meant a wasting disease (38). In Greek literature, records of TB (phthisis) could be found (33). Around 2,500 years ago, Hippocrates, in his aphorisms, clearly identified the symptoms of TB as the most widespread disease of that time and understood its clinical fatal presentation. He also wrote in his book, *Of the Epidemics*, "Phthisis makes its attacks chiefly between eighteen and thirty five" and "Consumption was the most considerable of the diseases which then prevailed and the only one which proved fatal to many persons" (34, 113).

Although the written records of TB were sparse in the middle ages, archeological evidence of the disease could be found and showed that TB was still widespread throughout Europe (104). One record about the death of St. Francis of Assisi at the age of 44 in 1226 indicated the etiological cause was probably TB (85). At the emergence of the Renaissance Period, the great anatomists at Padua (Italy) were supplanted at the helm of medicine by the French giants–Jean Nicolas Corvisart, Marie–Francois–Xavier Bichat, Gaspard Laurent Bayle, and Rene Theophile Hyacinthe Laennec– with new knowledge of disease. Dr. Corvisart and Dr. Bayle stimulated Dr. Laennec's interest in the clinical diagnosis of the chest, especially TB, from which Dr. Laennec himself suffered. He invented the stethoscope (1816) and clearly elucidated the pathogenesis of TB and recognized various forms of pulmonary or extrapulmonary TB as a single disease (35, 36, 108). In his great work, *D'Auscultation Mediate*, he expounded on the pathology of TB and most of the physical signs of pulmonary disease. In addition, he introduced terms to describe those findings that are still in use today. On the other hand, Sylvius was the first person to identify actual tubercles as a consistent and characteristic change in the lungs and other areas of consumptive patients with progression to abscesses and cavities (34).

Surrounded by patients with TB, medical practitioners and scientists struggled to understand its etiology. In Northern Europe, TB was generally considered a heritable disease; in Southern Europe it was felt to be infectious in nature. Meanwhile, the fact that TB was, indeed, infectious in nature was probably first suggested in 1790 by the English physician Benjamin Marten in his publication, *A New Theory of Consumption* (46). Dr. Marten's writings display a great degree of epidemiological insight (34). In contrast to the great level of understanding about the etiology of the disease, which was already enabling

prevention and a break in the chain of infection, those attempts to treat and manage the disease were still obscure. In 1865, the French doctor Jean–Antoine Villemin demonstrated that consumption could be transferred from humans to cattle and from cattle to rabbits. On the basis of this evidence, he postulated that a specific micro agent might be involved as the cause of the disease.

The fight against TB really began on March 24, 1882, when Hermann Heinrich Robert Koch made his justifiably famous presentation, *Die Aetiologie der Tuberculose*, to the Berlin Physiological Society (33, 37). By exploiting the exotic nature of the mycobacterial cell envelope, Dr. Koch developed a staining technique to definitely identify the etiological agent, *M. tuberculosis*, from infectious isolates and presented demonstrations of the tubercle bacillus. In addition, he was the first person to utilize solid media to propagate the bacilli. With these novel techniques, Dr. Koch applied a scientific method to develop a simplistic set of rational, stepwise postulates to conclusively identify the infectious agent responsible for a particular disease. These postulates bear his name in honor of his scientific contributions. Koch's postulates are as follows: 1) The bacteria must be present in every case of the disease; 2) The bacteria must be isolated from the host with the disease and grown in pure culture; 3) The specific disease must be reproduced when a pure culture of the bacteria is inoculated into a healthy susceptible host; 4) The bacteria must be recoverable from the experimentally infected host. He produced irrefutable evidence that *M. tuberculosis* is the causative agent of TB using this methodology (37, 71, 72). Dr. Koch's contributions to bacteriology were legion, and he was awarded the Nobel Prize in Medicine or Physiology in 1905 for his elucidation of the etiology of TB. In 1890, another great finding by Dr. Koch was a substance from tubercle

bacilli, which he thought was capable of arresting bacterial development *in vitro* and *in vivo*. He called this substance tuberculin. This news gave rise to tremendous hope throughout the world, which was soon replaced by disillusionment when the product turned out to be an ineffective therapeutic agent. However, tuberculin later proved to be a valuable diagnostic tool (118).

In the early 1900's, Clemens Freiherr von Pirquet had already recognized allergic reaction with serum sickness by the allergen (114). From the great finding of Dr. Koch's reaction to tuberculin, he used a vaccination lancet to introduce a small amount of diluted tuberculin intracutaneously (33, 34). On the basis of these findings, Florence Seibert developed purified protein derivative (PPD) essentially in the form in which it is currently used, in a series of investigations at the Phipps Institute of the University of Pennsylvania during the 1930s. After setting up the well–standardized PPD, tuberculin reaction sizes could be applied to diagnose the patients with mycobacterial infection. In 1952, Carroll Palmer and Leroy Bates studied the reactions to one test unit of PPD in more than 3,000 hospitalized TB patients (96). In this research, they found less than 1% of treated patients failed to react and reaction sizes showed averages of 15 mm. On the basis of these results, WHO expanded these skin tests to school children in various populations (7).

I.1.C. The diagnosis of tuberculosis

There are two major diagnostic tools for TB. One is the specific microbiological stain method and the other is culture procedure which is still widely used for detection of

M. tuberculosis. The most prevalent way is examining sputum smears for acid–fast bacilli (AFB) to obtain evidence of TB infection. Once stained with the primary stain, mycobacteria are very resistant to decolorization using acidified organic solvents, and hence are referred to as being "acid fast". Generally, two procedures are common: the carbolfuchsin methods, which include the Ziehl–Neelsen and Kinyoun methods, and a fluorochrome procedure using auramine O or auramine–rhodamine dyes (70). The stain method is the easiest and fastest to be performed as a diagnostic tool. It provides a preliminary confirmation of the diagnosis. Moreover, it gives a quantitative estimation of the number of bacilli, suggesting that the smear is of vital clinical and epidemiologic importance in assessing the patient's infectiousness. Approximately $0.5 - 1 \times 10^5$ microorganisms per ml of sample can be detected by staining sputum smears (63, 73, 103). However, not all infected individuals have detectable *M. tuberculosis* bacilli with AFB–stained smears and this staining method does not distinguish *M. tuberculosis* from non–tuberculous mycobacteria.

The gold standard of diagnostics is confirmation with its growth in selective media (5). Culture is 1000 times more sensitive than microscopy, allows precise species identification, can be applied to drug susceptibility testing, and may be useful to identify epidemiological links between patients or to detect laboratory cross–contamination. In general, the sensitivity and specificity of the culture method are 80 – 85% and 98%, respectively (65, 86). However, their outcome is delayed by the extremely low growth rate of mycobacteria. Contrary to a number of environmental mycobacteria that are rapid growers, yielding colonies in 7 days or less, *M. tuberculosis* exhibits a slow growth rate, requiring 14 – 21 days to generate visible colonies and does not produce any pigment.

With the advance of culture systems in 1980s, BACTEC and the biphasic culture methods were developed for faster recovery than traditional culture system (11, 98).

The introduction of nucleic acid amplification assays using polymerase chain reaction (PCR) in 1985 brought the most progress in TB diagnostics (107). In 1989, PCR was first applied to clinical samples, sputum, gastric aspirates, abscess aspirates, and biopsy samples, to detect a mycobacterial gene which allows the differential diagnosis of *M. tuberculosis* from non–tuberculous mycobacteria (21). A number of candidate genes have been tested for usage as diagnostic targets. Among them, IS6110 repeat sequence has been used to detect *M. tuberculosis* directly in clinical materials (50, 124). However, some other factors such as an endogenous amplification inhibiting factor of *M. tuberculosis* or unreliable quality control can influence susceptibility to both false positives and negatives and have hampered clinical use of this assay (14, 92). However, the severity of the problems began to be reduced after development of automated, robust, commercial tests (43, 67, 99, 100, 112, 126), which made clinical risk assessment possible. Therefore, the nucleic acid amplification diagnostic method has finally been shown to contribute to rapid identification of TB from the clinical spectrum (25, 75). Eventually, this method has been certificated for clinical application by the Centers for Disease Control and Prevention (CDC) in the United States, which recommends the use of the tests on sputum samples for pulmonary TB diagnosis.

Another old diagnostic method is the tuberculin skin test developed by Dr. Koch. The test is for the identification of host infected with *M. tuberculosis*. Tuberculin skin tests involve the intracutaneous injection of five tuberculin units of PPD prepared by the Mantoux technique (64). The standard PPD (PPD–S1) used in the United States was

prepared in 1941 and admitted in 1951 by the WHO Expert Committee on Biological Standardization (12). The skin reaction of *M. tuberculosis* infection may discriminate from *M. avium* or other non–tuberculous infections (97). However, the cross reactivity of PPD–S1 with *M. bovis* BCG vaccinated individuals represents a major limitation in applying this method to TB patients (1, 130). Therefore, the interpretation of the skin test needs to be made in the individual clinical context and with evaluation of other risk factors for infection.

The identification of regions of the *M. tuberculosis* genome that are not present in *M. bovis* BCG and non–tuberculous mycobacteria provides a unique opportunity to develop new specific diagnostic reagents. Fortunately, genomic studies have shown that the region of differentiation (RD)–1, is shared only by *M. tuberculosis*, *M. szulgai*, *M. marinum* and *M. kansasii*. The RD–1 region contains the early secretory antigen target–6 (ESAT–6) and the culture filtrate protein–10 (CFP–10) that are potential targets of the specific immune response against *M. tuberculosis* (15, 29). Interferon (IFN)–γ secreted by TB patients' memory and effector T–cells by the response of these proteins or overlapping peptides is a novel diagnostic marker of TB infection and could be discriminated from BCG vaccination or non–tuberculous mycobacteria infection (57, 58). *In vitro* blood test measuring IFN–γ is very useful to identify contacts of TB cases and shows remarkable concordance with the tuberculin skin test (95). Accordingly, the blood test has shown a greater sensitivity than the tuberculin skin test in active TB of HIV co–infected subjects. The clinical utility of this tool has been recently acknowledged by the U.S. Food and Drug Administration (FDA) (44, 81).

The recent progress in TB serology is also represented by the multi–antigen test using purified antigens. The recent studies of an Enzyme–Linked ImmunoSorbent Assay (ELISA) test using the 38kDa antigen, lipoarabinomannan (a mycobacterial lipoglycan, LAM), MPT–64, and glutamine synthase could achieve 93% sensitivity and 76% specificity with combination of AFB microscopy, suggesting that in the appropriate epidemiological and laboratory context this test could be used to improve the performances of the AFB smear test alone (68, 77, 102, 106, 132). However, serological tests alone do not appear to help diagnosis of sputum–positive pulmonary TB (26).

I.1.D. The chemotherapy of tuberculosis

In the middle of the 20th century, the outlook for TB patients and the history of TB dramatically changed with the introduction of chemotherapy. The discovery of para–amino salicylic acid (PAS) by Jorgen Lehmann in 1943 and of thiosemicarbazone by Berhard Domagk during World War I yielded the first therapeutic agents with efficacy in the treatment of TB. In 1944, Albert Schatz, Elizabeth Bugie, and Selman Waksman reported the isolation of streptomycin, the first antibiotic and first bactericidal agent effective against *M. tuberculosis* (109).

With the discovery of INH, the first oral mycobacterial drug in 1952, and RIF in 1957, a new chemotherapeutic era of TB treatment had dawned and sanatoria were closed. The discovery of the two effective drugs with their application in the armamentarium of anti–tuberculosis strategy in 1966 (30, 54, 76, 78, 91) accelerated investigations on reduction of treatment duration. In the middle of 1970s, the first clinical study in East

Africa and Zambia in association with the British Medical Research Council compared four different regimens [streptomycin, INH, and rifampicin; streptomycin, INH, and pyrazinamide (PZA); streptomycin, INH, and thiacetazone] with a standard 18–month streptomycin, INH, and thiacetazone regimen. This study demonstrated that the 6–month treating regimens containing RIF or PZA showed superior curing efficacy for patients (2). INH and RIF were considered as complete bactericidal drugs, being capable of killing bacteria in all environments, while streptomycin and PZA were of "half" effective, the former being active in the more alkaline milieu and the latter active in the more acidic intracellular environment. Thus, the combination with streptomycin or PZA was considered as a perfect complementary combination which made a very powerful bactericidal regimen (52). Therefore, the East African short course regimen began to employ streptomycin, INH, and rifampicin, which suggested that at least two full bactericidal drugs were required to successfully and dramatically cut treatment duration from 12 –18 months down to 6–months (52).

From the late 1970s, the main issue of TB chemotherapy has been focused on finding the best combination using the available antibiotics. In the earliest study, the 6–month regimen consisted of streptomycin, INH, RIF, and PZA for 4 months followed by the regimen containing streptomycin, INH, and PZA for 2 more months, and showed a relapse rate of 6% in patients infected with drug sensitive *M. tuberculosis* bacilli, with an even higher relapse rate with INH–resistant strains (4). A subsequent study evaluated another combination of streptomycin, INH, rifampicin, and PZA, and had lower than 1% relapse rate and the other combination, same regimen without streptomycin, around 2% relapse rate. However, without PZA, the relapse rate strikingly increased to 8% (3). More

valuable findings had shown that the regimens containing PZA were highly effective on patients infected with resistant strains against both INH and streptomycin with less than 4% relapse rate (6). A series of previous results had confirmed the importance of the sterilizing role of PZA used together with INH and rifampicin, in the reduction phase of chemotherapy.

A series of investigations during the 1980s proposed recommendations to the International Union Against Tuberculosis and Lung Disease (IUATLD), of the regimen including INH, rifampicin, and PZA for a 2–month induction phase followed by INH and rifampicin for a 4–month continuation phase (56). Thus, with these trial–validated, intermittent short course chemotherapy regimens, DOTS programs became feasible for TB services of high prevalence countries. With the DOTS programs developed by the IUATLD together with national TB programs, the WHO recommended directly supervised treatment consisting of a 2–month daily regimen of INH, rifampicin, PZA, ETH, and streptomycin followed by 4–month continuation with either daily or intermittent INH plus rifampicin for patients with newly diagnosed smear positive disease. As a second option, an entirely intermittent 6–month treatment was recommended (55).

I.1.E. The mode of action of current drugs for tuberculosis

According to their mode of action, first and second line TB drugs can be grouped as inhibitors of cell wall biosynthesis (D–cycloserine, INH, ETH, and EMB), inhibitors

of nucleic acid synthesis (RIF and quinolones), and inhibitors of membrane energy metabolism (PZA) (135).

D–Cycloserine targets peptidoglycan biosynthesis in various bacteria, including mycobacteria (27). It is a structural analogue of D–alanine and competitively inhibits the action of D–alanine racemase and D–alanyl–D–alanine synthetase (101). INH, ethionamide, and isoxyl all target mycolic acid biosynthesis. INH is a pro–drug that is activated by catalase–peroxidase encoded by *katG* (Rv1908c) (28). This was shown when KatG from *M. tuberculosis* was cloned and transformed into *M. smegmatis*, which is naturally more resistant to INH. KatG is thought to be able to oxidize INH into an electrophilic species, which is the presumed activated form of INH. The molecular target for INH has been debated for some time. Jacobs and colleagues proposed the target of INH is an enoyl reductase–NADH binary complex (17, 105). The enoyl reductase is encoded by *inhA*. Ethionamide is now thought to act in a similar manner to INH including the activation step. The proposed target of EMB was provided by Takayama and Kilburn who showed that it is likely arabinan biosynthesis of both arabinogalactan (AG) and LAM (121). They demonstrated that the incorporation of [^{14}C] from [^{14}C]glucose into AG arabinan was immediately inhibited upon exposure to EMB. This implicated that AG specific arabinosyltransferases were the target for EMB. Three putative arabinosyltransferases have been identified, *embC*, *embB*, and *embA* (18, 123). EMB resistance was observed upon the overexpression of the latter two genes and a third termed embR, which has been postulated to act as a regulator. Recent studies have shown that *embB* is the most mutated gene in EMB–resistant strains of mycobacteria and that

amino acid 306 of *embB* is the most mutated position in *M. tuberculosis*. From this, it is clear that arabinosyltransferases are the site of action of EMB (13, 74, 84, 117).

RIF is responsible for the reduction of the duration of therapy. Its mechanism of action is based on the inhibition of bacterial DNA dependent RNA polymerase, which is crucial for bacterial transcription. Despite the importance of RIF in the TB treatment, the emergence of different RIF–resistant bacteria, increase the problems to global TB control. This resistance occurs during therapy against active TB and normally arises from mutations in the β–subunit of the ribosomal polymerase gene (*rpoB*) (79, 133). Quinolone derivatives possess potent antibacterial activities with a broad spectrum organisms including *M. tuberculosis*. The inhibition of bacterial multiplication caused by quinolone derivatives is in general due to the inhibition of two bacterial enzymes: DNA gyrase (topoisomerase II) and topoisomerase IV enzymes. DNA gyrase is an essential protein involved in the replication, transcription and reparation of the bacterial DNA. Topoisomerase IV is responsible for decatenation that is removing the interlinking of daughter chromosomes thereby allowing segregation into two daughter cells at the end of the replication round (89, 93).

PZA is an important sterilizing drug. However, the mode of action is poorly understood. It is a prodrug and activated by *M. tuberculosis* pyrazinamidase which is only active at acidic pH. Pyrazinamidase converts PZA to the active form, pyrazinoic acid. Pyrazinoic acid and PZA de–energize the membrane by collapsing the membrane potential and affect the membrane transport function at acid pH (136).

I.1.F. The problems of current programs controlling tuberculosis

The currently popular treatments, DOTS programs, although highly effective, are far from ideal. Using the effective combination of available drugs, the curing period cannot be reduced below 6 months. In most developing countries, the treatment duration is still longer, an 8–month regimen. Because of the treatment over a long period of time, it has been difficult to anticipate that patients will complete their therapy on their own. Furthermore, all four of the most effective first–line drugs, INH, RIF, ETH, and PZA, must be taken together and in large quantities during the first 2 months. Therefore, although rates of serious adverse effects are low, many patients have suffered from side–effects. Improper implementation of DOTS programs lead to the development and spread of drug–resistant strains of TB, including MDR–TB. Especially, when given under suboptimal dose of drugs, these regimens are associated with a high risk of acquired–drug resistant cases, defined as the presence of drug resistant strains in a patient that previously had been treated for TB for at least one month (39). As one way to reduce the emergence of drug–resistant TB cases, it is recommended that treatment be directly observed by health care officers, especially during the first 2 months and whenever RIF is being used. However, this also requires a large infrastructure and is labor intensive, and is expensive.

Development of drug resistance is far more likely when supervised treatment is not given, when the patients are not compliant, when recommended regimens are not used, and when drugs with poor bioavailability are used. In the situations where MDR–TB is present, the cure rate using standard DOTS treatment drops from greater

than 90% to approximately 50% (51). In curing MDR–TB cases, short course chemotherapy is no longer effective and recommended. The WHO now recommends a modification of DOTS programs called DOTS–Plus, which consists of DOTS programs plus second–line TB drugs for a period of 24 months (16). The second–line drugs for treating MDR–TB are much more expensive, more toxic, and less effective. The problem of drug resistance has become so large, that within some regions such as Ivanovo Oblast in Russia, acquired–drug resistance to at least one anti–tuberculosis drug is 100% (94). Even more unsettling, the incidence of primary MDR–TB in Estonia increased from 10% to 14% in only four years (51). In addition, most existing TB drugs are only able to target actively growing bacilli through the inhibition of cell processes such as cell wall biogenesis and DNA replication. This implies that current TB chemotherapy is characterized by an efficient bactericidal activity but an extremely weak sterilizing activity, which is defined as the activity to kill persisters or dormant bacteria. The weak sterilizing property of available TB drugs is one of the major drawbacks of current TB chemotherapy. Although RIF and PZA are partially sterilizing drugs and play an important role in shortening the therapy period, there are still populations of persisting bacteria that are not killed by RIF and PZA.

In developing nations, political strife and economic collapse easily lead to an inadequate drug supply, poor infrastructure to support detection and follow–up of TB cases, and a failure to fully or correctly implement DOTS programs. All of these are reasons that DOTS programs are far from ideal for treatment of TB. From a purely epidemiological perspective, ineffective drug therapy is worse than no treatment at all, because it may extend the lives of chronically infected individuals and increases the

likelihood of transmission. Not only do these individuals spread TB for a longer period of time, but they serve as a reservoir for the dissemination of primary drug resistant strains within the community (137).

The TB–HIV co–infected patients show a significantly higher risk of presenting with active TB and a faster progression of disease. At this time, the usage of anti–tuberculosis drugs is usually limited to the patients who are receiving Highly Active Anti–Retroviral Therapy (HAART) due to the drug to drug interactions (115). In addition, chemotherapeutic treatment regimens are less effective and mortality rates can approach up to 80% in the TB–HIV co–infected cases.

With the rapidity of modern international travel and the increase in global emigration, this will eventually lead to more epidemics of MDR–TB occurring within industrialized nations, compromising once successful anti–tuberculosis programs and resulting in substantial financial and human costs. Therefore, expensive investigations mining for new drug targets have been undertaken. Three crucial purposes for developing novel anti–tuberculosis drugs are as follows: to improve current DOTS programs by shortening the total curing duration (48); to combat MDR–TB (10); and to provide for more effective treatment of persistent TB infection (119). The greatest impact would be to improve current DOTS programs by providing for new regimens that shorten the patient curing period and help their compliance. Obviously, a compound that would reduce the length of both the first bactericidal phase and the second sterilizing phase would provide the greatest improvement. On the other hand, a novel treatment with the purpose of improving therapy for patients with MDR–TB has been paid a great deal of attention. The final impetus to the development of new anti–tuberculosis drugs is for

improved treatment of persons with persistent TB infection. INH has been reported to be effective in persons with persistent TB and HIV co–infection and has recently been recommended by WHO for such persons (9). However, there are significant limitations to this intervention, and new drugs to improve persistent TB treatment have been deemed essential to the elimination of TB in low–incidence countries such as the United States (10). The priority of eliminating TB in the United States should be put on the development of new drugs for persistent TB infection treatment (66). Unless significant new resources are devoted to the detection and treatment of TB in developing countries, the worldwide increase in the incidence of TB will continue to escalate at an ever faster rate.

I.1.G. References

1. 2000. Control and prevention of tuberculosis in the United Kingdom: code of practice 2000. Joint Tuberculosis Committee of the British Thoracic Society. Thorax **55:**887-901.
2. 1974. Controlled clinical trial of four short-course (6-month) regimens of chemotherapy for treatment of pulmonary tuberculosis. Lancet **2:**1100-6.
3. 1982. Controlled trial of 4 three-times-weekly regimens and a daily regimen all given for 6 months for pulmonary tuberculosis. Second report: the results up to 24 months. Hong Kong Chest Service/British Medical Research Council. Tubercle **63:**89-98.
4. 1979. Controlled trial of 6-month and 8-month regimens in the treatment of pulmonary tuberculosis: the results up to 24 months. Tubercle **60:**201-10.
5. 2000. Diagnostic Standards and Classification of Tuberculosis in Adults and Children. This official statement of the American Thoracic Society and the Centers for Disease Control and Prevention was adopted by the ATS Board of

Directors, July 1999. This statement was endorsed by the Council of the Infectious Disease Society of America, September 1999. Am J Respir Crit Care Med **161:**1376-95.

6. 1987. Five-year follow-up of a controlled trial of five 6-month regimens of chemotherapy for pulmonary tuberculosis. Hong Kong Chest Service/British Medical Research Council. Am Rev Respir Dis **136:**1339-42.
7. 1955. FURTHER studies of geographic variation in naturally acquired tuberculin sensitivity. Bull World Health Organ **12:**63-83.
8. 2007. Global tuberculosis control: surveillance, planning, financing. WHO report 2007. Geneva, World Health Organization (WHO/HTM/TB/2007.376).
9. 1999. Preventive therapy against tuberculosis in people living with HIV. Wkly Epidemiol Rec **74:**385-98.
10. 1999. Tuberculosis elimination revisited: obstacles, opportunities, and a renewed commitment. Advisory Council for the Elimination of Tuberculosis (ACET). MMWR Recomm Rep **48:**1-13.
11. **Abe, C., S. Hosojima, Y. Fukasawa, Y. Kazumi, M. Takahashi, K. Hirano, and T. Mori.** 1992. Comparison of MB-Check, BACTEC, and egg-based media for recovery of mycobacteria. J Clin Microbiol **30:**878-81.
12. **Affronti, L. F., J. J. Caprio, P. Q. Edwards, M. L. Furculow, S. Grzybowski, J. Katz, F. E. Hesse, and F. B. Seibert.** 1969. What is PPD-S? A statement by the Committee on Diagnostic Skin Testing. Am Rev Respir Dis **99:**460-1.
13. **Alcaide, F., G. E. Pfyffer, and A. Telenti.** 1997. Role of *embB* in natural and acquired resistance to ethambutol in mycobacteria. Antimicrob Agents Chemother **41:**2270-3.
14. **Amicosante, M., L. Richeldi, G. Trenti, G. Paone, M. Campa, A. Bisetti, and C. Saltini.** 1995. Inactivation of polymerase inhibitors for *Mycobacterium tuberculosis* DNA amplification in sputum by using capture resin. J Clin Microbiol **33:**629-30.
15. **Andersen, P., M. E. Munk, J. M. Pollock, and T. M. Doherty.** 2000. Specific immune-based diagnosis of tuberculosis. Lancet **356:**1099-104.

16. **Aziz, M. A., and A. Wright.** 2005. The World Health Organization/International Union Against Tuberculosis and Lung Disease Global Project on Surveillance for Anti-Tuberculosis Drug Resistance: a model for other infectious diseases. Clin Infect Dis **41 Suppl 4:**S258-62.

17. **Banerjee, A., E. Dubnau, A. Quemard, V. Balasubramanian, K. S. Um, T. Wilson, D. Collins, G. de Lisle, and W. R. Jacobs, Jr.** 1994. *inhA*, a gene encoding a target for isoniazid and ethionamide in *Mycobacterium tuberculosis*. Science **263:**227-30.

18. **Belanger, A. E., G. S. Besra, M. E. Ford, K. Mikusova, J. T. Belisle, P. J. Brennan, and J. M. Inamine.** 1996. The *embAB* genes of *Mycobacterium avium* encode an arabinosyl transferase involved in cell wall arabinan biosynthesis that is the target for the antimycobacterial drug ethambutol. Proc Natl Acad Sci U S A **93:**11919-24.

19. **Bifani, P. J., B. B. Plikaytis, V. Kapur, K. Stockbauer, X. Pan, M. L. Lutfey, S. L. Moghazeh, W. Eisner, T. M. Daniel, M. H. Kaplan, J. T. Crawford, J. M. Musser, and B. N. Kreiswirth.** 1996. Origin and interstate spread of a New York City multidrug-resistant *Mycobacterium tuberculosis* clone family. JAMA **275:**452-7.

20. **Blower, S. M., and T. Chou.** 2004. Modeling the emergence of the 'hot zones': tuberculosis and the amplification dynamics of drug resistance. Nat Med **10:**1111-6.

21. **Brisson-Noel, A., B. Gicquel, D. Lecossier, V. Levy-Frebault, X. Nassif, and A. J. Hance.** 1989. Rapid diagnosis of tuberculosis by amplification of mycobacterial DNA in clinical samples. Lancet **2:**1069-71.

22. **Brosch, R., S. V. Gordon, M. Marmiesse, P. Brodin, C. Buchrieser, K. Eiglmeier, T. Garnier, C. Gutierrez, G. Hewinson, K. Kremer, L. M. Parsons, A. S. Pym, S. Samper, D. van Soolingen, and S. T. Cole.** 2002. A new evolutionary scenario for the *Mycobacterium tuberculosis* complex. Proc Natl Acad Sci U S A **99:**3684-9.

23. **Brown, R. E., B. Miller, W. R. Taylor, C. Palmer, L. Bosco, R. M. Nicola, J. Zelinger, and K. Simpson.** 1995. Health-care expenditures for tuberculosis in the United States. Arch Intern Med **155:**1595-600.

24. **Burgos, M., L. C. Gonzalez, E. A. Paz, E. Gournis, L. M. Kawamura, G. Schecter, P. C. Hopewell, and C. L. Daley.** 2005. Treatment of multidrug-resistant tuberculosis in San Francisco: an outpatient-based approach. Clin Infect Dis **40:**968-75.

25. **Catanzaro, A., S. Perry, J. E. Clarridge, S. Dunbar, S. Goodnight-White, P. A. LoBue, C. Peter, G. E. Pfyffer, M. F. Sierra, R. Weber, G. Woods, G. Mathews, V. Jonas, K. Smith, and P. Della-Latta.** 2000. The role of clinical suspicion in evaluating a new diagnostic test for active tuberculosis: results of a multicenter prospective trial. JAMA **283:**639-45.

26. **Chan, E. D., L. Heifets, and M. D. Iseman.** 2000. Immunologic diagnosis of tuberculosis: a review. Tuber Lung Dis **80:**131-40.

27. **Chopra, I., and P. Brennan.** 1997. Molecular action of anti-mycobacterial agents. Tuber Lung Dis **78:**89-98.

28. **Chouchane, S., I. Lippai, and R. S. Magliozzo.** 2000. Catalase-peroxidase (*Mycobacterium tuberculosis* KatG) catalysis and isoniazid activation. Biochemistry **39:**9975-83.

29. **Cockle, P. J., S. V. Gordon, A. Lalvani, B. M. Buddle, R. G. Hewinson, and H. M. Vordermeier.** 2002. Identification of novel *Mycobacterium tuberculosis* antigens with potential as diagnostic reagents or subunit vaccine candidates by comparative genomics. Infect Immun **70:**6996-7003.

30. **Covacev, L., and G. Monzali.** 1966. [Rifamycin SV in the therapy of tuberculosis]. Clin Ter **39:**547-66.

31. **Crubezy, E., B. Ludes, J. D. Poveda, J. Clayton, B. Crouau-Roy, and D. Montagnon.** 1998. Identification of *Mycobacterium* DNA in an Egyptian Pott's disease of 5,400 years old. C R Acad Sci III **321:**941-51.

32. **Daley, C. L., P. M. Small, G. F. Schecter, G. K. Schoolnik, R. A. McAdam, W. R. Jacobs, Jr., and P. C. Hopewell.** 1992. An outbreak of tuberculosis with accelerated progression among persons infected with the human

immunodeficiency virus. An analysis using restriction-fragment-length polymorphisms. N Engl J Med **326:**231-5.

33. **Daniel, T. M.** 1997. Captain of death : the story of tuberculosis. University of Rochester Press, Rochester, NY.
34. **Daniel, T. M.** 2006. The history of tuberculosis. Respir Med **100:**1862-70.
35. **Daniel, T. M.** 2000. Pioneers of medicine and their impact on tuberculosis. University of Rochester Press, Rochester, NY.
36. **Daniel, T. M.** 2004. Rene Theophile Hyacinthe Laennec and the founding of pulmonary medicine. Int J Tuberc Lung Dis **8:**517-8.
37. **Daniel, T. M.** 2005. Robert Koch and the pathogenesis of tuberculosis. Int J Tuberc Lung Dis **9:**1181-2.
38. **Daniel, V. S., and T. M. Daniel.** 1999. Old Testament biblical references to tuberculosis. Clin Infect Dis **29:**1557-8.
39. **Datta, M., M. P. Radhamani, R. Selvaraj, C. N. Paramasivan, B. N. Gopalan, C. R. Sudeendra, and R. Prabhakar.** 1993. Critical assessment of smear-positive pulmonary tuberculosis patients after chemotherapy under the district tuberculosis programme. Tuber Lung Dis **74:**180-6.
40. **David, H. L.** 1971. Resistance to D-cycloserine in the tubercle bacilli: mutation rate and transport of alanine in parental cells and drug-resistant mutants. Appl Microbiol **21:**888-92.
41. **David, H. L., and C. M. Newman.** 1971. Some observations on the genetics of isoniazid resistance in the tubercle bacilli. Am Rev Respir Dis **104:**508-15.
42. **Davies, J.** 1998. Antibiotic resistance in mycobacteria. Novartis Found Symp **217:**195-205; discussion 205-8.
43. **Devallois, A., E. Legrand, and N. Rastogi.** 1996. Evaluation of Amplicor MTB test as adjunct to smears and culture for direct detection of *Mycobacterium tuberculosis* in the French Caribbean. J Clin Microbiol **34:**1065-8.
44. **Dheda, K., A. Lalvani, R. F. Miller, G. Scott, H. Booth, M. A. Johnson, A. Zumla, and G. A. Rook.** 2005. Performance of a T-cell-based diagnostic test for tuberculosis infection in HIV-infected individuals is independent of CD4 cell count. Aids **19:**2038-41.

45. **Di Perri, G., M. Cruciani, M. C. Danzi, R. Luzzati, G. De Checchi, M. Malena, S. Pizzighella, R. Mazzi, M. Solbiati, E. Concia, and et al.** 1989. Nosocomial epidemic of active tuberculosis among HIV-infected patients. Lancet **2:**1502-4.

46. **Doetsch, R. N.** 1978. Benjamin Marten and his "New Theory of Consumptions". Microbiol Rev **42:**521-8.

47. **Dye, C., M. A. Espinal, C. J. Watt, C. Mbiaga, and B. G. Williams.** 2002. Worldwide incidence of multidrug-resistant tuberculosis. J Infect Dis **185:**1197-202.

48. **Dye, C., S. Scheele, P. Dolin, V. Pathania, and M. C. Raviglione.** 1999. Consensus statement. Global burden of tuberculosis: estimated incidence, prevalence, and mortality by country. WHO Global Surveillance and Monitoring Project. JAMA **282:**677-86.

49. **Eckstein, T. M., F. S. Silbaq, D. Chatterjee, N. J. Kelly, P. J. Brennan, and J. T. Belisle.** 1998. Identification and recombinant expression of a *Mycobacterium avium* rhamnosyltransferase gene (*rtfA*) involved in glycopeptidolipid biosynthesis. J Bacteriol **180:**5567-73.

50. **Eisenach, K. D., M. D. Cave, J. H. Bates, and J. T. Crawford.** 1990. Polymerase chain reaction amplification of a repetitive DNA sequence specific for *Mycobacterium tuberculosis*. J Infect Dis **161:**977-81.

51. **Espinal, M. A.** 2003. The global situation of MDR-TB. Tuberculosis (Edinb) **83:**44-51.

52. **Fox, W., and D. A. Mitchison.** 1975. Short-course chemotherapy for pulmonary tuberculosis. Am Rev Respir Dis **111:**845-8 CONTD.

53. **Gagneux, S., K. DeRiemer, T. Van, M. Kato-Maeda, B. C. de Jong, S. Narayanan, M. Nicol, S. Niemann, K. Kremer, M. C. Gutierrez, M. Hilty, P. C. Hopewell, and P. M. Small.** 2006. Variable host-pathogen compatibility in *Mycobacterium tuberculosis*. Proc Natl Acad Sci U S A **103:**2869-73.

54. **Gallo, G. G., C. R. Pasqualucci, N. Maggi, R. Ballotta, and P. Sensi.** 1966. Rifamycins. XLII. Rifazine, a new phenazinic derivative of rifamycins. Farmaco [Sci] **21:**68-75.

55. **Gbayisomore, A., A. A. Lardizabal, and L. B. Reichman.** 2000. Update: prevention and treatment of tuberculosis. Curr Opin Infect Dis **13:**155-159.

56. **Girling, D. J., P. Caulet, S. P. Pamra, and J. A. Pilheu.** 1988. Anti-tuberculosis regimens of chemotherapy. Recommendations from the Committee on Treatment of the International Union against Tuberculosis and Lung Disease. Indian J Chest Dis Allied Sci **30:**296-304.

57. **Goletti, D., O. Butera, F. Bizzoni, R. Casetti, E. Girardi, and F. Poccia.** 2006. Region of difference 1 antigen-specific CD4+ memory T cells correlate with a favorable outcome of tuberculosis. J Infect Dis **194:**984-92.

58. **Goletti, D., S. Carrara, D. Vincenti, C. Saltini, E. B. Rizzi, V. Schinina, G. Ippolito, M. Amicosante, and E. Girardi.** 2006. Accuracy of an immune diagnostic assay based on RD1 selected epitopes for active tuberculosis in a clinical setting: a pilot study. Clin Microbiol Infect **12:**544-50.

59. **Graessle, O. E., and J. J. Pietrowski.** 1949. The *in Vitro* Effect of Para-Aminosalicylic Acid (Pas) in Preventing Acquired Resistance to Streptomycin by *Mycobacterium tuberculosis*. J Bacteriol **57:**459-64.

60. **Gutierrez, M. C., S. Brisse, R. Brosch, M. Fabre, B. Omais, M. Marmiesse, P. Supply, and V. Vincent.** 2005. Ancient origin and gene mosaicism of the progenitor of *Mycobacterium tuberculosis*. PLoS Pathog **1:**e5.

61. **Hayman, J.** 1984. *Mycobacterium ulcerans*: an infection from Jurassic time? Lancet **2:**1015-6.

62. **Hirsh, A. E., A. G. Tsolaki, K. DeRiemer, M. W. Feldman, and P. M. Small.** 2004. Stable association between strains of *Mycobacterium tuberculosis* and their human host populations. Proc Natl Acad Sci U S A **101:**4871-6.

63. **Hobby, G. L., A. P. Holman, M. D. Iseman, and J. M. Jones.** 1973. Enumeration of tubercle bacilli in sputum of patients with pulmonary tuberculosis. Antimicrob Agents Chemother **4:**94-104.

64. **Huebner, R. E., M. F. Schein, and J. B. Bass, Jr.** 1993. The tuberculin skin test. Clin Infect Dis **17:**968-75.

65. **Ichiyama, S., K. Shimokata, and J. Takeuchi.** 1993. Comparative study of a biphasic culture system (Roche MB Check system) with a conventional egg

medium for recovery of mycobacteria. Aichi Mycobacteriosis Research Group. Tuber Lung Dis **74:**338-41.

66. **Jereb, J. A.** 2002. Progressing toward tuberculosis elimination in low-incidence areas of the United States. Recommendations of the Advisory Council for the Elimination of Tuberculosis. MMWR Recomm Rep **51:**1-14.

67. **Jonas, V., M. J. Alden, J. I. Curry, K. Kamisango, C. A. Knott, R. Lankford, J. M. Wolfe, and D. F. Moore.** 1993. Detection and identification of *Mycobacterium tuberculosis* directly from sputum sediments by amplification of rRNA. J Clin Microbiol **31:**2410-6.

68. **Kanaujia, G. V., P. K. Lam, S. Perry, P. N. Brusasca, A. Catanzaro, and M. L. Gennaro.** 2005. Integration of microscopy and serodiagnostic tests to screen for active tuberculosis. Int J Tuberc Lung Dis **9:**1120-6.

69. **Kapur, V., T. S. Whittam, and J. M. Musser.** 1994. Is *Mycobacterium tuberculosis* 15,000 years old? J Infect Dis **170:**1348-9.

70. **Koch, M. L., and R. A. Cote.** 1965. Comparison of Fluorescence Microscopy with Ziehl-Neelsen Stain for Demonstration of Acid-Fast Bacilli in Smear Preparations and Tissue Sections. Am Rev Respir Dis **91:**283-4.

71. **Koch, R.** 1982. Classics in infectious diseases. The etiology of tuberculosis: Robert Koch. Berlin, Germany 1882. Rev Infect Dis **4:**1270-4.

72. **Koch, R.** 1952. [Tuberculosis etiology.]. Dtsch Gesundheitsw **7:**457-65.

73. **Kox, L. F., D. Rhienthong, A. M. Miranda, N. Udomsantisuk, K. Ellis, J. van Leeuwen, S. van Heusden, S. Kuijper, and A. H. Kolk.** 1994. A more reliable PCR for detection of *Mycobacterium tuberculosis* in clinical samples. J Clin Microbiol **32:**672-8.

74. **Lety, M. A., S. Nair, P. Berche, and V. Escuyer.** 1997. A single point mutation in the *embB* gene is responsible for resistance to ethambutol in *Mycobacterium smegmatis*. Antimicrob Agents Chemother **41:**2629-33.

75. **Lim, T. K., A. Mukhopadhyay, A. Gough, K. L. Khoo, S. M. Khoo, K. H. Lee, and G. Kumarasinghe.** 2003. Role of clinical judgment in the application of a nucleic acid amplification test for the rapid diagnosis of pulmonary tuberculosis. Chest **124:**902-8.

76. **Lucchesi, M., G. Pallotta, P. Rossi, and M. Sbampato.** 1967. [The therapeutic action of Rifampicin, a derivative of 3-(4-methyl-1-piperazinyl-iminomethyl)-rifamycin SV, in pulmonary tuberculosis]. Ann Ist Carlo Forlanini **27:**199-227.

77. **Ma, Y., Y. M. Wang, and T. M. Daniel.** 1986. Enzyme-linked immunosorbent assay using *Mycobacterium tuberculosis* antigen 5 for the diagnosis of pulmonary tuberculosis in China. Am Rev Respir Dis **134:**1273-5.

78. **Maggi, N., C. R. Pasqualucci, R. Ballotta, and P. Sensi.** 1966. Rifampicin: a new orally active rifamycin. Chemotherapy **11:**285-92.

79. **Marianelli, C., F. Ciuchini, M. Tarantino, P. Pasquali, and R. Adone.** 2004. Genetic bases of the rifampin resistance phenotype in *Brucella* spp. J Clin Microbiol **42:**5439-43.

80. **Mathema, B., N. E. Kurepina, P. J. Bifani, and B. N. Kreiswirth.** 2006. Molecular epidemiology of tuberculosis: current insights. Clin Microbiol Rev **19:**658-85.

81. **Mazurek, G. H., J. Jereb, P. Lobue, M. F. Iademarco, B. Metchock, and A. Vernon.** 2005. Guidelines for using the QuantiFERON-TB Gold test for detecting *Mycobacterium tuberculosis* infection, United States. MMWR Recomm Rep **54:**49-55.

82. **Mc, L. J.** 1950. Streptomycin resistance in the tubercule bacillus. Edinburgh Med J **57:**547-56.

83. **Meyer, A. H., L. W. Kinsell, and R. J. Parsons.** 1952. Combined corticotropin (ACTH), para-aminosalicylic acid (PAS), and streptomycin in the treatment of pulmonary tuberculosis. Am Rev Tuberc **66:**542-7.

84. **Mokrousov, I., T. Otten, B. Vyshnevskiy, and O. Narvskaya.** 2002. Detection of *embB*306 mutations in ethambutol-susceptible clinical isolates of *Mycobacterium tuberculosis* from Northwestern Russia: implications for genotypic resistance testing. J Clin Microbiol **40:**3810-3.

85. **Moorman, L. J.** 1940. Tuberculosis and genius. University of Chicago Press, Chicago, Ill.,.

86. **Morgan, M. A., C. D. Horstmeier, D. R. DeYoung, and G. D. Roberts.** 1983. Comparison of a radiometric method (BACTEC) and conventional culture media

for recovery of mycobacteria from smear-negative specimens. J Clin Microbiol **18:**384-8.

87. **Morse, D., D. R. Brothwell, and P. J. Ucko.** 1964. Tuberculosis in Ancient Egypt. Am Rev Respir Dis **90:**524-41.

88. **Murray, C. J., and J. A. Salomon.** 1998. Modeling the impact of global tuberculosis control strategies. Proc Natl Acad Sci U S A **95:**13881-6.

89. **Musser, J. M.** 1995. Antimicrobial agent resistance in mycobacteria: molecular genetic insights. Clin Microbiol Rev **8:**496-514.

90. **Nerlich, A. G., C. J. Haas, A. Zink, U. Szeimies, and H. G. Hagedorn.** 1997. Molecular evidence for tuberculosis in an ancient Egyptian mummy. Lancet **350:**1404.

91. **Nitti, V., E. Catena, F. Bariffi, and F. Delli Veneri.** 1967. [Therapeutic activity of the Rifampicin in pulmonary tuberculosis]. Arch Tisiol Mal Appar Respir **22:**417-62.

92. **Noordhoek, G. T., J. D. van Embden, and A. H. Kolk.** 1996. Reliability of nucleic acid amplification for detection of *Mycobacterium tuberculosis*: an international collaborative quality control study among 30 laboratories. J Clin Microbiol **34:**2522-5.

93. **Onodera, Y., M. Tanaka, and K. Sato.** 2001. Inhibitory activity of quinolones against DNA gyrase of *Mycobacterium tuberculosis*. J Antimicrob Chemother **47:**447-50.

94. **Pablos-Mendez, A., M. C. Raviglione, A. Laszlo, N. Binkin, H. L. Rieder, F. Bustreo, D. L. Cohn, C. S. Lambregts-van Weezenbeek, S. J. Kim, P. Chaulet, and P. Nunn.** 1998. Global surveillance for antituberculosis-drug resistance, 1994-1997. World Health Organization-International Union against Tuberculosis and Lung Disease Working Group on Anti-Tuberculosis Drug Resistance Surveillance. N Engl J Med **338:**1641-9.

95. **Pai, M., K. Gokhale, R. Joshi, S. Dogra, S. Kalantri, D. K. Mendiratta, P. Narang, C. L. Daley, R. M. Granich, G. H. Mazurek, A. L. Reingold, L. W. Riley, and J. M. Colford, Jr.** 2005. *Mycobacterium tuberculosis* infection in

health care workers in rural India: comparison of a whole-blood interferon gamma assay with tuberculin skin testing. JAMA **293:**2746-55.

96. **Palmer, C. E., and L. E. Bates.** 1952. Tuberculin sensitivity of tuberculous patients. Bull World Health Organ **7:**171-88.

97. **Palmer, C. E., and L. B. Edwards.** 1967. Tuberculin test in retrospect and prospect. Arch Environ Health **15:**792-808.

98. **Park, C. H., D. L. Hixon, C. B. Ferguson, S. L. Hall, C. C. Risheim, and C. B. Cook.** 1984. Rapid recovery of mycobacteria from clinical specimens using automated radiometric technic. Am J Clin Pathol **81:**341-5.

99. **Pfyffer, G. E., P. Funke-Kissling, E. Rundler, and R. Weber.** 1999. Performance characteristics of the BDProbeTec system for direct detection of Mycobacterium tuberculosis complex in respiratory specimens. J Clin Microbiol **37:**137-40.

100. **Portaels, F., E. Serruys, H. De Beenhouwer, J. Degraux, K. De Ridder, K. Fissette, J. Gomez-Marin, H. Goossens, F. Muhlberger, S. R. Pattyn, F. Nturanye, F. Pouthier, and A. Van Deun.** 1996. Evaluation of the Gen-Probe amplified *Mycobacterium tuberculosis* direct test for the routine diagnosis of pulmonary tuberculosis. Acta Clin Belg **51:**144-9.

101. **Rastogi, N., and H. L. David.** 1993. Mode of action of antituberculous drugs and mechanisms of drug resistance in *Mycobacterium tuberculosis*. Res Microbiol **144:**133-43.

102. **Ratanasuwan, W., J. K. Kreiss, C. M. Nolan, B. A. Schaeffler, S. Suwanagool, S. Tunsupasawasdikul, C. Chuchottaworn, W. Dejsomritrutai, and H. M. Foy.** 1997. Evaluation of the MycoDot test for the diagnosis of tuberculosis in HIV seropositive and seronegative patients. Int J Tuberc Lung Dis **1:**259-64.

103. **Rickman, T. W., and N. P. Moyer.** 1980. Increased sensitivity of acid-fast smears. J Clin Microbiol **11:**618-20.

104. **Roberts, C. A., and J. E. Buikstra.** 2003. The bioarchaeology of tuberculosis : a global view on a reemerging disease. University Press of Florida, Gainesville.

105. **Rozwarski, D. A., G. A. Grant, D. H. Barton, W. R. Jacobs, Jr., and J. C. Sacchettini.** 1998. Modification of the NADH of the isoniazid target (InhA) from *Mycobacterium tuberculosis*. Science **279:**98-102.

106. **Sada, E., D. Aguilar, M. Torres, and T. Herrera.** 1992. Detection of lipoarabinomannan as a diagnostic test for tuberculosis. J Clin Microbiol **30:**2415-8.

107. **Saiki, R. K., S. Scharf, F. Faloona, K. B. Mullis, G. T. Horn, H. A. Erlich, and N. Arnheim.** 1985. Enzymatic amplification of beta-globin genomic sequences and restriction site analysis for diagnosis of sickle cell anemia. Science **230:**1350-4.

108. **Sakula, A.** 1981. R T H Laennec 1781--1826 his life and work: a bicentenary appreciation. Thorax **36:**81-90.

109. **Schatz, A., E. Bugie, and S. A. Waksman.** 2005. Streptomycin, a substance exhibiting antibiotic activity against Gram-positive and Gram-negative bacteria. 1944. Clin Orthop Relat Res:3-6.

110. **Selwyn, P. A., D. Hartel, V. A. Lewis, E. E. Schoenbaum, S. H. Vermund, R. S. Klein, A. T. Walker, and G. H. Friedland.** 1989. A prospective study of the risk of tuberculosis among intravenous drug users with human immunodeficiency virus infection. N Engl J Med **320:**545-50.

111. **Selwyn, P. A., B. M. Sckell, P. Alcabes, G. H. Friedland, R. S. Klein, and E. E. Schoenbaum.** 1992. High risk of active tuberculosis in HIV-infected drug users with cutaneous anergy. JAMA **268:**504-9.

112. **Shah, J. S., J. Liu, D. Buxton, A. Hendricks, L. Robinson, G. Radcliffe, W. King, D. Lane, D. M. Olive, and J. D. Klinger.** 1995. Q-beta replicase-amplified assay for detection of *Mycobacterium tuberculosis* directly from clinical specimens. J Clin Microbiol **33:**1435-41.

113. **Siegel, R. E.** 1964. Clinical Observation in Hippocrates: an Essay on the Evolution of the Diagnostic Art. J Mt Sinai Hosp N Y **31:**285-303.

114. **Silverstein, A. M.** 2000. Clemens Freiherr von Pirquet: explaining immune complex disease in 1906. Nat Immunol **1:**453-5.

115. **Spradling, P., D. Drociuk, S. McLaughlin, L. M. Lee, C. A. Peloquin, K. Gallicano, C. Pozsik, I. Onorato, K. G. Castro, and R. Ridzon.** 2002. Drug-drug interactions in inmates treated for human immunodeficiency virus and *Mycobacterium tuberculosis* infection or disease: an institutional tuberculosis outbreak. Clin Infect Dis **35:**1106-12.

116. **Sreevatsan, S., X. Pan, K. E. Stockbauer, N. D. Connell, B. N. Kreiswirth, T. S. Whittam, and J. M. Musser.** 1997. Restricted structural gene polymorphism in the *Mycobacterium tuberculosis* complex indicates evolutionarily recent global dissemination. Proc Natl Acad Sci U S A **94:**9869-74.

117. **Sreevatsan, S., K. E. Stockbauer, X. Pan, B. N. Kreiswirth, S. L. Moghazeh, W. R. Jacobs, Jr., A. Telenti, and J. M. Musser.** 1997. Ethambutol resistance in *Mycobacterium tuberculosis*: critical role of *embB* mutations. Antimicrob Agents Chemother **41:**1677-81.

118. **Stuper-Essen, P., and R. Koch.** 1951. [On the tuberculin sensitivity of guinea pigs treated by TB I in infections due to TB I resistant strains.]. Beitr Klin Tuberk Spezif Tuberkuloseforsch **106:**210-5.

119. **Styblo, K., and J. Meijer.** 1976. Impact of BCG vaccination programmes in children and young adults on the tuberculosis problem. Tubercle **57:**17-43.

120. **Sutherland, I.** 1976. Recent studies in the epidemiology of tuberculosis, based on the risk of being infected with tubercle bacilli. Adv Tuberc Res **19:**1-63.

121. **Takayama, K., and J. O. Kilburn.** 1989. Inhibition of synthesis of arabinogalactan by ethambutol in *Mycobacterium smegmatis*. Antimicrob Agents Chemother **33:**1493-9.

122. **Telenti, A., and M. Iseman.** 2000. Drug-resistant tuberculosis: what do we do now? Drugs **59:**171-9.

123. **Telenti, A., W. J. Philipp, S. Sreevatsan, C. Bernasconi, K. E. Stockbauer, B. Wieles, J. M. Musser, and W. R. Jacobs, Jr.** 1997. The *emb* operon, a gene cluster of *Mycobacterium tuberculosis* involved in resistance to ethambutol. Nat Med **3:**567-70.

124. **Thierry, D., M. D. Cave, K. D. Eisenach, J. T. Crawford, J. H. Bates, B. Gicquel, and J. L. Guesdon.** 1990. IS6110, an IS-like element of *Mycobacterium tuberculosis* complex. Nucleic Acids Res **18:**188.

125. **Tinne, J. E., and J. L. Henderson.** 1950. Primary streptomycin-resistant tuberculosis in a newborn child. Simple method of assessing streptomycin resistance. Lancet **2:**901-4.

126. **Tortoli, E., F. Lavinia, and M. T. Simonetti.** 1997. Evaluation of a commercial ligase chain reaction kit (Abbott LCx) for direct detection of *Mycobacterium tuberculosis* in pulmonary and extrapulmonary specimens. J Clin Microbiol **35:**2424-6.

127. **Tsolaki, A. G., A. E. Hirsh, K. DeRiemer, J. A. Enciso, M. Z. Wong, M. Hannan, Y. O. Goguet de la Salmoniere, K. Aman, M. Kato-Maeda, and P. M. Small.** 2004. Functional and evolutionary genomics of *Mycobacterium tuberculosis*: insights from genomic deletions in 100 strains. Proc Natl Acad Sci U S A **101:**4865-70.

128. **Vareldzis, B. P., J. Grosset, I. de Kantor, J. Crofton, A. Laszlo, M. Felten, M. C. Raviglione, and A. Kochi.** 1994. Drug-resistant tuberculosis: laboratory issues. World Health Organization recommendations. Tuber Lung Dis **75:**1-7.

129. **Vynnycky, E., and P. E. Fine.** 1997. The natural history of tuberculosis: the implications of age-dependent risks of disease and the role of reinfection. Epidemiol Infect **119:**183-201.

130. **Wang, L., M. O. Turner, R. K. Elwood, M. Schulzer, and J. M. FitzGerald.** 2002. A meta-analysis of the effect of Bacille Calmette Guerin vaccination on tuberculin skin test measurements. Thorax **57:**804-9.

131. **Wier, J. A., P. B. Storey, C. W. Tempel, and O. L. Weiser.** 1956. Streptomycin, isoniazid, and para-aminosalicylic acid in the treatment of pulmonary tuberculosis. Am Rev Tuberc **73:**117-22.

132. **Wilkins, E. G., and J. Ivanyi.** 1990. Potential value of serology for diagnosis of extrapulmonary tuberculosis. Lancet **336:**641-4.

133. **Williams, D. L., L. Spring, L. Collins, L. P. Miller, L. B. Heifets, P. R. Gangadharam, and T. P. Gillis.** 1998. Contribution of *rpoB* mutations to

development of rifamycin cross-resistance in *Mycobacterium tuberculosis*. Antimicrob Agents Chemother **42:**1853-7.

134. **Williston, E. H., and G. P. Youmans.** 1950. The inability of p-aminosalicylic acid to delay the emergence of streptomycin resistant tubercle bacilli in mice. Am Rev Tuberc **62:**156-9.

135. **Zhang, Y.** 2005. The magic bullets and tuberculosis drug targets. Annu Rev Pharmacol Toxicol **45:**529-64.

136. **Zhang, Y., M. M. Wade, A. Scorpio, H. Zhang, and Z. Sun.** 2003. Mode of action of pyrazinamide: disruption of *Mycobacterium tuberculosis* membrane transport and energetics by pyrazinoic acid. J Antimicrob Chemother **52:**790-5.

137. **Zignol, M., M. S. Hosseini, A. Wright, C. L. Weezenbeek, P. Nunn, C. J. Watt, B. G. Williams, and C. Dye.** 2006. Global incidence of multidrug-resistant tuberculosis. J Infect Dis **194:**479-85.

138. **Zimmerman, M. R.** 1979. Pulmonary and osseous tuberculosis in an Egyptian mummy. Bull N Y Acad Med **55:**604-8.

139. **Zink, A. R., C. Sola, U. Reischl, W. Grabner, N. Rastogi, H. Wolf, and A. G. Nerlich.** 2003. Characterization of *Mycobacterium tuberculosis* complex DNAs from Egyptian mummies by spoligotyping. J Clin Microbiol **41:**359-67.

Chapter I–2.

Literature review on isopentenyl diphosphate biosynthesis via the methylerythritol phosphate pathway

I.2.A. Discovery of the methylerythritol phosphate pathway, an alternative route for isopentenyl diphosphate biosynthesis

Isoprenoids are one of the largest groups of natural products formally derived from the branched five–carbon skeleton of isoprene, encompassing over 30,000 known compounds (12, 42). Isoprenoids include essential primary metabolites, which participate in nutrition and in metabolic processes, as well as secondary metabolites, which influence ecological interactions with the environment and are of less obvious physiological significance. Subgroups of isoprenoids comprise sterols, carotenoids, cholorophylls, quinones, as well as polyprenols. They are derived from a five–carbon subunit, cyclization reactions, rearrangements and further oxidation or reduction of the carbon skeleton, responsible for the enormous diversity of structures (13, 14). Despite their functional and structural diversity, all isoprenoids derive from the biological equivalents of isoprene, isopentenyl diphosphate (IPP) and dimethylallyl diphosphate (DMAPP), ubiquitous precursors in all living organisms (25).

Intensive efforts for discovering the early steps of isoprenoid biosynthesis in liver tissue and in yeast lead to the discovery of the mevalonate (MVA) pathway (8, 9, 82) (Fig.I.2.1). The first step in the MVA pathway involves condensing acetyl–CoA and acetoacetyl–CoA to form 3–hydroxy–3–methylglutaryl–CoA (HMG–CoA) catalyzed by HMG–CoA synthase. 3–Hydroxy–3–methylglutaryl–CoA reductase (HMGR) then catalyzes the irreversible formation of mevalonate. HMGR is one of the most stringently regulated enzymes known and is the enzymatic target for the cholesterol lowering drug such as lovastatin or compactin (7, 46). Mevalonate is then subject to two ATP–

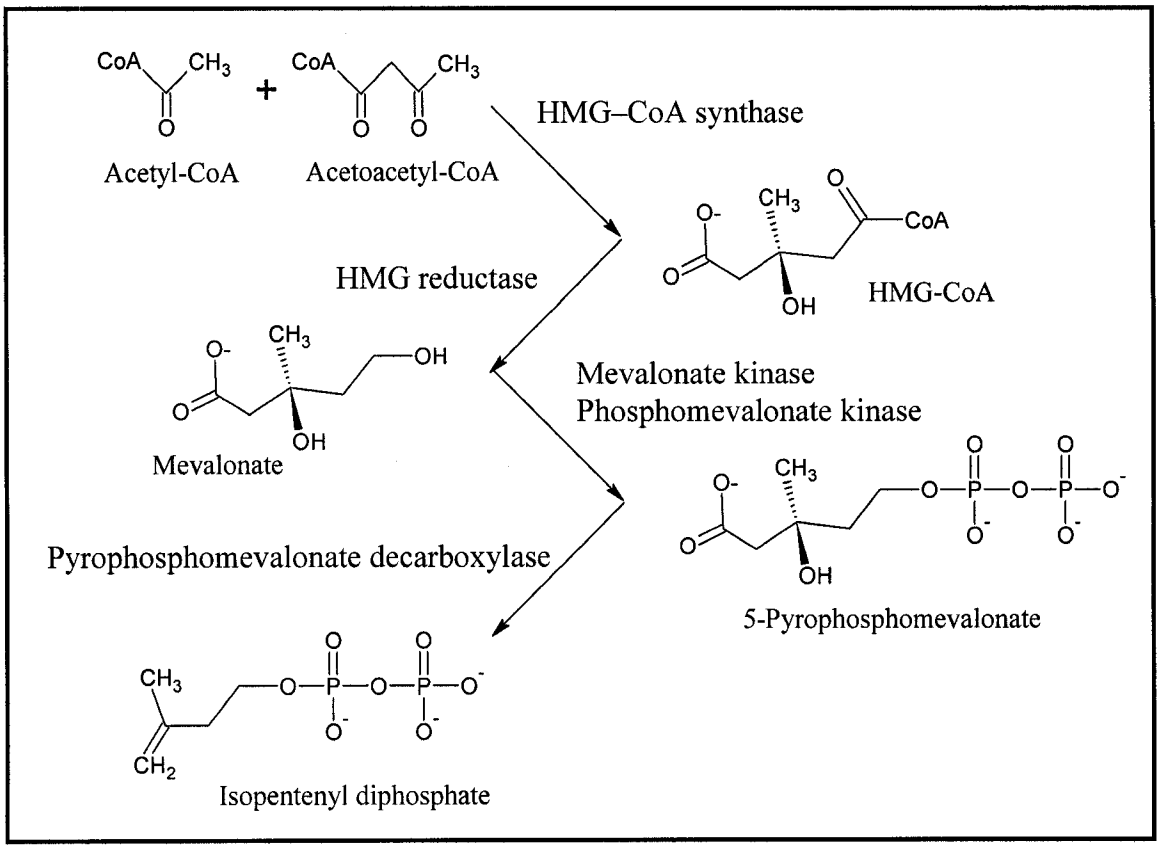

FIGURE I.2.1. **The mevalonate pathway for IPP biosynthesis**. This pathway is an important cellular metabolic pathway present in all higher eukaryotes and some eubacteria. DMAPP and IPP serve the repeating units for the biosynthesis of isoprenoid molecules (39). Abbreviation: HMG–CoA, 3–Hydroxy–3–methylglutaryl CoA.

dependent phosphorylation events yielding 5–pyrophosphomevalonate. Finally, pyrophosphomevalonate decarboxylase catalyzes the decarboxylation of 5–pyrophosphomevalonate to IPP. This step requires ATP and probably begins with the phosphorylation of the 3–hydroxy group, followed by a trans–elimination of both the phosphate and carboxyl moieties. IPP can be isomerized to DMAPP, the five–carbon allylic diphosphate used in isoprenoid synthesis. A series of studies confirmed the distribution of this metabolic route over a broad–spectrum of organisms.

For several decades, the MVA pathway was accepted as the paradigm for the biosynthesis of all isoprenoid building blocks in all organisms, despite mounting evidence against such universality by the biosynthetic mechanisms producing chloroplast isoprenoids, plant mono– and diterpenes and some bacterial isoprenoids (68, 70). Historically, there were limited studies addressing the early steps of bacterial isoprenoid biosynthesis because low concentrations of isoprenoids were typically encountered in bacteria in comparison with these found in other living organisms (60). However, bacteria synthesize essential isoprenoids such as polyprenyl phosphate, which is a carbohydrate carrier used in peptidoglycan biosynthesis of the cell wall or in prenyl chains of the ubiquinones and menaquinones, important components of electron transport chains. Other species of isoprenoids with restricted distribution include: carotenoids or triterpenoids of the hopane series which act as membrane stabilizers and which modulate membrane rigidity and fluidity (70). Due to relatively higher intracellular concentration of hopanoid (0.5 to 30 mg/g), hopanoid biosynthesis could be investigated after one study was published to prove the origin of the additional five–carbon isoprene building block linked to the triterpene skeleton using [^{13}C]–NMR spectroscopy (69). That study showed

that the five–carbon isoprene side chain was not derived from the MVA pathway, but from a pentose, and disclosed an unexpected and novel pathway for the formation of isoprene units (24). From a series of labeling experiments with [U–$^{13}C_6$] glucose isotopomers, [1–$^{13}C_1$] glucose, [6–$^{13}C_1$] glucose, and [$^{13}C_1$] acetate, the labeling patterns of the hopanoid couldn't be explained by the MVA pathway (90). In addition, the unexpected isotope patterns were able to be explained by condensation of 'activated acetaldehyde' with a triose phosphate as an initial step of an alternative biosynthetic pathway (68). Extensive experiments indicated that the isoprene units were derived from glyceraldehyde 3–phosphate (GAP) and a two–carbon component from decarboxylation of pyruvate (70, 71). These findings were confirmed in subsequent studies with mutants of *E. coli* (41, 80). The hypothesis was that *E. coli* auxotrophic mutants requiring 2–C–methyl–D–erythritol (ME) should be affected in isoprenoid biosynthesis. A genetic strategy based on this mutant strain succeeded in identifying the first bacterial gene encoding DXP reductoisomerase (IspC) (80). Incorporation of isotope–labeled 1–deoxy–D–xylulose (DX) or ME derivatives into the prenyl chains of ubiquinone and menaquinone from *E. coli* with extraordinary efficacy provided decisive proof for the existence of an unknown pathway (70). Earlier work had already shown that the carbon skeleton of DX could be incorporated into pyridoxol (vitamin B_6) (30, 31) and into the thiazole ring of thiamine (vitamin B_1) (86). Thus, DX or a derivative thereof appeared to qualify as the branching intermediate for the biosynthetic pathway of vitamins B_1 and B_6 and a novel means, the MVA–independent pathway, of isoprenoid biosynthesis. Several studies have elucidated the full extent of the methylerythritol phosphate (MEP) pathway (45, 64, 68) (Fig.I.2.2). Therefore, only the most striking features concerning this novel

metabolic route will be outlined here (Fig.I.2.2). These novel findings were expanded to other bacterial species, including those that do not produce hopanoids (eg, *E. coli*), and to other isoprenoid series such as the prenyl side chains of ubiquinone and menaquinone. Several studies have shown that the same pathway is also utilized in plastids of higher plant systems (20).

I.2.B. Identification and elucidation of the enzymes and intermediates in the methylerythritol phosphate pathway

The MEP pathway is now known to be initiated by the condensation of GAP and pyruvate to create 1–deoxy–D–xylulose 5–phosphate (DXP), a reaction catalyzed by DXP synthase (DXS) (Fig.I.2.3). This catalytic mechanism of condensation can also be seen in the reaction catalyzed by transketolases. The *dxs* gene encoding this enzyme was first isolated from *E. coli* (48, 74) and has subsequently been cloned and expressed *in vitro* from a variety of plants and microorganisms (5, 26, 40, 85). The cognate enzyme has a conserved thiamine–binding domain and both thiamine and a divalent cation such as Mg^{2+} or Mn^{2+} are required for its activity in *E. coli* (55, 74). DXS requires thiamine diphosphate as a reaction center for an acyl anion molecule, in parallel with the mechanisms of transketolase (26, 85). In *Arabidopsis thaliana*, the albino phenotype is a result of knock–out of the CLA1 gene, which encodes the first enzyme in the plant MEP pathway. The normal phenotype can be restored by supplementing the diet with DX, the free alcohol of DXP (21). Trapping experiments with [^{14}C]–labeled CO indicated a ping–pong mechanism in which pyruvate binds to thiamine diphosphate, CO_2 is released, then

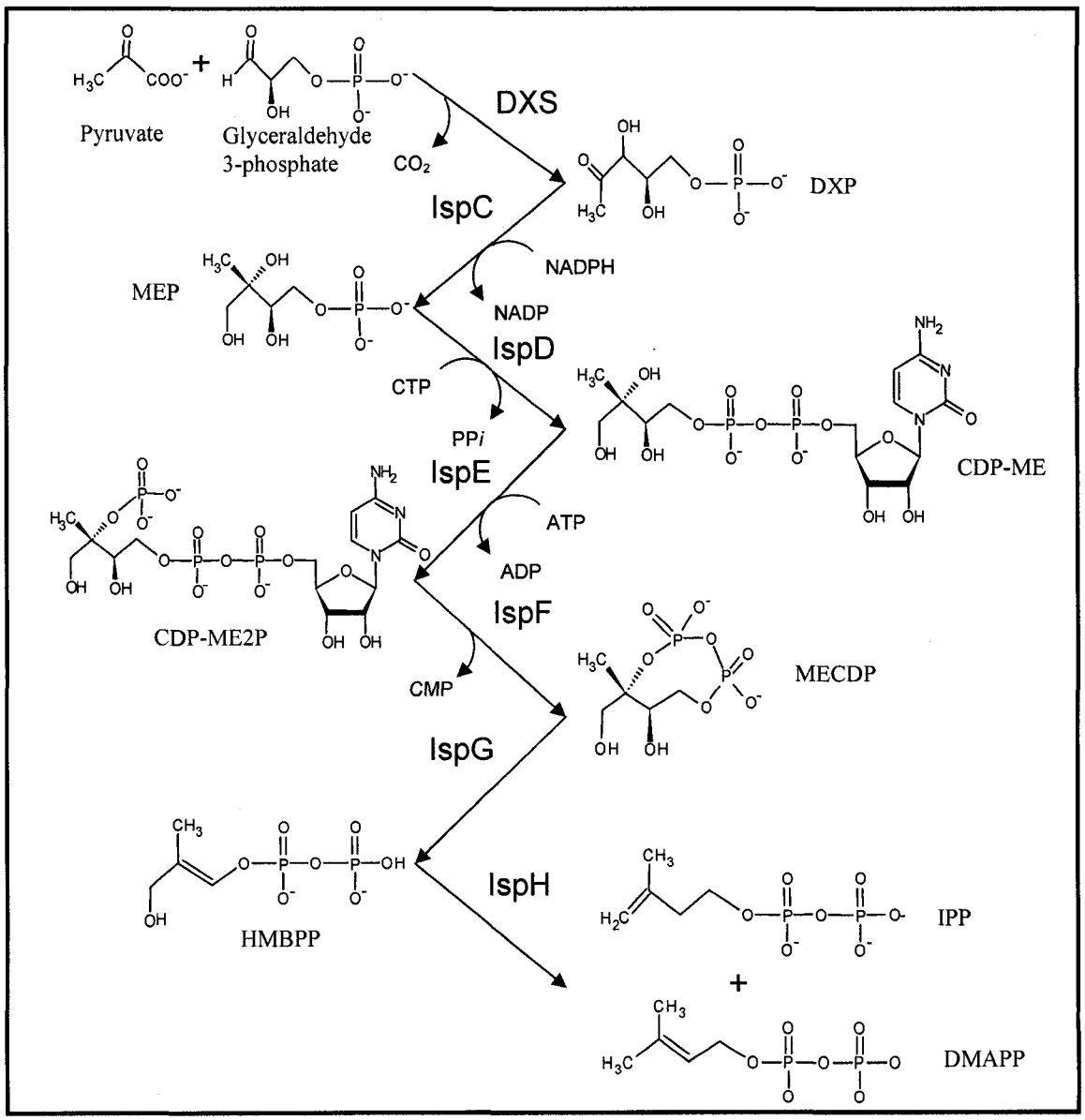

FIGURE I.2.2. **The methylerythritol phosphate pathway**. Most eubacteria utilize this pathway for the biosynthesis of IPP and DMAPP. Abbreviations: The names of structures are in the text. DXS, DXP synthase; IspC, DXP reductoisomerase; IspD, 4–(cytidine 5'–diphosphate)–2–C–methyl–D–erythritol synthetase; IspE, 4–(cytidine 5'–diphosphate)–2–C–methyl–D–erythritol kinase; IspF, 2–C–methyl–D–erythritol 2,4–cyclodiphosphate synthase; IspG, 1–hydroxy–2–methyl–2–(E)–butenyl 4–diphosphate synthase; IspH, 1–hydroxy–2–methyl–2–(E)–butenyl 4–diphosphate reductase (39).

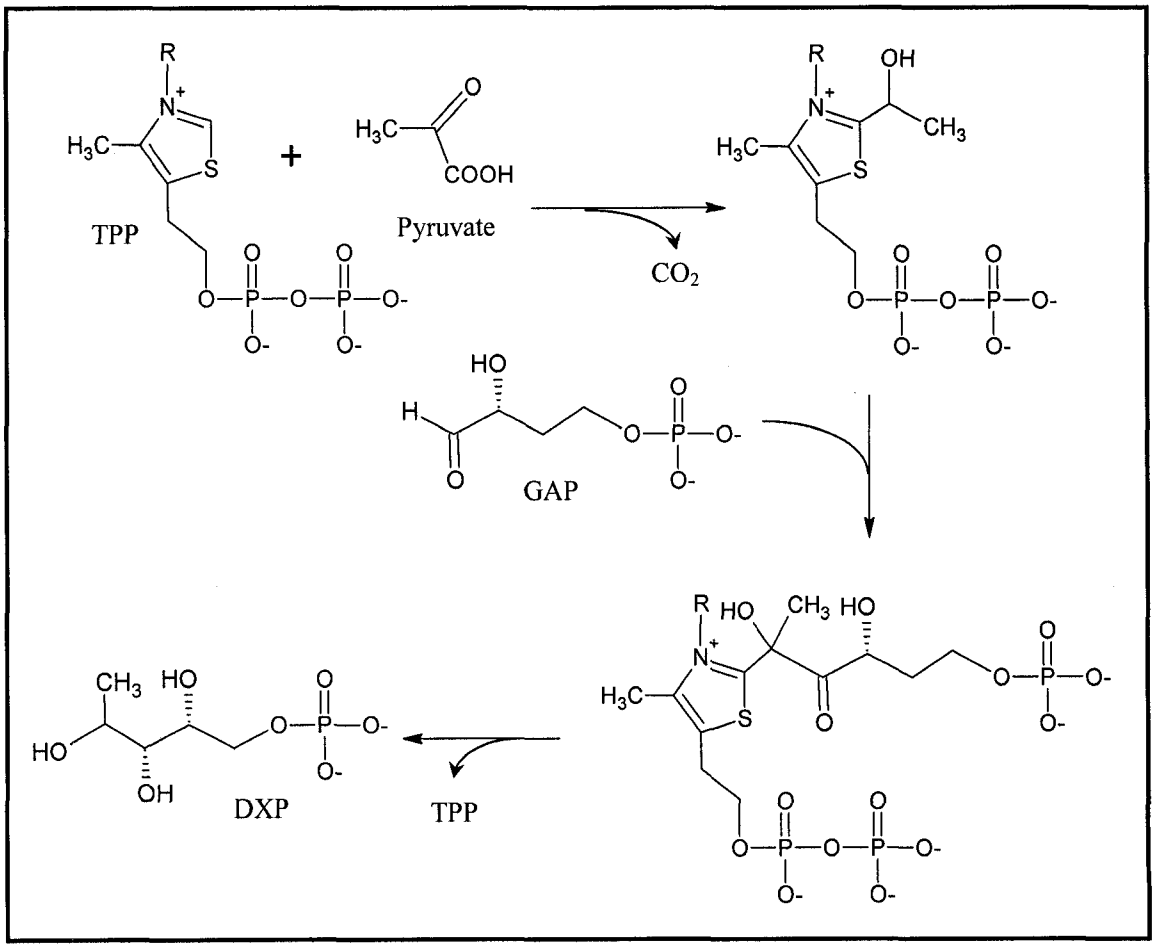

FIGURE.I.2.3. **Proposed reaction catalyzed by the DXS enzyme.** This step is for the formation of 1–deoxy–D–xylulose 5–phosphate (DXP) from pyruvate and glyceraldehyde 3–phosphate (GAP) catalyzed by DXS enzyme. Thiamine diphosphate (TPP) is required for its catalytic activity as a cofactor (39).

GAP binds next and, finally, DXP is released from the DXS (Fig.I.2.3) (22). Besides GAP, DXS from *E. coli* and *M. tuberculosis* can use other sugar phosphates as well as short–chain aldehydes as acceptor substrates (5, 81). Several studies with *A. thaliana* and tomato (*Lycopersicon esculentum*) have shown that the levels of the plastidic isoprenoids correlate with changes in DXS levels, suggesting that DXS is the rate–limiting enzyme for IPP and DMAPP biosynthesis in these plants (22, 49). As noted earlier, DXP is a biosynthetic intermediate not only for the MEP pathway but also for the biosynthesis of thiamine and the pyridoxol in *E. coli* (30). Therefore, DXS activity is not a committed step in the MEP pathway.

The finding that ME is incorporated into the prenyl side chain of ubiquinone in *E. coli* suggested that the branched chain isoprenoid precursors from the linear carbon skeleton of DXP requires an intramolecular rearrangement in order to yield 2–C–methyl–erythrose 4–phosphate. Subsequent conversion to 2–C–methyl–D–erythritol 4–phosphate (MEP) occurs by a reducing process. These skeletal rearrangements have been documented in a variety of studies (4, 19). The fourth carbon of DXP is rearranged which connects to the second carbon by an intra–molecular process. Therefore, it was originally believed that two enzymes were involved in the transformation of MEP from DXP. Studies on *E. coli* mutants in which MEP or ME was required for survival indicated that defects within the *yaeM* gene were responsible for the phenotype and the gene was subsequently cloned (41, 80). Homologous proteins were later isolated from various bacteria, plants, and protozoa (16, 44, 52, 61). Incubation of the YaeM enzyme with DXP and NADPH resulted in a decrease in the NADPH level, indicating the enzyme converted DXP into the reaction product which was identified as MEP (80). Therefore, in the

presence of NADPH, MEP is the next product in the pathway and is created by rearrangement of DXP with DXP reductoisomerase, encoded by *dxr* (*ispC*; renamed later in *E. coli*) (37, 80) (Fig.I.2.4). The DXP reductoisomerase requires a divalent cation, Mg^{2+} or Mn^{2+}, as a cofactor. The identification of the reaction intermediate, 2–C–methylerythrose 4–phosphate, provided solid evidence of the reversibility of the reaction (16, 32, 37). The structure of *E. coli* IspC was recently determined to be a homodimer consisting of an N–terminal dinucleotide binding domain and C–terminal helical domain (56, 76, 89). The forward reaction proceeds as an ordered process with NADPH binding to the IspC prior to the substrate (32, 37). This step is the first committed step in the MEP pathway. DXP reductoisomerase is widely distributed in plants and many eubacteria, including human pathogens, possibly utilized as bioterrorism agents, but not in mammals.

Many studies concerning the development of herbicides and anti–bacterial drugs have targeted this enzyme, IspC. Previously, fosmidomycin was well known to have dramatic bactericidal activity against most Gram–negative bacteria (38, 54). Studies in *Micrococcus luteus* indicated that fosmidomycin could inhibit menaquinone and carotenoid biosynthesis, suggesting this compound targeted isoprenoid biosynthesis (73). Using rapid screening for IspC inhibitors, fosmidomycin displayed strong dose–dependent inhibition, having an IC_{50} (50% inhibiting concentration) of 24 nM (33, 59). Further investigation determined that fosmidomycin could completely inhibit *E. coli* growth at a concentration of 6.25 μg/ml. However, inhibition was abolished by adding ME to the growth medium, indicating that DXP reductoisomerase is the target of fosmidomycin in the MEP pathway (41). Interestingly, the substrate (DXP) structure can be superimposed onto fosmidomycin, indicating fosmidomycin may act as a competitive

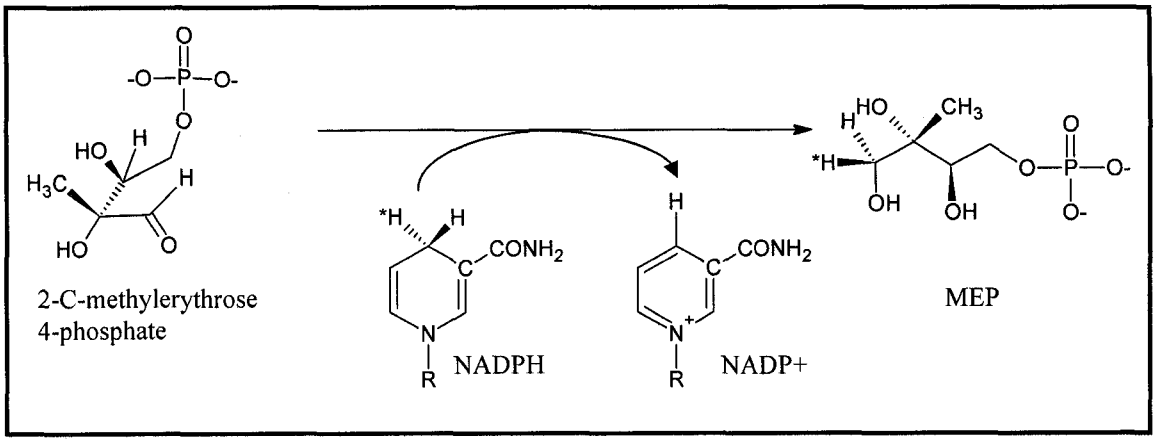

FIGURE I.2.4. **Proposed reaction catalyzed by the IspC enzyme.** The reaction is initiated by the skeletal rearrangement of 1–deoxy–D–xylulose 5–phosphate (DXP) followed by a two electron reduction step requiring NADPH as cofactor (39). 2–C–methylerythrose 4–phosphate is generated by rearrangement of DXP.

inhibitor of IspC (75).

In order to identify the downstream steps in the MEP pathway, *E. coli* mutants with metabolic blocks between MEP and IPP were used. Such mutants would show lethal phenotype in *E. coli* and therefore a strain was designed by transformation to express mevalonate kinase, phosphomevalonate kinase, and pyrophosphomevalonate decarboxylase, thus allowing partial generation of IPP by the MVA pathway upon the addition of mevalonate (40, 78, 79). Mevalonate was required for the mutant growth and this showed unequivocally that the mutants had a defect in the MEP pathway leading to IPP biosynthesis from MEP. Using these mutants, four genes, *ygbP* (*ispD*), *ychB* (*ispE*), *ygbB* (*ispF*), and *gcpE* (*ispG*) were identified that could complement the defects of these blocked mutants and restore IPP synthesis from MEP.

Crude cell extracts of *E. coli* were shown to form unidentified products from MEP in the presence of nucleoside triphosphate, preferentially cytidine 5'–triphosphate (CTP) (66). A database search retrieved the unidentified protein having phosphocytidyl transferase function, *acs1* of *Haemophilus influenzae* (66). This protein harbors N–terminal domain for the transfer of a cytidine 5'–monophosphate (CMP) moiety to ribitol 5–phosphate producing 5–pyrophosphocytidyl ribitol. Acs1 sequence similarity searches revealed an unannotated *E. coli* protein as IspD. The IspD enzyme was cloned and purified and was shown to convert MEP into 4–(cytidine 5'–diphosphate)–2–C–methyl–D–erythritol (CDP–ME) in the presence of CTP (Fig.I.3.2). In addition, the gene was shown to be essential for IPP biosynthesis in *E. coli* (66). *E. coli* IspD requires Mn^{2+} or Co^{2+}, in addition to Mg^{2+}, and the *A. thaliana* IspD utilizes also Ni^{2+} as a cofactor (37, 65, 66). L–erythritol–4–phosphate showed a weak inhibitory effect on the *E. coli* IspD with

IC_{50} of 1.4 mM (47). The IspD forms a homodimer and Mg^{2+} is coordinated to the α, β, and γ phosphates of CTP (57). In the genome of *E. coli* and several other eubacteria, the *ispD* gene was found to be closely linked to or fused with the unannotated *ispF* gene or its putative orthologs.

The fourth reaction step in the MEP pathway is the conversion of CDP–ME to 2–phospho–4–(cytidine 5'–diphospho)–2–C–methyl–D–erythritol (CDP–ME2P) in the presence of ATP and is catalyzed by the *ispE* gene product. The recombinant *E. coli* IspE protein was shown to phosphorylate the hydroxyl group at the second position of CDP–ME (Fig.I.4.1) (50). A sequence alignment revealed that *E. coli* IspE showed similarities to other ATP–dependent kinases such as mevalonate kinase, homoserine kinase, and phosphomevalonate kinase. Crystal structure analyses showed that *E. coli* IspE forms homodimers and *Thermus thermophilus* IspE is a single molecule in the asymmetric subunit but the subunits of both IspE structures follow an α/β fold, characteristic of the galactose/ homoserine/ mevalonate/ phosphomevalonate (GHMP) kinase superfamily present in mammalian cells (51, 84). Although architectural comparison showed bacterial IspE has a close relationship with mammalian GHMP kinase superfamily, there are distinct differences in the catalytic centers and substrate binding pockets. The differences in the catalytic centers indicate its substrate specificity according to the species of the enzyme and the substrate binding site of bacterial IspE, especially the pyrimidine binding site, is located in an extension to the β–turn–β motif, which is lacking in the GHMP kinase superfamily.

The product of IspE, CDP–ME2P, is then converted into 2–C–methyl–D–erythritol 2,4–cyclodiphosphate (MECDP) with the release of CMP by the fifth enzyme

in the MEP pathway, the *ispF* gene product (29). More recently, the orthologous IspF protein from *Plasmodium falciparum* was shown to generate not only MECDP but also the 2–C–methyl–D–erythritol 3,4–cyclophosphate, albeit at a reduced rate (23, 62) (Fig.I.2.5). The structures of the IspF protein from *E. coli*, *H. influenzae*, and *T. thermophilus* have shown that IspF proteins forms homotrimers and contain three active sites, each of which is formed in a cleft between pairs of subunits. The subunit pairs recognize and bind Zn^{2+} with tetrahedral coordination (34, 35, 43, 58, 77). The Zn^{2+} supports the correct binding of the substrate at the active site and facilitates the nucleophilic attack of the 2–phosphate group.

The role of the *ispG* gene product was analyzed by *in vivo* experiments in which recombinant *E. coli* overexpressing *ispC*, *ispD*, *ispE*, *ispF*, and *ispG* catalyzed the conversion of exogenous DX into 1–hydroxy–2–methyl–2–(E)–butenyl 4–diphosphate (HMBPP) (28). This finding indicated the involvement of the *ispG* gene product in the MEP pathway and was confirmed by a study showing the accumulation of HMBPP in a mutant of *E. coli* carrying a defect in the *lytB* (*ispH*) gene (2). Recombinant IspG reduces MECDP ring opening using a photoreduced deazaflavin derivative as an artificial electron donor (67, 72). One report has shown that IspG has a prosthetic $[4Fe–4S]^{2+}$ cluster, suggesting the reduction reaction involves a free radical. If so, reduction of MECDP could also occur via the shuttle of redox equivalents from NADPH through flavodoxin reductase (36, 67, 72). The hypothetical IspG catalytic mechanism is illustrated in Fig.I.2.6. In this process, the epoxide of the first intermediate is a potential point for the reduction reaction. Notably, IspG protein has been shown to catalyze that reaction more efficiently with an artificial electron donor system comprised of dithionite

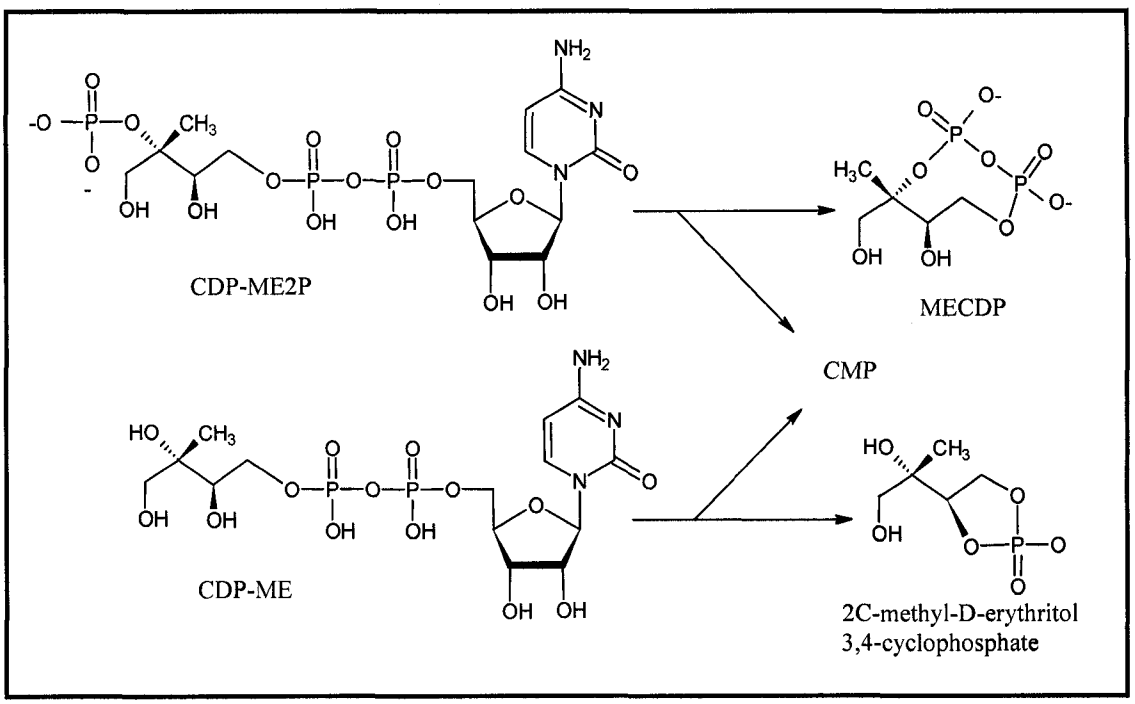

FIGURE I.2.5. **Proposed reaction catalyzed by the IspF enzyme**. IspF can utilize 2–phospho–4–(cytidine 5'–diphospho)–2–C–methyl–D–erythritol (CDP–ME2P) converting it into 2C–methyl D–erythritol 2,4–cyclodiphosphate (MECDP) and utilize also 4–(cytidine 5'–diphosphate)–2–C–methyl–D–erythritol (CDP–ME) converting it into 2C–methyl D–erythritol 3,4–cyclophosphate (62). In both reactions, cytidine 5'–monophosphate (CMP) is released.

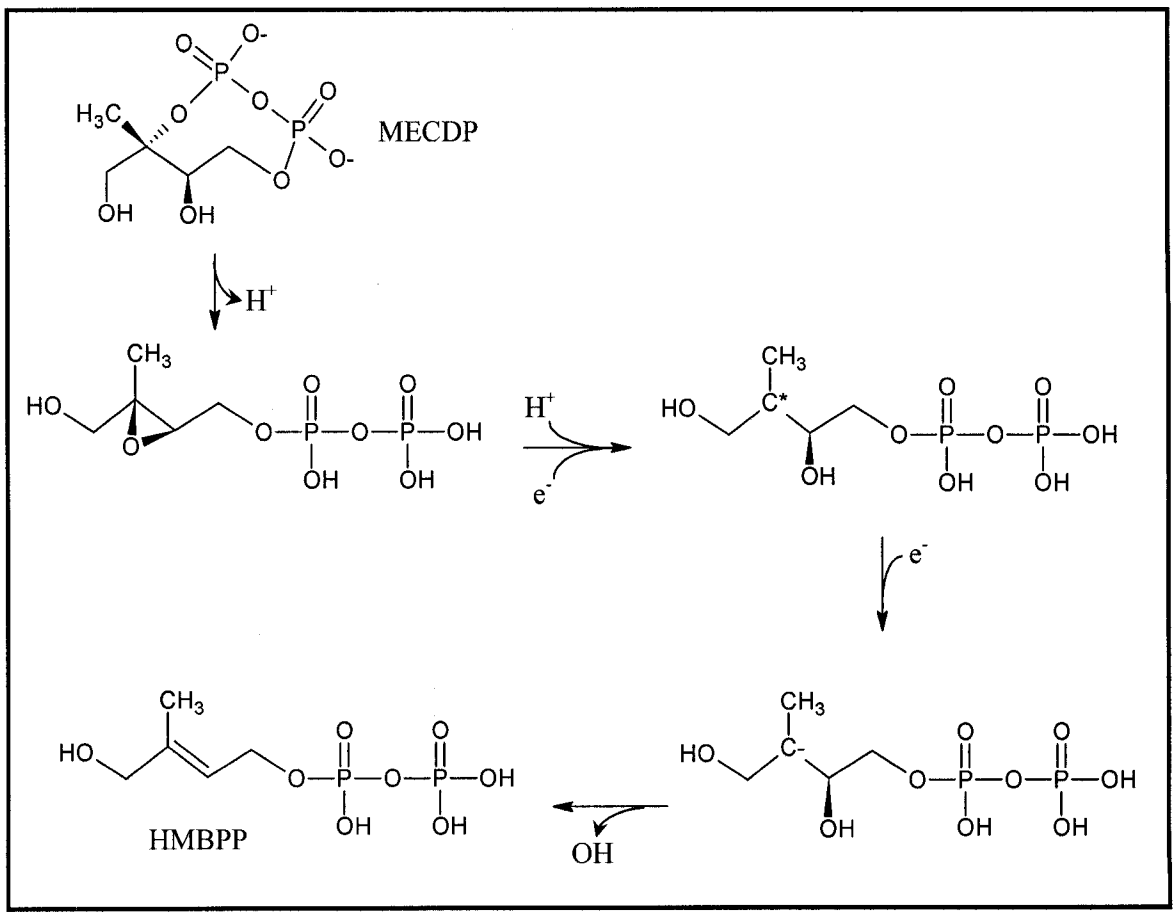

FIGURE I.2.6. **Hypothetical reaction catalyzed by the IspG enzyme.** This step is for the conversion of 2C–methyl–D–erythritol 2,4–cyclodiphosphate (MECDP) into 1–hydroxy–2–methyl–2–(E)–butenyl 4–diphosphate (HMBPP) catalyzed by the IspG enzyme. (*, radical) (28, 67).

compared with NADPH, flavodoxin and flavodoxin reductase as a redox shuttle system.

The *ispH* gene product is responsible for the conversion of HMBPP into IPP and DMAPP and this function was previously determined to be essential in *E. coli* as well as *Synechocystis sp.* (3, 15). *In vivo* experiments using an *E. coli* strain overexpressing the genes *xylB* and *ispC,D,E,F,* and *G* converted exogenous [^{13}C]–labeled DX into HMBPP and co–expression of *ispH* could yield IPP and DMAPP at a molar ratio of 5:1 (63). Interestingly, the recombinant IspH enzyme from *E. coli* has no activity by itself and must be stimulated by *E. coli* crude extract. The reaction requires NADH, flavin–adenine dinucleotide (FAD) and divalent cations (preferably Co^{2+}), and at least one more unidentified electron shuttle (1). The IspH enzyme can be also activated under anaerobic conditions, restoring reduction capacity in the presence of flavodoxin, flavodoxin reductase, and NADPH (67, 88). UV/visible and electron paramagnetic resonance spectroscopy revealed that the recombinant IspH from *E. coli* possesses a prosthetic dioxygen–sensitive $[4Fe–4S]^{2+}$ cluster (88). The hypothetical reaction catalyzed by IspH involves a two–electron transfer, resulting in the cleavage of a nonactivated C–OH bond in HMBPP. Like IspG, the prosthetic $[4Fe–4S]^{2+}$ cluster suggests the involvement of radical intermediates (Fig.I.2.7).

I.2.C. Evolutionary perspectives of the methylerythritol phosphate pathway and the mevalonate pathway

All organisms except for obligate intracellular parasites need at least one pathway for biosynthesizing IPP for their survival. Eukaryotes including animals and fungi use

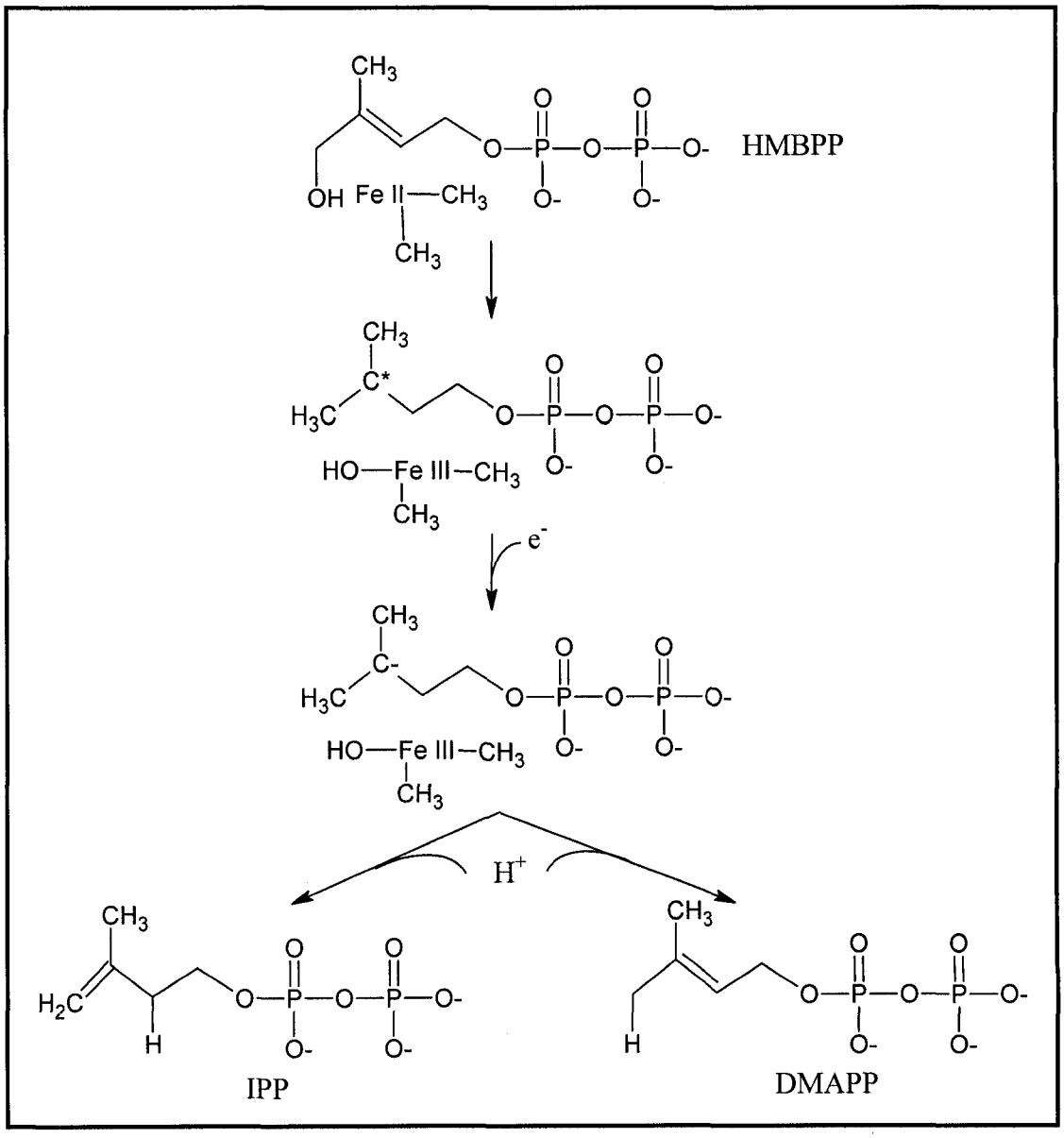

FIGURE.I.2.7. **Hypothetical the reaction catalyzed by the IspH enzyme**. This diagram represents the hypothetical procedure by which the IspH enzyme converts of 1–hydroxy–2–methyl–2–(*E*)–butenyl 4–diphosphate (HMBPP) into isopentenyl diphosphate (IPP) and dimethylallyl diphosphate (DMAPP). (*, radical) (67, 88).

only the MVA pathway. Plants and algae have the MEP pathway together with the MVA pathway in many cases. Many green algae and some photosynthetic protists (*P. falciparum*) use the MEP pathway (11). Although archaea possess solely the MVA pathway, it is difficult to explain the distribution pattern of the last two enzymes of the MVA pathway; phosphomevalonate kinase and pyrophosphomevalonate decarboxylase (11). Bacteria are more complex because they use either or both of the pathways, although the majority of them utilize only the MEP pathway as probably ancestral route (10). Bacteria possessing both pathways, usually use the MEP pathway to generate essential primary metabolites, with those of the MVA pathway being dedicated to secondary metabolites (10). For example, a few actinomycetes (*Streptomyces aeriouvifer* and *Kitasatospora griseola*) possess both pathways. *S. aeriouvifer* synthesizes menaquinone through the MEP pathway at an early growth stage, and switches to the MVA pathway for synthesis of the antibiotic naphterpin at a later growth stage. Furthermore, pravastatin, an HMGR inhibitor, can suppress the production of naphterpin without affecting its growth, indicating that the MVA pathway is specifically involved in the synthesis of this antibiotic (11). The patchy distribution and dispensability of the MVA pathway indicate that all the genes of the MVA pathway likely were acquired by horizontal gene transfer (HGT) in these actinomycetes. The genes encoding the last two enzymes of the MVA pathway, as it is known in eukaryotes, are missing from most archaea; these functions being fulfilled by unidentified analogs. However, some archaea have acquired those genes through HGT. Indeed, *Sulfolobus* possesses the last two genes that are very similar to their eukaryotic homologs and both *Thermoplasma* and *Halobacterium* have the genes seemingly of bacterial origin (53).

The genes of the MEP pathway are usually scattered around a genome without forming a cluster. Although the MEP pathway might not be transferred as a unit, its genes can be individually acquired. Some firmicutes, although they use the MVA pathway, also harbor genes of the MEP pathway: *dxs* is found in *Lactococcus lactis* and *ispE* is found in *Staphylococcus aureus*. Similarly, *ispD* gene is present in the archea *Pyrococcus horikoshii* but is absent from the genome of any other archaea, even the closely related *Pyrococcus abyssii*, indicating that is the result of a recent HGT. The MEP pathway genes also acquired through homologous gene replacement between different bacteria harboring this pathway. For example, the *ispG* was transferred from plants to *Chlamydia* and to *Chlorobium* (42). On the other hand, *dxr* and *ispH* support a cyanobacterial origin of the MEP pathway found in eukaryotes, as a strong clustering of photosynthetic eukaryotes with cyanobacteria can be seen in the phylogenetic trees of both genes (42).

I.2.D. Distribution of the methylerythritol phosphate pathway and its potential as new targets for anti–bacterial drugs

Most of the eubacteria with completely sequenced genomes including human pathogens exclusively utilize the MEP pathway. Although genes encoding parts of the enzymes in the MVA pathway have been found in some bacteria, the MEP pathway likely represents the most widespread pathway for isoprenoid biosynthesis in eubacteria (69). However, the spirochete *Borrelia burgdorferi* and Gram– positive cocci, such as *Staphylococcus aureus* (83, 87), carry complete sets of the MVA pathway genes, including the gene for type II isopentenyl diphosphate isomerase (18). Another type of

eubacteria, as well as some *Streptomyces* species and *Listeria monocytogenes* (6) have complete sets of both the MVA pathway and the MEP pathway genes. As mentioned in the previous section, these distributions of the two sets of genes for isoprenoid biosynthesis reflect HGT rather than phylogenetic relationship (10, 17, 42). In line with genetic data, various isoprenoids from actinomycetes have been shown to originate via the MEP route.

Most bacterial pathogens, listed as Category A, B, and C agents in the biothreat groups classified by the National Institute of Allergy and Infectious Diseases (NIAID) (Table II.1.1) and the Centers for Disease Control and Prevention (CDC) (Table II.1.2), utilize the MEP pathway. Three (*Yersinia pestis*, *Fransicella tularensis*, and *Clostridium botulinum*) of the six Category A agents utilize or appear to utilize the MEP pathway. Among the twelve Category B agents listed, eight (*Brucella* spp., *Burkholderia mallei, Burkholderia pseudomallei*, *Staphylococcus* spp., *Salmonella* spp., *Shigella dysenteriae*, *Escherichia coli* O157: H7 and *Vibrio cholerae*) appear to utilize the MEP pathway with the exception of *Coxiella burnetii* and *Staphylococcus* spp. (18). Several minor anomalies in the distribution of orthologs should be noted. *V. cholerae* has a full set of genes for the MEP pathway and a single gene with similarity to HMGR of the MVA pathway. Some eubacteria with full sets of the MEP pathway genes such as *E. coli* and *M. tuberculosis* possess both orthologs of the IPP isomerases (*idi*) type I or II. Since IPP and DMAPP can be synthesized independently by the catalytic action of the IspH protein, it can be assumed that the isomerases serve as non–essential salvage pathway proteins in these organisms; indeed, *idiI* deletion mutants of *E. coli* were found to be viable on minimal medium (27).

Whole genome sequencing of numerous pathogenic bacteria has enabled the systematic search for essential genes. Approximately 30 *E. coli* genes with widely distributed orthologs have been identified as essential, including the entire MEP pathway genes described above. Many of the other genes have, as yet, no known function. Therefore, the MEP pathway enzymes are prime candidates for high throughput screening of chemical libraries aimed at rational drug development. The MEP pathway is exclusively used for early step of isoprenoid biosynthesis by the majority of pathogenic bacteria, including *M. tuberculosis*, and there is no evidence for its presence in animals, yeasts and fungi. This makes the MEP metabolic route an important target for the design of novel anti–bacterial and anti–parasitic drugs, with potential for minimal side effects for the human host.

I.2.E. References

1. **Adam, P., S. Hecht, W. Eisenreich, J. Kaiser, T. Grawert, D. Arigoni, A. Bacher, and F. Rohdich.** 2002. Biosynthesis of terpenes: studies on 1-hydroxy-2-methyl-2-(E)-butenyl 4-diphosphate reductase. Proc Natl Acad Sci U S A **99:**12108-13.
2. **Altincicek, B., A. Kollas, M. Eberl, J. Wiesner, S. Sanderbrand, M. Hintz, E. Beck, and H. Jomaa.** 2001. LytB, a novel gene of the 2-C-methyl-D-erythritol 4-phosphate pathway of isoprenoid biosynthesis in *Escherichia coli*. FEBS Lett **499:**37-40.
3. **Altincicek, B., A. K. Kollas, S. Sanderbrand, J. Wiesner, M. Hintz, E. Beck, and H. Jomaa.** 2001. GcpE is involved in the 2-C-methyl-D-erythritol 4-phosphate pathway of isoprenoid biosynthesis in *Escherichia coli*. J Bacteriol **183:**2411-6.

4. **Arigoni, D., S. Sagner, C. Latzel, W. Eisenreich, A. Bacher, and M. H. Zenk.** 1997. Terpenoid biosynthesis from 1-deoxy-D-xylulose in higher plants by intramolecular skeletal rearrangement. Proc Natl Acad Sci U S A **94:**10600-5.

5. **Bailey, A. M., S. Mahapatra, P. J. Brennan, and D. C. Crick.** 2002. Identification, cloning, purification, and enzymatic characterization of *Mycobacterium tuberculosis* 1-deoxy-D-xylulose 5-phosphate synthase. Glycobiology **12:**813-20.

6. **Begley, M., C. G. Gahan, A. K. Kollas, M. Hintz, C. Hill, H. Jomaa, and M. Eberl.** 2004. The interplay between classical and alternative isoprenoid biosynthesis controls gammadelta T cell bioactivity of *Listeria monocytogenes*. FEBS Lett **561:**99-104.

7. **Betteridge, D. J., W. Krone, J. P. Reckless, and D. J. Galton.** 1978. Compactin inhibits cholesterol synthesis in lymphocytes and intestinal mucosa from patients with familial hypercholesterolaemia. Lancet **2:**1342-3.

8. **Bloch, K.** 1992. Sterol molecule: structure, biosynthesis, and function. Steroids **57:**378-83.

9. **Bochar, D. A., C. V. Stauffacher, and V. W. Rodwell.** 1999. Sequence comparisons reveal two classes of 3-hydroxy-3-methylglutaryl coenzyme A reductase. Mol Genet Metab **66:**122-7.

10. **Boucher, Y., and W. F. Doolittle.** 2000. The role of lateral gene transfer in the evolution of isoprenoid biosynthesis pathways. Mol Microbiol **37:**703-16.

11. **Boucher, Y., C. J. Douady, R. T. Papke, D. A. Walsh, M. E. Boudreau, C. L. Nesbo, R. J. Case, and W. F. Doolittle.** 2003. Lateral gene transfer and the origins of prokaryotic groups. Annu Rev Genet **37:**283-328.

12. **Brocks, J. J., G. A. Logan, R. Buick, and R. E. Summons.** 1999. Archean molecular fossils and the early rise of eukaryotes. Science **285:**1033-6.

13. **Connolly, J. D., and R. A. Hill.** 1989. Triterpenoids. Nat Prod Rep **6:**475-501.

14. **Connolly, J. D., R. A. Hill, and B. T. Ngadjui.** 1994. Triterpenoids. Nat Prod Rep **11:**467-92.

15. **Cunningham, F. X., Jr., T. P. Lafond, and E. Gantt.** 2000. Evidence of a role for LytB in the nonmevalonate pathway of isoprenoid biosynthesis. J Bacteriol **182:**5841-8.

16. **Dhiman, R. K., M. L. Schaeffer, A. M. Bailey, C. A. Testa, H. Scherman, and D. C. Crick.** 2005. 1-Deoxy-D-xylulose 5-phosphate reductoisomerase (IspC) from *Mycobacterium tuberculosis*: towards understanding mycobacterial resistance to fosmidomycin. J Bacteriol **187:**8395-402.

17. **Eberl, M., M. Hintz, A. Reichenberg, A. K. Kollas, J. Wiesner, and H. Jomaa.** 2003. Microbial isoprenoid biosynthesis and human gammadelta T cell activation. FEBS Lett **544:**4-10.

18. **Eisenreich, W., A. Bacher, D. Arigoni, and F. Rohdich.** 2004. Biosynthesis of isoprenoids via the non-mevalonate pathway. Cell Mol Life Sci **61:**1401-26.

19. **Eisenreich, W., B. Menhard, P. J. Hylands, M. H. Zenk, and A. Bacher.** 1996. Studies on the biosynthesis of taxol: the taxane carbon skeleton is not of mevalonoid origin. Proc Natl Acad Sci U S A **93:**6431-6.

20. **Eisenreich, W., M. Schwarz, A. Cartayrade, D. Arigoni, M. H. Zenk, and A. Bacher.** 1998. The deoxyxylulose phosphate pathway of terpenoid biosynthesis in plants and microorganisms. Chem Biol **5:**R221-33.

21. **Estevez, J. M., A. Cantero, C. Romero, H. Kawaide, L. F. Jimenez, T. Kuzuyama, H. Seto, Y. Kamiya, and P. Leon.** 2000. Analysis of the expression of CLA1, a gene that encodes the 1-deoxyxylulose 5-phosphate synthase of the 2-C-methyl-D-erythritol-4-phosphate pathway in *Arabidopsis*. Plant Physiol **124:**95-104.

22. **Eubanks, L. M., and C. D. Poulter.** 2003. *Rhodobacter capsulatus* 1-deoxy-D-xylulose 5-phosphate synthase: steady-state kinetics and substrate binding. Biochemistry **42:**1140-9.

23. **Fellermeier, M., M. Raschke, S. Sagner, J. Wungsintaweekul, C. A. Schuhr, S. Hecht, K. Kis, T. Radykewicz, P. Adam, F. Rohdich, W. Eisenreich, A. Bacher, D. Arigoni, and M. H. Zenk.** 2001. Studies on the nonmevalonate pathway of terpene biosynthesis. The role of 2C-methyl-D-erythritol 2,4-cyclodiphosphate in plants. Eur J Biochem **268:**6302-10.

24. **Flesch, G., and M. Rohmer.** 1988. Prokaryotic hopanoids: the biosynthesis of the bacteriohopane skeleton. Formation of isoprenic units from two distinct acetate pools and a novel type of carbon/carbon linkage between a triterpene and D-ribose. Eur J Biochem **175:**405-11.

25. **Gabrielsen, M., C. S. Bond, I. Hallyburton, S. Hecht, A. Bacher, W. Eisenreich, F. Rohdich, and W. N. Hunter.** 2004. Hexameric assembly of the bifunctional methylerythritol 2,4-cyclodiphosphate synthase and protein-protein associations in the deoxy-xylulose-dependent pathway of isoprenoid precursor biosynthesis. J Biol Chem **279:**52753-61.

26. **Hahn, F. M., L. M. Eubanks, C. A. Testa, B. S. Blagg, J. A. Baker, and C. D. Poulter.** 2001. 1-Deoxy-D-xylulose 5-phosphate synthase, the gene product of open reading frame (ORF) 2816 and ORF 2895 in *Rhodobacter capsulatus*. J Bacteriol **183:**1-11.

27. **Hahn, F. M., A. P. Hurlburt, and C. D. Poulter.** 1999. *Escherichia coli* open reading frame 696 is *idi*, a nonessential gene encoding isopentenyl diphosphate isomerase. J Bacteriol **181:**4499-504.

28. **Hecht, S., W. Eisenreich, P. Adam, S. Amslinger, K. Kis, A. Bacher, D. Arigoni, and F. Rohdich.** 2001. Studies on the nonmevalonate pathway to terpenes: the role of the GcpE (IspG) protein. Proc Natl Acad Sci U S A **98:**14837-42.

29. **Herz, S., J. Wungsintaweekul, C. A. Schuhr, S. Hecht, H. Luttgen, S. Sagner, M. Fellermeier, W. Eisenreich, M. H. Zenk, A. Bacher, and F. Rohdich.** 2000. Biosynthesis of terpenoids: YgbB protein converts 4-diphosphocytidyl-2C-methyl-D-erythritol 2-phosphate to 2C-methyl-D-erythritol 2,4-cyclodiphosphate. Proc Natl Acad Sci U S A **97:**2486-90.

30. **Hill, R. E., K. Himmeldirk, I. A. Kennedy, R. M. Pauloski, B. G. Sayer, E. Wolf, and I. D. Spenser.** 1996. The biogenetic anatomy of vitamin B6. A 13C NMR investigation of the biosynthesis of pyridoxol in *Escherichia coli*. J Biol Chem **271:**30426-35.

31. **Hill, R. E., A. Iwanow, B. G. Sayer, W. Wysocka, and I. D. Spenser.** 1987. The regiochemistry and stereochemistry of the biosynthesis of vitamin B6 from triose units. J Biol Chem **262:**7463-71.

32. **Hoeffler, J. F., D. Tritsch, C. Grosdemange-Billiard, and M. Rohmer.** 2002. Isoprenoid biosynthesis via the methylerythritol phosphate pathway. Mechanistic investigations of the 1-deoxy-D-xylulose 5-phosphate reductoisomerase. Eur J Biochem **269:**4446-57.

33. **Jomaa, H., J. Wiesner, S. Sanderbrand, B. Altincicek, C. Weidemeyer, M. Hintz, I. Turbachova, M. Eberl, J. Zeidler, H. K. Lichtenthaler, D. Soldati, and E. Beck.** 1999. Inhibitors of the nonmevalonate pathway of isoprenoid biosynthesis as antimalarial drugs. Science **285:**1573-6.

34. **Kemp, L. E., C. S. Bond, and W. N. Hunter.** 2002. Structure of 2C-methyl-D-erythritol 2,4- cyclodiphosphate synthase: an essential enzyme for isoprenoid biosynthesis and target for antimicrobial drug development. Proc Natl Acad Sci U S A **99:**6591-6.

35. **Kishida, H., T. Wada, S. Unzai, T. Kuzuyama, M. Takagi, T. Terada, M. Shirouzu, S. Yokoyama, J. R. Tame, and S. Y. Park.** 2003. Structure and catalytic mechanism of 2-C-methyl-D-erythritol 2,4-cyclodiphosphate (MECDP) synthase, an enzyme in the non-mevalonate pathway of isoprenoid synthesis. Acta Crystallogr D Biol Crystallogr **59:**23-31.

36. **Kollas, A. K., E. C. Duin, M. Eberl, B. Altincicek, M. Hintz, A. Reichenberg, D. Henschker, A. Henne, I. Steinbrecher, D. N. Ostrovsky, R. Hedderich, E. Beck, H. Jomaa, and J. Wiesner.** 2002. Functional characterization of GcpE, an essential enzyme of the non-mevalonate pathway of isoprenoid biosynthesis. FEBS Lett **532:**432-6.

37. **Koppisch, A. T., D. T. Fox, B. S. Blagg, and C. D. Poulter.** 2002. *E. coli* MEP synthase: steady-state kinetic analysis and substrate binding. Biochemistry **41:**236-43.

38. **Kuroda, Y., M. Okuhara, T. Goto, M. Okamoto, H. Terano, M. Kohsaka, H. Aoki, and H. Imanaka.** 1980. Studies on new phosphonic acid antibiotics. IV.

Structure determination of FR-33289, FR-31564 and FR-32863. J Antibiot (Tokyo) **33:**29-35.

39. **Kuzuyama, T.** 2002. Mevalonate and nonmevalonate pathways for the biosynthesis of isoprene units. Biosci Biotechnol Biochem **66:**1619-27.

40. **Kuzuyama, T., M. Takagi, S. Takahashi, and H. Seto.** 2000. Cloning and characterization of 1-deoxy-D-xylulose 5-phosphate synthase from *Streptomyces* sp. Strain CL190, which uses both the mevalonate and nonmevalonate pathways for isopentenyl diphosphate biosynthesis. J Bacteriol **182:**891-7.

41. **Kuzuyama, T., S. Takahashi, and H. Seto.** 1999. Construction and characterization of *Escherichia coli* disruptants defective in the *yaeM* gene. Biosci Biotechnol Biochem **63:**776-8.

42. **Lange, B. M., T. Rujan, W. Martin, and R. Croteau.** 2000. Isoprenoid biosynthesis: the evolution of two ancient and distinct pathways across genomes. Proc Natl Acad Sci U S A **97:**13172-7.

43. **Lehmann, C., K. Lim, J. Toedt, W. Krajewski, A. Howard, E. Eisenstein, and O. Herzberg.** 2002. Structure of 2C-methyl-D-erythrol-2,4-cyclodiphosphate synthase from *Haemophilus influenzae*: activation by conformational transition. Proteins **49:**135-8.

44. **Liao, Z., R. Chen, M. Chen, C. Yang, Q. Wang, and Y. Gong.** 2007. A new 1-deoxy-D-xylulose 5-phosphate reductoisomerase gene encoding the committed-step enzyme in the MEP pathway from *Rauvolfia verticillata*. Z Naturforsch [C] **62:**296-304.

45. **Lichtenthaler, H. K.** 1999. The 1-Deoxy-D-Xylulose-5-Phosphate Pathway of Isoprenoid Biosynthesis in Plants. Annu Rev Plant Physiol Plant Mol Biol **50:**47-65.

46. **Lichtenthaler, H. K., J. Schwender, A. Disch, and M. Rohmer.** 1997. Biosynthesis of isoprenoids in higher plant chloroplasts proceeds via a mevalonate-independent pathway. FEBS Lett **400:**271-4.

47. **Lillo, A. M., C. N. Tetzlaff, F. J. Sangari, and D. E. Cane.** 2003. Functional expression and characterization of EryA, the erythritol kinase of *Brucella abortus*,

and enzymatic synthesis of L-erythritol-4-phosphate. Bioorg Med Chem Lett **13:**737-9.

48. **Lois, L. M., N. Campos, S. R. Putra, K. Danielsen, M. Rohmer, and A. Boronat.** 1998. Cloning and characterization of a gene from *Escherichia coli* encoding a transketolase-like enzyme that catalyzes the synthesis of D-1-deoxyxylulose 5-phosphate, a common precursor for isoprenoid, thiamin, and pyridoxol biosynthesis. Proc Natl Acad Sci U S A **95:**2105-10.

49. **Lois, L. M., M. Rodriguez-Concepcion, F. Gallego, N. Campos, and A. Boronat.** 2000. Carotenoid biosynthesis during tomato fruit development: regulatory role of 1-deoxy-D-xylulose 5-phosphate synthase. Plant J **22:**503-13.

50. **Luttgen, H., F. Rohdich, S. Herz, J. Wungsintaweekul, S. Hecht, C. A. Schuhr, M. Fellermeier, S. Sagner, M. H. Zenk, A. Bacher, and W. Eisenreich.** 2000. Biosynthesis of terpenoids: YchB protein of *Escherichia coli* phosphorylates the 2-hydroxy group of 4-diphosphocytidyl-2C-methyl-D-erythritol. Proc Natl Acad Sci U S A **97:**1062-7.

51. **Miallau, L., M. S. Alphey, L. E. Kemp, G. A. Leonard, S. M. McSweeney, S. Hecht, A. Bacher, W. Eisenreich, F. Rohdich, and W. N. Hunter.** 2003. Biosynthesis of isoprenoids: crystal structure of 4-diphosphocytidyl-2C-methyl-D-erythritol kinase. Proc Natl Acad Sci U S A **100:**9173-8.

52. **Miller, B., T. Heuser, and W. Zimmer.** 2000. Functional involvement of a deoxy-D-xylulose 5-phosphate reductoisomerase gene harboring locus of *Synechococcus leopoliensis* in isoprenoid biosynthesis. FEBS Lett **481:**221-6.

53. **Ng, W. V., S. P. Kennedy, G. G. Mahairas, B. Berquist, M. Pan, H. D. Shukla, S. R. Lasky, N. S. Baliga, V. Thorsson, J. Sbrogna, S. Swartzell, D. Weir, J. Hall, T. A. Dahl, R. Welti, Y. A. Goo, B. Leithauser, K. Keller, R. Cruz, M. J. Danson, D. W. Hough, D. G. Maddocks, P. E. Jablonski, M. P. Krebs, C. M. Angevine, H. Dale, T. A. Isenbarger, R. F. Peck, M. Pohlschroder, J. L. Spudich, K. W. Jung, M. Alam, T. Freitas, S. Hou, C. J. Daniels, P. P. Dennis, A. D. Omer, H. Ebhardt, T. M. Lowe, P. Liang, M. Riley, L. Hood, and S. DasSarma.** 2000. Genome sequence of *Halobacterium* species NRC-1. Proc Natl Acad Sci U S A **97:**12176-81.

54. **Okuhara, M., Y. Kuroda, T. Goto, M. Okamoto, H. Terano, M. Kohsaka, H. Aoki, and H. Imanaka.** 1980. Studies on new phosphonic acid antibiotics. III. Isolation and characterization of FR-31564, FR-32863 and FR-33289. J Antibiot (Tokyo) **33:**24-8.

55. **Querol, J., M. Rodriguez-Concepcion, A. Boronat, and S. Imperial.** 2001. Essential role of residue H49 for activity of *Escherichia coli* 1-deoxy-D-xylulose 5-phosphate synthase, the enzyme catalyzing the first step of the 2-C-methyl-D-erythritol 4-phosphate pathway for isoprenoid Synthesis. Biochem Biophys Res Commun **289:**155-60.

56. **Reuter, K., S. Sanderbrand, H. Jomaa, J. Wiesner, I. Steinbrecher, E. Beck, M. Hintz, G. Klebe, and M. T. Stubbs.** 2002. Crystal structure of 1-deoxy-D-xylulose-5-phosphate reductoisomerase, a crucial enzyme in the non-mevalonate pathway of isoprenoid biosynthesis. J Biol Chem **277:**5378-84.

57. **Richard, S. B., M. E. Bowman, W. Kwiatkowski, I. Kang, C. Chow, A. M. Lillo, D. E. Cane, and J. P. Noel.** 2001. Structure of 4-diphosphocytidyl-2-C-methylerythritol synthetase involved in mevalonate- independent isoprenoid biosynthesis. Nat Struct Biol **8:**641-8.

58. **Richard, S. B., J. L. Ferrer, M. E. Bowman, A. M. Lillo, C. N. Tetzlaff, D. E. Cane, and J. P. Noel.** 2002. Structure and mechanism of 2-C-methyl-D-erythritol 2,4-cyclodiphosphate synthase. An enzyme in the mevalonate-independent isoprenoid biosynthetic pathway. J Biol Chem **277:**8667-72.

59. **Ridley, R. G.** 1999. Planting the seeds of new antimalarial drugs. Science **285:**1502-3.

60. **Rodriguez-Concepcion, M.** 2004. The MEP pathway: a new target for the development of herbicides, antibiotics and antimalarial drugs. Curr Pharm Des **10:**2391-400.

61. **Rodriguez-Concepcion, M., I. Ahumada, E. Diez-Juez, S. Sauret-Gueto, L. M. Lois, F. Gallego, L. Carretero-Paulet, N. Campos, and A. Boronat.** 2001. 1-Deoxy-D-xylulose 5-phosphate reductoisomerase and plastid isoprenoid biosynthesis during tomato fruit ripening. Plant J **27:**213-22.

62. **Rohdich, F., W. Eisenreich, J. Wungsintaweekul, S. Hecht, C. A. Schuhr, and A. Bacher.** 2001. Biosynthesis of terpenoids. 2C-Methyl-D-erythritol 2,4-cyclodiphosphate synthase (IspF) from *Plasmodium falciparum*. Eur J Biochem **268:**3190-7.

63. **Rohdich, F., S. Hecht, K. Gartner, P. Adam, C. Krieger, S. Amslinger, D. Arigoni, A. Bacher, and W. Eisenreich.** 2002. Studies on the nonmevalonate terpene biosynthetic pathway: metabolic role of IspH (LytB) protein. Proc Natl Acad Sci U S A **99:**1158-63.

64. **Rohdich, F., K. Kis, A. Bacher, and W. Eisenreich.** 2001. The non-mevalonate pathway of isoprenoids: genes, enzymes and intermediates. Curr Opin Chem Biol **5:**535-40.

65. **Rohdich, F., J. Wungsintaweekul, W. Eisenreich, G. Richter, C. A. Schuhr, S. Hecht, M. H. Zenk, and A. Bacher.** 2000. Biosynthesis of terpenoids: 4-diphosphocytidyl-2C-methyl-D-erythritol synthase of *Arabidopsis thaliana*. Proc Natl Acad Sci U S A **97:**6451-6.

66. **Rohdich, F., J. Wungsintaweekul, M. Fellermeier, S. Sagner, S. Herz, K. Kis, W. Eisenreich, A. Bacher, and M. H. Zenk.** 1999. Cytidine 5'-triphosphate-dependent biosynthesis of isoprenoids: YgbP protein of *Escherichia coli* catalyzes the formation of 4-diphosphocytidyl-2-C-methylerythritol. Proc Natl Acad Sci U S A **96:**11758-63.

67. **Rohdich, F., F. Zepeck, P. Adam, S. Hecht, J. Kaiser, R. Laupitz, T. Grawert, S. Amslinger, W. Eisenreich, A. Bacher, and D. Arigoni.** 2003. The deoxyxylulose phosphate pathway of isoprenoid biosynthesis: studies on the mechanisms of the reactions catalyzed by IspG and IspH protein. Proc Natl Acad Sci U S A **100:**1586-91.

68. **Rohmer, M.** 1999. The discovery of a mevalonate-independent pathway for isoprenoid biosynthesis in bacteria, algae and higher plants. Nat Prod Rep **16:**565-74.

69. **Rohmer, M.** 1998. Isoprenoid biosynthesis via the mevalonate-independent route, a novel target for antibacterial drugs? Prog Drug Res **50:**135-54.

70. **Rohmer, M., M. Knani, P. Simonin, B. Sutter, and H. Sahm.** 1993. Isoprenoid biosynthesis in bacteria: a novel pathway for the early steps leading to isopentenyl diphosphate. Biochem J **295 (Pt 2):**517-24.

71. **Schwender, J., M. Seemann, H. K. Lichtenthaler, and M. Rohmer.** 1996. Biosynthesis of isoprenoids (carotenoids, sterols, prenyl side-chains of chlorophylls and plastoquinone) via a novel pyruvate/glyceraldehyde 3-phosphate non-mevalonate pathway in the green alga *Scenedesmus obliquus*. Biochem J **316 (Pt 1):**73-80.

72. **Seemann, M., B. T. Bui, M. Wolff, D. Tritsch, N. Campos, A. Boronat, A. Marquet, and M. Rohmer.** 2002. Isoprenoid biosynthesis through the methylerythritol phosphate pathway: the (E)-4-hydroxy-3-methylbut-2-enyl diphosphate synthase (GcpE) is a [4Fe-4S] protein. Angew Chem Int Ed Engl **41:**4337-9.

73. **Shigi, Y.** 1989. Inhibition of bacterial isoprenoid synthesis by fosmidomycin, a phosphonic acid-containing antibiotic. J Antimicrob Chemother **24:**131-45.

74. **Sprenger, G. A., U. Schorken, T. Wiegert, S. Grolle, A. A. de Graaf, S. V. Taylor, T. P. Begley, S. Bringer-Meyer, and H. Sahm.** 1997. Identification of a thiamin-dependent synthase in *Escherichia coli* required for the formation of the 1-deoxy-D-xylulose 5-phosphate precursor to isoprenoids, thiamin, and pyridoxol. Proc Natl Acad Sci U S A **94:**12857-62.

75. **Steinbacher, S., J. Kaiser, W. Eisenreich, R. Huber, A. Bacher, and F. Rohdich.** 2003. Structural basis of fosmidomycin action revealed by the complex with 2-C-methyl-D-erythritol 4-phosphate synthase (IspC). Implications for the catalytic mechanism and anti-malaria drug development. J Biol Chem **278:**18401-7.

76. **Steinbacher, S., J. Kaiser, S. Gerhardt, W. Eisenreich, R. Huber, A. Bacher, and F. Rohdich.** 2003. Crystal structure of the type II isopentenyl diphosphate:dimethylallyl diphosphate isomerase from *Bacillus subtilis*. J Mol Biol **329:**973-82.

77. **Steinbacher, S., J. Kaiser, J. Wungsintaweekul, S. Hecht, W. Eisenreich, S. Gerhardt, A. Bacher, and F. Rohdich.** 2002. Structure of 2C-methyl-d-

erythritol-2,4-cyclodiphosphate synthase involved in mevalonate-independent biosynthesis of isoprenoids. J Mol Biol **316:**79-88.

78. **Takagi, M., T. Kuzuyama, S. Takahashi, and H. Seto.** 2000. A gene cluster for the mevalonate pathway from *Streptomyces* sp. Strain CL190. J Bacteriol **182:**4153-7.

79. **Takahashi, S., T. Kuzuyama, and H. Seto.** 1999. Purification, characterization, and cloning of a eubacterial 3-hydroxy-3-methylglutaryl coenzyme A reductase, a key enzyme involved in biosynthesis of terpenoids. J Bacteriol **181:**1256-63.

80. **Takahashi, S., T. Kuzuyama, H. Watanabe, and H. Seto.** 1998. A 1-deoxy-D-xylulose 5-phosphate reductoisomerase catalyzing the formation of 2-C-methyl-D-erythritol 4-phosphate in an alternative nonmevalonate pathway for terpenoid biosynthesis. Proc Natl Acad Sci U S A **95:**9879-84.

81. **Thorell, S., M. Schurmann, G. A. Sprenger, and G. Schneider.** 2002. Crystal structure of decameric fructose-6-phosphate aldolase from *Escherichia coli* reveals inter-subunit helix swapping as a structural basis for assembly differences in the transaldolase family. J Mol Biol **319:**161-71.

82. **Toth, M. J., and L. Huwyler.** 1996. Molecular cloning and expression of the cDNAs encoding human and yeast mevalonate pyrophosphate decarboxylase. J Biol Chem **271:**7895-8.

83. **Voynova, N. E., S. E. Rios, and H. M. Miziorko.** 2004. *Staphylococcus aureus* mevalonate kinase: isolation and characterization of an enzyme of the isoprenoid biosynthetic pathway. J Bacteriol **186:**61-7.

84. **Wada, T., T. Kuzuyama, S. Satoh, S. Kuramitsu, S. Yokoyama, S. Unzai, J. R. Tame, and S. Y. Park.** 2003. Crystal structure of 4-(cytidine 5'-diphospho)-2-C-methyl-D-erythritol kinase, an enzyme in the non-mevalonate pathway of isoprenoid synthesis. J Biol Chem **278:**30022-7.

85. **Walter, M. H., J. Hans, and D. Strack.** 2002. Two distantly related genes encoding 1-deoxy-d-xylulose 5-phosphate synthases: differential regulation in shoots and apocarotenoid-accumulating mycorrhizal roots. Plant J **31:**243-54.

86. **White, R. H.** 1978. Stable isotope studies on the biosynthesis of the thiazole moiety of thiamin in *Escherichia coli*. Biochemistry **17:**3833-40.

87. **Wilding, E. I., D. Y. Kim, A. P. Bryant, M. N. Gwynn, R. D. Lunsford, D. McDevitt, J. E. Myers, Jr., M. Rosenberg, D. Sylvester, C. V. Stauffacher, and V. W. Rodwell.** 2000. Essentiality, expression, and characterization of the class II 3-hydroxy-3-methylglutaryl coenzyme A reductase of *Staphylococcus aureus*. J Bacteriol **182:**5147-52.

88. **Wolff, M., M. Seemann, B. Tse Sum Bui, Y. Frapart, D. Tritsch, A. Garcia Estrabot, M. Rodriguez-Concepcion, A. Boronat, A. Marquet, and M. Rohmer.** 2003. Isoprenoid biosynthesis via the methylerythritol phosphate pathway: the (E)-4-hydroxy-3-methylbut-2-enyl diphosphate reductase (LytB/IspH) from *Escherichia coli* is a [4Fe-4S] protein. FEBS Lett **541:**115-20.

89. **Yajima, S., T. Nonaka, T. Kuzuyama, H. Seto, and K. Ohsawa.** 2002. Crystal structure of 1-deoxy-D-xylulose 5-phosphate reductoisomerase complexed with cofactors: implications of a flexible loop movement upon substrate binding. J Biochem (Tokyo) **131:**313-7.

90. **Zhou, D., and R. H. White.** 1991. Early steps of isoprenoid biosynthesis in *Escherichia coli.* Biochem J **273 (Pt 3):**627-34.

Chapter I–3.

Characterization of the *Mycobacterium tuberculosis* 4–(cytidine 5'–diphosphate)–2–C–methyl–D–erythritol synthase: Potential for drug development

Parts of the results in this chapter have been published in the Journal of Bacteriology (12)

I.3.A. Introduction

Isoprenoid synthesis is being studied with the goal of identifying new drug targets for anti–bacterial drugs. In *M. tuberculosis*, isoprenoids play diverse essential roles. For example, polyprenyl phosphate (Pol–P) acts as a carrier of activated sugar in the biosynthesis of the arabinan portion of AG, arabinomannan, and LAM (40), the "linker unit" of mycobacterial AG (21), and lipid I and lipid II, which are fundamental to peptidoglycan synthesis (19). In addition, the prenylated side–chain of menaquinones, the only lipoquinones in the electron transport chain in *M. tuberculosis* is derived from a polyprenyl diphosphate molecule (31, 34). Recent reports have shown that NADH type II dehydrogenase and F_1F_0–ATP synthase are effective drug targets in drug resistant *M. tuberculosis* (1, 39). In addition, it has been shown that the bactericidal effect of PZA is due to interference in maintenance of mycobacterial transmembrane proton gradient, resulting in depletion of energy (42). Therefore, it is reasonable to predict that the enzymes involved in isoprenoid biosynthesis will also provide new and valid drug targets, a hypothesis supported by the fact that disruption of any step in the MEP pathway is lethal for *E. coli* (14, 36).

Although structurally and functionally complex, all isoprenoids of eubacteria are generated from two simple five–carbon precursors, IPP and its isomer, DMAPP (4, 28). Until recently, these precursors were thought to be synthesized exclusively through the MVA pathway (10), as is seen in animals. However, intensive work with *E. coli* revealed the existence of an alternative means of synthesis, the MEP pathway (3, 13, 16, 18, 29). It is now accepted that the MEP pathway is the only source of IPP and DMAPP in many

eubacteria including *M. tuberculosis*. In this pathway, IPP and DMAPP are produced by a series of catalytic reactions starting with condensation of GAP and pyruvate (Fig.I.2.2, Fig.I.3.1). The first two enzymes of this pathway in *M. tuberculosis*, DXS and IspC from *M. tuberculosis* have previously been characterized (2, 5, 11). The product of IspC is MEP, which provides the substrate for the subject of this chapter, CDP–ME synthase (IspD). In this step, IspD catalyzes transfer of the CMP moiety of CTP to MEP producing CDP–ME, with the corresponding release of inorganic pyrophosphate (Fig.I.3.1). We now report the identification, cloning, characterization and essentiality of this enzyme in *M. tuberculosis*. Furthermore, we developed the new spectrophotometry based assays and validated it by determining Z'–Factor value to apply high throughput screening (HTS) assay for finding IspD specific inhibitors.

I.3.B. Materials and Methods

Materials. $H_{37}Rv$ genomic DNA was provided through NIH/NIAID Contract N01–AI–75320, "Tuberculosis Research Material and Vaccine Testing" at Colorado State University. All PCR reagents and cloning materials were purchased from Qiagen (Valencia, CA). [γ–^{32}P]CTP (25 Ci/mmol) was purchased from ICN (Costa Mesa, CA) or enzymatically synthesized as previously described (9). An EnzChek® Phosphate Assay Kit was purchased from Invitrogen (Eugene, OR). MEP was purchased from Echelon Research Laboratories, Inc. (Salt Lake City, UT). All other chemicals used were at least analytical grade and were obtained from Sigma Aldrich (St. Louis, MO).

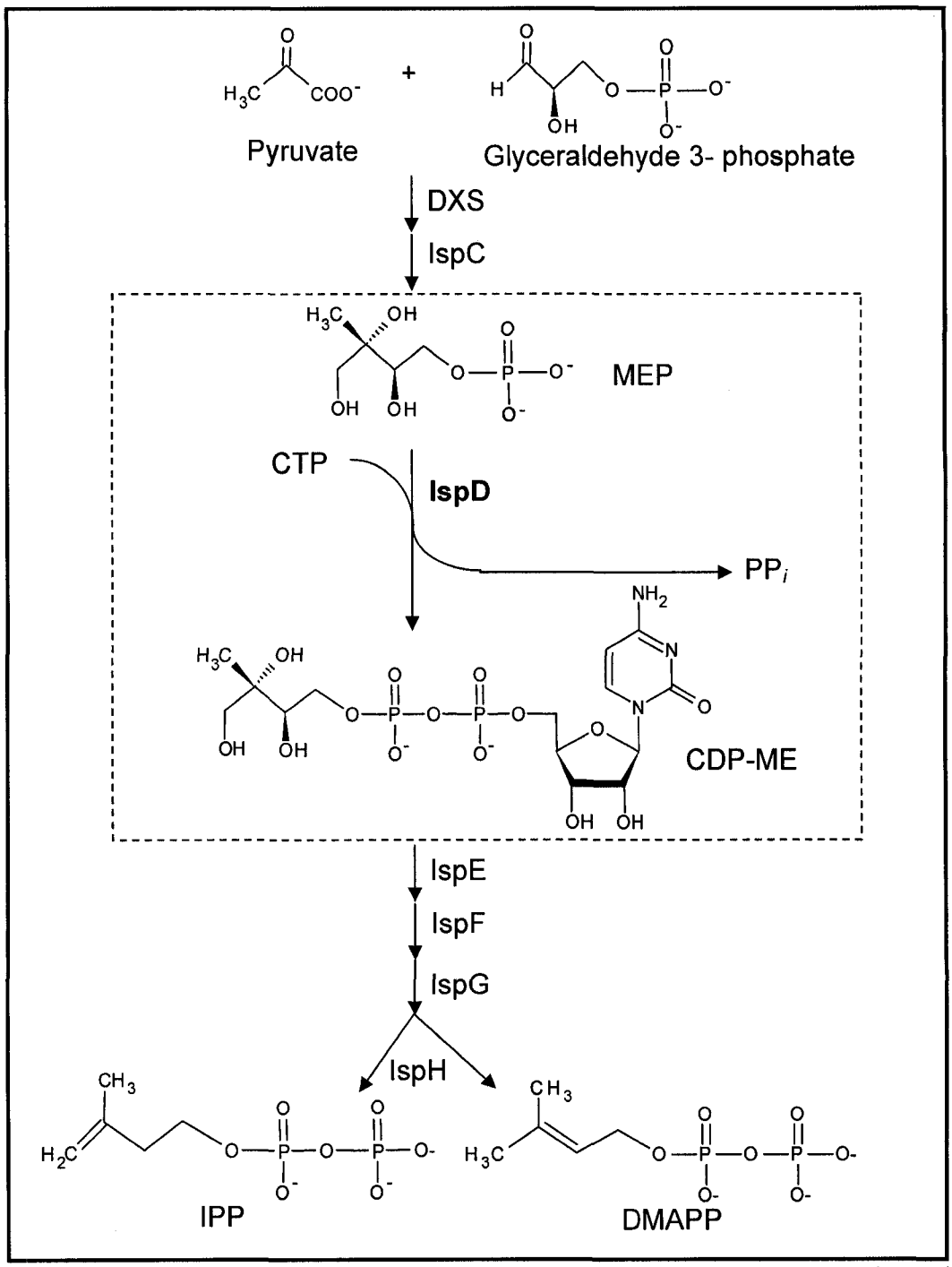

FIGURE I.3.1. **The methylerythritol phosphate pathway and the IspD reaction.** The reaction catalyzed by CDP–ME synthase (IspD), is highlighted. In *M. tuberculosis*, IPP and DMAPP are synthesized through the activities of a cascade of enzymes: DXS and IspC through IspH.

PCR amplification and cloning of *Rv3582c* from *M. tuberculosis.* *Rv3582c* was amplified using the oligonucleotide primers designed from the sequences available in Tuberculist (http://genolist.pasteur.fr/TubercuList/). The oligonucleotides used were IspDFor and IspDRev containing *Nde*I and *Xho*I restriction enzyme sites, respectively (Table I.3.1). The PCR products were digested with *Nde*I and *Xho*I, and ligated into the pET28a(+) vector (EMD Biosciences, Inc., San Diego, CA) that had been digested with the same enzymes and subsequently purified. Ligation mixtures were used to transform *E. coli* DH5α cells (Life Technologies, Rockville, MD) creating DH5α[pET28a(+)::*Rv3582c*], in which the target construct (pET28a(+)::*Rv3582c*) was propagated. The plasmid was isolated using Qiagen Plasmid Miniprep Kits and sequenced by Macromolecular Resources, Colorado State University.

Expression and purification of the recombinant Rv3582c. Recombinant Rv3582c was expressed and purified as previously described (5, 17). Briefly, transformation of BL21 (DE3) (Novagen, Madison, WI) with pET28a(+)::*Rv3582c* afforded the recombinant strain BL21(DE3)[pET28a(+)::*Rv3582c*]. Protein expression was induced in the presence of 0.5 mM isopropyl–β–D–thiogalactopyranoside (IPTG) at 20°C for 10 hours. The recombinant protein carrying a hexa–histidine tag was purified by immobilized metal affinity chromatography (IMAC) using a linear gradient of 50 to 200 mM imidazole in washing buffer [50 mM 4–morpholine propane sulfonic acid (MOPS) (pH 7.9), 1 mM $MgCl_2$, 10 % glycerol and 1 mM β–mercaptoethanol]. Eluted fractions were analyzed by SDS–PAGE and Western blot analysis with an anti–Histidine antibody (Sigma Aldrich) visualized with Coomassie Brilliant Blue 250R and alkaline phosphatase, respectively.

TABLE I.3.1. **PCR primers used in this study.** The sequences recognized by the restriction enzymes are underlined.

Primer name	Sequence	Enzyme
IspDFor	CATATGAGGGAAGCGGGCGAAGTAG	*Nde*I
IspDRev	CTCGAGTCACCCGCGGAGTATAGCTTG	*Xho*I
IspDNFor	AAGCTTAGCATCCCGCATGCGGGCAGT	*Hin*dIII
IspDNRev	GGATCCGAGAGTCTGCCCGTCGAGCTG	*Bam*HI
IspDCFor	GGATCCACCACCAAACTGGATCTGTTGC	*Bam*HI
IspDCRev	GGTACCGGCGATTTCGTTCTCATGATCCG	*Kpn*I
IspDint1	CTCCGACCTTGAAAATCATCT	
IspDint2	TACGACGTCGCGTTTATCC	
IspD/FCompPro	TTAATTAAGGCCGGCTGTTAGCATGGAGTAACG	*Pac*I
IspD/FCompRev	TTAATTAAGCCAGCTTACCTGCCCAATTGCTG	*Pac*I
IspD/FCompSh	TTAATTAAGACGCCAAAGCCGAGACCATCCTT	*Pac*I
IspD US Probe For	GACGAGAATCAATGAGACCT	
IspD US Probe Rev	AGTGATATCGGCTCGGTGAC	

Fractions containing recombinant Rv3582c estimated to be at least 95% pure by Coomassie staining of SDS–PAGE gels were pooled, desalted on a PD–10 column (Millipore, Bedford, MA), and stored at –70°C.

Preparation of cytosolic fractions from control and recombinant *E. coli* strain. Control and recombinant BL21(DE3) strains were grown in LB media without antibiotics or supplemented with 50 μg/ml of kanamycin, respectively. Bacilli were harvested, resuspended in lysis buffer [50 mM MOPS (pH 7.9), 10 mM $MgCl_2$, 5 mM β–mercaptoethanol] at 4°C, and disrupted by probe sonication with a Soniprep 150 (Integrated Services, TCP, Palisades Park, NJ) on ice. Homogenates were centrifuged at 27,000 × *g* for 30 minutes and the pellets were discarded. The supernatants were subsequently centrifuged at 100,000 × *g* in a Beckman 70.1 Ti rotor for 2 hours. The resulting cytosol was analyzed for expression of Rv3582c by Western blot analysis.

Radiochemical *in vitro* assay for IspD activity. IspD activity was monitored by [^{32}P]PP*i* release employing liquid scintillation spectrometry (Fig.I.3.2). Reaction mixtures contained 50 mM Tris–HCl (pH 7.9), 20 mM sodium fluoride, 10 mM $MgCl_2$, 1 mM DTT, 38.5 pmols of purified IspD enzyme, MEP and [γ–^{32}P]CTP (10 dpm/pmol at the indicated concentrations) in a final volume of 100 μl. Incubations were carried out at 37°C for 30 minutes. Reactions were terminated by adding 200 μl of a slurry of activated charcoal in 10 mM Tris–HCl buffer (pH 8.0). The slurry was then loaded into an empty spin column and centrifuged at 5,000 × *g* for 3 minutes to elute [^{32}P]PP*i*, residual [γ–^{32}P]CTP was retained on the charcoal.

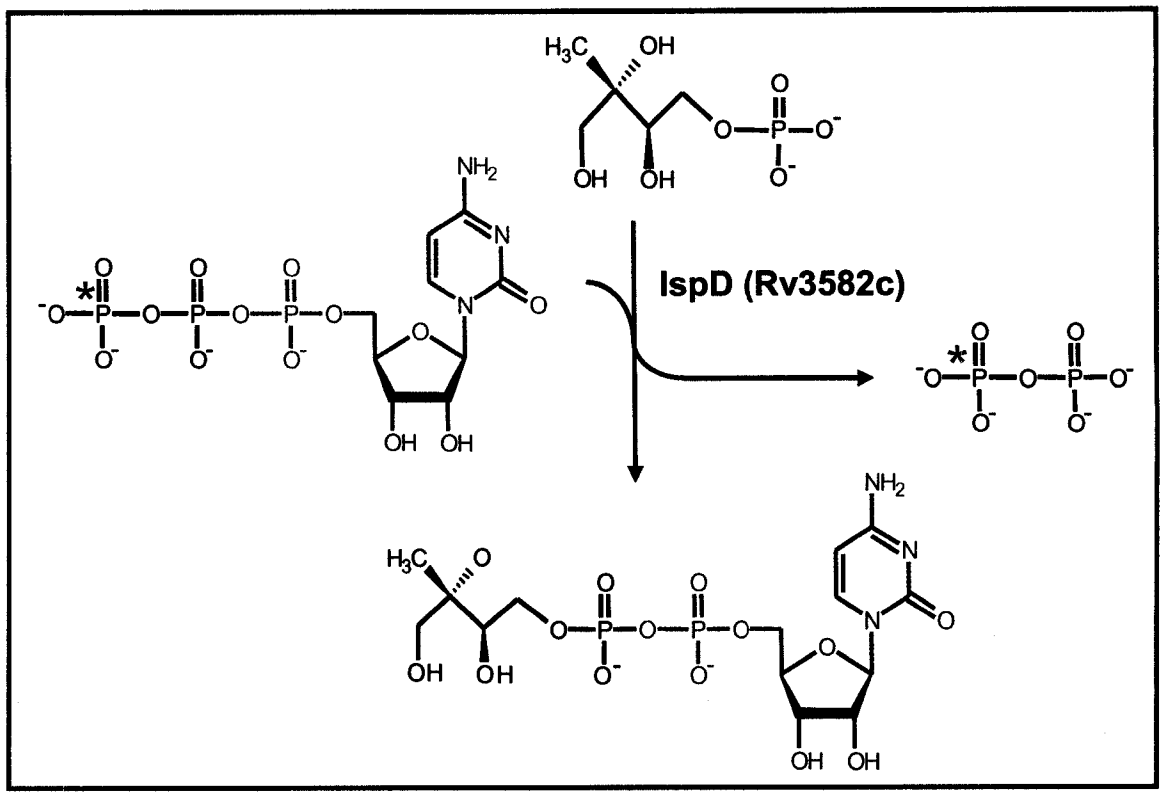

FIGURE I.3.2. **Schematic diagram of the radiochemical IspD assay.** [γ–^{32}P]CTP was used for the reaction. The released [^{32}P]PP*i* was measured using liquid scintillation spectrometry. The enzyme activity is proportional to the PP*i* release. The substrate in this reaction was 2–C–methyl–D–erythritol 4–phosphate and cytidine 5'–triphosphate and the product was 4–(cytidine 5'–diphosphate)–2–C–methyl–D–erythritol. Asterisks indicate the position of the radioisotope.

Spectrophotometry based *in vitro* assay for IspD activity. IspD activity was also monitored by coupling to the spectrophotometric reactions linked by released PP*i* using the commercially available EnzChek® Phosphate Assay Kit (Invitrogen) (Fig.I.3.3). Spectrophotometry based assays were performed according to the kit instructions except that the volumes were reduced to accommodate 96–well or 384–well microplates. Final assay mixtures contained 50 mM Tris–HCl (pH 7.4), 200 μM MESG, 1 mM DTT, 100 μM MEP, 100 μM CTP, 0.03 U inorganic pyrophosphatase, 1U purine nucleoside phosphorylase and 3.9 pmols of purified IspD enzyme in 96–well or 384–well microplates (Costar, Bethesda, MD). Reactions were incubated at room temperature for 30 minutes after which their endpoint absorbance at 360 nm was determined.

Determination of enzymatic properties of Rv3582c. To determine the optimal pH for enzyme activity, reaction mixtures at various pH values containing pH appropriate buffers (MES, MOPS, Tris, or TAPS) were used. Optimal concentrations for divalent cations were determined in assay mixtures containing $MgCl_2$, $MnCl_2$, $CaCl_2$ or $ZnCl_2$ at the indicated concentrations. The effect of CTP concentration on activity was determined using a constant concentration of MEP (100 μM) and varying concentrations of CTP. The effect of MEP concentration was determined using a constant concentration of CTP (100 μM) and varying concentrations of MEP. The K_m and V_{max} values of substrates for the enzyme were calculated by nonlinear regression analysis (SigmaPlot V.8.02A).

Determination of Rv3582c essentiality by gene switching analysis. The experiments

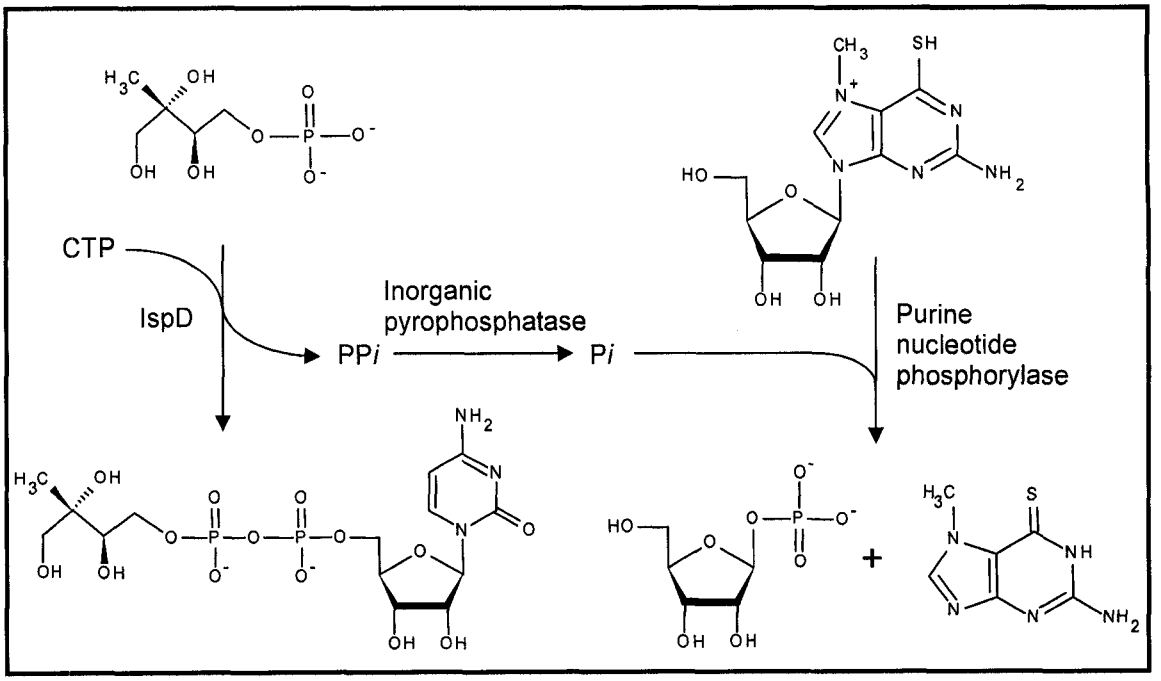

FIGURE I.3.3. **Spectrophotometry based assay for IspD activity**. The EnzChek® Phosphate Assay Kit includes inorganic pyrophosphatase, which catalyzes conversion of PP*i* into two equivalents of P*i*. The P*i* is consumed by the MESG/ purine nucleotide phosphorylase reaction and detected by an increase of the product (2–amino–6–mercapto–7–methyl purine) absorbance at 360 nm.

relating to the Rv3582c essentiality were performed by Dr. Tanya Parish's group at Queen Mary's School of Medicine and Dentistry in the United Kingdom. Previously published methods were employed to determine the essentiality of *Rv3582c* (22, 24, 35). Briefly, a deletion delivery vector was constructed. The primer pairs IspDNFor and IspDNRev, and IspDCFor and IspDCRev were used to amplify the regions either side of *Rv3582c* and introduce relevant restriction enzyme sites (Table.I.3.1). PCR products were cloned into pCR–Blunt II–TOPO (Invitrogen). The fragments were then cloned as *Hin*dIII–*Bam*HI and *Bam*HI–*Kpn*I fragments into p2NIL (24) and the marker gene from pGOAL19 was cloned into the *Pac*I site to generate the final delivery vector, where 537 bp of Rv3582c was deleted. Single cross–overs were generated by electroporation into *M. tuberculosis* and selection on 100 μg/ml hygromycin, 20 μg/ml kanamycin, and 50 μg/ml X–gal. A single colony was selected and streaked out in the absence of any antibiotics to allow the second cross–over to occur. Double crossovers were selected on 2 % w/v sucrose and 50 μg/ml X–gal; white colonies were patch tested for kanamycin and hygroymcin sensitivity to ensure that they had lost the plasmid by recombination. PCR was then used to determine whether the each double cross–over had the wild type or deletion allele. Primers used were IspDint1 and IspDint2 (Table.I.3.1), which amplify 2.0 kbp and 1.3 kbp fragments from the wild type and deletion alleles, respectively. Two merodiploid strains carrying an extra copy of Rv3582c were constructed as follows: the primer pairs IspD/FCompPro and IspD/FCompRev, and the primer pairs IspD/FCompSh and IspD/FCompRev were used to amplify Rv3582c and the regions to either side and to introduce *Pac*I sites (Table.I.3.1). PCR products were ligated into pCR–Blunt II–TOPO. The products were then cloned as *Pac*I fragments into the integrating vector pAPA3 to

generate pIspD–PRO and pIspD–SH, respectively. The integrity and direction of the construct were confirmed by DNA sequencing. Both vectors were electroporated into the single cross–over strain and recombinants isolated on 10 μg/ml gentamicin, 100 μg/ml hygromycin, 20 μg/ml kanamycin, and 50 μg/ml X–gal. The merodiploids were streaked out on the plates without any antibiotics and double cross–overs were isolated as described above, except that gentamicin was included at all stages. Deletion of the chromosomal copy of Rv3582c was confirmed by Southern blotting. To generate a probe for Southern analysis, the region upstream of the ispD was PCR–amplified using primers IspD US Probe For and IspD US Probe Rev (Table.I.3.1); the isolated fragment was labeled with AlkPhos Direct system (GE Healthcare). Genomic *M. tuberculosis* DNA (2 μg) was digested with *Bam*HI; the digestion products were separated on an agarose gel and transferred by vacuum blotter onto a Hybond N+ membrane (GE Healthcare). The membrane was hybridized for 16 hours in AlkPhos Direct hybridization buffer with blocking added (GE Healthcare) at 65°C with the labeled probe. Primary and secondary post hybridization washes were carried out (two primary washes for 10 minutes each at 55 °C and two secondary for 5 minutes each at room temperature, as per manufactures' instructions), and the probe detected by CDP–Star (GE Healthcare). The requirement of the integrated gene copy was established via gene switching, using pUC–Hyg–Int (20), as previously described (25).

Z'–Factor. The spectrophotometry based assays were employed as described above. The reaction volumes tested were 20 μl, 30 μl, 40 μl, and 50 μl to find the most suitable reaction volume for applying to high throughput screening assays. The Z'–Factor was

determined as described by Zhang and coworkers (41). For automation, all the steps in this assay were performed using an automated fluid transfer system in 384–well microplates (Precision XS microplate sample processor, BioTek instruments). The reaction numbers were fifty in both positive and negative samples.

Other procedures. The reactions were performed under conditions that were linear for both time (up to 30 minutes) and concentration (up to 192.5 pmols) of purified recombinant Rv3582c and all reported values are averages of triplicated assays. Protein concentrations were estimated using a bicinchoninic acid (BCA) protein assay kit (Pierce, Rockford, IL). Radioactive samples were analyzed using a Beckman (Fullerton, CA) LS6500 liquid scintillation spectrometer. BLAST searches were performed using the National Center for Biotechnology Information (NCBI) Web site and the Tuberculist website [http://bioweb.pasteur.fr/GenoList/TubercuList/]. Multiple alignments were performed using the Multalin interface (8).

I.3.C. Results

Identification and overexpression of *M. tuberculosis* IspD. Rv3582c from *M. tuberculosis* showed 31% identity with the amino acid sequence of *E. coli* IspD (Fig.I.3.4), suggesting an analogous function in *M. tuberculosis*. *Rv3582c* is 696 bp in length, encoding a polypeptide of 234 amino acids with a molecular weight of 26 kDa, and is predicted to be cytosolic. *Rv3582c* was amplified by PCR from the *M. tuberculosis* H_{37}Rv genome and cloned into the pET28a(+) vector for overexpression in *E. coli* [BL21

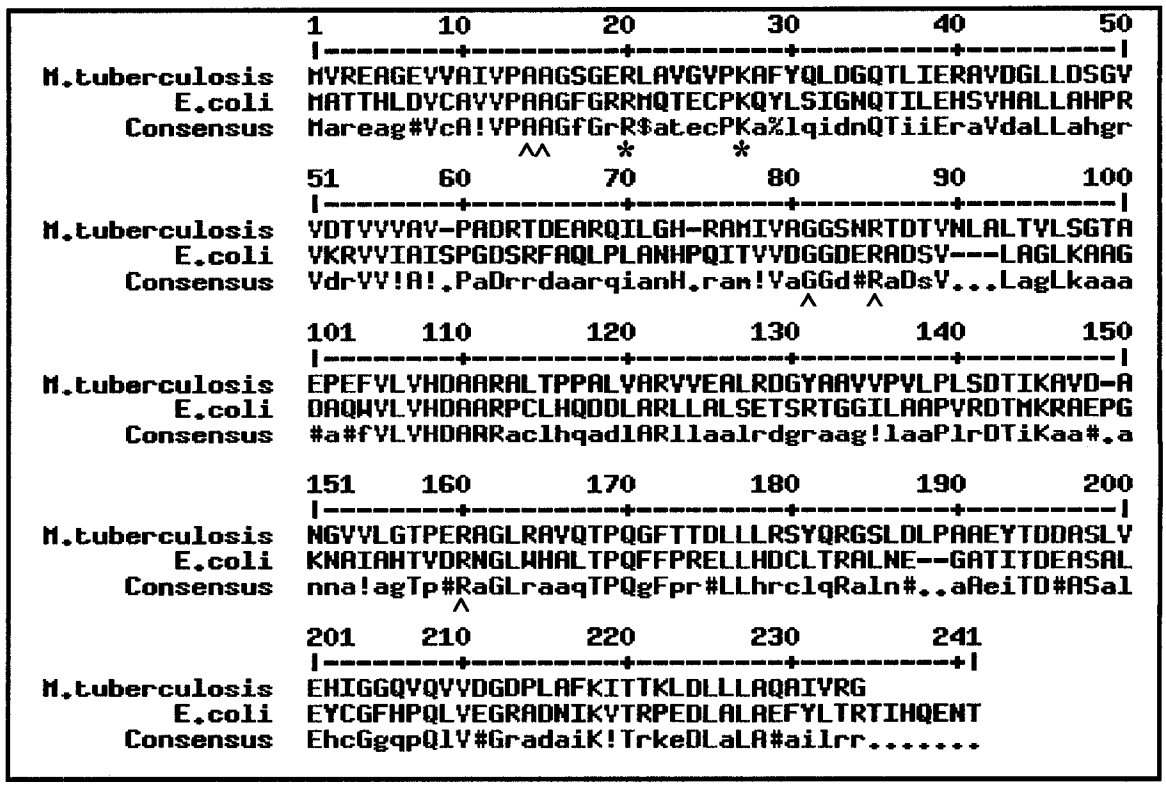

FIGURE I.3.4. **Alignment of the amino acid sequence of IspD from *E. coli* and the ortholog (Rv3582c) identified in the *M. tuberculosis* genome**. Identities are indicated in red and similarities are indicated in blue. The *E. coli* amino acids involved in CTP specificity are highlighted with (*) and the essential amino acids for catalytic function are highlighted with (^) (26).

(DE3)]. The cytosolic fractions from the control and recombinant BL21(DE3) strains were tested for IspD activity. The specific activity of the cytosol from the recombinant strain was about 1.5 fold higher than that of the control strain (Fig.I.3.5), indicating that *Rv3582*c encodes functional IspD in *M. tuberculosis*. Overexpression of the predicted 26 kDa polypeptide was confirmed by Western blot analysis using an anti–His antibody

Determination of *M. tuberculosis* Rv3582c essentiality. All attempts to generate an *Rv3582c* deletion mutant in the wild–type background failed. Forty double cross–over strains were tested and all were wild–type. Two different merodiploid strains were used to demonstrate that *Rv3582c* was essential; the pIspD–SH strain carried the *Rv3582c* gene expressed from the Ag85A promoter and the pIspD–PRO strain carried a larger DNA fragment containing not only the *Rv3582c* gene but also the surrounding genes predicted to be in the same operon, including the probable native promoter. Using this method, double cross–over strains of both wild–type and deletion alleles were isolated for both merodiploid strains. Three out of eight mutant double cross–over strains for the strain carrying pIspD–SH and seven out of thirty two for the strain carrying pIspD–PRO were isolated ($p=0.003$ and $p= 0.002$ respectively). One of each strain was selected for further study (named AS1 and AS2 respectively). A previously described "gene switching" method (25) was employed to show that the integrated wild–type allele cannot be removed when it is the only functional copy present in the cell. The integrated vector could be efficiently replaced by an alternative version after transformation and used to confirm essentiality with other *M. tuberculosis* genes (23). Replacement of the integrated vectors (gentamicin resistance) in strains AS1 and AS2 with an "empty" vector (pUC–

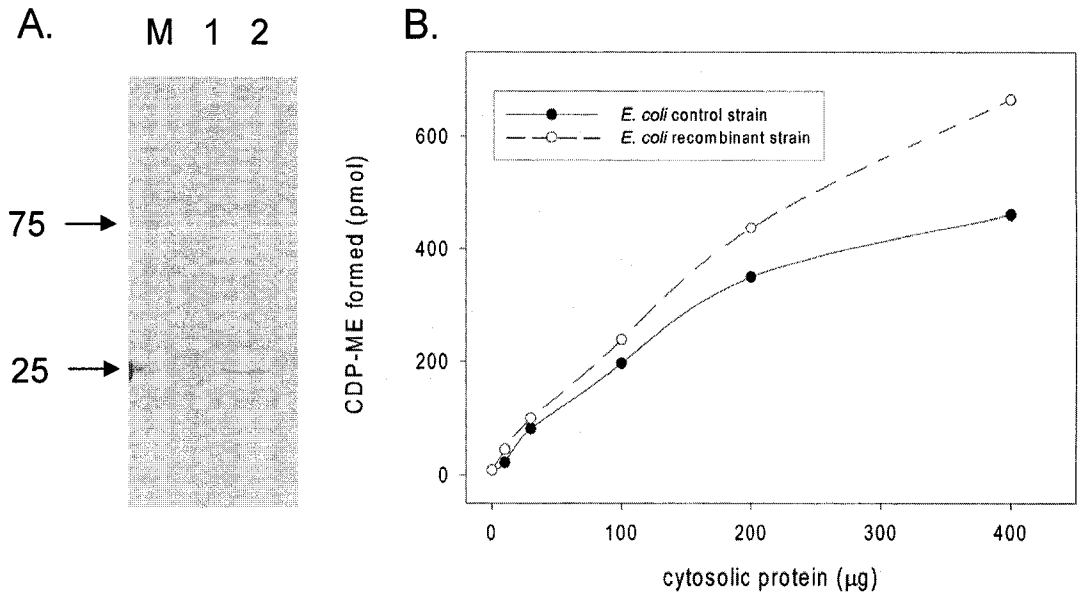

FIGURE I.3.5. **The effect of overexpression of *Rv3582c* on IspD activity**. A. Confirmation of Rv3582c expression on *E. coli* control strain with Western blot analysis with anti–His antibody. B. IspD activity in cytosol isolated from *E. coli* transformed with pET28a(+)::Rv3582c (open circles) or empty vector (closed circles).

Hyg–Int) which did not have the *Rv3582c* gene but carried an alternative marker gene (hygomycin resistance) was attempted. In both cases, no viable colonies could be obtained with hygromycin resistance after electroporation, indicating that the cells cannot survive without a functional copy of *Rv3582c*. The PCR primers IspDint1 and IspDint2 were used to verify the presence of the wild–type (2.0 kb) or deletion (1.3 kb) allele of *ispD* from genomic DNA (Fig.I.3.6).

***In vitro* reaction requirements for Rv3582c.** Recombinant Rv3582c was purified by immobilized nickel affinity chromatography (Fig.I.3.7). The reaction catalyzed by purified recombinant Rv3582c was tested for optimal pH, divalent cation specificity, and nucleotide 5–triphosphate (NTP) specificity. The enzyme was active over a broad pH range (pH 6.0 – pH 9.0), with optimal activity at pH 8.0 (Fig.I.3.8A) and showed an absolute dependence on divalent cations (Fig.I.3.8B). The activity was optimal in the presence of 20 mM Mg^{2+}. Mn^{2+} also supported the activity at a comparable level. Zn^{2+} also supported activity up to a concentration of 2.5 mM. Ca^{2+} was relatively ineffective at supporting catalytic activity at all concentrations tested (Fig.I.3.8B). The addition of 10 mM EDTA to the reaction mixture completely abolished the activity. The enzyme is specific for CTP was absolute as other NTPs were poor substrates [less than 6% of the activity seen with CTP under optimal conditions (data not shown)].

Kinetic characterization of Rv3582c. Purified IspD enzyme activity was linear with increasing protein concentration up to a concentration of 192.5 pmols, reactions were also linear with time up to 30 min. The effects of MEP or CTP concentrations on reaction

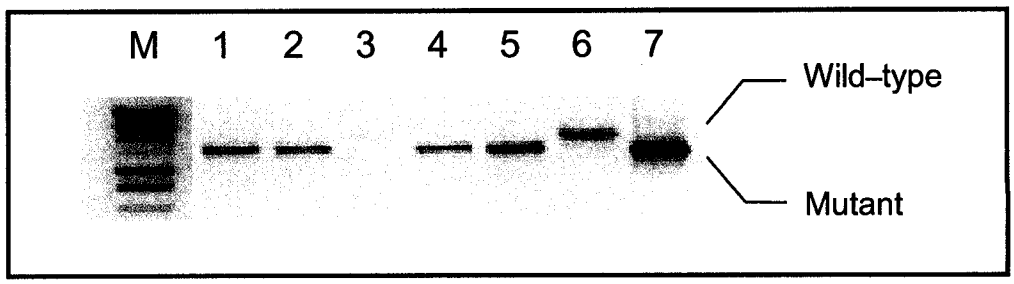

FIGURE I.3.6. **PCR analysis of the gene switching experiment for determining *ispD* essentiality for *M. tuberculosis* H_{37}Rv survival.** The PCR primers IspDint1 and IspDint2 were used to determine *ispD* identity. Lane M: Lamdba *Hin*dIII marker, Lanes 1–5, Double cross–over strains, Lane 6, wild–type genomic control, Lane 7, delivery vector control. Lanes 1–2, 4–5 show the product expected for a mutant strain and lane 3 shows the product expected for a wild–type strain.

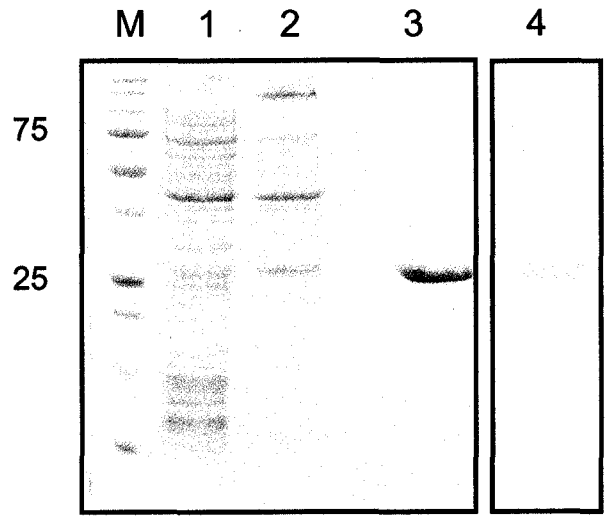

FIGURE I.3.7. **SDS–PAGE analysis of expression and purification of histidine tagged IspD.** Proteins were visualized by Coommassie brilliant blue 250R and Western blot hybridization by alkaline phosphatase. *M. tuberculosis IspD* was cloned into pET28a(+) and transformed into the *E. coli* BL21(DE3) for expression of the hexa histidine IspD fusion protein. Lane 1, transformed BL21(DE3) cell lysates prior to IPTG treatment. Lane 2, transformed BL21(DE3) cell lysates after IPTG treatment. Lane 3, purified hexa–histidine IspD elute fraction from an Immobilized Metal Affinity Chromatography (IMAC) column. Lane 4, Western blot hybridization of purified IspD using an anti–Histidine antibody. M: Molecular weight standards.

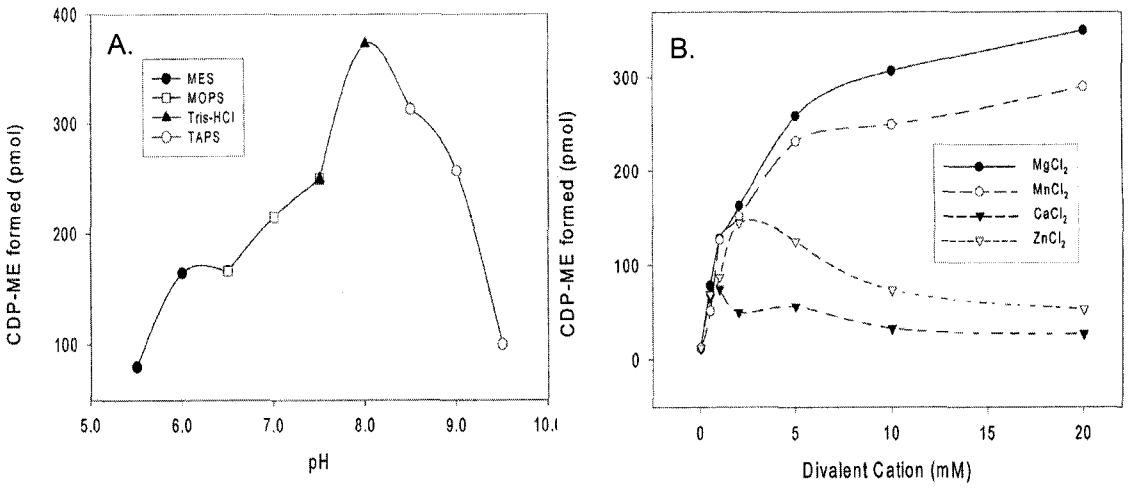

FIGURE I.3.8. **The effect of pH and divalent cation concentration on *M. tuberculosis* IspD catalytic activity**. A. The optimal pH for catalytic activity was determined using MES (pH 5.5 – pH 6.5), MOPS (pH 6.5 – pH 7.5), Tris–HCl (pH 7.5 – pH 8.5), and TAPS (pH 8.5 – pH 9.5). B. Divalent cations (Mg^{2+}, Mn^{2+}, Zn^{2+}, or Ca^{2+}) were added to the reaction mixtures at the indicated concentrations. Reaction mixtures were described in Materials and Methods.

rates were determined by varying the concentration of one substrate while keeping the other fixed (Fig.I.3.9). The K_m^{MEP} and K_m^{CTP} were calculated to be 58.5 μM and 53.2 μM, respectively (Table.I.3.2).

Determination of Z′–Factor values. For the spectrophotometry based assays to be useful in a high throughput screening assay, it must be reliable in a small–well format. Assay optimization and validation require the determination of the Z′–Factor value, a dimensionless statistical characteristic used to assess the quality of data generated in a potential high throughput screening assay (41). The Z′–Factor values for the current assay were calculated based on the negative control (without purified Rv3582c) and positive control (with purified Rv3582c) in 384–well microplates using the equation:

$$\text{Z′–Factor value} = 1 - \frac{(3\sigma_{\text{positive}} - 3\sigma_{\text{negative}})}{|\mu_{\text{positive}} - \mu_{\text{negative}}|}$$

where σ represents the standard deviation and μ is the mean of each set of data points. Z′–Factor value is a commonly used measure of assay performance and reliability that takes into account both the assay signal dynamic range (signal–to–background ratio) and variation (signal–to–noise ratio) associated with the measured signals. A perfect assay would have a Z′–Factor value of 1, while an excellent assay would score between 0.5 and 1. Using four different reaction volumes (20 μl, 30 μl, 40 μl, and 50 μl), Z′–Factor values ranging between 0.75 and 0.93 were obtained, indicating excellent assay reliability (Table.I.3.3).

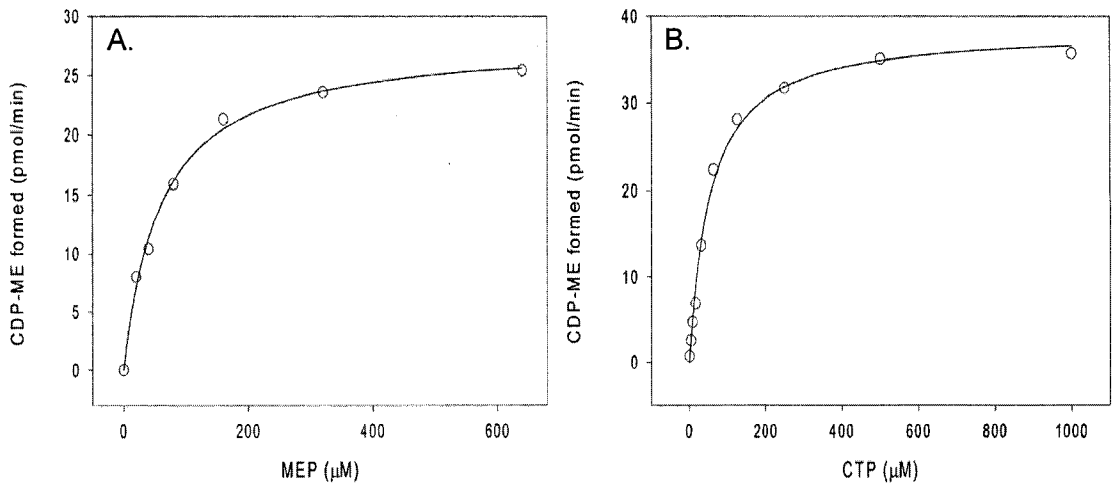

FIGURE I.3.9. **The effect of MEP and CTP concentrations on *M. tuberculosis* IspD catalytic activity**. A. To determine the effect of MEP concentration, CTP concentration was held at 100 μM and the concentration of MEP was varied as indicated. B. To determine the effect of CTP concentration, MEP concentration was held at 100 μM and the concentration of CTP was varied as indicated. Reaction mixtures were as described in Materials and Methods.

TABLE I.3.2. **Calculated kinetic parameters for *M. tuberculosis* IspD.**

Reaction/ Substrate	Calculated parameter			
	K_m (μM)	V_{max} (pmol/min)	K_{cat} (min^{-1})	K_{cat}/K_m ($mM^{-1}min^{-1}$)
MEP	58.5	27.9	0.7	12.3
CTP	53.2	38.5	1.0	1.9

Each reaction contained 38.5 pmols of *M. tuberculosis* IspD. The K_m and V_{max} values were calculated from the experiments shown in Fig.I.3.9 using non–linear regression analysis (SigmaPlot V. 8.02A)

TABLE I.3.3. **Z'–Factor values for the spectrophotometry based assay.**

Reaction volume		20 µl	30 µl	40 µl	50 µl
Sample Number	Positive	50	50	50	50
	Negative	50	50	50	50
Z' –Factor		0.75 ± 0.02	0.92 ± 0.01	0.91 ± 0.01	0.93 ± 0.01

The assays were performed in 384 well microplates using an automated precision XS fluid transfer system.

I.3.D. Discussion

The enzyme encoded by *Rv3582c* is clearly a functional CDP–ME synthase. The inability to isolate a non–functional mutant using the two step disrupting strategy indicates that *Rv3582c* is essential for *M. tuberculosis* survival, *in vivo*. These results are consistent with Himar1–based transposon mutagenesis experiments performed by Sassetti *et al.* (32). The essentiality of the IspD enzyme for the growth of other bacteria has also been reported (7, 14, 33). *M. tuberculosis* IspD was active over a broad pH range as was previously reported for the *E. coli* enzyme (27). Addition of EDTA or BioRex 70 to reaction mixtures showed that divalent cations are absolutely required for its cytidylyltransferase activity (data not shown). A concentration of 20 mM Mg^{2+} supported optimal activity; however, Zn^{2+} could also support the *M. tuberculosis* IspD activity at low concentrations. Interestingly, *E. coli* IspD catalytic activity could not be supported by Zn^{2+} at all (30). In *E. coli* IspD, Mg^{2+} forms coordinate bonds with the three phosphate moieties of CTP and the α–phosphate oxygen of CDP–ME, as was shown for the glycerol 3–phosphate cytidyltransferase of *Bacillus subtilis* (26, 38), and it is assumed that the divalent cations play a similar role in IspD from *M. tuberculosis*. Not surprisingly, *M. tuberculosis* IspD showed a high degree of specificity for CTP. This specificity is likely achieved from the pyrimidine base forming hydrogen bonds to the backbone amides of conserved amino acids and the cytosine moiety for stacking interactions inside the catalytic domain (26, 27). In fact, mutation of these conserved amino acids abolished or reduced catalytic activity in *E. coli* IspD (27). The K_m^{MEP} for the *M. tuberculosis* IspD is significantly higher than the value reported for the *E. coli* enzyme as determined by [^{13}C]

NMR spectrometry; however, the K_m^{CTP} values are similar (27, 30). The specificity constants (K_{cat}/K_m) of the *M. tuberculosis* IspD for the both substrates were lower than that determined for the *E. coli* enzyme (27), suggesting that the IspD of *M. tuberculosis* is less efficient.

To achieve minimal toxicity for clinical trials, any potential drug therapy for TB should ideally target factors absent in the host but essential for bacilli survival. In humans, the MVA pathway is exclusively employed for the IPP biosynthesis and no ortholog of *M. tuberculosis* IspD exists. Furthermore, isoprenoid compounds have crucial roles in cell wall biosynthesis and energy production in *M. tuberculosis*. Recent data suggested that the F_1F_0 ATP synthase is required for mycobacterial growth, suggesting that ATP generation from substrate level phosphorylation is insufficient for survival (37). Thus, inhibition of menaquinone synthesis, which ultimately would be achieved by inhibition of IspD enzyme, may well be lethal to *M. tuberculosis* in non–replicating persistence, a state of thought to be prevalent in latent infections with *M. tuberculosis* (6).

The characterization of IspD orthologs of other organisms was previously done using [^{1}H] or [^{13}C] NMR spectroscopy (15, 29, 30) or TLC based assays (26, 27) which are complicated, require expensive equipment or tedious. In the present study, the PP*i* released during the reaction catalyzed by IspD was utilized to monitor the *M. tuberculosis* IspD activity. This assay is facile, direct, and relatively inexpensive. Moreover, another non–radioactive enzyme assay, the spectrophotometry based assay, was developed and validated as a HTS assay. The validation determined by *Z'*–factor values indicated that three different reaction volumes (30 µl, 40 µl, and 50 µl) of the spectrophotometry based assay can be applied to screen *M. tuberculosis* IspD specific inhibitors (Table I.3.3).

Therefore, the 30 μl reaction volume will be chosen for 384–well microplate format to screen inhibitors. The results in this chapter facilitate high throughput screening for finding novel inhibitors of IspD.

I.3.E. References

1. **Andries, K., P. Verhasselt, J. Guillemont, H. W. Gohlmann, J. M. Neefs, H. Winkler, J. Van Gestel, P. Timmerman, M. Zhu, E. Lee, P. Williams, D. de Chaffoy, E. Huitric, S. Hoffner, E. Cambau, C. Truffot-Pernot, N. Lounis, and V. Jarlier.** 2005. A diarylquinoline drug active on the ATP synthase of *Mycobacterium tuberculosis*. Science **307:**223-7.
2. **Argyrou, A., and J. S. Blanchard.** 2004. Kinetic and chemical mechanism of *Mycobacterium tuberculosis* 1-deoxy-D-xylulose-5-phosphate isomeroreductase. Biochemistry **43:**4375-84.
3. **Arigoni, D., S. Sagner, C. Latzel, W. Eisenreich, A. Bacher, and M. H. Zenk.** 1997. Terpenoid biosynthesis from 1-deoxy-D-xylulose in higher plants by intramolecular skeletal rearrangement. Proc Natl Acad Sci U S A **94:**10600-5.
4. **Bach, T. J.** 1995. Some new aspects of isoprenoid biosynthesis in plants--a review. Lipids **30:**191-202.
5. **Bailey, A. M., S. Mahapatra, P. J. Brennan, and D. C. Crick.** 2002. Identification, cloning, purification, and enzymatic characterization of *Mycobacterium tuberculosis* 1-deoxy-D-xylulose 5-phosphate synthase. Glycobiology **12:**813-20.
6. **Cho, S. H., D. Goodlett, and S. Franzblau.** 2006. ICAT-based comparative proteomic analysis of non-replicating persistent *Mycobacterium tuberculosis*. Tuberculosis (Edinb) **86:**445-60.
7. **Cornish, R. M., J. R. Roth, and C. D. Poulter.** 2006. Lethal mutations in the isoprenoid pathway of *Salmonella enterica*. J Bacteriol **188:**1444-50.

8. **Corpet, F.** 1988. Multiple sequence alignment with hierarchical clustering. Nucleic Acids Res **16:**10881-90.

9. **Crick, D. C., J. R. Scocca, J. S. Rush, D. W. Frank, S. S. Krag, and C. J. Waechter.** 1994. Induction of dolichyl-saccharide intermediate biosynthesis corresponds to increased long chain cis-isoprenyltransferase activity during the mitogenic response in mouse B cells. J Biol Chem **269:**10559-65.

10. **Dhe-Paganon, S., J. Magrath, and R. H. Abeles.** 1994. Mechanism of mevalonate pyrophosphate decarboxylase: evidence for a carbocationic transition state. Biochemistry **33:**13355-62.

11. **Dhiman, R. K., M. L. Schaeffer, A. M. Bailey, C. A. Testa, H. Scherman, and D. C. Crick.** 2005. 1-Deoxy-D-xylulose 5-phosphate reductoisomerase (IspC) from *Mycobacterium tuberculosis*: towards understanding mycobacterial resistance to fosmidomycin. J Bacteriol **187:**8395-402.

12. **Eoh, H., A. C. Brown, L. Buetow, W. N. Hunter, T. Parish, D. Kaur, P. J. Brennan, and D. C. Crick.** 2007. Characterization of the *Mycobacterium tuberculosis* 4 diphosphocytidyl 2 C methyl D erythritol synthase: Potential for Drug Development. J Bacteriol.

13. **Flesch, G., and M. Rohmer.** 1988. Prokaryotic hopanoids: the biosynthesis of the bacteriohopane skeleton. Formation of isoprenic units from two distinct acetate pools and a novel type of carbon/carbon linkage between a triterpene and D-ribose. Eur J Biochem **175:**405-11.

14. **Freiberg, C., B. Wieland, F. Spaltmann, K. Ehlert, H. Brotz, and H. Labischinski.** 2001. Identification of novel essential *Escherichia coli* genes conserved among pathogenic bacteria. J Mol Microbiol Biotechnol **3:**483-9.

15. **Gabrielsen, M., F. Rohdich, W. Eisenreich, T. Grawert, S. Hecht, A. Bacher, and W. N. Hunter.** 2004. Biosynthesis of isoprenoids: a bifunctional IspDF enzyme from *Campylobacter jejuni*. Eur J Biochem **271:**3028-35.

16. **Horbach, S., H. Sahm, and R. Welle.** 1993. Isoprenoid biosynthesis in bacteria: two different pathways? FEMS Microbiol Lett **111:**135-40.

17. **Kaur, D., P. J. Brennan, and D. C. Crick.** 2004. Decaprenyl diphosphate synthesis in *Mycobacterium tuberculosis*. J Bacteriol **186:**7564-70.

18. **Lois, L. M., N. Campos, S. R. Putra, K. Danielsen, M. Rohmer, and A. Boronat.** 1998. Cloning and characterization of a gene from *Escherichia coli* encoding a transketolase-like enzyme that catalyzes the synthesis of D-1-deoxyxylulose 5-phosphate, a common precursor for isoprenoid, thiamin, and pyridoxol biosynthesis. Proc Natl Acad Sci U S A **95:**2105-10.

19. **Mahapatra, S., T. Yagi, J. T. Belisle, B. J. Espinosa, P. J. Hill, M. R. McNeil, P. J. Brennan, and D. C. Crick.** 2005. Mycobacterial lipid II is composed of a complex mixture of modified muramyl and peptide moieties linked to decaprenyl phosphate. J Bacteriol **187:**2747-57.

20. **Mahenthiralingam, E., B. I. Marklund, L. A. Brooks, D. A. Smith, G. J. Bancroft, and R. W. Stokes.** 1998. Site-directed mutagenesis of the 19-kilodalton lipoprotein antigen reveals No essential role for the protein in the growth and virulence of *Mycobacterium intracellulare*. Infect Immun **66:**3626-34.

21. **Mikusova, K., M. Mikus, G. S. Besra, I. Hancock, and P. J. Brennan.** 1996. Biosynthesis of the linkage region of the mycobacterial cell wall. J Biol Chem **271:**7820-8.

22. **Parish, T., J. Lewis, and N. G. Stoker.** 2001. Use of the mycobacteriophage L5 excisionase in *Mycobacterium tuberculosis* to demonstrate gene essentiality. Tuberculosis (Edinb) **81:**359-64.

23. **Parish, T., M. Schaeffer, G. Roberts, and K. Duncan.** 2005. HemZ is essential for heme biosynthesis in *Mycobacterium tuberculosis*. Tuberculosis (Edinb) **85:**197-204.

24. **Parish, T., and N. G. Stoker.** 2000. *glnE* is an essential gene in *Mycobacterium tuberculosis*. J Bacteriol **182:**5715-20.

25. **Pashley, C. A., and T. Parish.** 2003. Efficient switching of mycobacteriophage L5-based integrating plasmids in *Mycobacterium tuberculosis*. FEMS Microbiol Lett **229:**211-5.

26. **Richard, S. B., M. E. Bowman, W. Kwiatkowski, I. Kang, C. Chow, A. M. Lillo, D. E. Cane, and J. P. Noel.** 2001. Structure of 4-diphosphocytidyl-2-C-methylerythritol synthetase involved in mevalonate- independent isoprenoid biosynthesis. Nat Struct Biol **8:**641-8.

27. **Richard, S. B., A. M. Lillo, C. N. Tetzlaff, M. E. Bowman, J. P. Noel, and D. E. Cane.** 2004. Kinetic analysis of Escherichia coli 2-C-methyl-D-erythritol-4-phosphate cytidyltransferase, wild type and mutants, reveals roles of active site amino acids. Biochemistry **43:**12189-97.

28. **Rohdich, F., A. Bacher, and W. Eisenreich.** 2005. Isoprenoid biosynthetic pathways as anti-infective drug targets. Biochem Soc Trans **33:**785-91.

29. **Rohdich, F., J. Wungsintaweekul, W. Eisenreich, G. Richter, C. A. Schuhr, S. Hecht, M. H. Zenk, and A. Bacher.** 2000. Biosynthesis of terpenoids: 4-diphosphocytidyl-2C-methyl-D-erythritol synthase of *Arabidopsis thaliana*, p. 6451-6, Proc Natl Acad Sci U S A, vol. 97.

30. **Rohdich, F., J. Wungsintaweekul, M. Fellermeier, S. Sagner, S. Herz, K. Kis, W. Eisenreich, A. Bacher, and M. H. Zenk.** 1999. Cytidine 5'-triphosphate-dependent biosynthesis of isoprenoids: YgbP protein of *Escherichia coli* catalyzes the formation of 4-diphosphocytidyl-2-C-methylerythritol. Proc Natl Acad Sci U S A **96:**11758-63.

31. **Saito, Y., and K. Ogura.** 1981. Biosynthesis of menaquinones. Enzymatic prenylation of 1,4-dihydroxy-2-naphthoate by *Micrococcus luteus* membrane fractions. J Biochem (Tokyo) **89:**1445-52.

32. **Sassetti, C. M., D. H. Boyd, and E. J. Rubin.** 2003. Genes required for mycobacterial growth defined by high density mutagenesis. Mol Microbiol **48:**77-84.

33. **Sauret-Gueto, S., A. Ramos-Valdivia, E. Ibanez, A. Boronat, and M. Rodriguez-Concepcion.** 2003. Identification of lethal mutations in *Escherichia coli* genes encoding enzymes of the methylerythritol phosphate pathway. Biochem Biophys Res Commun **307:**408-15.

34. **Sharma, V., M. E. Hudspeth, and R. Meganathan.** 1996. Menaquinone (vitamin K2) biosynthesis: localization and characterization of the *menE* gene from *Escherichia coli*. Gene **168:**43-8.

35. **Smith, D. A., T. Parish, N. G. Stoker, and G. J. Bancroft.** 2001. Characterization of auxotrophic mutants of *Mycobacterium tuberculosis* and their potential as vaccine candidates. Infect Immun **69:**1142-50.

36. **Testa, C. A., and M. J. Brown.** 2003. The methylerythritol phosphate pathway and its significance as a novel drug target. Curr Pharm Biotechnol **4:**248-59.

37. **Tran, S. L., and G. M. Cook.** 2005. The F1Fo-ATP synthase of *Mycobacterium smegmatis* is essential for growth. J Bacteriol **187:**5023-8.

38. **Weber, C. H., Y. S. Park, S. Sanker, C. Kent, and M. L. Ludwig.** 1999. A prototypical cytidylyltransferase: CTP:glycerol-3-phosphate cytidylyltransferase from *Bacillus subtilis*. Structure **7:**1113-24.

39. **Weinstein, E. A., T. Yano, L. S. Li, D. Avarbock, A. Avarbock, D. Helm, A. A. McColm, K. Duncan, J. T. Lonsdale, and H. Rubin.** 2005. Inhibitors of type II NADH:menaquinone oxidoreductase represent a class of antitubercular drugs. Proc Natl Acad Sci U S A **102:**4548-53.

40. **Wolucka, B. A., M. R. McNeil, E. de Hoffmann, T. Chojnacki, and P. J. Brennan.** 1994. Recognition of the lipid intermediate for arabinogalactan/arabinomannan biosynthesis and its relation to the mode of action of ethambutol on mycobacteria. J Biol Chem **269:**23328-35.

41. **Zhang, J. H., T. D. Chung, and K. R. Oldenburg.** 1999. A Simple Statistical Parameter for Use in Evaluation and Validation of High Throughput Screening Assays. J Biomol Screen **4:**67-73.

42. **Zhang, Y., M. M. Wade, A. Scorpio, H. Zhang, and Z. Sun.** 2003. Mode of action of pyrazinamide: disruption of *Mycobacterium tuberculosis* membrane transport and energetics by pyrazinoic acid. J Antimicrob Chemother **52:**790-5.

Chapter I–4.

Characterization of an *in vitro* HTS assay targeting *Mycobacterium tuberculosis* 4–(cytidine 5'–diphosphate)–2–C–methyl–D–erythritol kinase

I.4.A. Introduction

The reaction catalyzed by IspD is performed at the third step in the MEP pathway and the *M. tuberculosis* IspD was identified and characterized in chapter I–3. The next enzyme in the MEP pathway is the ATP–dependent CDP–ME kinase (IspE). This ATP–dependent kinase catalyzes the transfer of γ–phosphate moiety of ATP to the substrate, CDP–ME, forming CDP–ME2P and corresponding release of ADP (Fig.I.4.1) (7, 9). The *E. coli* IspE has been reported to be essential for bacterial viability, *in vivo* (2) and there is no homolog in mammalian cells, indicating that IspE is also an attractive drug target.

Structural comparison using DALI (3) indicated the bacterial IspE belongs to the GHMP kinase superfamily (6, 11), so–named for four members: galactokinase, homoserine kinase, mevalonate kinase and phosphomevalonate kinase. A non–hydrolyzable ATP derivative was used to determine the *E. coli* IspE structure (8). In addition, *Thermus thermophilus* IspE structure has also been studied (11). *T. thermophilus* IspE is a single molecule in the asymmetric unit and has no conserved residues for divalent cation binding (11). In contrast, other members of the GHMP superfamily mostly form homodimers and require divalent cation as a cofactor. *E. coli* IspE forms homodimer and each subunit displays the α/β fold which is the conserved characteristic of GHMP kinase superfamily. The α/β fold of each subunit arranged into cofactor and substrate–binding domains with catalytic center positioned in a deep cleft between two domains. Despite the high structural similarity with the GHMP superfamily, the conserved residues for coordinating divalent cation (Mg^{2+}) and triphosphate moiety of

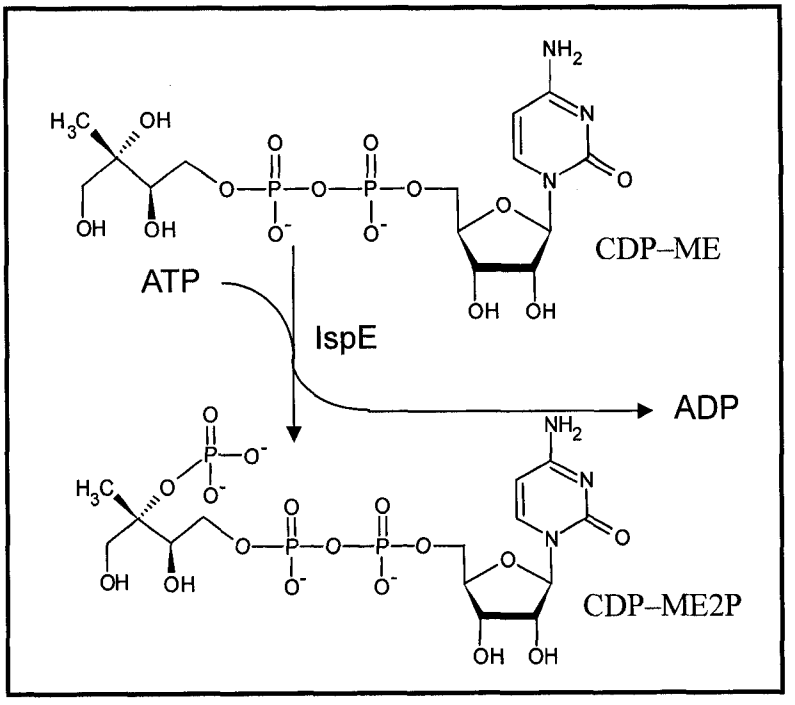

FIGURE I.4.1. **The reaction catalyzed by IspE.** The substrate is 4–(cytidine 5'–diphosphate)–2–C–methyl–D–erythritol (CDP–ME) and the product is 2–phospho–4–(cytidine 5'–diphopho)–2–C–methyl–D–erythritol. IspE has the ATP–dependent kinase activity and release corresponding ADP.

ATP are missing in *E. coli* IspE and there is no evidence for divalent cation binding in the crystal structure. However, *E. coli* IspE activity requires divalent cations (4, 6). Moreover, the pyrimidine–binding site is constructed with an extension to the first β–turn–β unit, a distinct feature in only *E. coli* IspE and the cofactor purine moiety forms hydrogen–bonding interactions that stabilize the less common syn orientation with respect to the base. (5, 8, 11). These conformational differences between bacterial and mammalian members of the GHMP superfamily support the hypothesis that IspE is an attractive and potential drug target.

The putative ATP–binding domains (10) and glycine–rich sequence motif (6) are well conserved over the GHMP kinase superfamily. These motifs are also present in protein kinases and *E. coli* IspE. The *Rv1011* gene product of *M. tuberculosis* showed strong similarity with *E. coli* IspE with the conserved glycine–rich motif and ATP–binding domains (Fig.I.4.2). Therefore, we have cloned, expressed, and purified Rv1011 and defined its biochemical role in the *M. tuberculosis* MEP pathway. In addition, an *in vitro* HTS assay using purified recombinant Rv1011 was developed.

Even though Rv1011 is predicted to be cytosolic and soluble, the intact Rv1011 failed to be expressed in *E. coli* at reasonable levels, presumably because of low solubility. Therefore, eight truncated versions of Rv1011 by deleting either N–terminal or C–terminal or both were tested to optimize the expression level and its activity. The expression level was dramatically increased when 6–amino acid residues at the C–terminal end were removed and the truncated Rv1011 was active and stable. Thus, those constructs were purified and used to define the role of *M. tuberculosis* IspE and develop the *in vitro* HTS assay.

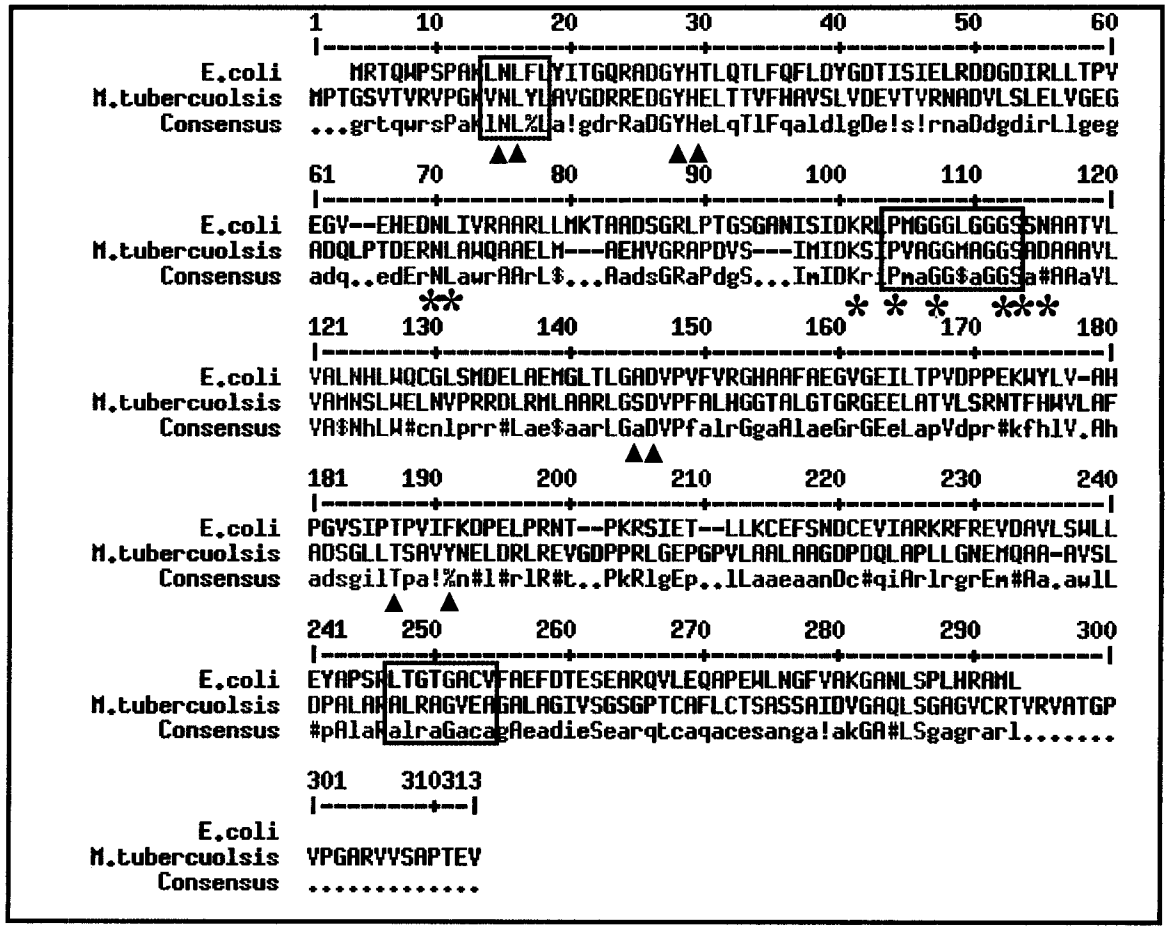

FIGURE I.4.2. **Alignment of the amino acid sequence of IspE from *E. coli* and the ortholog (Rv1011) identified in the *M. tuberculosis* genome.** Identities are indicated in red. Similarities are indicated in blue. The *E. coli* amino acids involved in the ATP–binding are indicated (*) and those involved in substrate (CDP–ME) binding are also indicated (▲). The three blue boxes indicate the conserved amino acids required for the catalytic activity of IspE (6, 7). The second blue box shows conserved glycine–rich domain.

I.4.B. Materials and Methods

Materials. CDP–ME was purchased from Echelon Research Laboratories, Inc. (Salt Lake City, UT). The Kinase–Glo® Luminescent Kinase Assay Kit was obtained from Promega Corporation (Madison, WI). The ADP Quest HS Kinase Assay Kit was purchased from GE healthcare Bio–Sciences Corp. (Piscataway, NJ). All other reagents and solvents were of at least analytical grade.

Preparation of cytosolic fractions of *M. smegmatis* control strain and recombinant *M. smegmatis* strain. Putative *ispE* open reading frame from *M. tuberculosis* (*Rv1011*) was amplified using oligonucleotide primers designed from the sequences available in Tuberculist (http://genolist.pasteur.fr/TubercuList/). The primers used in this study were synthesized in macromolecular resources (Colorado State University) and summarized in Table I.4.1. All the primers contain the sequences recognized by *Nde*I and *Hin*dIII restriction enzymes (underlined). The intact *Rv1011* PCR products were obtained by using the primer set, Rv1011For and Rv1011Rev. The PCR fragments were digested with *Nde*I and *Hin*dIII and ligated into pVV2, a mycobacterial expression plasmid. Transformation of *E. coli* DH5α subcloning cells (Life Technologies, Rockville, MD) with ligation mixtures created the recombinant strains DH5α[pVV2::*Rv1011*] for propagation. The constructs were isolated using Qiagen Plasmid Miniprep Kits. Transformation of *M. smegmatis* mc^2155 with the construct pVV2::*Rv1011* created the recombinant strains *M. smegmatis* mc^2155[pVV2::*Rv1011*]. The control strain was obtained by transforming *M. smegmatis* mc^2155 with empty pVV2 vector. Control and

recombinant *M. smegmatis* mc^2155 strains were grown in LB media supplemented with 50 μg/ml of kanamycin and 34 μg/ml of hygromycin. Both strains were harvested by centrifugation at 10,000 × *g* for 10 minutes and stored at –70°C. Recombinant and control cell pellets were resuspended and washed with MOPS buffer [50 mM MOPS (pH 7.9), 10 mM $MgCl_2$, 5 mM β–mercaptoethanol] at 4°C. The resuspended solutions were disrupted by probe sonication on ice for 10 cycles of 25 seconds on and 90 seconds off in a Soniprep 150 (Integrated Services, TCP, Palisades Park, NJ). Homogenates were centrifuged at 27,000 × *g* for 30 minutes, and the supernatants collected separately. The supernatants were ultra–centrifuged at 55,000 × *g* in a Beckman 70.1 Ti rotor for 2 hours. The supernatants were aliquot and stored at –70°C. The expression of Rv1011 of the cytosol fraction obtained recombinant strain was confirmed by Western blot analysis with an anti–Histidine antibody (Sigma Aldrich).

PCR amplification and cloning of eight truncated versions of *Rv1011* from *M. tuberculosis*. The *Rv1011* PCR products obtained above were ligated into pET28a(+) vector (EMD Biosciences, Inc., San Diego, CA). Transformation of *E. coli* DH5α with ligation mixtures created the recombinant strains DH5α[pET28a(+)::*Rv1011*]. The constructs were isolated using Qiagen Plasmid Miniprep Kits. Unfortunately, the expression of the intact Rv1011 failed under all conditions. Therefore, we tried to express eight different versions of truncated Rv1011 to optimize the expression and solubility (Fig.I.4.3, Table I.4.2). Different truncated *Rv1011* PCR products were obtained using PCR reaction containing various set of primers, as described in Table.I.4.2. The eight different truncated *Rv1011* genes encode corresponding mutant Rv1011 enzymes. The

TABLE I.4.1. **PCR primers used in this study.** The sequences recognized by the restriction enzymes are underlined.

Primer name	Sequence	Enzyme
Rv1011For	CATATGCCCACCGGGTCGGTCACCGTT	*Nde*I
Rv1011Rev	AAGCTTTCACACTTCGGTCGGCGCAGA	*Hin*dIII
Rv1011–primer1	CATATGGCCGTCTCGCTGGTCGACGAG	*Nde*I
Rv1011–primer2	CATATGGTCTCGATCATGATCGAC	*Nde*I
Rv1011–primer3	AAGCTTCGCAGACACCACGCGGGCGCC	*Hin*dIII
Rv1011–primer4	AAGCTTCGAGGTGCACAGGAAGGCACA	*Hin*dIII

constructs were purified and sequence confirmed by Marcomolecular Resources, Colorado State University.

Expression and purification of the recombinant mutant Rv1011. *E. coli* BL21(DE3) (Novagen, Madison, WI) was used as the expression host. Transformation of BL21(DE3) with the eight different versions of truncated construct afforded the BL21(DE3)[pET28a(+)::truncated *Rv1011*]. The expression strains were propagated in LB media supplemented with kanamycin (50 μg/ml) at 37°C and then induced with 0.5 mM IPTG at 20°C for 10 hours. Cells were resuspended in lysis buffer [50 mM MOPS (pH 7.9), 10 mM $MgCl_2$, 10 % glycerol, 5 mM β–mercaptoethanol, and 1 mg/ml lysozyme] and disrupted by sonication using a Sanyo Soniprep 150 (Integrated Serviecs, TCP Inc, Palisades Park, NJ) on ice. Mutant recombinant Rv1011 proteins carrying a histidine extension were purified by IMAC. Histidine–select nickel affinity gel (Sigma Aldrich, St Louis, MO) was added to the disrupted cell supernatant and rocked at 4°C for 30 minutes. The resulting slurry was used to pack columns, which were then washed with 50 mM MOPS (pH 7.9), 1 mM $MgCl_2$, 10 % glycerol and 1 mM β–mercaptoethanol. Histidine tagged recombinant mutant Rv1011 was eluted with the washing buffer containing a linear gradient of 10 mM to 200 mM imidazole. Fractions containing the protein were pooled and desalted by a PD–10 desalting column (Amersham, Piscataway, NJ). The pooled material was analyzed by SDS–PAGE and Western blot analysis with an anti–Histidine antibody. Recombinant proteins were concentrated by ultrafiltration (5000 molecular weight cutoff, Centricon, Millipore, Bedford, MA).

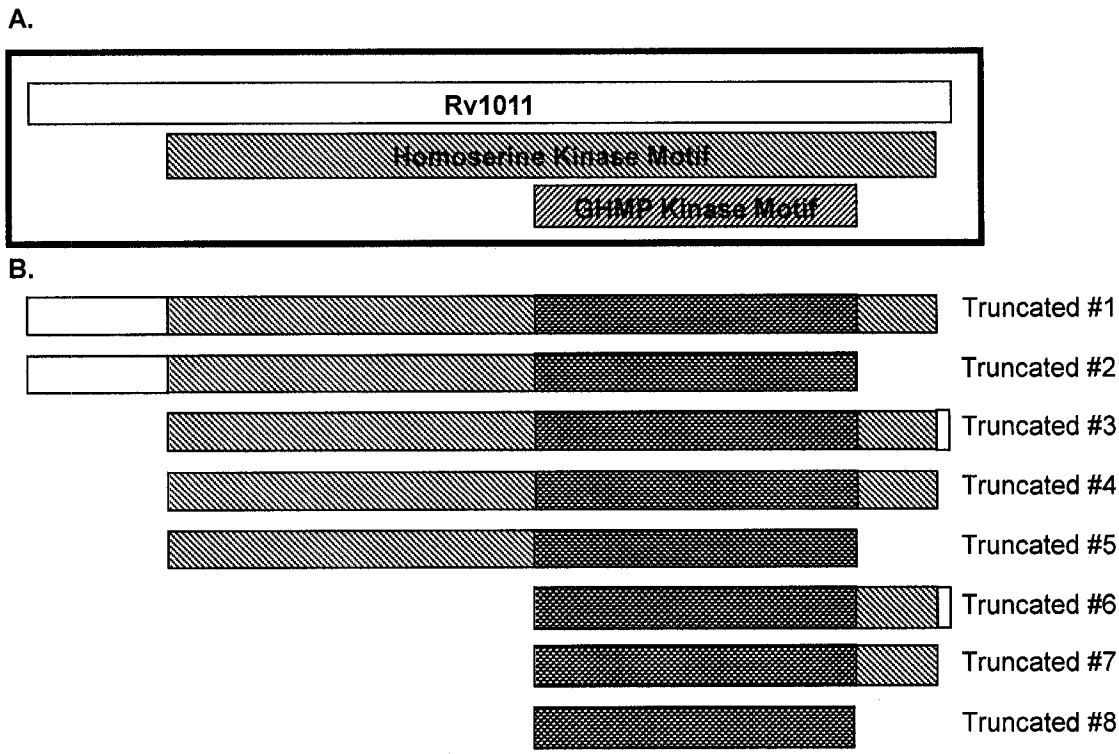

FIGURE I.4.3. **Schematic diagram showing the kinase domains and eight different mutant Rv1011 fragments.** A. Rv1011 contains two overlapped motifs (Homoserine Kinase Motif and GHMP Kinase Motif). B. diagrams of domains contained by eight mutant Rv1011 proteins. Truncated #1 fragment contained intact Rv1011 removing the 6 C–terminal amino acids. Truncated #4 mutated Rv1011 fragment contained the whole Homeserine Kinase Motif. Truncated #8 mutated Rv1011 fragment contained the whole GHMP Kinase Motif.

TABLE I.4.2.**The properties of eight recombinant mutant Rv1011 enzymes and wild type Rv1011**

Truncated Rv1011	Primers used	Size	Solubility	Activity	Stability
Wild type	Rv1011For, Rv1011Rev	306 a.a.	–	N.A.	N.A.
#1	Rv1011For, Primer 3	300 a.a.	+++	+++	+++
#2	Rv1011For, Primer 4	267 a.a.	++	+	+
#3	Primer 1, Rv1011Rev	270 a.a.	++	++	+
#4	Primer 1, Primer 3	265 a.a.	++	++	+
#5	Primer1, Primer 4	230 a.a.	+	+	+
#6	Primer 2, Rv1011Rev	215 a.a.	+++	++	+
#7	Primer2, Primer3	210 a.a.	++	+++	–
#8	Primer2, Primer4	140 a.a.	+++	–	N.A.

Truncated PCR products were obtained from the PCR reactions using different sets of primers. Symbols used: N.A., not applicable; –, no; +, low; ++, intermediate; +++, good. Solubility was checked using SDS–PAGE analysis, activity was checked using the enzyme assay, and enzyme stability was checked after storing for one week at –70°C.

Development of *in vitro* IspE HTS assay using the Kinase–Glo® Luminescent Kinase Kit and ADP Quest HS Kinase Assay Kit. IspE is an ATP–dependent kinase. Therefore, the Kinase–Glo® Luminescent Kinase Assay Kit and the ADP Quest HS Kinase Assay Kit were utilized to monitor. The Kinase–Glo® Luminescent Kinase Assay Kit is used to measure ATP concentration remained in the reaction mixtures. In contrast, the ADP Quest HS Kinase Assay Kit measures ADP concentration produced by the kinase reaction. Reaction mixtures contained 50 mM Tris–HCl (pH 7.9), 200 μM ATP, 2 mM DTT, 100 μM CDP–ME, 5 mM $MgCl_2$ and 97.2 pmols of purified truncated Rv1011 enzyme in a 50 μl final reaction volume in 96–well luminescence microtiter microplates (Thermo Fisher Scientific) when using the Kinase–Glo® Luminescent Kinase Assay Kit. The reactions were incubated at 37°C for 30 minutes and 50 μl of the Kinase–Glo® Reagent was added to make a total volume of 100 μl. Final mixtures were incubated at room temperature for 10 minutes and IspE activity was measured by Synergy™ HT Multi–Detection Microplate Reader (BioTek instruments). On the other hand, the ADP Quest HS Kinase Assay Kit produces a fluorescent signal which is directly proportional to the ADP concentration produced in the kinase reactions. The measurable fluorescent signal is produced by coupling enzymes within the Kit (Fig.I.4.4). The same reaction mixture as that of the Kinase–Glo® Luminescent Kinase Assay Kit was used in the 96–well black microplates with clear bottom (Costar, NY). After incubating at 37°C for 15 minutes, 25 μl of reagent A and 50 μl of reagent B were added, sequentially. After incubating at room temperature for 15 minutes, the fluorescence was measured by Synergy™ HT Multi–Detection Microplate Reader (BioTek instruments) at excitation wavelength 530 nm and emission wavelength 590 nm.

Determination of optimal reaction conditions for the *in vitro* HTS enzyme assay using mutant Rv1011. To determine the optimal pH for the *in vitro* HTS enzyme assay using mutant IspE, reaction mixtures at various pH values containing pH appropriate buffers (MES, MOPS, Tris, TAPS, or CAPS) were used. Optimal concentrations for divalent cations were determined in assay mixtures containing $MgCl_2$ or $MnCl_2$ at the indicated concentrations.

Determination of kinetic properties of mutant Rv1011. The effect of ATP concentration on activity was determined using a constant concentration of CDP–ME (100 μM) and varying concentrations of ATP. The effect of CDP–ME concentration was determined using a constant concentration of ATP (200 μM) and varying concentrations of CDP–ME. The K_m and V_{max} values of substrates for the enzyme were calculated by non–linear regression analysis (SigmaPlot V. 8.02A).

I.4.C. Results

Identification of *M. tuberculosis* IspE. The amino acid sequence of Rv1011 from *M. tuberculosis* has only 21% identity with that of *E. coli* IspE (Fig.I.4.2). However, all known catalytic domains, including the glycine–rich domains and ATP–binding motifs, are conserved in Rv1011, suggesting an analogous function in *M. tuberculosis*. Intact Rv1011 encodes a protein of 306 amino acids with a molecular weight of 31.8 kDa, which is predicted to be soluble.

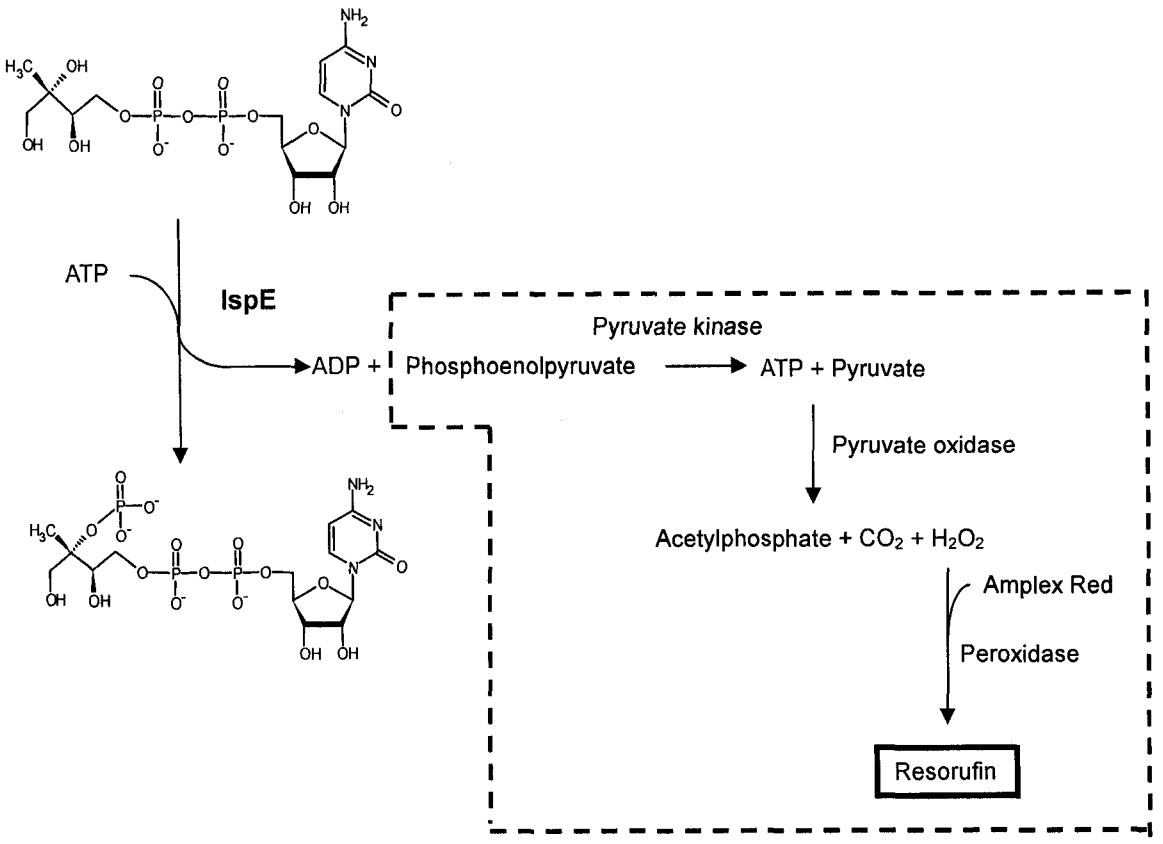

FIGURE I.4.4. **An overview of the ADP Quest HS Kinase Kit coupling ADP produced from the IspE catalytic reaction and the enzymes within the kit.** The ADP Quest HS Kinase Assay Kit is used to generate hydrogen peroxide (H_2O_2) from ADP. H_2O_2, when combined with Amplex Red (fluorescent dye precursor) in the presence of peroxidase generates fluorescent resorufin. The addition of a stop solution is required to stabilize background signal.

The effect of overexpression of *Rv1011* in *M. smegmatis* mc^{2}155. *Rv1011* was amplified by PCR from the *M. tuberculosis* H_{37}Rv genome and cloned into the pVV2 vector for overexpression in *M. smegmatis* mc^{2}155. The cytosolic fractions from the control (*M. smegmatis* mc^{2}155[pVV2]) and recombinant (*M. smegmatis* mc^{2}155[pVV2::*Rv1011*] strains were tested for the IspE activity using the Kinase–Glo® Luminescent Kinase Assay Kit. The specific activity of the cytosol from the recombinant strain was significantly higher than that of the control strain (Fig.I.4.5), indicating that *Rv1011* encodes functional IspE in *M. tuberculosis*. Overexpression of the predicted 31.8 kDa polypeptide was confirmed by Western blot analysis using an anti–Histidine antibody (data not shown). The amount of the purified Rv1011 in *M. smegmatis* was too small to use and develop the HTS assay.

Optimal reaction conditions of the *in vitro* Rv1011 HTS assays. In order to optimize protein expression, various *E. coli* hosts and vector systems were used. However, all the trials for expression of intact Rv1011 failed. To facilitate the purification of large quantities of recombinant Rv1011 for further characterization, eight different mutated versions of Rv1011 were tested (Fig.I.4.3). Among them, Rv1011 fragment truncating 6–amino acid at C–terminal end was chosen because this truncated version showed the highest expression level and could be induced under all conditions tested (Table.I.4.2). Moreover, recombinant mutant Rv1011 obtained by removing 6–amino acids at C–terminal end was the most stable and active (Table I.4.2). Therefore, mutant Rv1011 was purified by IMAC for further characterization (Fig.I.4.6). The expression was confirmed by Western blot analysis, at the expected molecular weight of 30.8 kDa (Fig.I.4.6). The

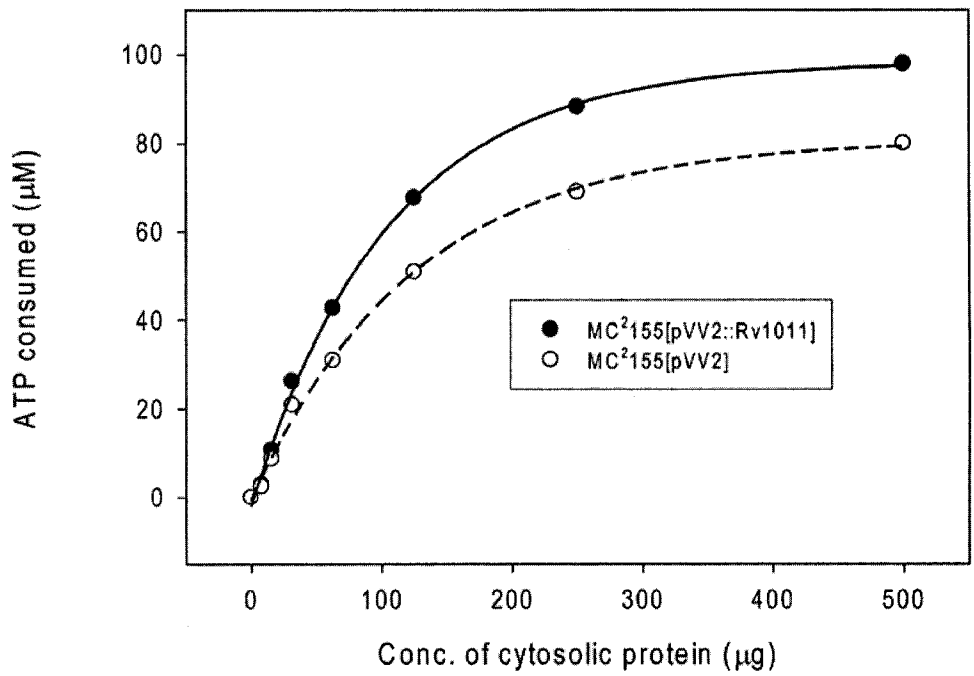

FIGURE I.4.5. **The effect of overexpression of *Rv1011* in *M. smegmatis* mc^{2}155 on IspE activity**. The dashed line shows IspE activity of cytosolic fraction from control strain (*M. smegmatis* mc^{2}155[pVV2]) and the solid line shows the that of the recombinant strain (*M. smegmatis* mc^{2}155[pVV2::*Rv1011*]). Overexpression of Rv1011 in *M. smegmatis* mc^{2}155 was confirmed by Western blot analysis with an anti–Histidine antibody (data not shown).

recombinant mutant Rv1011 showed ATP–dependent kinase activity. The catalytic reaction of the *in vitro* HTS assay using the mutant Rv1011 was tested for finding optimal pH and divalent cations. The ADP Quest HS Kinase Assay Kit was utilized. Plots of the fluorescent signal of the *in vitro* HTS assay in terms of pH were bell shaped with the highest signal at pH 8.0 (Fig.I.4.7A). The *in vitro* HTS assay was optimal in the presence of 10 mM Mg^{2+}. However, Mn^{2+} was ineffective at supporting the *in vitro* HTS assay at all concentrations tested (Fig.I.4.7B).

Kinetic properties of Rv1011. Most truncated Rv1011 enzymes showed various degrees of ATP–dependent kinase activity except for truncated #8 Rv1011 which showed no activity (Table I.4.2). All the truncated Rv1011 enzymes were very unstable and they lost the activity in less than 1 week at –70°C except for 6 C–terminal amino acid removing mutant Rv1011 (Table I.4.2). The activities of purified the mutant Rv1011 were linear with increasing the concentration up to 162.3 pmols and the reactions were also linear with time up to 30 minutes. The effects of CDP–ME or ATP concentrations on reaction rates were determined by varying the concentration of one substrate while keeping the other fixed (Fig.I.4.8). The K_m^{CDP-ME} and K_m^{ATP} were calculated to be 515.1 μM and 75.2 μM, respectively (Table I.4.3).

I.4.D. Discussion

Truncation of Rv1011 was used to improve expression in *E. coli*. Surprisingly, most of recombinant truncated versions of Rv1011 tested in this chapter showed

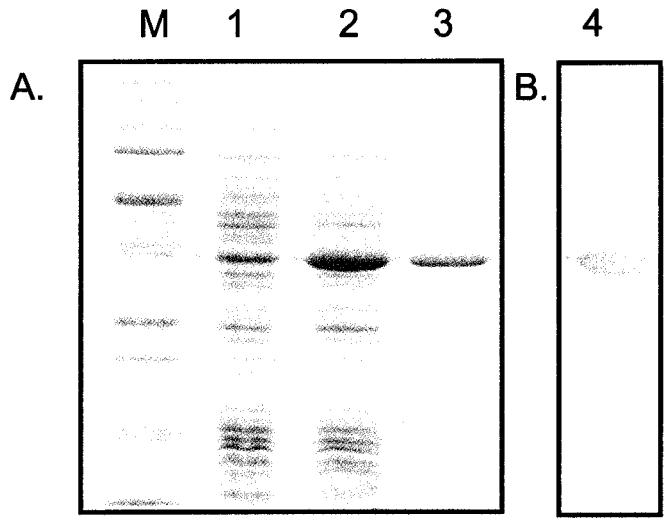

FIGURE I.4.6. **SDS–PAGE analysis of expression and purification of histidine tagged mutant IspE.** Proteins were visualized by Coomassie brilliant blue 250R (panel A) and Western blot hybridization using conjugated alkaline phosphatase (panel B). Lane 1, transformed BL21(DE3) cell lysates prior to IPTG treatment. Lane 2, transformed BL21(DE3) cell lysates after IPTG treatment. Lane 3, purified histidine truncated IspE eluted from an IMAC column. Lane 4, Western blot hybridization of purified truncated IspE using an anti–Histidine antibody.

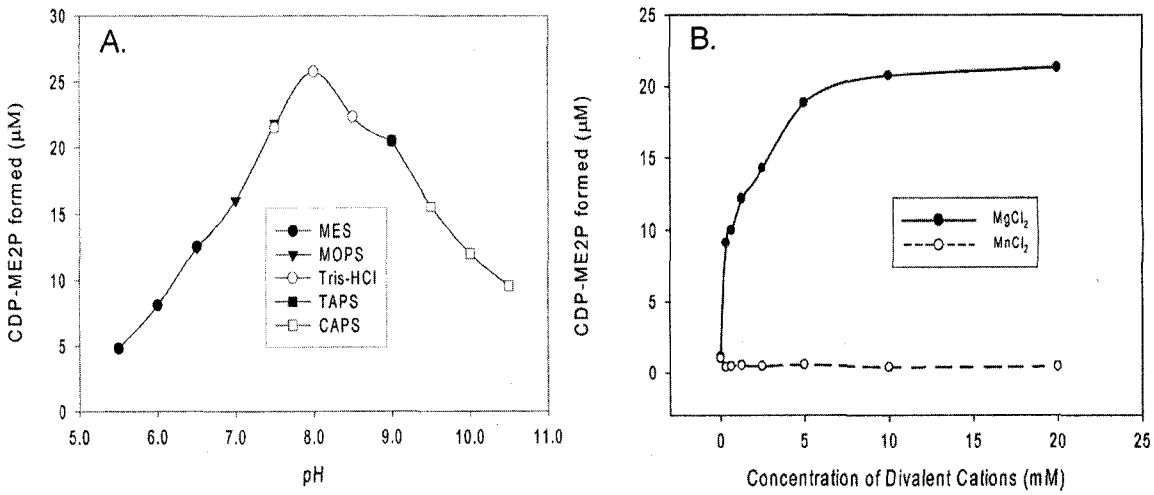

FIGURE I.4.7. **The effects of pH and divalent cation concentration on the *in vitro* HTS assay using mutant *M. tuberculosis* IspE**. A. The optimal pH for catalytic activity was determined using MES (pH 5.5 - pH 7.0), MOPS (pH 7.0 - pH 7.5), Tris (pH 7.5 - pH 8.5), TAPS (pH 8.5 - pH 9.0), and CAPS (pH 9.0 - pH 10.5). B. Divalent cations were added to the reaction mixtures at the indicated concentrations. The reaction mixtures were as described in Materials and Methods.

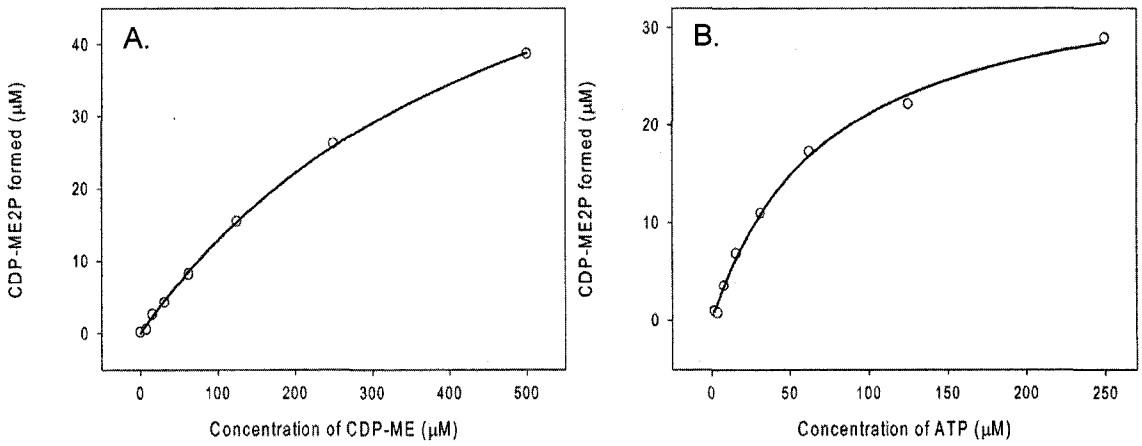

FIGURE I.4.8. **The effects of CDP–ME and ATP concentrations on mutant *M. tuberculosis* IspE activity**. A. To determine the effect of CDP–ME concentration, ATP concentration was held at 200 μM and the concentration of CDP–ME was varied from 0 to 640 μM. B. To determine the effect of ATP concentration, CDP–ME concentration was held at 100 μM and the concentration of ATP was varied from 0 to 250 μM. Reaction mixtures were as described in Materials and Methods.

TABLE I.4.3. **Calculated kinetic parameters for mutant *M. tuberculosis* IspE.**

Reaction/ Substrate	Calculated parameter			
	K_m (μM)	V_{max} (μmol/min)	K_{cat} (min^{-1})	K_{cat}/K_m ($\mu M^{-1}min^{-1}$)
ATP	75.2	2.5	2.5×10^4	3.4×10^2
CDP–ME	515	5.3	5.4×10^4	1.1×10^2

Each reaction contained 97.2 pmols of recombinant mutant Rv1011. The K_m and V_{max} values were calculated from the experiments shown in Fig.I.4.8 using non–linear regression analysis (Sigma Plot V.8.02A)

improved expression levels and ATP–dependent kinase activity. However, the smallest Rv1011 version (#8 Rv1011, Table I.4.2) harboring only the GHMP kinase motif, although its expression level was dramatically increased, showed no activity. These results indicated that both N–terminal and C–terminal ends of Rv1011 are required for its catalytic activity. Among eight different truncated versions of Rv1011, mutant Rv1011 removing 6–amino acids at the C–terminal end (#1 truncated Rv1011) showed the highest activity and were the most stable. Therefore, it was assumed that the C–terminal end of the Rv1011 contain little functional contribution to its activity. In contrast, *E. coli* IspE subunit comprises 10 α–helices and 12 β–strands. ATP–binding motif comprises four–stranded β sheet on one side with a five–helix bundle on the other, where the 6–amino acids of the C–terminal end contribute to form the part of a five–helix bundle for composing ATP–binding motif (8).

The highest fluorescent signal of the *in vitro* HTS IspE assay using mutant Rv1011 was obtained in the presence of 20 mM of divalent cation (Mg^{2+}) and at pH 8.0. The *in vitro* HTS IspE assay reactions were stopped before adding the reagents of the ADP Quest HS Kinase Assay Kit. Therefore, it is not worrisome that the divalent cation in the kit influences the IspE reactions. However, the kit contains extra enzymes for generating the measurable fluorescent signal from ADP produced by the IspE reaction. Various pH values or divalent cations tested in this study may influence the coupling enzymes within the kit. Although the optimal pH and divalent cations for the *in vitro* HTS IspE assay were identified, it is required to develop the radiochemical enzyme assay using [γ–^{32}P]ATP to find the optimal *in vitro* requirements of *M. tuberculosis* IspE in terms of pH and divalent cations.

Previous literature has shown that K_m^{ATP} and K_m^{CDP-ME} for *E. coli* IspE are 420 μM and 150 μM, respectively (1). The K_m^{ATP} and K_m^{CDP-ME} for the mutant *M. tuberculosis* IspE are 75.2 μM and 515.1 μM, respectively. The different K_m values indicated that the IspE isolated from distinct sources shows different affinity to the substrates. This is also supported from the results obtained from the *S. typhi* IspE, the *V. cholerae* IspE and the *B. mallei* IspE (chapter II–3). When the calculated kinetic values are compared with those of the *S. typhi* IspE, the *V. cholerae* IspE, or the *B. mallei* IspE, The K_m^{ATP} is similar but the $K_m^{CDP\text{–ME}}$ is higher than other values. However, the specificity constants (K_{cat}/K_m) of *M. tuberculosis* IspE in terms of both substrates were similar to those of the *S. typhi* IspE, the *V. cholerae* IspE, or the *B. mallei* IspE. The higher values of $Km^{CDP\text{–ME}}$ for *M. tuberculosis* suggested that *M. tuberculosis* IspE has lower affinity for CDP–ME. As part of future directions, it is required to compare K_m values obtained using cytosolic fraction from wild *M. tuberculosis* strain with those using the mutant Rv1011.

Either radiochemical assays using [2–^{14}C]CDP–ME (7, 11) or *in vitro* assays in which the product is analyzed by reverse–phase HPLC (9) were employed to characterize IspE enzymes of other organisms. These methods are sensitive and specific. However, they are not suitable for automation to apply the HTS assays in multi–well microplate formats. A HTS assay should be non–radioactive and miniaturized by reducing the reaction volume to apply multi–well microplate formats. In the present study, we have monitored *M. tuberculosis* IspE activity in two different ways. One method measures the ATP concentration coupling to produce luminescent signal and the other measures the ADP concentration by generating a fluorescent signal. Unfortunately, we have failed to

get consistent and reproducible results using the former way. Therefore, the latter method is preferred as this produces a positive fluorescent signal that is directly proportional to the ADP concentration in the kinase reaction. Moreover, unlike the ATP depletion approach, it gives robust performance even with high ATP concentration or low enzyme activity. Therefore, we will use this assay to screen the specific inhibitors against *M. tuberculosis* IspE.

I.4.E. References

1. **Bernal, C., C. Palacin, A. Boronat, and S. Imperial.** 2005. A colorimetric assay for the determination of 4-diphosphocytidyl-2-C-methyl-D-erythritol 4-phosphate synthase activity. Anal Biochem **337:**55-61.
2. **Freiberg, C., B. Wieland, F. Spaltmann, K. Ehlert, H. Brotz, and H. Labischinski.** 2001. Identification of novel essential *Escherichia coli* genes conserved among pathogenic bacteria. J Mol Microbiol Biotechnol **3:**483-9.
3. **Holm, L., and C. Sander.** 1995. Dali: a network tool for protein structure comparison. Trends Biochem Sci **20:**478-80.
4. **Hunter, W. N.** 2007. The non-mevalonate pathway of isoprenoid precursor biosynthesis. J Biol Chem **282:**21573-7.
5. **Krishna, S. S., T. Zhou, M. Daugherty, A. Osterman, and H. Zhang.** 2001. Structural basis for the catalysis and substrate specificity of homoserine kinase. Biochemistry **40:**10810-8.
6. **Lange, B. M., and R. Croteau.** 1999. Isopentenyl diphosphate biosynthesis via a mevalonate-independent pathway: isopentenyl monophosphate kinase catalyzes the terminal enzymatic step. Proc Natl Acad Sci U S A **96:**13714-9.
7. **Luttgen, H., F. Rohdich, S. Herz, J. Wungsintaweekul, S. Hecht, C. A. Schuhr, M. Fellermeier, S. Sagner, M. H. Zenk, A. Bacher, and W. Eisenreich.** 2000. Biosynthesis of terpenoids: YchB protein of *Escherichia coli* phosphorylates the

2-hydroxy group of 4-diphosphocytidyl-2C-methyl-D-erythritol. Proc Natl Acad Sci U S A **97:**1062-7.

8. **Miallau, L., M. S. Alphey, L. E. Kemp, G. A. Leonard, S. M. McSweeney, S. Hecht, A. Bacher, W. Eisenreich, F. Rohdich, and W. N. Hunter.** 2003. Biosynthesis of isoprenoids: crystal structure of 4-diphosphocytidyl-2C-methyl-D-erythritol kinase. Proc Natl Acad Sci U S A **100:**9173-8.

9. **Rohdich, F., J. Wungsintaweekul, H. Luttgen, M. Fischer, W. Eisenreich, C. A. Schuhr, M. Fellermeier, N. Schramek, M. H. Zenk, and A. Bacher.** 2000. Biosynthesis of terpenoids: 4-diphosphocytidyl-2-C-methyl-D-erythritol kinase from tomato. Proc Natl Acad Sci U S A **97:**8251-6.

10. **Tsay, Y. H., and G. W. Robinson.** 1991. Cloning and characterization of ERG8, an essential gene of *Saccharomyces cerevisiae* that encodes phosphomevalonate kinase. Mol Cell Biol **11:**620-31.

11. **Wada, T., T. Kuzuyama, S. Satoh, S. Kuramitsu, S. Yokoyama, S. Unzai, J. R. Tame, and S. Y. Park.** 2003. Crystal structure of 4-(cytidine 5'-diphospho)-2-C-methyl-D-erythritol kinase, an enzyme in the non-mevalonate pathway of isoprenoid synthesis. J Biol Chem **278:**30022-7.

Chapter I–5.

Drug candidate screening from small directed compound libraries against *Mycobacterium tuberculosis* 1–deoxy–D–xylulose 5–phosphate synthase

I.5.A. Introduction

A new TB treatment should offer at least one of three improvements over the existing DOTS programs: shorten the total duration of effective treatment; significantly reduce the total doses required to be taken to improve the treatment of MDR–TB; and provide a more effective treatment of persistent TB infection (17). Ideally, a new, highly effective drug will achieve all. As myriad part of efforts to develop new treatments for TB, drug discovery programs are aimed at targeting proteins the function of which is known to be essential for the *M. tuberculosis* survival and which lack homologs in mammalian cells. In most cases, lead compounds are screened and identified through the *in vitro* enzyme assays using recombinant purified enzyme which has been selected as a drug target. Each of the resulting inhibitors then represents a starting point whose structure is further modified to improve binding and other important characteristics (4). Lead compounds also can be identified based on known inhibitors, chemical intuition, or even known drugs. All of these processes together can produce a series of lead compounds that might be suitable for further medicinal chemical manipulation to produce candidates for preclinical evaluation.

The MEP pathway has been paid intensive attention as sources of a drug target. The initiation of the pathway involves condensing pyruvate and GAP in the presence of TPP (Fig. I.5.1) (16). In *M. tuberculosis*, *Rv2682c* encodes the responsible enzyme for this step and has previously been characterized as the *M. tuberculosis* DXS (2). *M. tuberculosis* DXS showed optimal activity at pH 7.0, in the presence of divalent metal ions, 1 mM of Mg^{2+} and has 40 μM for $K_m^{pyruvate}$ and 6.1 μM for K_m^{GAP}. It utilizes

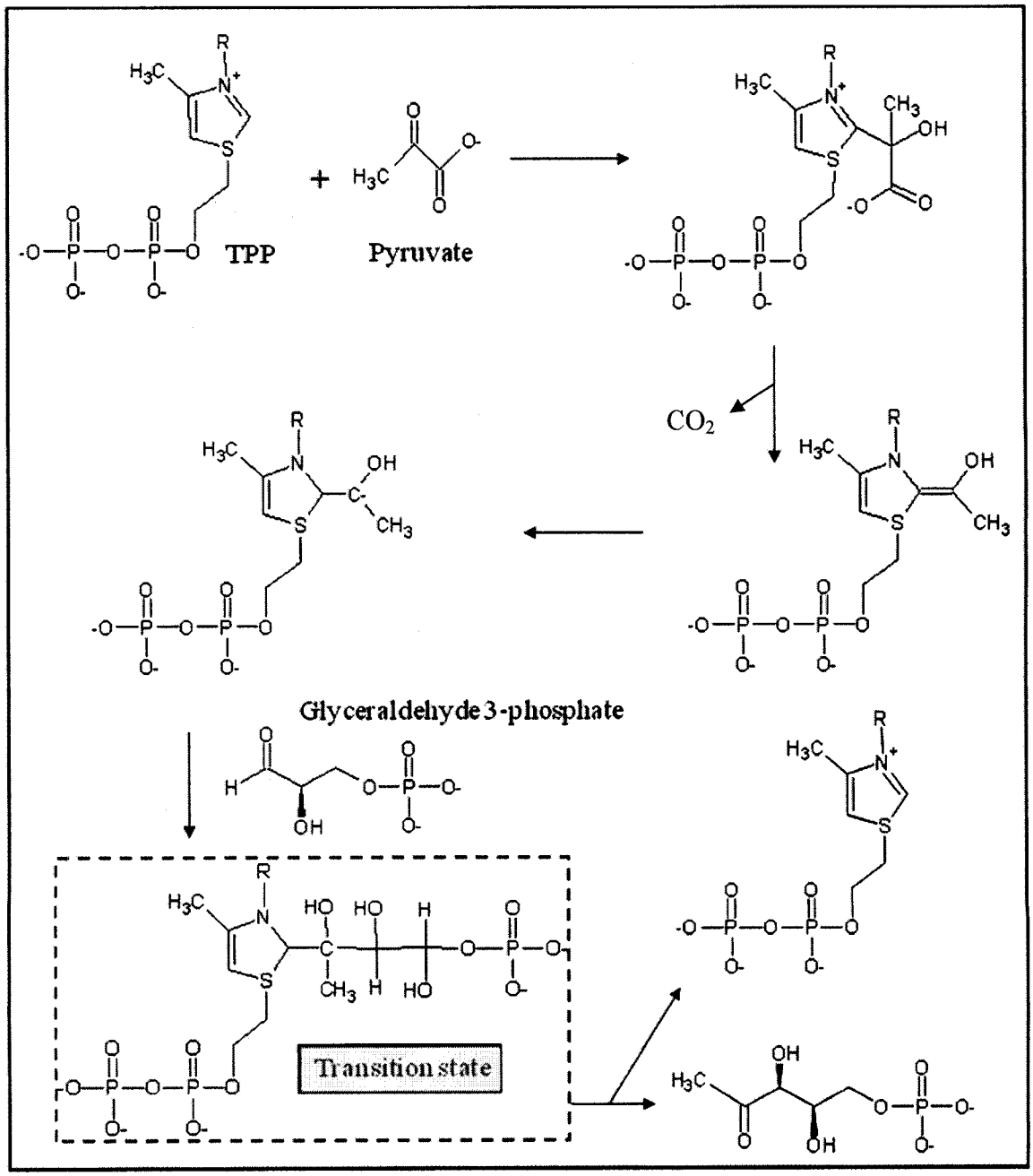

FIGURE I.5.1. **Proposed procedure of producing 1–deoxy–D–xylulose–5–phosphate from pyruvate and glyceraldehyde–3–phosphate.** Thiamine diphosphate (TPP) contributes to the reaction center and forms the transition state with pyruvate and glyceraldehyde 3–phosphate after decarboxylation which is depicted with a dashed box.

D–glyceraldehyde and L–glyceraldehyde as substrates, both of which have much larger K_m values than that of GAP, suggesting that this enzyme has relatively broad substrate ranges. Interestingly, *M. tuberculosis* contains another homolog of *E. coli* DXS, the *Rv3379c* gene product. However, an alignment with *E. coli* DXS indicated that Rv3379c contains a partially truncated DRAG motif, a conserved domain among members of the transketolase (TK) superfamily (2, 6), and purified recombinant Rv3379c showed no DXS activity (2).

In vitro enzyme assays for monitoring *M. tuberculosis* DXS activity were previously been established and the *M. tuberculosis* DXS (Rv2682c) was predicted to be essential for bacterial survival *in vivo* by Himar1–based transposon mutagenesis experiments performed by Sassetti *et al* (14). As part of a collaboration with Dr. Scott Franzblau at University of Illinois at Chicago (UIC), a small directed compound library against the *M. tuberculosis* DXS was designed and synthesized for the purpose of identifying specific inhibitors. The compounds screened in this study could be divided into two groups. The first group was designed by mimicking the structure of the transition state, depicted in the dashed boxes in Fig.I.5.1. The second group included the previously reported TK inhibitors and various modifications. The general rationale of modifying the compounds was to improve the penetrating capacity through the unusual *M. tuberculosis* cell wall, which was acquired by replacing the polar pyrophosphate moiety of TPP with the bioisosteres such as the sulfonamide groups or 2–thioxo 4–thiazolidinone.

The synthesized compounds should be drug–like. "Lipinski's rule of five" (7) helps to determine whether the compounds are drug–like or not according to their properties and structural features. This guideline helps to predict that poor absorption or

permeation of orally administered substances are more likely if the compound meets the following criteria: molecular mass is more than 500 Da; high lipophilicity (expressed as cLogP is greater than 5); more than 5 hydrogen bond donors; and more than 10 hydrogen bond acceptors. In this chapter, we screened inhibitors against *M. tuberculosis* DXS using a previously established *in vitro* enzyme assay (2).

I.5.B. Materials and Methods

Materials. [2–^{14}C]pyruvate (50mCi/mmol) was purchased from NEN Life Science products Inc. (Boston MA). AG1–X2 anion exchange (chloride form) was obtained from BioRad (Hercules, CA). D–Glyceraldehyde and GAP were purchased from Sigma Aldrich (St. Louis, MO) and TPP was purchased from ICN (Costa Mesa, CA). Silica gel $_{60}$ F254 aluminum backed TLC plates were purchased from EM Science (Darmstadt, Gemany). All other reagents and solvents were of at least analytical grade.

Expression and purification of the recombinant Rv2682c. BL21(DE3) cells harboring pET28a(+)::*Rv2682c* were grown at 37°C in LB broth medium containing kanamycin (50 μg/ml) to an OD_{600} ~0.6 with aeration. The culture was allowed to cool on ice and the expression was induced by adding 0.5 mM IPTG for 16 hours at 20°C with shaking. Cells were harvested by centrifugation at 8,000 × *g* for 10 minutes and stored at –70°C overnight. The frozen cells were resuspended in a lysis buffer (2ml/gm of wet weight of cells) containing 50 mM MOPS (pH 7.9), 10 mM $MgCl_2$, 15% glycerol and 1 mM β–mercaptoethanol and 1mg/ml lysozyme, broken by sonication using a Sanyo Soniprep

150 (Integrated Services, TCP Inc, Palisades Park, NJ) on ice and centrifugated at 27,000 × *g* at 4°C for 30 minutes. The volume of the supernatant was adjusted to 30 ml and imidazole was added to achieve a final concentration of 5 mM. A packed volume of 0.75 ml of Histidine–select nickel affinity gel (Sigma Aldrich, St. Louis, MO) pre–equilibrated with lysis buffer was added to the resulting solution and rocked at 4 °C for 20 minutes. A small column (BioRad) was packed with the slurry and the column was washed sequentially with 2 ml of lysis buffer followed by 50 ml of washing buffer containing 50 mM MOPS (pH 7.9), 1 mM $MgCl_2$, 10% glycerol and 1 mM β–mercaptoethanol. The hexa–histidine tagged recombinant Rv2682c was eluted with washing buffer containing linear gradient of 50 mM to 200 mM imidazole and each fraction was analyzed by SDS–PAGE. The fractions containing hexa–histidine tagged recombinant Rv2682c were pooled, concentrated and desalted on a PD–10 column (Amersham, Piscataway, NJ). Recombinant Rv2682c was then concentrated by ultrafiltration using a 5 kDa molecular weight cutoff Centricon (Millipore, Bedford, MA). Final storage buffer contained 20% glycerol in a final concentration and resulting mixture was aliquot and stored at –70°C.

The *in vitro* DXS assay using GAP. Activity was monitored essentially as previously described (2). The reaction mixtures contained 250 mM MOPS (pH 7.9), 5 mM TPP, 120 μM [2–^{14}C]pyruvate, 59 pmols of purified DXS and various concentrations of GAP (0 to 50 μM) in a final volume of 75 μl. The reactions were incubated at 37°C for 30 minutes and terminated by heating at 80°C for 3 minutes. Following centrifugation at 13,000 × *g* for 5 minutes, the residual pellet was discarded and the supernatant was transferred to new tubes. The aliquots were counted by a liquid scintillation counter and spotted on

Silica gel $_{60}$ TLC plates. The [^{14}C] labeled products were developed with a solvent system of n–propanol/ethyl acetate/ H_2O (6:1:3, v/v/v) to separate from [2–^{14}C]pyruvate (10) and identified the locations of the product by the Bioscan Imaging System. To confirm the identity of the product, an aliquot of the products, [^{14}C]DXP, were treated with bovine alkaline phosphatase, and spotted on Silica gel $_{60}$ TLC plates.

The *in vitro* DXS assay using glyceraldehyde. The reaction mixture contained 100 mM MOPS (pH 7.9), 5 mM TPP, 120 μM [2–^{14}C]pyruvate, 26 mM glyceraldehyde and 59 pmols of purified DXS in a final volume of 75 μl. The reactions were started by adding purified DXS, incubated at room temperature for 30 minutes, and terminated by adding 1ml 50% methanol. The reaction mixtures were then loaded into an anion exchanger, AG1–X2, in the form of 1.5 ml bed volume in a Pasteur pipette at room temperature. The product, [^{14}C]DX was eluted with 5 ml 50% methanol. The eluates were dried under N_2, resuspended in 500 μl 50% methanol and 300 μl of which was subjected to be counted by liquid scintillation spectrometry. Aliquots were also spotted on Silica gel $_{60}$ TLC plates and the plates were developed in n–propanol/ethyl acetate/ H_2O (6:1:3, v/v/v) as previously described (10). The locations of eluting radiolabeled product were identified using a Bioscan System 200 Imaging System (Bioscan Inc., Washington, D.C.).

Determining the IC_{50} values of the chemical compounds tested. Thirty six transition state mimicking compounds and twenty reported TK inhibitors, designed and supplied from the UIC, were tested. All compounds were supplied at 12.8 mM concentration dissolved in DMSO. They were first tested at 200 μM, if they showed inhibitory activity,

then detailed inhibition curves were generated. The *in vitro* enzyme assay using glyceraldehyde was employed to evaluate their inhibitory effects. Selected inhibitors were used at concentrations of 0, 8, 16, 32, 64, 128, 256, and 512 μM to determine their mode of inhibition and IC_{50} values were calculated using GraFit 5.0. The negative control (without purified DXS and without compound) and positive control (with purified DXS and without compound) containing the same volume of DMSO as that of the individual chemical compounds should be included. All assays were started by adding purified DXS and terminated by adding 1ml 50% of methanol. Nonlinear regression analysis was done using SigmaPlot V.8.02A.

Other procedures. The reactions were performed under conditions that were linear for both time and concentration of purified recombinant DXS and all values are averages of triplicated assays. Protein concentrations were estimated using a BCA Protein Assay Kit (Pierce, Rockford. IL). Radioactivity was measured in Ecolume (ICN, Costa Mesa, CA) using a Beckman (Fullerton, CA) LS 6500 liquid scintillation spectrometer.

I.5.C. Results

Expression and purification of *M. tuberculosis* DXS. Rv2682c was cloned, expressed, and purified in *E. coli* as a fusion protein bearing a hexa–histidine tag. The purified *M. tuberculosis* DXS was estimated to be at least 95% pure by 12% SDS–PAGE analysis and was active. A clear band was observed corresponding to molecular weight (67.8 kDa) consistent with the expected size with a hexa–histidine tag. Western blot analysis with

anti–histidine antibody confirmed the single band corresponds to DXS. 59 pmols of purified DXS were used for the *in vitro* enzyme assay to screen the compounds.

Optimization of the *in vitro* enzyme assay with purified *M. tuberculosis* DXS. In the *in vitro* enzyme assays using glyceraldehyde, the product of the reaction was easily isolated from [2–^{14}C]pyruvate by using the anion exchange column (AG1–X2) (Fig.I.5.2). We have confirmed that the eluted radiolabeled material from the AG1–X2 column contained only the product, [^{14}C]DX, and that [2–^{14}C]pyruvate was completely removed (Fig.I.5.2). The radioactivity of the eluting product was proportional to the amount of purified DXS used.

Determining the inhibitory effects of the selected compounds. Thirty six DXS transition state mimicking compounds and twenty previously reported TK inhibitors were tested. Their structures are summarized in Table I.5.1 and Table I.5.2. Three (#19, #21, and #29) from the former group and seven (#37, #39, #40, #41, #46, #52, and #55) from the latter group showed significant inhibitory effects on the *M. tuberculosis* DXS. The detailed inhibition curves of the selected compounds are shown in Fig.I.5.3 and Fig.I.5.4. Compound #19 (3–deaza thiamin diphosphate, Deaza–TPP) showed the greatest inhibitory effect as expected based on the previously reported data (12). However, Deaza–TPP must have high affinities with all the mammalian enzymes requiring TPP as a cofactor, resulting in mammalian cell toxicity. Beside compound #19, compounds #21 and #29 showed comparable effects with IC_{50} values of 13 μM and 24 μM, respectively (Table I.5.3). The structures of #21 and #29 contain benzene ring and furan ring.

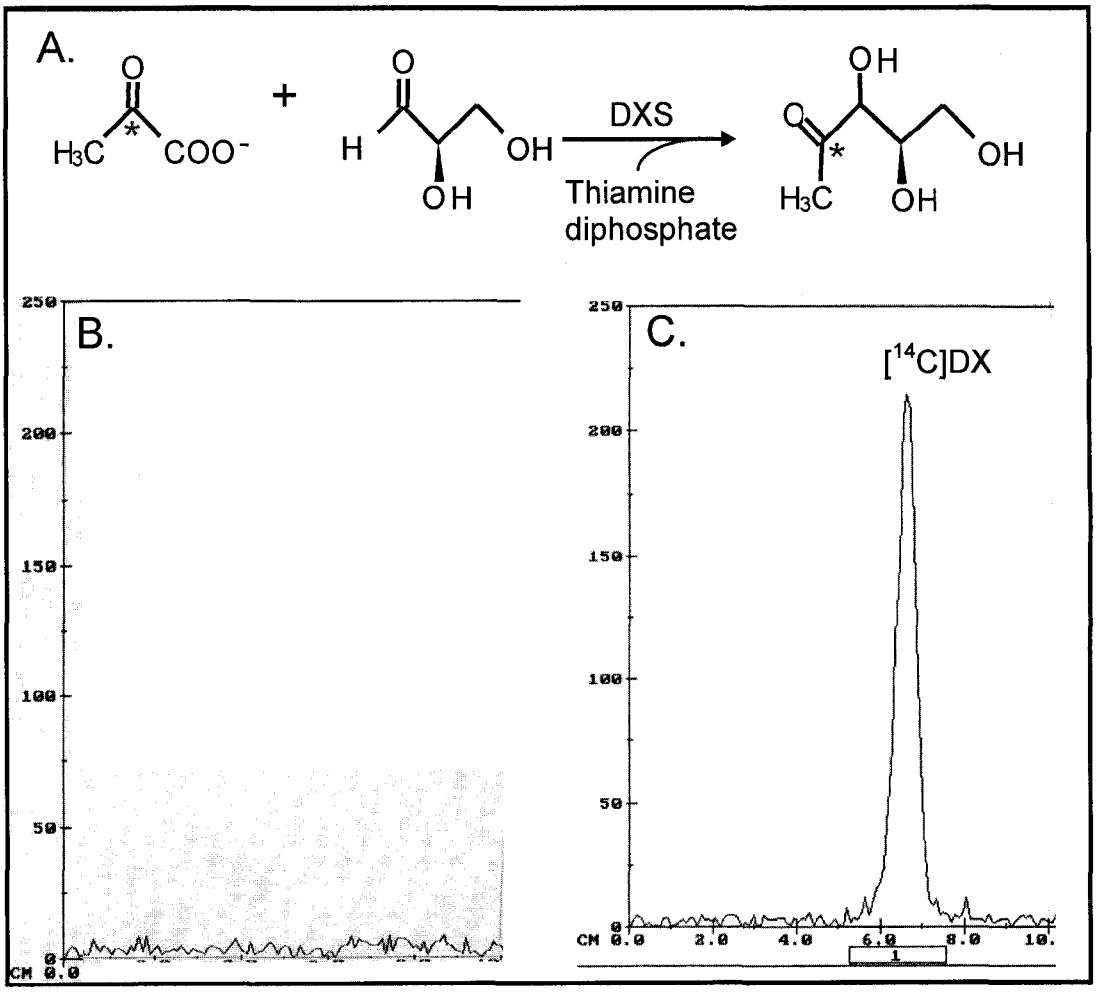

FIGURE I.5.2. ***In vitro* enzyme assay with glyceraldehyde**. When the reaction mixtures contained [2–^{14}C]pyruvate and glyceraldehyde, the product, [^{14}C]DX, can be isolated by AG1–X2 anion exchanger and identified by the Bioscan. A. The proposed reaction catalyzed by DXS. B. The Bioscan image of the eluate from AG1–X2 column of the reaction mixtures without the active DXS enzyme. C. The Bioscan image of the eluate from AG1–X2 column of the reaction mixtures with active DXS enzyme. A single peak was identified and corresponds to [^{14}C]DX. Asterisks indicate the position of the radioisotope.

TABLE I.5.1. **Transition state mimicking compounds**

ID	Structure	ID	Structure
#1	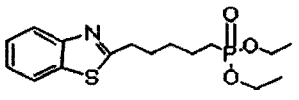	#7	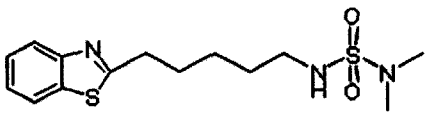
#2	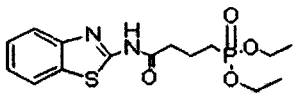	#8	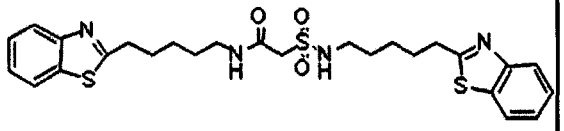
#3	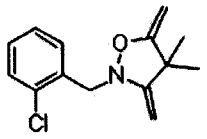	#9	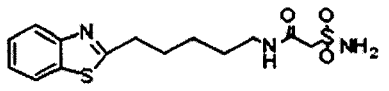
#4	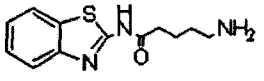	#10	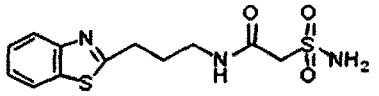
#5	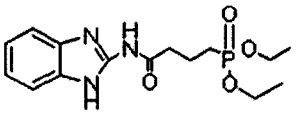	#11	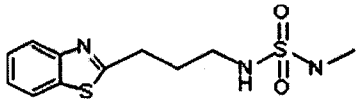
#6	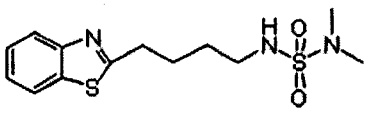	#12	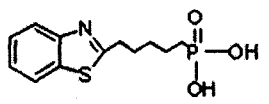

ID	Structure	ID	Structure
#13	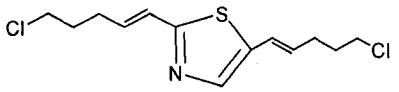	#19	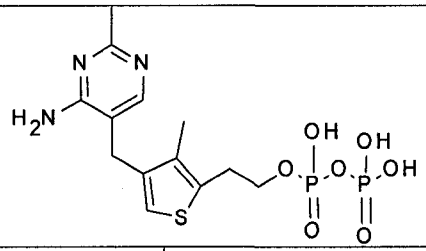
#14	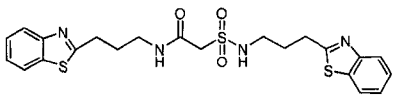	#20	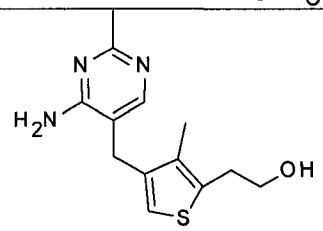
#15	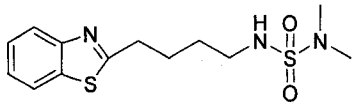	#21	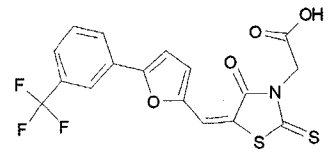
#16	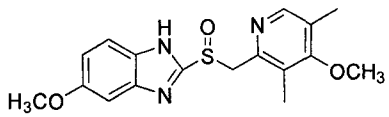	#22	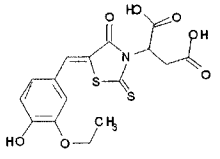
#17	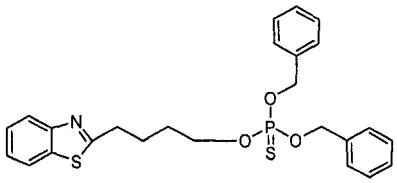	#23	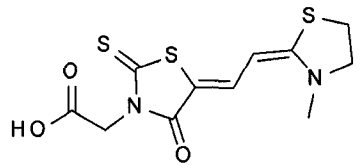
#18	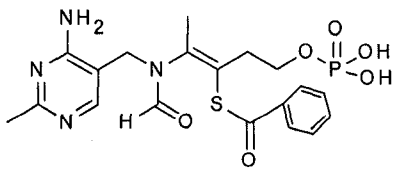	#24	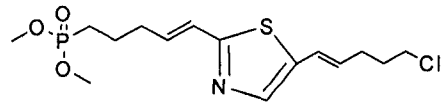

ID	Structure	ID	Structure
#25	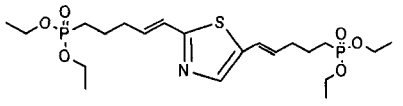	#31	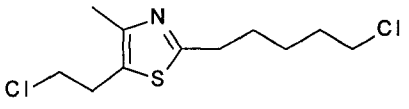
#26	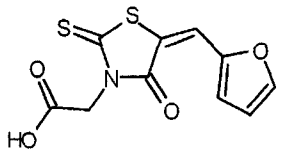	#32	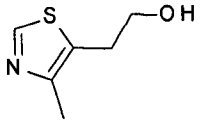
#27	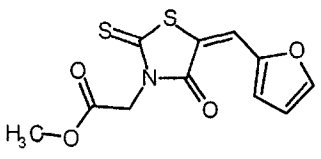	#33	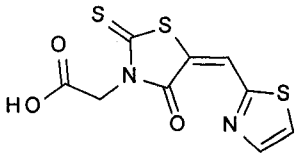
#28	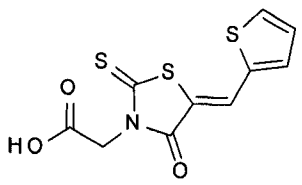	#34	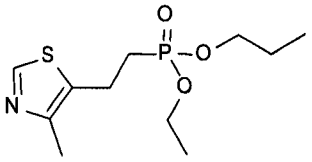
#29	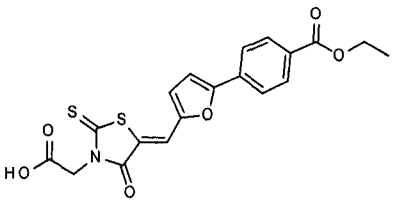	#35	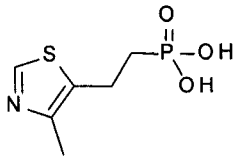
#30	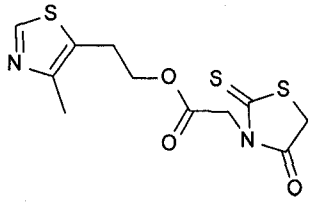	#36	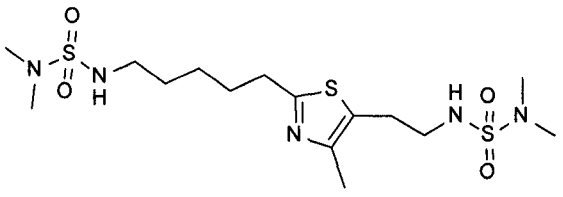

TABLE I.5.2. **Reported transketolase inhibitors**

ID	Structure	ID	Structure
#37	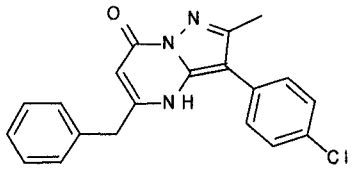	#43	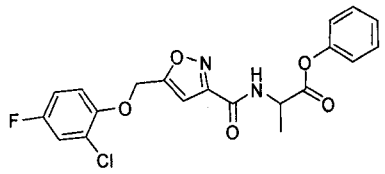
#38	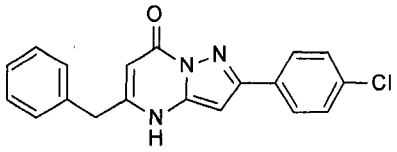	#44	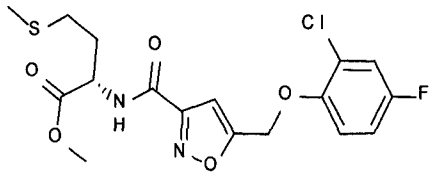
#39	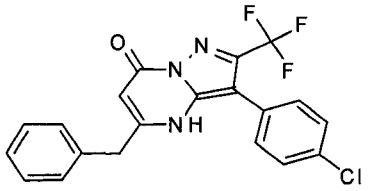	#45	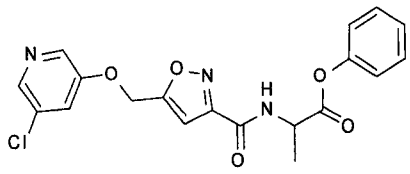
#40	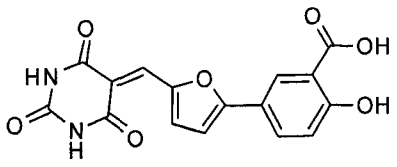	#46	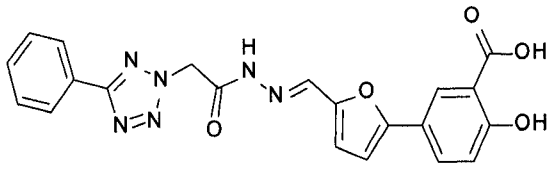
#41	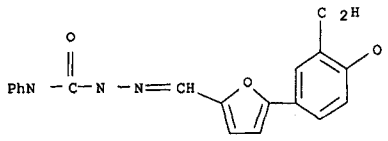	#47	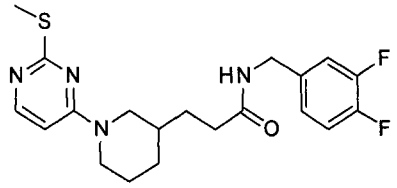
#42	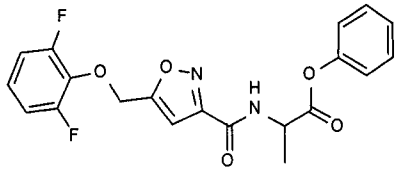	#48	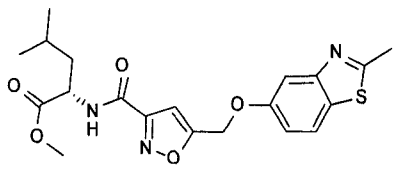

ID	Structure	ID	Structure
#49	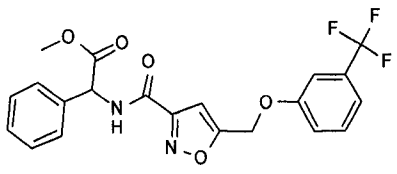	#53	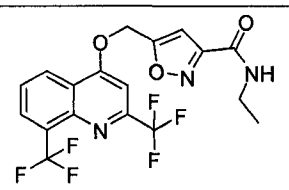
#50	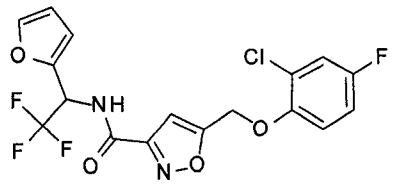	#54	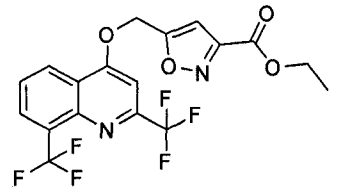
#51	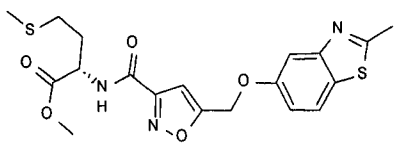	#55	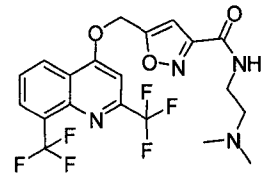
#52	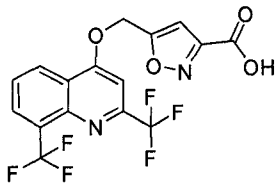	#56	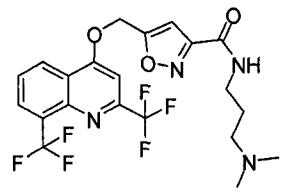

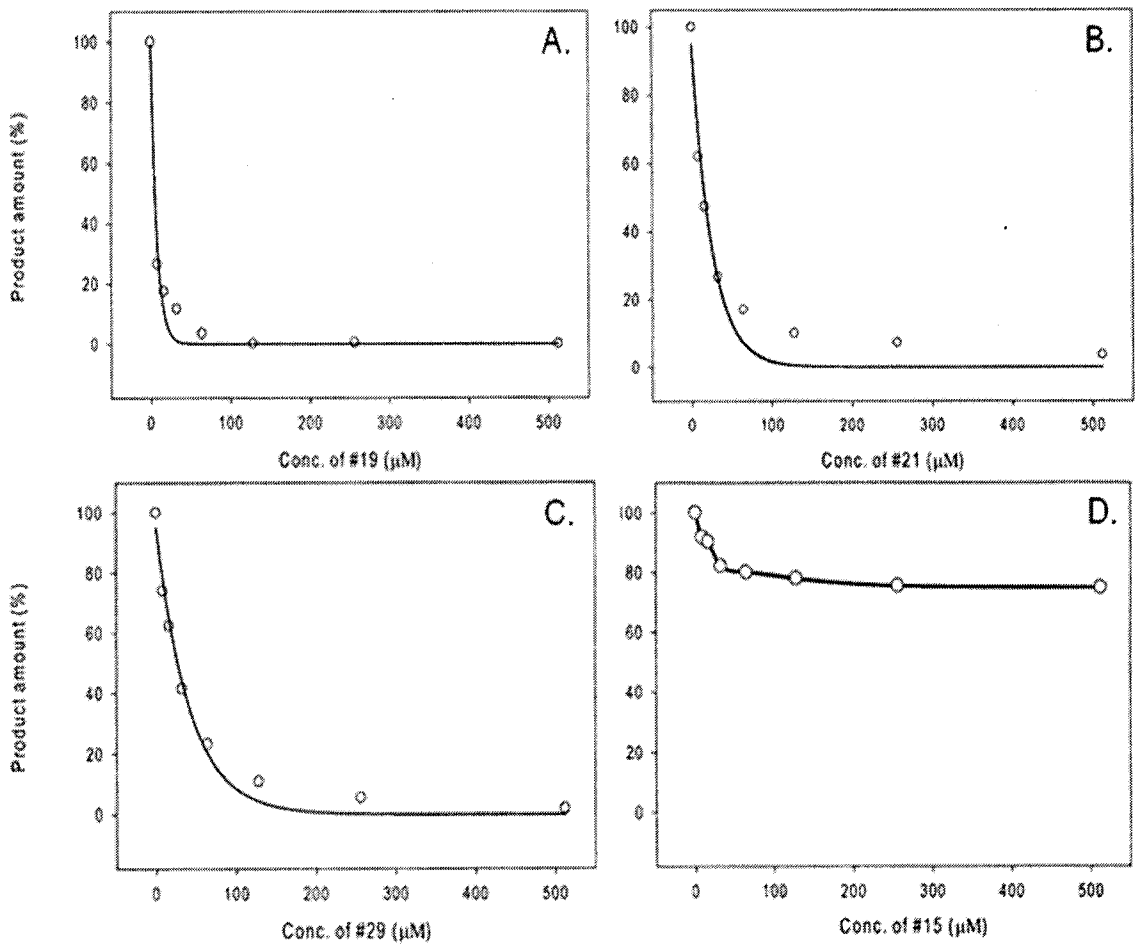

FIGURE I.5.3. **Inhibition curves of the selected transition state mimicking compounds**. The *in vitro* assay using glyceraldehyde was employed to generate their inhibition curves according to the concentrations (0 ~ 512 μM). The inhibition curves were drawn using Sigma Plot and IC_{50} values were calculated using GraFit 5.0.13. The amount of purified *M. tuberculosis* DXS in each reaction mixture was 59 pmols. A. compound #19, B. compound #21, C. compound #29, and D. compound #15.

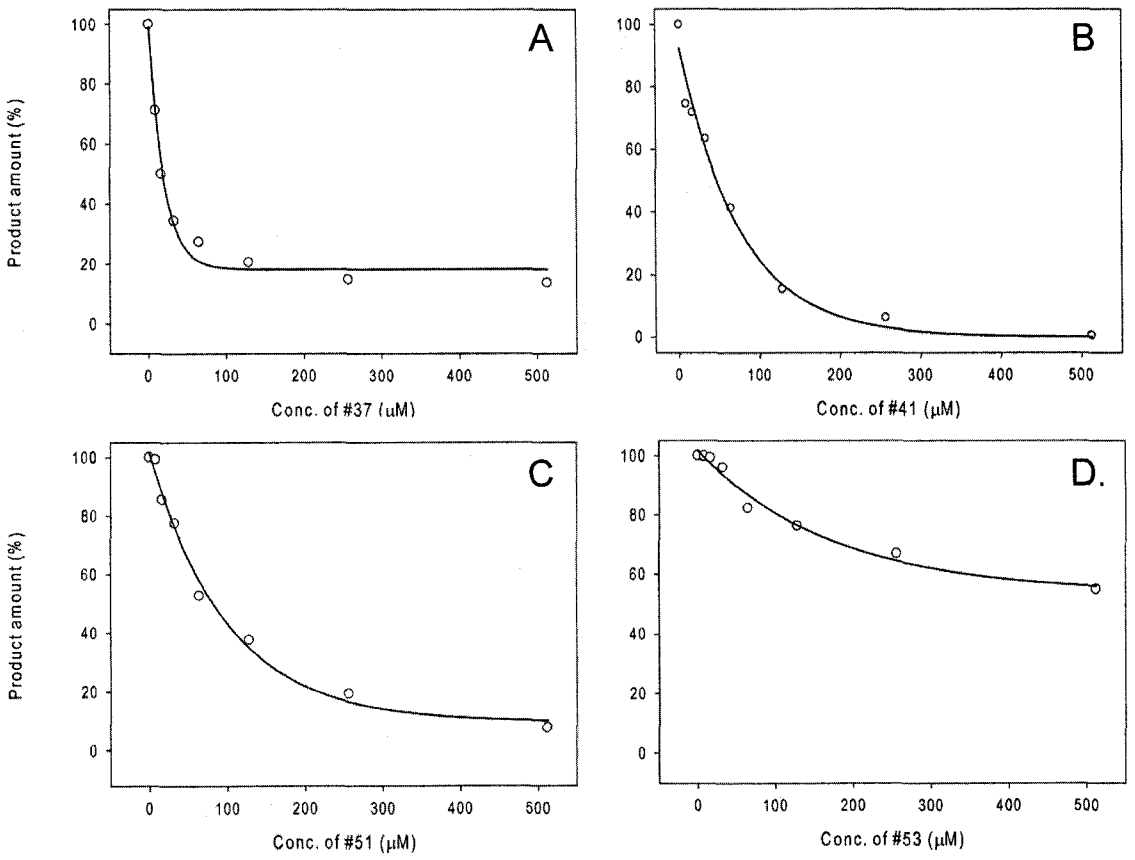

FIGURE I.5.4. **Inhibition curves of the selected reported TK inhibitors.** The *in vitro* assay using glyceraldehyde was employed to generate their inhibition curves according to the concentrations (0 ~ 512 μM). The inhibition curves were drawn using Sigma Plot and IC_{50} values were calculated using GraFit 5.0.13. The amount of purified *M. tuberculosis* DXS in each reaction mixture was 59 pmols. A. compound #37, B. compound #41, C. compound #51, and D. compound #53.

However, #26 and #27, although they are structurally similar to compounds #21 and #29, showed no inhibitory effects (data not shown).

Among twenty reported TK inhibitors tested, the compounds #37 and #39 showed the greatest inhibitory effects with IC_{50} values of 34 μM and 14 μM, respectively (Fig. I.5.4, Table I.5.3). The structures of #37 and #39 indicate that the chloride group at 3–position of benzene ring is preferred (Table I.5.2). Compound #38 showed no effect on the DXS activity, suggesting that the linkage pattern of the benzene ring is also one of crucial factors determining inhibitory effects. The IC_{50} values of selected compounds are summarized in Table I.5.3.

Determining the synergistic effects of compounds #39 and #46. Compounds #39 and #46 showed high inhibitory effects with different properties. Compound #39 showed lower IC_{50} value (14 μM) than that of compound #46 (40 μM). However, DXS activity was maintained at over 10% at even the high concentration (512 μM) of #39. On the contrary, compound #46 abolished the DXS activity at 200 μM concentration. When they were co–treated, the IC_{50} value was improved to 11 μM (of each concentration) and the DXS activity was almost abolished at 50 μM of each concentration (Fig. I.5.5), suggesting that compounds #39 and #46 interact with *M. tuberculosis* DXS in different modes.

TABLE I.5.3. **Summary of IC_{50} values and structures of the selected compounds**

Compound ID	IC_{50} (μM)	Compound ID	IC_{50} (μM)
#14 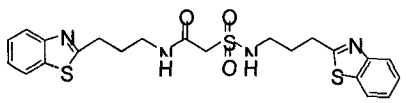	**73**	#17 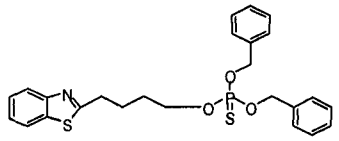	**61**
#19 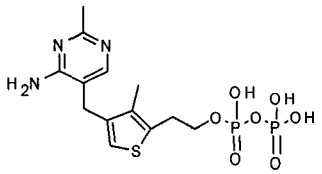	**2**	#21 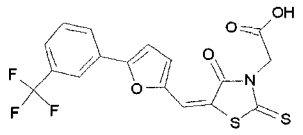	**13**
#29 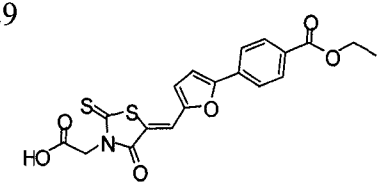	**24**	#37 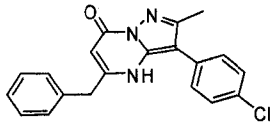	**34**
#39 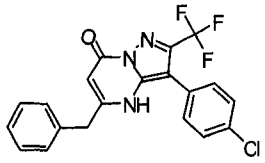	**14**	#40 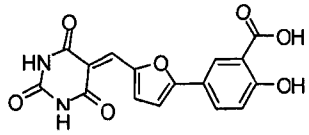	**96**
#41 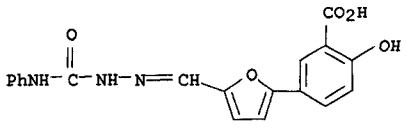	**63**	#46 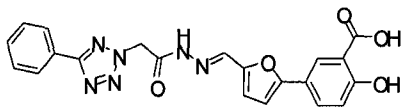	**41**
#52 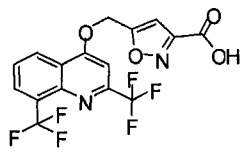	**73**	#55 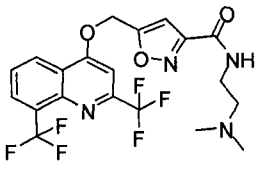	**133**

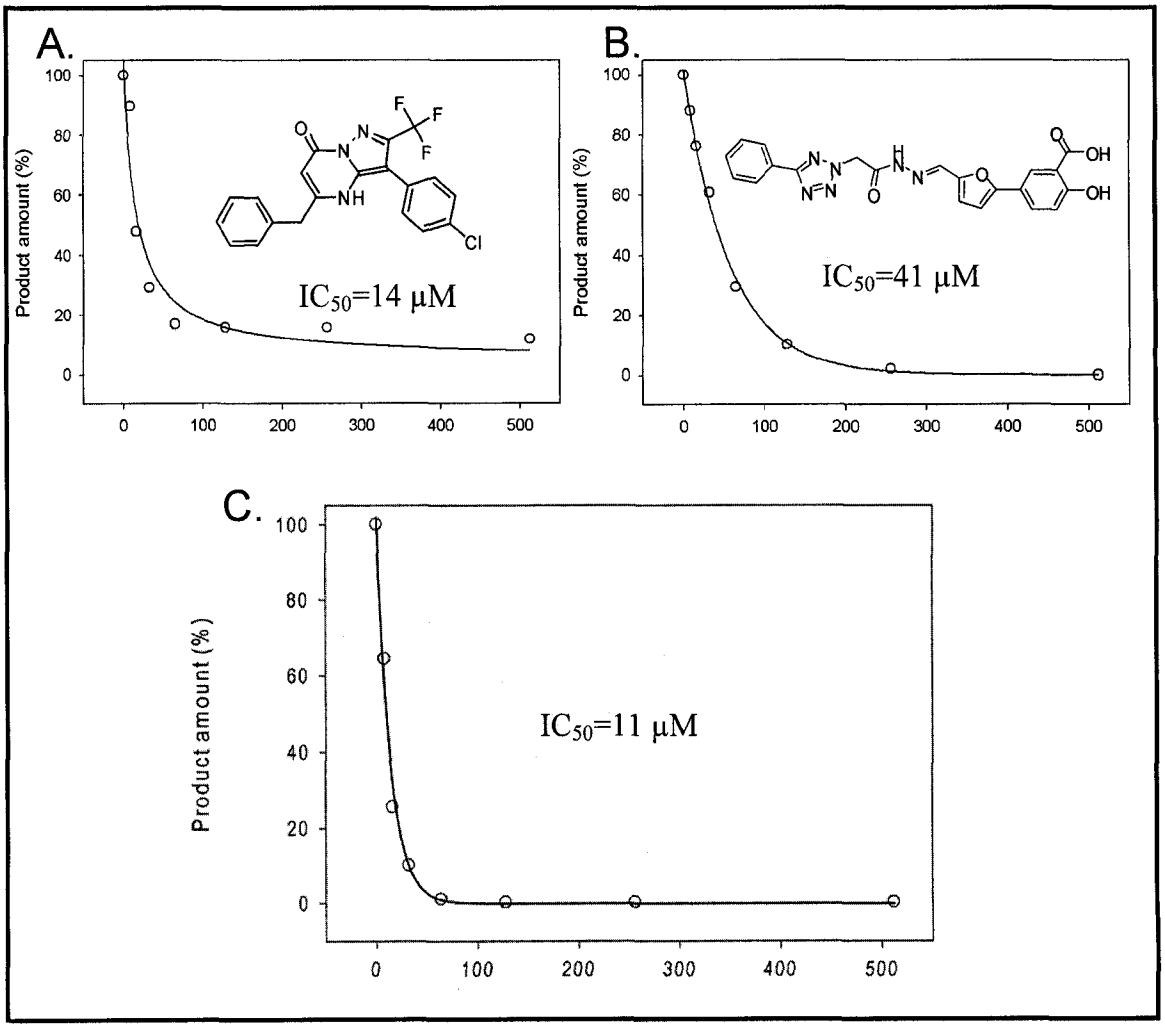

FIGURE I.5.5. **Inhibition curves of the co–treatment with two compounds #39 and #46.** A. The inhibition curve of compound #39 against *M. tuberculosis* DXS showed 14 μM for its IC_{50} value. B. The inhibition curve of compound #46 against *M. tuberculosis* DXS indicated 41 μM for its IC_{50} value. C. When compounds #39 and #46 were combined, the inhibition curves showed 11μM of each compound for the IC_{50} value.

I.5.D. Discussion

In an effort to mine new pharmacophores for TB therapeutics, we optimized previously established *in vitro* assay of the *M. tuberculosis* DXS and screened the lead compounds from small directed compound libraries designed and generated at UIC. We sought the specific inhibitors against the *M. tuberculosis* DXS. The transition state mimicking compounds and reported TK inhibitors have shown inhibitory effects on the DXS activity. A relatively small amount of compounds screening involving fifty six substances identified twelve compounds that inhibited the DXS activity with IC_{50} values between 2 to 133 μM (Table I.5.3). Among the twelve selected compounds, five compounds (#19, #21, #37, #39, and #46) showed IC_{50} values below 50 μM. We considered these to be reasonable starting structure for identifying and modifying candidates as lead compounds. Despite the highest inhibitory effects, Deaza–TPP (#19) is anticipated to have mammalian cell toxicity due to the interactions with a broad range of enzymes such as pyruvate decarboxylase, E1 subunit of pyruvate dehydrogenase, α–ketoglutarate dehydrogenase (1, 12). The catalytic reactions of them also require TPP. The mechanisms of E1 subunit of pyruvate dehydrogenase include deprotonation of TPP, attack on the carbonyl group of the substrate to give 2–lactyl TPP, decarboxylation from the substrate to give the enamine intermediate, and finally release of products (1, 18). Deaza–TPP has been shown to be an exceptionally strong inhibitor of both TPP–dependent enzymes, with much tighter binding capacity to those enzymes (8, 12). Therefore, the most potent substance other than #19, #39 (IC_{50}, 14 μM), was chosen for further modification. These syntheses are ongoing at UIC.

Inhibition curves obtained from the compounds #39 and #46 co–treatment inferred that the two compounds have different enzymatic properties (Fig.I.5.5). The K_m and V_{max} values of glyceraldehyde were determined when the compounds were treated or not. We concluded that compound #39 is the non–competitive inhibitor defined as the substance that binds to a site other than the active site to interfere the product generation, and compound #46 is uncompetitive inhibitor defined as the substance binding to only the substrate–enzyme binding complex to interfere the product generation (data not shown).

M. tuberculosis DXS shows 38% identity with *E. coli* DXS. This high level of conservation suggests a strong maintenance of primary structures, indicating the crucial motifs may contribute the structural conformation in the catalytic properties of the DXS. Therefore, the *M. tuberculosis* DXS structure is likely similar to that of *E. coli* DXS (19). The DXS active site is located at the interface inside of the monomer, with no direct contribution from the other monomer of the DXS dimeric structure. In contrast, the catalytic active site of TK superfamily (E1 subunit of pyruvate dehydrogenase, pyruvate decarboxylase, and α–ketoglutarate dehydrogenase) is located at the interface formed by the two identical subunits of two monomers (5, 9, 13). The main reason for the differences in the active sites is coming from the domain organization with exceptionally longer linker region between the two domains (20). Although, *M. tuberculosis* DXS and TK superfamily commonly require TPP as a cofactor with a similar catalytic mechanisms, there are huge differences in the active site position or the arrangement of subunits which are the major clues for reducing the cytotoxicity (2).

The disruption of the *A. thaliana* CLA1 gene, the ortholog of the DXS (3), showed an albino phenotype due to an arrest of chloroplast development and an absence of accumulation of carotenoid and cholorophylls (11). Himar1–based transposon mutagenesis study showed the *M. tuberculosis* DXS is predicted to be essential for *M. tuberculosis* viability, *in vivo* (14). In addition, DXS is exclusively present in pathogenic bacteria such as *M. tuberculosis* and in protozoan *P. falciparum*. There is no evidence that mammals have a DXS homolog. Hence, the development of small molecule inhibitors for the *M. tuberculosis* DXS constitutes a novel approach in the treatment of TB. To our knowledge, this is the first study that describes a specific inhibitor of the *M. tuberculosis* DXS activity that is capable of interfering with essential functions of key intermediates in bacterial metabolism. 1–deoxy–D–xylulose 5–phosphate is the crucial substrate for the biosynthesis of not only the major building blocks of isoprenoids but also thiamine and pyridoxol (10, 15). The lead compounds that efficiently inhibit the first enzyme in the MEP pathway of *M. tuberculosis* and thereby blocked the biological activity of the system as a whole would be potential substances for anti–tuberculosis drugs.

I.5.E. References

1. **Aevarsson, A., K. Seger, S. Turley, J. R. Sokatch, and W. G. Hol.** 1999. Crystal structure of 2-oxoisovalerate and dehydrogenase and the architecture of 2-oxo acid dehydrogenase multienzyme complexes. Nat Struct Biol **6:**785-92.
2. **Bailey, A. M., S. Mahapatra, P. J. Brennan, and D. C. Crick.** 2002. Identification, cloning, purification, and enzymatic characterization of

Mycobacterium tuberculosis 1-deoxy-D-xylulose 5-phosphate synthase. Glycobiology **12:**813-20.

3. **Crowell, D. N., C. E. Packard, C. A. Pierson, J. L. Giner, B. P. Downes, and S. N. Chary.** 2003. Identification of an allele of CLA1 associated with variegation in *Arabidopsis thaliana.* Physiol Plant **118:**29-37.
4. **Duncan, K.** 2003. Progress in TB drug development and what is still needed. Tuberculosis (Edinb) **83:**201-7.
5. **Gerhardt, S., S. Echt, M. Busch, J. Freigang, G. Auerbach, G. Bader, W. F. Martin, A. Bacher, R. Huber, and M. Fischer.** 2003. Structure and properties of an engineered transketolase from maize. Plant Physiol **132:**1941-9.
6. **Hahn, F. M., L. M. Eubanks, C. A. Testa, B. S. Blagg, J. A. Baker, and C. D. Poulter.** 2001. 1-Deoxy-D-xylulose 5-phosphate synthase, the gene product of open reading frame (ORF) 2816 and ORF 2895 in *Rhodobacter capsulatus.* J Bacteriol **183:**1-11.
7. **Jorgensen, W. L.** 2004. The many roles of computation in drug discovery. Science **303:**1813-8.
8. **Leeper, F. J., D. Hawksley, S. Mann, C. Perez Melero, and M. D. Wood.** 2005. Studies on thiamine diphosphate-dependent enzymes. Biochem Soc Trans **33:**772-5.
9. **Lindqvist, Y., G. Schneider, U. Ermler, and M. Sundstrom.** 1992. Three-dimensional structure of transketolase, a thiamine diphosphate dependent enzyme, at 2.5 A resolution. Embo J **11:**2373-9.
10. **Lois, L. M., N. Campos, S. R. Putra, K. Danielsen, M. Rohmer, and A. Boronat.** 1998. Cloning and characterization of a gene from *Escherichia coli* encoding a transketolase-like enzyme that catalyzes the synthesis of D-1-deoxyxylulose 5-phosphate, a common precursor for isoprenoid, thiamin, and pyridoxol biosynthesis. Proc Natl Acad Sci U S A **95:**2105-10.
11. **Mandel, M. A., K. A. Feldmann, L. Herrera-Estrella, M. Rocha-Sosa, and P. Leon.** 1996. CLA1, a novel gene required for chloroplast development, is highly conserved in evolution. Plant J **9:**649-58.

12. **Mann, S., C. Perez Melero, D. Hawksley, and F. J. Leeper.** 2004. Inhibition of thiamin diphosphate dependent enzymes by 3-deazathiamin diphosphate. Org Biomol Chem **2:**1732-41.

13. **Nilsson, U., Y. Lindqvist, R. Kluger, and G. Schneider.** 1993. Crystal structure of transketolase in complex with thiamine thiazolone diphosphate, an analogue of the reaction intermediate, at 2.3 A resolution. FEBS Lett **326:**145-8.

14. **Sassetti, C. M., D. H. Boyd, and E. J. Rubin.** 2003. Genes required for mycobacterial growth defined by high density mutagenesis. Mol Microbiol **48:**77-84.

15. **Schwender, J., M. Seemann, H. K. Lichtenthaler, and M. Rohmer.** 1996. Biosynthesis of isoprenoids (carotenoids, sterols, prenyl side-chains of chlorophylls and plastoquinone) via a novel pyruvate/glyceraldehyde 3-phosphate non-mevalonate pathway in the green alga *Scenedesmus obliquus*. Biochem J **316 (Pt 1):**73-80.

16. **Sprenger, G. A., U. Schorken, T. Wiegert, S. Grolle, A. A. de Graaf, S. V. Taylor, T. P. Begley, S. Bringer-Meyer, and H. Sahm.** 1997. Identification of a thiamin-dependent synthase in *Escherichia coli* required for the formation of the 1-deoxy-D-xylulose 5-phosphate precursor to isoprenoids, thiamin, and pyridoxol. Proc Natl Acad Sci U S A **94:**12857-62.

17. **Tomioka, H., K. Sato, T. Shimizu, and C. Sano.** 2002. Anti-*Mycobacterium tuberculosis* activities of new fluoroquinolones in combination with other antituberculous drugs. J Infect **44:**160-5.

18. **Wang, J., H. Dong, S. Li, and H. He.** 2005. Theoretical study toward understanding the catalytic mechanism of pyruvate decarboxylase. J Phys Chem B **109:**18664-72.

19. **Xiang, S., G. Usunow, G. Lange, M. Busch, and L. Tong.** 2006. Crystal structure of 1-deoxy-D-xylulose 5-phosphate synthase (DXS), a crucial enzyme for isoprenoids biosynthesis. J Biol Chem.

20. **Xiang, S., G. Usunow, G. Lange, M. Busch, and L. Tong.** 2007. Crystal structure of 1-deoxy-D-xylulose 5-phosphate synthase, a crucial enzyme for isoprenoids biosynthesis. J Biol Chem **282:**2676-82.

Chapter II.

The methylerythritol phosphate pathway of three selected human pathogens: *Salmonella typhi*, *Vibrio cholerae*, and *Burkholderia mallei*: potential as drug targets

Chapter II–1.

Literature review on the need for new therapeutics in the context of bioterrorism

II.1.A. Threat of bioterrorism and biodefense efforts

A bioterrorist attack is defined as the deliberate release of a wide range of microorganisms or plants, or their components for the purpose of causing human illness, social disruption, and finally heavy casualties in a large percentage of those exposed (15). Although often perceived as a recent invention, bioterrorism has been used for hundreds of years. In 1346, the Tatars catapulted the dead bodies of plague victims into Kaffa (now Ukraine), causing the second European plague pandemic (10). Following World War II, several countries still maintain biological weaponizing programs. However, the United States, Canada, and the United Kingdom all ended their biological weaponizing programs by the early 1970s. In 1972, most countries in the world signed the contract for Biological and Toxin Weapons Convention, which called for the termination of all offensive biological weaponizing programs and agreed with the destruction of existing biological weapon stocks. Despite these positive events, the Soviet Union continued to expand its biological weaponizing programs throughout the 1980s and early 1990s (2, 20). The biggest concern of the biological weaponizing programs included the production of large amounts of smallpox virus and its development of mechanisms to weaponize it. The naturally occurring smallpox incidence was already eradicated and the production of its vaccine was also stopped as early as 1980, could give bioterrorists the most suitable opportunity to use smallpox virus as an agents of bioterrorist attacks (27).

Terrorists would possibly employ bioterrorism because they would be capable of producing a threat that was extremely difficult to detect, did not cause illness for several hours to several days, and had the potential to cause considerable mortality within the

target population. Bioterrorism has recently become an important political issue in the world. The budget of the United States for counter–bioterrorism is rising exponentially–for example, it rose from 91 million dollars in 1998 to 336 million dollars in 2000 (30). The budget has consistently increased and was more than 4 billion dollars in 2006. The recent elevation of the threat of bioterrorism has heightened awareness of terrorism in the public and has increased fears of an attack around the world. For example, the introduction of *Bacillus anthracis* (the causative agent of Anthrax) into the United States postal system in October 2001 alerted the public to the realities of bioterrorism.

There are several facts contributing to the growing danger of bioterrorism: only minute amounts of the biological agents are needed to generate mass casualties; the amount of various agents required to manufacture biological weapons are easily acquired with currently available technology; only limited financing and training are required to establish a biological weaponizing programs; and biological weapons are relatively easy to deliver (3). Out of the thousands of biological agents capable of causing human infection, only a few are ideal agents for bioterror weapons production because they are required to be disseminated easily, be stable and infectious upon environmental exposure, and be available for mass production (31).

Acts of bioterrorism can potentially be extremely devastating due to the fact that they invade the protective immune system of a target population by introducing agents to which that population is immunologically naïve (16). After this protective immunity has been weakened by a large scale biological attack, high levels of morbidity will most likely overwhelm public health facilities. The intense fear of bioterrorism is also likely to cause mass terror in the population exposed, which can ultimately lead to socioeconomic

disruption. Moreover, many bioterrorism agents harbor genetic mutations which confer resistance to current antibiotics. Therefore, basic laboratory research should include study of pathogen biology and identification of potential targets for new diagnostics, vaccines, chemotherapheutics, and new therapeutic strategies for preventing and suppressing these biothreats.

II.1.B. Ranking of bioweapons

The September 11th, 2001attacks upon the World Trade Center and the Pentagon were particularly terrifying due to the sheer scale of the operation. As part of the governmental response aimed at preventing future terrorist attacks, NIAID (National Center of Allergy and Infectious Diseases), part of NIH (National Institutes of Health) and the CDC (Centers for Disease Control and Prevention), an agency within the United States Department of Health and Human Services identified several organisms with the greatest potential for use by bioterrorists (1). They independently classified or categorized the potential biological agents hierarchically into three priority categories (A, B, and C) based on the degree of dangers they pose and the likelihood that they will be used as an agent of bioterrorism (Table II.1.1, Table II.1.2). The classifications performed by the CDC and the NIAID are very similar. However, NIAID includes antimicrobial resistance bacterial diseases such as MDR–TB to the category C. These classes are organized based on the overall public health impact of the agent (disease and mortality rates), public perception of the agent, dissemination potential, the need and/or availability for special health preparations, and the ability of the agent to be converted into a weapon.

TABLE II.1.1. **NIAID Category A, B, and C priority pathogens.**

Category A agents	**Category B agents**
Bacteria *Bacillus anthracis* (anthrax) *Clostridium botulinum* toxin (botulism) *Francisella tularensis* (tularemia) *Yersinia pestis* (plague) Viral hemorrhagic fevers Arenaviruses Bunyaviruses Flaviruses Filoviruses *Variola major* (smallpox) and other related pox viruses	Bacteria *Burkholderia pseudomallei* (Melioidosis) *Burkholderia mallei* (Glanders) *Clostridium perfringens* (Epsilon toxin) *Coxiella burnetii* (Q fever) *Brucella species*(Brucellosis) *Staphylococcus aureus* (Enterotoxin B) *Rickettsia prowazekii* (Epidemic typhus) *Chlamydia psittaci* (Psittacosis) Food and Waterborne Pathogens *Escherichia coli* O157:H7, *Vibrio cholera,* *Salmonella species,* *Shigella species,* *Listeria monocytogenes,* *Campylobacter jejuni,* *Yersinia enterocolitica* Viral encephalitis West Nile virus Eastern equine encephalitis viruses Western equine encephalitis viruses Venezuelan equine encephalitis viruses La Crosse viruses Japanese encephalitis viruses Kyasanur forest California encephalitis viruses *Ricinus communis* Castor bean (Ricin toxin)
Category C agents	
Bacteria *Mycobacterium tuberculosis* (Multidrug– resistant Tuberculosis) Other *Rickettsia* (Rickettsial diseases) Viruses Nipah virus (Nipah virus encephalitis) Tickborne hemorrhagic fever viruses Crimean–Congo hemorrhagic fever virus (Crimean–Congo hemorrhagic fever) Tickborne encephalitis viruses (Tick–borne encephalitis) Yellow fever virus (Yellow fever) Influenza viruses (Flu) Rabies virus (Rabies) Other Hantaviruses	

[http://pathema.tigr.org/pathema/AbcGenomes.shtml].

TABLE II.1.2. **CDC categorization of potential bioweapons.**

Category A Agents	
Disease or Symptoms	Causative pathogen
Anthrax	*Bacillus anthracis*
Botulism	*Clostridium botulinum toxin*
Plaque	*Yersinia pestis*
Smallpox	*Variola major*
Tularemia	*Fransicella tularensis*
Viral hemorrhagic fever	filoviruses and arenaviruses
Category B Agents	
Disease or Symptoms	Causative pathogen
Brucellosis	*Brucella* species
Glanders	*Burkholderia mallei*
Melioidosis	*Burkholderia pseudomallei*
Psittacosis	*Chlamydia psittaci*
Q fever	*Coxiella burnetii*
Typhoid fever	*Rickettsia prowazekii*
Viral encephalitis	alphaviruses
Water safety threat	*Vibrio cholerae, Cryptosporidium parvum*
Food safety threat	*Salmonella* species, *Escherichia coli, Shigella*
Category C Agents	
Disease or Symptoms	Causative pathogen
Nipah encephalitis	Nipah virus
Hemorrhagic fever with renal syndrome	Hanta virus
Hemorrhagic fever	Tick borne hemorrhagic fever viruses

Category A agents

Category A agents are considered the highest threat to the public (9). They include some of the deadliest organisms known to man. These agents are easily disseminated from person to person and have the potential to cause widespread panic. Most importantly, the agents belonging to this category have the ability to cause a high level of mortality, with a huge impact on public health. In 1998, the Working Group on Civilian Biodefense (an expert panel of academic and government leaders) defined that the agents within Category A would cause the largest scale illness and death if employed as biological weapons and therefore are of critical importance and require immediate attention (9).

The threat of these bioterrorism agents has made clinicians and scientists aware of limitations in the current understanding of the diseases caused by a number of virulent pathogens. For a variety of reasons, most illnesses caused by bioterrorism agents are rarely seen by physicians (23): anthrax, plague, and tularemia occur only in rural areas; filoviral hemorrhagic fevers are limited to central Africa; small pox has long been eradicated; and the infections caused by aerosolized encephalitis viruses do not occur under natural conditions. Although large number *in vitro* or *in vivo* models for the research have been developed to investigate their pathogenic mechanisms, these diseases remain poorly characterized. The events of September 11th, 2001 and the subsequent anthrax scare serve as reminders that any method used by terrorists will likely be unpredictable and will be aimed at circumventing current surveillance technology and national security policy. For example, although airplane hijackings were well known

prior to September 11th, 2001, the use of hijacked airplanes as missiles was completely unexpected. Likewise, the use of anthrax in the form of a white powder sent through the U.S. Portal Service as a means of bioterrorism was highly unpredictable at the time (11).

Category B agents

Category B agents have lower potential for large–scale dissemination with resulting mass illness of a target population and are considered as causing less illness and death than those caused by Category A agents. Therefore, Category B agents are expected to have a lower medical and public health impact (31). These agents also have lower general public awareness and relatively fewer special public health preparedness efforts have been taken. Several agents in this category even utilize unusual dissemination routes, such as food or water (*Salmonella* spp. or *Vibrio cholerae*), through which many bioterrorist attacks have been performed. Therefore, Category B agents require elevated improvement in medical preparedness, surveillance, and diagnostic capabilities to prevent a mass impact. For Category B agents, public health awareness efforts will focus on identified deficiencies, such as improving awareness and enhancing surveillance or chemotherapeutic capabilities.

Category C agents

Biological agents that are currently not believed to present a high bioterrorism risk to public health but which could emerge as future threats were placed in Category C (31). These agents are considered as part of the ongoing development of public health infrastructure for detecting and addressing emerging infectious diseases. The agents in

this category have also high potential for morbidity and mortality and include pathogens that could be engineered for mass dissemination. Therefore, Category C agents are further assessed for their potential to threaten large populations as additional information becomes available on their epidemiology. In addition, special epidemiologic and laboratory capacity are required to be maintained to assist in the investigation of naturally occurring outbreaks due to Category C "emerging" agents. Various established programs for the emerging infectious diseases and unexplained illnesses augment the overall bioterrorism preparedness efforts for many Category C agents (36).

II.1.C. Three bacterial pathogens selected by relative phylogenetic distance of the enzymes in the MEP pathway from those of *E. coli*

Salmonella typhi

Although most agents considered likely to be used for bioterrorism would be disseminated by way of an aerosol, it is also possible for pathogens to be food or water borne. In fact, intentional exposure to *S. typhimurium* has already been used in the United States for religious reasons (38). Bacteria of the genus *Salmonella* account for the majority of food poisoning cases in the United States, with the CDC estimating 1.4 million cases, annually. This bacteria is a rod–shaped, Gram–negative, and facultative anaerobe that infects a wide variety of organisms. *Salmonella* infection results in either typhoid fever or gastroenteritis (13, 14, 18, 37). Typhoid fever was a potent killer prior to the development of modern antibiotics. The pathogen's potential for development as a

weapon and the severe gastrointestinal symptoms it inflicts on the majority of infected individuals have led to its classification as a Category B agent.

The ease with which it can be isolated and cultured makes *Salmonella* a unique bioterrorist threat. Although death due to infection is rare, the pathogen can cause death or severe complications in immune compromised individuals. *Salmonella* is generally not considered a life–threatening bioterrorist agent because of the relative transience of symptoms and low mortality. However, this pathogen does have potential as a powerful psychological tool for rogue groups wishing to spread panic and cause doubt concerning food safety. Chemotherapeutics provide a method of treating *Salmonella* victims, but the range of antibiotics that can be used for successful treatment has narrowed because of the rise of antibiotic–resistant strains. Although mortality rates would probably not be as high now owing to improved supportive measures, steps must be taken to deal with the possibility of purposeful incorporation of multiple drug resistance into *S. typhi* (8, 22, 26, 33, 35).

Vibrio cholerae

V. cholerae is the causative agent of a gastrointestinal disease, cholera, notorious for its characteristic dehydration and massive diarrhea (32). The disease devastated the world's populations in the 19th and early 20th centuries, causing major pandemics. Although vaccines and therapeutic measures have been developed, the disease is still a public health concern in parts of Africa, Asia, and Latin America, where health care is poor and extreme poverty precludes adequate medical care and preventive measures (25). An epidemic in central Africa in 1994 and 1995 presented case fatality rates as high as

30% in areas where medical facilities were limited. Clinical symptoms appear soon after *V. cholerae* secretes the cholera toxin. Because of cholera's severe symptoms, its high rate of fatality when untreated, and the potential for genetic engineering of a more potent strain, *V. cholerae* represents a significant threat as a biological weapon (21, 28).

Wild–type cholera is not likely to be used as a bioterror weapon because of the ease of treatment, the almost complete lack of fatality (less than 1%) if treated properly, and its inability to survive drying and temperatures above 70°C. Also, it is not contagious. It is, therefore, likely that cholera would be used against military rather than civilian populations. Although not lethal with proper treatment, cholera is a powerful incapacitating agent for a military force for 24 – 72 hours (34). The use of appropriate antibiotics in cholera infection can reduce both the severity of diarrhea and the duration of the disease by speeding the excretion of *V. cholerae*. Tetracycline, furazolidane, and doxycycline have all been recommended for use against cholera. However, over the past decade, *V. cholerae* has steadily developed resistance to those antibiotics. Recent studies of cholera strains indicate the presence of mutated genes requiring multidrug resistance, especially among O1 strains. The O139 strains have been shown to be more resistant to antimicrobial agents. *V. cholerae* has developed resistance even to fluoroquinones, thus eliminating their use in disease treatment (24), frustrating clinicians because fluoroquinones have not yet been used against cholera infection. Antibiotic resistance genes are generally located on plasmids, suggesting that *V. cholerae* can acquire the plasmids from resistant, avirulent, gut coliforms in the organisms it infects (6, 7, 17).

Burkholderia mallei

Infection with *B. mallei* causes a subcutaneous infection known as farcy or can disseminate to cause the condition known as glanders. *B. mallei* is a nonmotile, Gram–negative bacillus that is an obligate animal pathogen (29). In humans, acute infection with *B. mallei* is characterized by necrosis of the tracheobronchial tree, pustular skin lesions, and either a febrile pneumonia, if the organism was inhaled, or signs of sepsis and multiple abscesses, if the skin was the portal of entry. At the turn of the 20th century, glanders was a common cause of death among horses, and there were secondary, often fatal, infections in humans. Because of the lethal and contagious nature of the disease, *B. mallei* was considered an ideal agent for biologic warfare (5).

Glanders may have been the first biologic agent employed in the 20th century (39). The destruction of livestock and the transmission caused by *B. mallei* were highly contagious. It is suspected that bioterrorists have attempted to develop an aerosolized form of antibiotic resistant *B. mallei* that could become a biological weapon as potent as Category A agents (4, 5).

II.1.D. The requirements of new antibiotics for counter–bioterrorism initiatives

The early recognition and prevention of a bioterrorist event are essential for ensuring effective containment and reduction of casualties (19). Enhanced disease surveillance activities including development of novel broad–spectrum antibiotics targeting biological pathogens will also be required for rapid response to bioterrorist

events. The diversity of existing biological agents and the various possibilities through genetic recombination preclude simple therapeutic counter-measures to bioterrorist attacks. The former Soviet Union is known to have developed at least 30 biological agents for use as potential weapons (20). Although the average period for developing a new drug or vaccine is around 8 to 10 years, one report suggests only 1 to 3 years may be needed for developing a novel bioweapon (12). Thus, an urgent requirement exists for continuous investigation and development of broad–spectrum antibiotics. Existing counter-measures for known threats are very restricted. There are only a few vaccines available or in production and a limited number of classes of antibiotics. For example, the smallpox vaccine is highly effective, but it elicits dangerous and potentially lethal complications in a number of individuals, and because it is a live-attenuated vaccine, it poses a significant risk for all immune compromised individuals (12). The limited availability of an antibiotic is also one of the huge concerns with respect to future threats, especially in light of the increase in the number of new and re-emerging infectious diseases and the marked rise in resistance to current existing antibiotics. When the issue of drug–resistance is laid against the dearth of new classes of antibiotics being developed and commercialized today, it becomes clear that there is no effective public health response against bioterrorism. New antibiotic discovery is dependent on an understanding of the fundamental cellular mechanisms that are conserved over the broad–spectrum of human pathogens and are required for their viability. In this context, the enzymes in the MEP pathway of bacterial pathogens which are likely used as bioterrorism agents have been elucidated and validated as potential drug targets.

II.1.E. References

1. 2003. From the Centers for Disease Control and Prevention. Additions to terrorism preparedness compendium. JAMA **289:**296.
2. **Alibek, K.** 1999. The Soviet Union's anti-agricultural biological weapons. Ann N Y Acad Sci **894:**18-9.
3. **Atlas, R. M.** 2002. Bioterriorism: from threat to reality. Annu Rev Microbiol **56:**167-85.
4. **Bossi, P., A. Guihot, and F. Bricaire.** 2005. [Emerging or re-emerging infections that can be used for bioterrorism]. Presse Med **34:**149-55.
5. **Coenye, T., and J. J. LiPuma.** 2003. Molecular epidemiology of *Burkholderia* species. Front Biosci **8:**e55-67.
6. **Colmer, J. A., J. A. Fralick, and A. N. Hamood.** 1998. Isolation and characterization of a putative multidrug resistance pump from *Vibrio cholerae*. Mol Microbiol **27:**63-72.
7. **Dalsgaard, A., A. Forslund, A. Petersen, D. J. Brown, F. Dias, S. Monteiro, K. Molbak, P. Aaby, A. Rodrigues, and A. Sandstrom.** 2000. Class 1 integron-borne, multiple-antibiotic resistance encoded by a 150-kilobase conjugative plasmid in epidemic *Vibrio cholerae* O1 strains isolated in Guinea-Bissau. J Clin Microbiol **38:**3774-9.
8. **Dargatz, D. A., and J. L. Traub-Dargatz.** 2004. Multidrug-resistant *Salmonella* and nosocomial infections. Vet Clin North Am Equine Pract **20:**587-600.
9. **Darling, R. G., C. L. Catlett, K. D. Huebner, and D. G. Jarrett.** 2002. Threats in bioterrorism. I: CDC category A agents. Emerg Med Clin North Am **20:**273-309.
10. **Derbes, V. J.** 1966. De Mussis and the great plague of 1348. A forgotten episode of bacteriological warfare. JAMA **196:**59-62.

11. **Ferguson, N. E., L. Steele, C. Y. Crawford, N. L. Huebner, J. C. Fonseka, J. C. Bonander, and M. J. Kuehnert.** 2003. Bioterrorism web site resources for infectious disease clinicians and epidemiologists. Clin Infect Dis **36:**1458-73.

12. **Greenfield, R. A., and M. S. Bronze.** 2003. Prevention and treatment of bacterial diseases caused by bacterial bioterrorism threat agents. Drug Discov Today **8:**881-8.

13. **Hadjichristodoulou, C., E. Nikolakopoulou, K. Karabinis, E. Karakou, A. Markogiannakis, C. Panoulis, M. Lampiri, and P. Tassios.** 1999. Outbreak of *Salmonella* gastroenteritis among attendees of a restaurant opening in Greece, June 1998. Euro Surveill **4:**72-75.

14. **Hall, R.** 2002. Outbreak of gastroenteritis due to *Salmonella typhimurium* phage type I 35a following consumption of raw egg. Commun Dis Intell **26:**285-7.

15. **Han, S. Z., M. C. Alfano, W. J. Psoter, and E. D. Rekow.** 2003. Bioterrorism and catastrophe response: a quick-reference guide to resources. J Am Dent Assoc **134:**745-52.

16. **Henderson, D. A.** 1999. The looming threat of bioterrorism. Science **283:**1279-82.

17. **Huda, M. N., J. Chen, Y. Morita, T. Kuroda, T. Mizushima, and T. Tsuchiya.** 2003. Gene cloning and characterization of VcrM, a Na+-coupled multidrug efflux pump, from *Vibrio cholerae* non-O1. Microbiol Immunol **47:**419-27.

18. **Janssen van Doorn, K., D. Pierard, and H. Spapen.** 2006. Acute renal dysfunction in *salmonella* gastroenteritis. J Clin Gastroenterol **40:**910-2.

19. **Kaufmann, A. F., M. I. Meltzer, and G. P. Schmid.** 1997. The economic impact of a bioterrorist attack: are prevention and postattack intervention programs justifiable? Emerg Infect Dis **3:**83-94.

20. **Knoph, J. T., and K. S. Westerdahl.** 2006. Re-evaluating Russia's biological weapons policy, as reflected in the Criminal Code and Official Admissions: insubordination leading to a president's subordination. Crit Rev Microbiol **32:**1-13.

21. **Kochi, S. K., K. P. Killeen, and U. S. Ryan.** 2003. Advances in the development of bacterial vector technology. Expert Rev Vaccines **2:**31-43.

22. **Kohbata, S., M. Takahashi, and E. Yabuuchi.** 1983. Lactose-fermenting, multiple drug-resistant *Salmonella typhi* strains isolated from a patient with postoperative typhoid fever. J Clin Microbiol **18:**920-5.

23. **Kortepeter, M. G., and G. W. Parker.** 1999. Potential biological weapons threats. Emerg Infect Dis **5:**523-7.

24. **Krishna, B. V., A. B. Patil, and M. R. Chandrasekhar.** 2006. Fluoroquinolone-resistant *Vibrio cholerae* isolated during a cholera outbreak in India. Trans R Soc Trop Med Hyg **100:**224-6.

25. **Lan, R., and P. R. Reeves.** 2002. Pandemic spread of cholera: genetic diversity and relationships within the seventh pandemic clone of *Vibrio cholerae* determined by amplified fragment length polymorphism. J Clin Microbiol **40:**172-81.

26. **Lee, K., D. Yong, J. H. Yum, Y. S. Lim, H. S. Kim, B. K. Lee, and Y. Chong.** 2004. Emergence of multidrug-resistant *Salmonella enterica* serovar *typhi* in Korea. Antimicrob Agents Chemother **48:**4130-5.

27. **Levy-Bruhl, D., and N. Guerin.** 2001. The use of smallpox virus as a biological weapon: the vaccination situation in France. Euro Surveill **6:**171-8.

28. **Lipp, E. K., A. Huq, and R. R. Colwell.** 2002. Effects of global climate on infectious disease: the cholera model. Clin Microbiol Rev **15:**757-70.

29. **Manzeniuk, I. N., E. A. Galina, V. V. Dorokhin, I. Kalachev, V. N. Borzenkov, and E. A. Svetoch.** 1999. [*Burkholderia mallei* and *Burkholderia pseudomallei*. Study of immuno- and pathogenesis of glanders and melioidosis. Heterologous vaccines]. Antibiot Khimioter **44:**21-6.

30. **Marshall, E.** 1999. Bioterror defense initiative injects shot of cash. Science **283:**1234-5.

31. **Moran, G. J.** 2002. Threats in bioterrorism. II: CDC category B and C agents. Emerg Med Clin North Am **20:**311-30.

32. **Morris, J. G., Jr., J. L. Picardi, S. Lieb, J. V. Lee, A. Roberts, M. Hood, R. A. Gunn, and P. A. Blake.** 1984. Isolation of nontoxigenic *Vibrio cholerae* O

group 1 from a patient with severe gastrointestinal disease. J Clin Microbiol **19:**296-7.

33. **Olsen, S. J., M. Ying, M. F. Davis, M. Deasy, B. Holland, L. Iampietro, C. M. Baysinger, F. Sassano, L. D. Polk, B. Gormley, M. J. Hung, K. Pilot, M. Orsini, S. Van Duyne, S. Rankin, C. Genese, E. A. Bresnitz, J. Smucker, M. Moll, and J. Sobel.** 2004. Multidrug-resistant *Salmonella Typhimurium* infection from milk contaminated after pasteurization. Emerg Infect Dis **10:**932-5.

34. **Ongradi, J.** 2002. [Microbial warfare and bioterrorism]. Orv Hetil **143:**1935-9.

35. **Rabatsky-Ehr, T., J. Whichard, S. Rossiter, B. Holland, K. Stamey, M. L. Headrick, T. J. Barrett, and F. J. Angulo.** 2004. Multidrug-resistant strains of *Salmonella enterica Typhimurium*, United States, 1997-1998. Emerg Infect Dis **10:**795-801.

36. **Rotz, L. D., A. S. Khan, S. R. Lillibridge, S. M. Ostroff, and J. M. Hughes.** 2002. Public health assessment of potential biological terrorism agents. Emerg Infect Dis **8:**225-30.

37. **Shpargel, J. S., R. S. Berardi, and D. Lenz.** 1985. *Salmonella typhi* carrier state 52 years after illness with typhoid fever: a case study. Am J Infect Control **13:**122-3.

38. **Torok, T. J., R. V. Tauxe, R. P. Wise, J. R. Livengood, R. Sokolow, S. Mauvais, K. A. Birkness, M. R. Skeels, J. M. Horan, and L. R. Foster.** 1997. A large community outbreak of salmonellosis caused by intentional contamination of restaurant salad bars. JAMA **278:**389-95.

39. **Wheelis, M.** 1998. First shots fired in biological warfare. Nature **395:**213.

Chapter II–2.

Characterization of 4–(cytidine 5'–diphosphate)–2–C–methyl–D–erythritol synthase from Category B bioterrorism agents: *Salmonella typhi, Vibrio cholerae, and Burkholderia mallei*

II.2.A. Introduction

Many bacterial pathogens harbor genetic mutations which confer resistance to current antibiotics (14) and multi–drug resistance is one of the most serious problems for controlling bacterial infection. Therefore, drug development is urgently required. The NIAID and the CDC have divided potential bioterrorism agents into three hierarchical categories, based upon their risks for causing mass casualties in the event of a bioterrorist attack and how easily they can be spread (Table.II.1.1 and Table II.1.2). Category A includes the agents which are considered the highest risk and Category C includes the organisms being considered as the emerging infectious threats (4, 12). Category B includes agents are moderately easy to disseminate, cause moderate morbidity and low mortality (14). Nonetheless, there is an example of terrorists using Category B agents in the United States as recently as 1984. Restaurant salad bars were contaminated with *Salmonella* by the Rajneeshee cult, which sickened hundreds of people in Oregon (8). In another example, members of anti–government groups used ricin toxin in an attempt to assassinate law enforcement agents in Minnesota (9). Generally, most of the successful bioterrorist events recognized to date have used water or food as a vehicle of dissemination.

Salmonella typhi, *Vibrio cholerae* and *Burkholderia mallei* were selected as the representative sources of IspD orthologs because of their relative genetic distances from *M. tuberculosis* IspD. *In silico* studies have shown that *S. typhi*, *V. cholerae*, and *B. mallei* have no homologous enzymes of the MVA pathway, with the exception of *V. cholerae*, which has a HMGR homolog. This suggests that all these organisms utilize the

MEP pathway, exclusively. A multiple alignment of *E. coli* IspD, *M. tuberculosis* IspD, and those of these bacterial pathogens indicated the IspD orthologs possess the conserved amino acids for substrate binding domain as well as catalytic motifs. In addition, IspD has already been reported as an essential enzyme in *E. coli* (20) and is predicted to be essential in *M. tuberculosis* (19). In the present chapter, IspD orthologs from *S. typhi*, *V. cholerae*, and *B. mallei* were identified, purified and characterized for the purpose of developing the HTS assay mining a new broad–spectrum antimicrobial agent. Z′–Factor values were determined to validate the reliability of the HTS assay.

II.2.B. Materials and Methods

Materials. *S. typhi* (700931D) and *V. cholerae* (39315D) chromosomal DNA were purchased from American Type Culture Collection (ATCC). *B. mallei* chromosomal DNA was kindly provided by Dr. Herbert Schweitzer at Colorado State University. All PCR reagents and cloning materials were purchased from Qiagen (Valencia, CA). MEP was purchased from Echelon Research Laboratories, Inc. (Salt Lake City, UT). Histidine–select nickel affinity resin, other chemicals, and solvents which are not otherwise noted were at least analytical grade or higher and obtained from Sigma Aldrich (St. Louis, MO).

PCR amplification and cloning of *ispD* orthologs of *S. typhi*, *V. cholerae* and *B. mallei*. Putative *ispD* gene open reading frames of *S. typhi*, *V. cholerae* and *B. mallei* chromosomes were amplified by using oligonucleotide primers designed based on the

sequences available in Kyoto Encyclopedia of Genes and Genomes (KEGG) (http://www.genome.jp/kegg/). The primers were synthesized by Macromolecular Resources (Colorado State University) and are summarized in Table II.2.1. All the primers contain *Nde*I and *Hin*dIII restriction enzyme sites in the forward and reverse primers, respectively. PCR products were digested with *Nde*I and *Hin*dIII, and ligated into the pET28a(+) vector (EMD Biosciences, Inc., San Diego, CA). Ligation mixtures were used to transform *E. coli* DH5α (Life Technologies, Rockville, MD), plasmids were amplified, and the recombinant IspD plasmids were isolated using a Plasmid Miniprep Kit from Qiagen (Valencia, CA). Three expression constructs were purified and sequences were confirmed by Marcomolecular Resources (Colorado State University).

Expression and purification of the recombinant IspD orthologs. Transformation of BL21(DE3) (Novagen, Madison, WI) with the three constructs created BL21(DE3)[pET28a(+)::*S. typhi ispD*], BL21(DE3)[pET28a(+)::*V. cholerae ispD*] and BL21(DE3)[pET28a(+)::*B. mallei ispD*]. These strains were propagated in LB media supplemented with kanamycin (50 μg/ml) and induced with 0.5 mM IPTG at 20°C for 16 hours. Cells were harvested and disrupted by sonication using a Sanyo Soniprep 150 (Integrated Services, TCP Inc, Palisades Park, NJ) on ice. Recombinant IspD enzymes carrying a hexa–histidine tag were purified by Histidine–select nickel affinity gel (Sigma Aldrich). Recombinant IspD orthologs were eluted using a linear gradient of imidazole (50 to 200 mM) in 50 mM 4–morpholine propane sulfonic acid (MOPS) (pH 7.9), 1 mM $MgCl_2$, 10% glycerol, and 1mM β–mercaptoethanol. Fractions containing recombinant IspD enzymes were pooled and the purified pools desalted by a PD–10 column

TABLE II.2.1. **PCR primers used in this study**. The sequences recognized by restriction enzymes are underlined

Organism	Primer	Sequence	Enzyme
S. typhi	Forward	CATATGAACAACATGACAGCGATTGT	*Nde*I
	Reverse	AAGCTTTCTGATCATGATTTTCCTTATTACG	*Hin*dIII
V. cholerae	Forward	CATATGGCAGCCACTTTATTGGA	*Nde*I
	Reverse	AAGCTTTCGCATTATGCTTTCTCCTG	*Hin*dIII
B. mallei	Forward	CATATGACCTCCCGACTTTTTGCC	*Nde*I
	Reverse	AAGCTTTCAGGAAGCGCGCGCCGGTT	*Hin*dIII

(Amersham, Piscataway, NJ). The recombinant IspD enzymes were concentrated by a 5000 molecular weight cutoff Centricon (Millipore, Bedford, MA).

Preparation of [γ–^{32}P]CTP. [γ–^{32}P]CTP was enzymatically synthesized essentially as described (3). Baker's yeast nucleoside 5'–diphosphate kinase (Sigma Aldrich) was utilized to catalyze the transfer of the [^{32}P]γ–phosphate moiety from [γ–^{32}P]ATP to CDP to generate [γ–^{32}P]CTP. Reaction mixtures contained 40 mM CDP, 5 mM $MgCl_2$, 80 mM Tris–HCl (pH 7.4), 4 units of yeast nucleoside 5'–diphosphate kinase, and 2 mCi [γ–^{32}P]ATP in a final volume of 50 µl. After incubating for 2 hours at room temperature, the mixture was subjected to chromatography on a Benzyl–DEAE cellulose column (1.5 cm × 15 cm) in 10 mM NH_4HCO_3. [γ–^{32}P]CTP was eluted from the column with a linear gradient (250 ml) of 0 – 0.5 M NH_4HCO_3. The eluted radioactive material was detected on a PEI cellulose TLC plate developed with 0.7 M NaH_2PO_4 (pH 3.8). Fractions corresponding to [γ–^{32}P]CTP were combined, concentrated to a volume of 1 ml by rotary evaporation under reduced pressure at 30°C, desalted by gel filtration chromatography on a Sephadex G–10 column (1.5 cm × 30 cm). Fractions containing [γ–^{32}P]CTP were combined, concentrated again, and stored at –20°C.

Radiochemical *in vitro* assay for the activity of IspD orthologs. The IspD catalytic activities were monitored by measuring [^{32}P]PP*i* release using liquid scintillation spectrometry as described in chapter I–3. Reactions were started by the addition of 19 pmols, 19.5 pmols, and 19.3 pmols of IspD orthologs of *S. typhi*, *V. cholerae*, and *B. mallei*, respectively and terminated by adding 200 µl of a slurry of activated charcoal in

10 mM Tris–HCl buffer (pH 8.0). The slurries were then loaded onto an empty spin column to remove residual [γ–^{32}P]CTP retained on the charcoal and to elute [^{32}P]PP*i* by centrifugation at 7,000 rpm for 3 minutes.

Spectrophotometry based *in vitro* assay for the catalytic activities of IspD orthologs. EnzChek® Phosphate Assay Kits (Invitrogen) were utilized to monitor the IspD activity by coupling released PP*i*, as described in chapter I–3 (Fig.I.3.3). This spectrophotometry based *in vitro* assay was performed on 384–well microplates (Costar, Bethesda, MD). The reaction mixtures were the same as those of *M. tuberculosis* IspD (chapter I–3) in a 30 µl final reaction volume. Reactions were incubated at room temperature for 30 minutes and the end point absorbance at 360 nm was determined by Synergy™ HT Multi–Detection Microplate Reader (BioTek instruments).

Determination of enzymatic properties of IspD orthologs. To determine the optimal pH for the activities of IspD orthologs, the reaction buffers (MES, MOPS, Tris, or TAPS) at different pH values containing appropriate counter ions were used. Optimal concentrations for divalent cations were determined in the assay mixtures using different metal ions such as $MgCl_2$, $MnCl_2$, $CaCl_2$ and $ZnCl_2$ at the indicated concentrations. The effect of CTP concentration on activity was determined using a constant concentration of MEP (100 µM) and varying concentrations of CTP. The effect of MEP concentration was determined using a constant concentration of CTP (100 µM) and varying concentrations of MEP. The K_m and V_{max} values of substrates for IspD orthologs were calculated by nonlinear regression analysis (SigmaPlot V. 8.02A).

Z'–Factor. The spectrophotometry based *in vitro* assay could be applied to the HTS assay for screening specific inhibitors. Therefore, Z'–Factor values were determined as described in chapter I–3 for 30 µl reaction volumes. All the steps were performed using an automated fluid transfer system in 384–well microplates (Precision XS microplate sample processor, BioTek instruments).

Other procedures. All enzyme assays were performed in triplicate, under conditions that were linear for both time (up to 30 minutes) and concentration of recombinant IspD orthologs (up to approximately 95 pmols of each). Recombinant protein concentrations were estimated using a BCA protein assay kit (Pierce, Rockford, IL). Radioactivity was measured using a LS6500 liquid scintillation spectrometer (Beckman Coulter Inc). BLAST searches were performed at the National Center for Biotechnology Information (NCBI) Web site using standard protein–protein BLAST. Multiple alignments were performed using the Multalin interface Align show from the Sequence Manipulation suite [http://www.ualberta.ca/~stothard/javascript/index.html] available at the university of Alberta Web site. Clustal W analysis was performed on the European Molecular Biology Network (EMBnet) World Wide Web site, and the unrooted dendrogram was graphically displayed using TreeView version 1.6.1.

II.2.C. Results

Identification of IspD orthologs in Category B agents: *S. typhi*, *V. cholerae*, and *B. mallei*. The amino acid sequences of putative IspD orthologs identified from *S. typhi*, *V.*

cholerae and *B. mallei* chromosomes were aligned and compared with *E. coli* IspD (18) and *M. tuberculosis* IspD (Fig.II.2.1). The *M. tuberculosis* IspD was identified, characterized, and validated as an anti–tuberculosis drug target in chapter I–3. Comparison of the predicted primary sequences of these IspD orthologs of five organisms (*M. tuberculosis*, *E. coli*, *S. typhi*, *V. cholerae*, and *B. mallei*) revealed significant similarities, suggesting that all organisms utilize the MEP pathway as early steps of isoprenoid biosynthesis. The phylogenetic distances could be estimated on the basis of amino acid similarities. The phylogenetic distance between *E. coli* IspD and *S. typhi* IspD was closest with 91 % identity. *V. cholerae* IspD showed 53% identity and *B. mallei* IspD showed 38 % identity with *E. coli* IspD. These three IspD orthologs share conserved crucial amino acids forming catalytic domains and substrate binding sites, suggesting all three open reading frames encode orthologous enzymes of *E. coli* IspD and *M. tuberculosis* IspD (Fig.II.2.1). An unrooted dendrogram obtained from the IspD sequences of ten bacterial pathogens is shown in Fig.II.2.2. *S. typhi* is closest to *E. coli*, *V. cholerae* is intermediate, and *B. mallei* is farthest from *E. coli.* Therefore, *S. typhi*, *V. cholerae* and *B. mallei* were selected as representative sources of IspD for comparison. Three IspD orthologs of *S. typhi*, *V. cholerae*, and *B. mallei* are predicted to encode cytosolic proteins and have the similar molecular masses of around 26 kDa.

Expression and purification of recombinant IspD orthologs from *S. typhi*, *V. cholerae* and *B. mallei*. IspD orthologs of *S. typhi*, *V. cholerae*, and *B. mallei* were overexpressed in *E. coli* with an N–terminal hexa–histidine fusion tag. The recombinant IspD orthologs were highly induced under the conditions tested. Western blot analysis

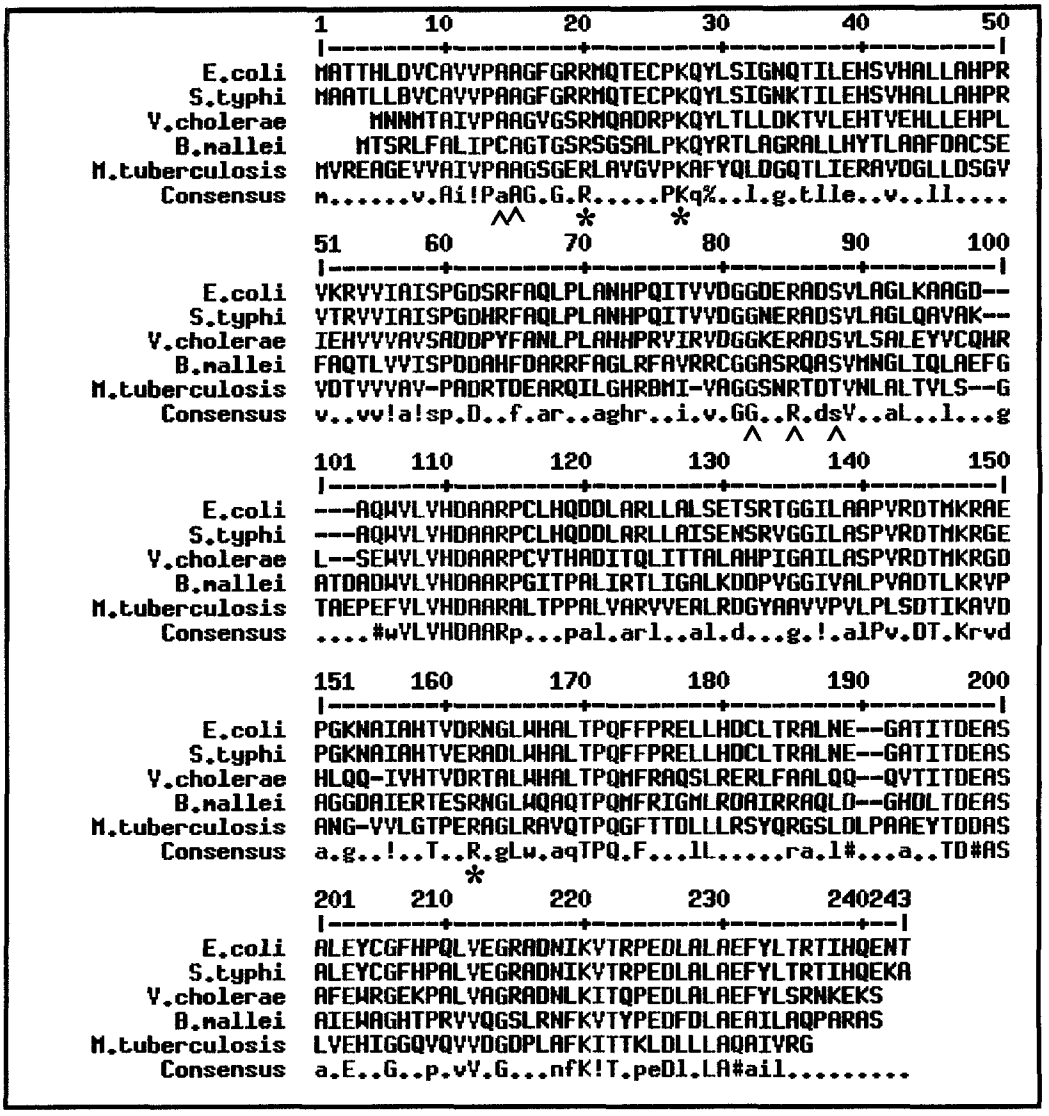

FIGURE II.2.1. **Multiple alignment of IspD amino acid sequences from five bacterial pathogens; *E. coli*, *M. tuberculosis*, *S. typhi*, *V. cholerae* and *B. mallei*.** Identities are indicated by red and similarities are indicated by blue. The identities of the IspD orthologs of *S. typhi*, *V. cholerae*, *B. mallei* and *M. tuberculosis* with *E. coli* IspD were 91%, 53%, 38% and 31% respectively. The conserved amino acids involved in substrate specificity (15) are highlighted with (*). The conserved amino acids related to catalytic activity (15) were highlighted with (^).

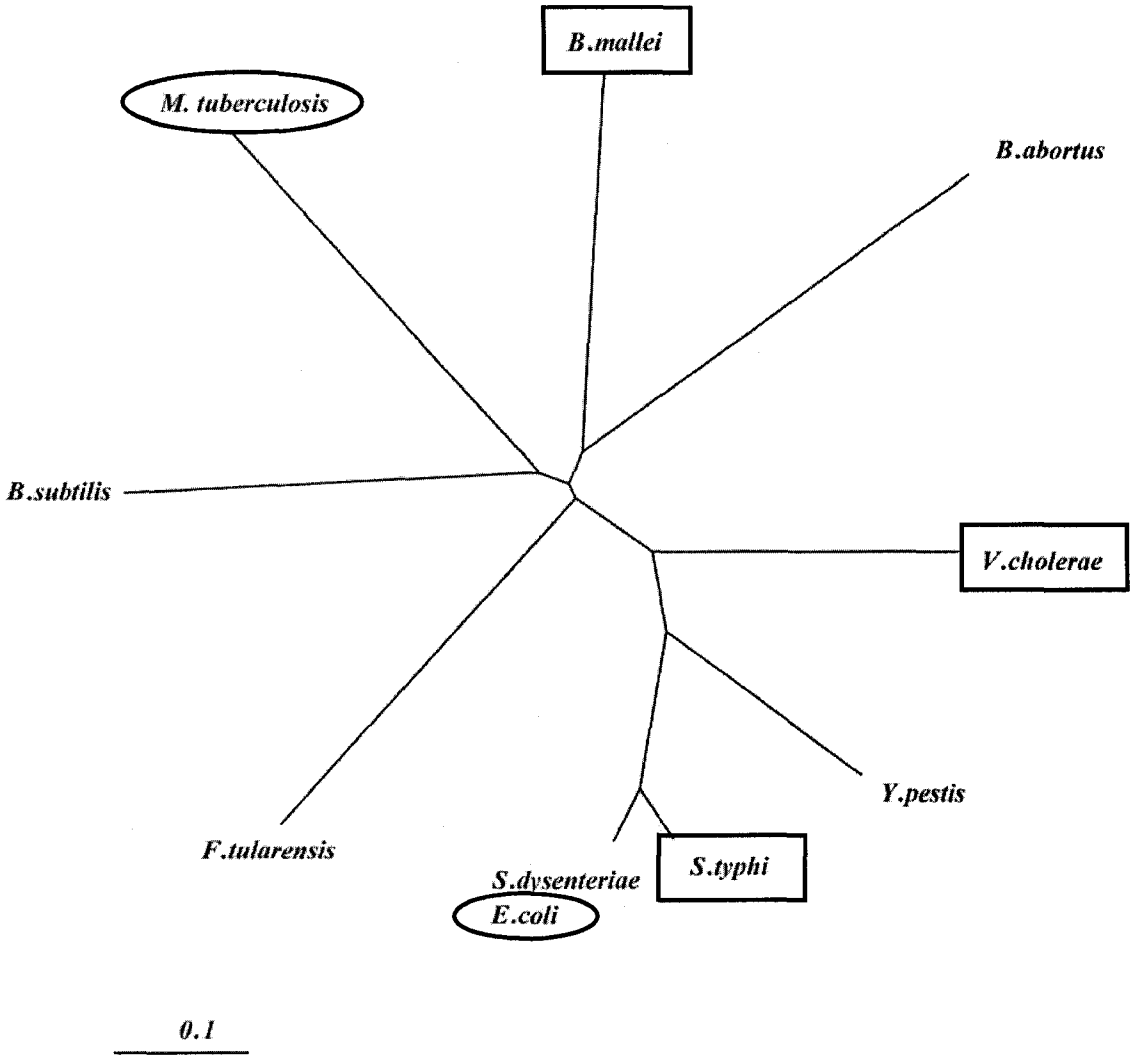

FIGURE II.2.2. **Unrooted dendrogram of IspD orthologs identified from ten representative bacterial pathogens.** *Bacillus spp. Yersinia pestis* and *Fransicella tularensis* are Category A agents. *Brucella abortus*, *Escherichia coli*, *Shigella dysenteriae*, *S. typhi*, *V. cholerae*, and *B. mallei* are Category B agents. Multidrug resistant *M. tuberculosis* is a Category C agent (according to the NIAID classification). The organisms utilizes in this study are depicted with solid square boxes and *E. coli* and *M. tuberculosis* were depicted with solid ellipse.

confirmed all enzymes were expressed as full length proteins with the expected molecular mass (26 kDa). The recombinant IspD orthologs were purified by IMAC. The eluted recombinant IspD orthologs were estimated to be over 90% pure as estimated by SDS–PAGE analysis (Fig.II.2.3).

Biochemical properties of IspD orthologs of *S. typhi*, *V. cholerae* and *B. mallei*. All three recombinant IspD orthologs were stable for more than 6 months at –20°C in 20 % glycerol without significant loss of catalytic activity. Plots of three IspD activities in terms of pH were bell shaped with optimal activities at pH 8.0. All the activities of IspD orthologs were maintained at least 80% at pH 6.0 and pH 9.0, showing IspD orthologs were active over a relatively broad pH range. *B. mallei* IspD, however, showed a narrower pH range than others (Fig.II.2.4A). All IspD orthologs showed an absolute requirement for divalent cations. The addition of 10 mM EDTA to the reaction mixtures completely abolished catalytic activity in all cases. The activities were optimal in the presence of 20 mM Mn^{2+}. Mg^{2+} also supported all IspD activities at a comparable level to Mn^{2+}. Interestingly, the effects of low concentrations (below 2.5 mM) of Zn^{2+} were similar to those of Mn^{2+} or Mg^{2+} for the *B. mallei* IspD activity (Fig.II.2.4B). However, Ca^{2+} showed minimal supports for their catalytic activities at only low concentration. In all cases, replacement of CTP with other NTPs such as ATP, TTP, GTP, or UTP abolished enzymatic activity, suggesting they don't act as substrates.

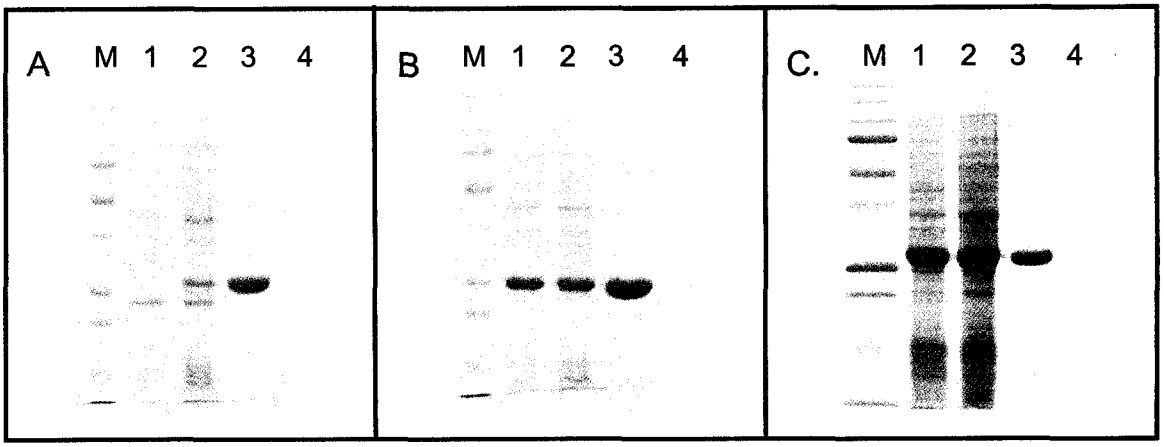

FIGURE II.2.3. **Expression and purification of histidine tagged IspD orthologs of three selected human pathogens; *S. typhi* (Panel A), *V. cholerae* (Panel B) and *B. mallei* (Panel C).** The proteins were visualized by Coommassie brilliant blue 250R and Western blot hybridization. IspD orthologs were cloned into pET28a(+) and used to transform *E. coli* BL21(DE3) for expression of the hexa–histidine fusion proteins. Lane 1: transformed BL21(DE3) cell lysates prior to IPTG treatment. Lane 2: transformed BL21(DE3) cell lysates after IPTG treatment. Lane 3: purified histidine tagged IspD fraction from an IMAC column. Lane 4: Western blot analysis of purified hexa–histidine tagged IspD orthologs using an anti–Histidine antibody. M: Molecular weight standard.

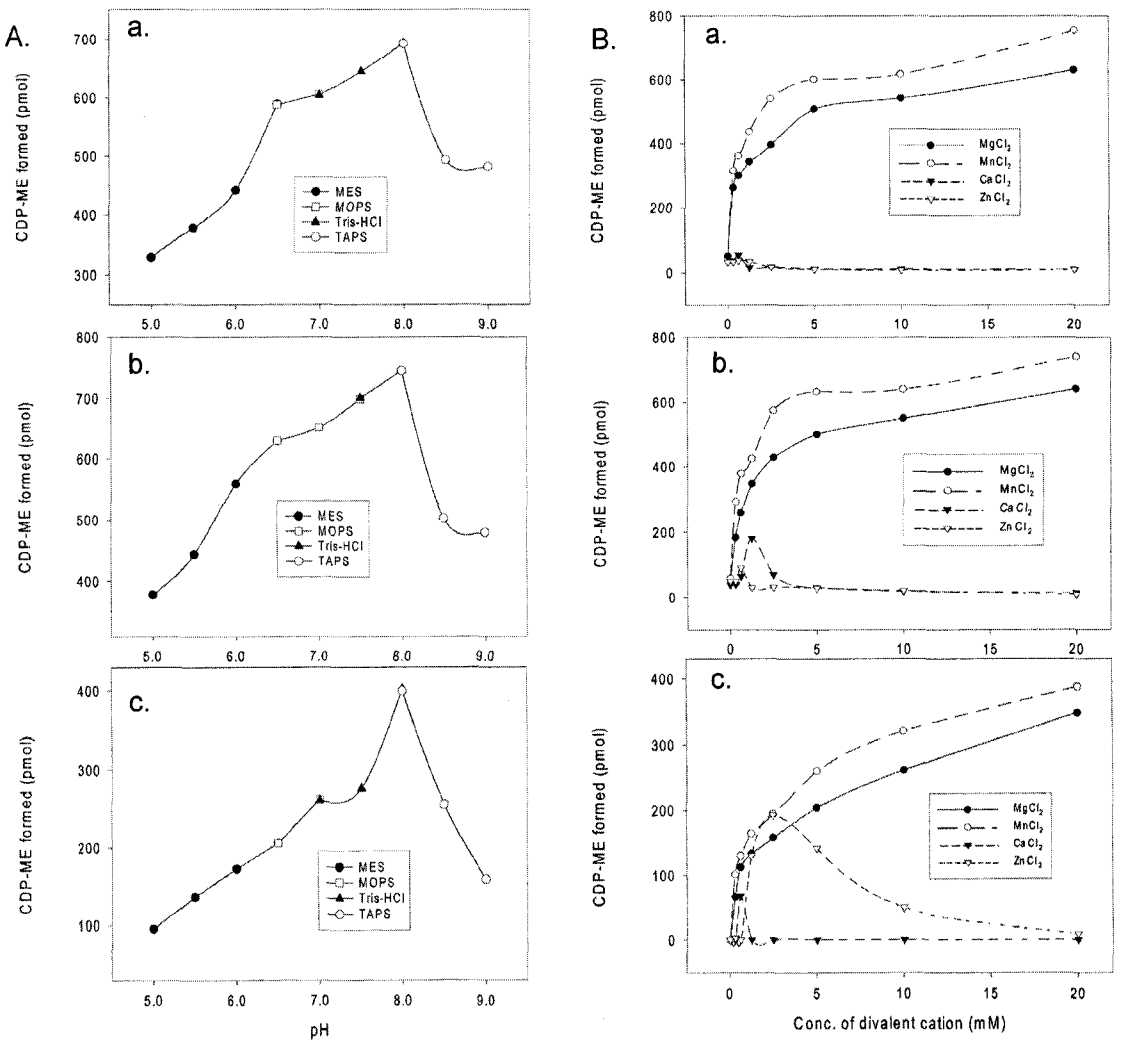

FIGURE II.2.4. **The effect of pH and divalent cation concentration on *S. typhi* (a), *V. cholerae* (b), and *B. mallei* (c) IspD activities**. Panel A: The buffer systems used to achieve the indicated pH values were: MES (pH 5.5 – pH 7.0), MOPS (pH 7.0 – pH 7.5), Tris (pH 7.5 – pH 8.5), and TAPS (pH 8.5 – pH 9.5). Panel B: Divalent cation (Mg^{2+}, Mn^{2+}, Zn^{2+}, or Ca^{2+}) concentrations were as indicated.

Kinetic properties of *S. typhi*, *V. cholerae* and *B. mallei* IspD orthologs. Three IspD orthologs displayed linear relationship between enzymatic activity and purified enzyme concentrations (up to 95 pmols for *S. typhi* IspD, 97.5 pmols for *V. cholerae* IspD, and 96.5 pmols for *B. mallei* IspD). The effects of MEP or CTP concentrations on reaction rates were determined by varying concentrations of one substrate while maintaining a fixed concentration of the other substrate (Fig.II.2.5). The K_m^{MEP} values of IspD orthologs of *S. typhi*, *V. cholerae* and *B. mallei* were 67.0 μM, 44.1 μM and 87.7 μM, respectively. The K_m^{CTP} values of IspD orthologs of *S. typhi*, *V. cholerae* and *B. mallei* were 80.7 μM, 83.6 μM and 61.4 μM, respectively (Table.II.2.2). These three genetically distinct IspD orthologs showed very similar K_m^{MEP} and K_m^{CTP} values, suggesting that they have similar affinities and catalytic properties (K_m/K_{cat}) with respect to their substrates. Calculated kinetic parameters are summarized in Table II.2.2, and suggest that three IspD orthologs analyzed in this study have similar enzymatic properties.

Determination of Z′–Factor values. The Z′–Factor values for the spectrophotometry based *in vitro* assays were calculated as discussed in chapter I–3. The Z′–Factor values for the assays using *S. typhi* IspD, *V. cholerae* IspD, and *B. mallei* IspD were 0.93, 0.91, and 0.91, respectively, suggesting the spectrophotometry based *in vitro* assays with a 30 μl reaction volume are reliable to apply to HTS assays (Table II.2.3).

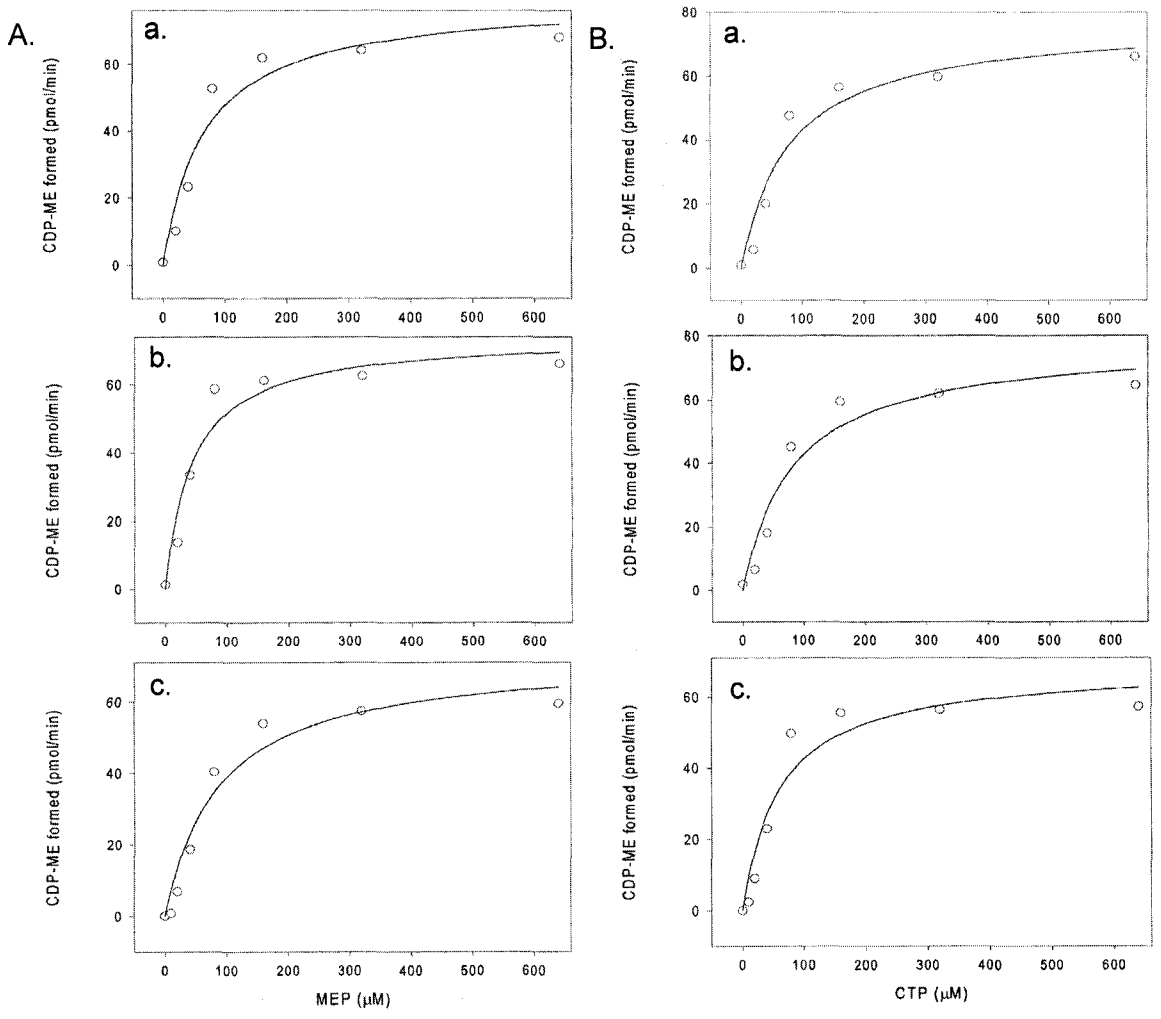

FIGURE II.2.5. **The effect of MEP and CTP concentrations on *S. typhi* (a), *V. cholerae* (b), and *B. mallei* (c) IspD activities.** Panel A: To determine the effect of MEP, the CTP concentration was held at 100 μM and the concentration of MEP was varied from 0 to 640 μM. Panel B: To determine the effect of CTP, the concentration of MEP was held at 100 μM and the concentration of CTP was varied from 0 to 640 μM.

TABLE II.2.2. **Calculated kinetic parameters for IspD orthologs of *S. typhi*, *V. cholerae* and *B. mallei***

IspD origin/ Substrates		Calculated parameters			
		K_m (μM)	V_{max} (pmol/min)	K_{cat} (min^{-1})	K_{cat}/K_m ($mM^{-1}min^{-1}$)
S. typhi	MEP	67.0	79.6	4.2	62.3
	CTP	80.7	77.5	4.1	50.6
V. cholerae	MEP	44.1	74.3	3.8	86.3
	CTP	83.6	78.4	4.0	48.1
B. mallei	MEP	87.7	72.8	3.8	43.0
	CTP	61.4	68.6	3.6	57.8

The concentrations of recombinant IspD orthologs from *S. typhi, V. cholerae* and *B. mallei* in each reaction were 19 pmols, 19.5 pmols and 19.3 pmols, respectively. SigmaPlot V. 8.02A was utilized to calculate K_m and V_{max} values for MEP and CTP.

TABLE II.2.3. **Z'–Factor values for the spectrophotometry based assay**. (Reaction volumes, 30μl)

IspD sources		*S. typhi*	*V. cholerae*	*B. mallei*
Sample Number	Positive	50	50	50
	Negative	50	50	50
Z'–Factor		0.93 ± 0.01	0.91 ± 0.02	0.91 ± 0.02

The assays were performed in 384–well microplates using an automated precision XS fluid transfer system.

II.2.D. Discussion

Many countries are known to either have generated agents for biological weapons or to possess the technology to do so. A large majority of the biological agents classified by the CDC and the NIAID as potential biological warfare/terrorism agents (Table II.1.1 and Table II.1.2) (4, 12) appear to utilize the MEP pathway. Three of the six entities designated as Category A agents utilize or appear to utilize the MEP pathway. Among the twelve Category B agents listed, eight are organisms that appear to utilize the MEP pathway (21). *M. tuberculosis*, classified as a Category C agent by the NIAID, has been shown to also utilize the MEP pathway. Studies using *A. thaliana* (17), barley (13), *P. falciparum* (1), *M. tuberculosis* (5), and *E. coli* (10) have shown that IspC, the second enzyme in the MEP pathway, is inhibited by the antibiotic fosmidomycin. Therefore, a large number of experiments have already shown that enzymes in the MEP pathway are attractive targets for developing broad–spectrum antibiotics. Because the MEP pathway is a relatively new discovery with few known inhibitors, it is unlikely that any bioterrorist organization has been able to develop bacteria that are resistant to MEP pathway–specific inhibitors. Coupled with the fact that the pathway is absent in humans, these make the MEP pathway a viable target for the development of treatments effective against many bioterrorist agents.

Although the *S. typhi* IspD, the *V. cholerae* IspD and the *B. mallei* IspD showed different levels of identity with the *E. coli* IspD, the biochemical and kinetic properties of three IspD orthologs are very similar, indicating IspD, the third enzyme in the MEP pathway, can be exploited as a potential drug target for broad–spectrum antibacterial

drugs (16). However, the identity between *E. coli* IspD and *B. mallei* IspD is 38%, lower than those between *E. coli* and the other organisms examined in this study. Slight differences in the optimal levels of divalent cation and pH support these ideas. Nonetheless, the biochemical catalytic requirements and the specificity constants (K_{cat}/K_m) of *S. typhi* IspD, *V. cholerae* IspD and *B. mallei* IspD, including those of *M. tuberculosis* IspD, are significantly similar. Therefore, three selected pathogens are excellent representatives of IspD sources for developing broad–spectrum antibiotics. In chapter I–3, a two step strategy was employed to show the essentiality of *M. tuberculosis* IspD. The essentiality of the IspD orthologs for the growth of other organisms has also been reported (2, 6, 20). Therefore, we anticipate the IspD orthologs of three human pathogens characterized in this study are also essential for their survival, *in vivo*. The spectrophotometry based *in vitro* assay is more facile and inexpensive than previously used NMR spectroscopy (7, 18) and Z′–Factor values indicated that the assay is excellently reliable for the HTS assay.

II.2.E. References

1. **Borrmann, S., A. A. Adegnika, F. Moussavou, S. Oyakhirome, G. Esser, P. B. Matsiegui, M. Ramharter, I. Lundgren, M. Kombila, S. Issifou, D. Hutchinson, J. Wiesner, H. Jomaa, and P. G. Kremsner.** 2005. Short-course regimens of artesunate-fosmidomycin in treatment of uncomplicated *Plasmodium falciparum* malaria. Antimicrob Agents Chemother **49:**3749-54.
2. **Cornish, R. M., J. R. Roth, and C. D. Poulter.** 2006. Lethal mutations in the isoprenoid pathway of *Salmonella enterica*. J Bacteriol **188:**1444-50.

3. **Crick, D. C., J. R. Scocca, J. S. Rush, D. W. Frank, S. S. Krag, and C. J. Waechter.** 1994. Induction of dolichyl-saccharide intermediate biosynthesis corresponds to increased long chain cis-isoprenyltransferase activity during the mitogenic response in mouse B cells. J Biol Chem **269:**10559-65.

4. **Darling, R. G., C. L. Catlett, K. D. Huebner, and D. G. Jarrett.** 2002. Threats in bioterrorism. I: CDC category A agents. Emerg Med Clin North Am **20:**273-309.

5. **Dhiman, R. K., M. L. Schaeffer, A. M. Bailey, C. A. Testa, H. Scherman, and D. C. Crick.** 2005. 1-Deoxy-D-xylulose 5-phosphate reductoisomerase (IspC) from *Mycobacterium tuberculosis*: towards understanding mycobacterial resistance to fosmidomycin. J Bacteriol **187:**8395-402.

6. **Freiberg, C., B. Wieland, F. Spaltmann, K. Ehlert, H. Brotz, and H. Labischinski.** 2001. Identification of novel essential *Escherichia coli* genes conserved among pathogenic bacteria. J Mol Microbiol Biotechnol **3:**483-9.

7. **Gabrielsen, M., F. Rohdich, W. Eisenreich, T. Grawert, S. Hecht, A. Bacher, and W. N. Hunter.** 2004. Biosynthesis of isoprenoids: a bifunctional IspDF enzyme from *Campylobacter jejuni*. Eur J Biochem **271:**3028-35.

8. **Jacobs, M. K.** 2004. The history of biologic warfare and bioterrorism. Dermatol Clin **22:**231-46, v.

9. **Klietmann, W. F., and K. L. Ruoff.** 2001. Bioterrorism: implications for the clinical microbiologist. Clin Microbiol Rev **14:**364-81.

10. **Leon, A., L. Liu, Y. Yang, M. P. Hudock, P. Hall, F. Yin, D. Studer, K. J. Puan, C. T. Morita, and E. Oldfield.** 2006. Isoprenoid biosynthesis as a drug target: bisphosphonate inhibition of *Escherichia coli* K12 growth and synergistic effects of fosmidomycin. J Med Chem **49:**7331-41.

11. **Meadows, M.** 2004. Project Bioshield: protecting Americans from terrorism. FDA Consum **38:**32-3.

12. **Moran, G. J.** 2002. Threats in bioterrorism. II: CDC category B and C agents. Emerg Med Clin North Am **20:**311-30.

13. **Mueller, C., J. Schwender, J. Zeidler, and H. K. Lichtenthaler.** 2000. Properties and inhibition of the first two enzymes of the non-mevalonate pathway of isoprenoid biosynthesis. Biochem Soc Trans **28:**792-3.

14. **Pappas, G., P. Panagopoulou, L. Christou, and N. Akritidis.** 2006. Category B potential bioterrorism agents: bacteria, viruses, toxins, and foodborne and waterborne pathogens. Infect Dis Clin North Am **20:**395-421, x.

15. **Richard, S. B., M. E. Bowman, W. Kwiatkowski, I. Kang, C. Chow, A. M. Lillo, D. E. Cane, and J. P. Noel.** 2001. Structure of 4-diphosphocytidyl-2-C-methylerythritol synthetase involved in mevalonate- independent isoprenoid biosynthesis. Nat Struct Biol **8:**641-8.

16. **Richard, S. B., A. M. Lillo, C. N. Tetzlaff, M. E. Bowman, J. P. Noel, and D. E. Cane.** 2004. Kinetic analysis of *Escherichia coli* 2-C-methyl-D-erythritol-4-phosphate cytidyltransferase, wild type and mutants, reveals roles of active site amino acids. Biochemistry **43:**12189-97.

17. **Rohdich, F., S. Lauw, J. Kaiser, R. Feicht, P. Kohler, A. Bacher, and W. Eisenreich.** 2006. Isoprenoid biosynthesis in plants - 2C-methyl-D-erythritol-4-phosphate synthase (IspC protein) of *Arabidopsis thaliana*. Febs J **273:**4446-58.

18. **Rohdich, F., J. Wungsintaweekul, M. Fellermeier, S. Sagner, S. Herz, K. Kis, W. Eisenreich, A. Bacher, and M. H. Zenk.** 1999. Cytidine 5'-triphosphate-dependent biosynthesis of isoprenoids: YgbP protein of *Escherichia coli* catalyzes the formation of 4-diphosphocytidyl-2-C-methylerythritol. Proc Natl Acad Sci U S A **96:**11758-63.

19. **Sassetti, C. M., D. H. Boyd, and E. J. Rubin.** 2003. Genes required for mycobacterial growth defined by high density mutagenesis. Mol Microbiol **48:**77-84.

20. **Sauret-Gueto, S., A. Ramos-Valdivia, E. Ibanez, A. Boronat, and M. Rodriguez-Concepcion.** 2003. Identification of lethal mutations in *Escherichia coli* genes encoding enzymes of the methylerythritol phosphate pathway. Biochem Biophys Res Commun **307:**408-15.

21. **Testa, C. A., and M. J. Brown.** 2003. The methylerythritol phosphate pathway and its significance as a novel drug target. Curr Pharm Biotechnol **4:**248-59.

Chapter II–3.

Characterization of an *in vitro* HTS assay targeting 4–(cytidine 5'–diphosphate)–2–C–methyl–D–erythritol kinase of three selected pathogens: *Salmonella typhi*, *Vibrio cholerae* and *Burkholderia mallei*

II.3.A. Introduction

The severity of the bioterrorism has been increased by the emergence of antimicrobial–resistant organisms and lack of health–care facilities. Therefore, early detection of and response to bioterrorist attacks are absolutely crucial. In the long term, the only way to defend against bioterrorist attacks may be achieved through a combination of constant surveillance, accurate diagnostics and continuous innovation of high–quality vaccines and broad–spectrum antibiotics (5). Currently, it has been reported that the increasing prevalence of antimicrobial–resistant pathogens is mainly related to the emergence of genetic mutant strains. The investigation of the mechanisms emerging drug resistance is important. Besides, it is also required for identifying and investigating new drug targets for the preparedness for bioterrorism and the MEP pathway has been investigated as the target.

The IspD orthologs were identified in *S. typhi*, *V. cholerae*, and *B. mallei*, characterized and validated as a potential drug target in the chapter II–2. The following step in the MEP pathway is unique kinase reaction performed by CDP–ME kinase (IspE, YchB in *E. coli*), which belongs to GHMP kinase superfamily. The IspE catalytic reaction involves the transfer of the γ–phosphate moiety of ATP to CDP–ME forming CDP–ME2P, with the corresponding release of ADP (Fig.I.4.1) (3, 7). A multiple alignment of *E. coli* IspE (3) and *M. tuberculosis* IspE (chapter I–4) with the *S. typhi, V. cholerae* and *B. mallei* genomes indicated that putative IspE orthologs of *S. typhi*, *V. cholerae*, and *B. mallei* share the conserved domains involved in ATP–binding and glycine–rich motif, major characteristics of the GHMP kinase superfamily (Fig.II.3.1). *In silico* studies have

shown that three bacterial pathogens utilize exclusively the MEP pathway for the isoprenoid biosynthesis. Therefore, IspE can be a potential drug target for developing broad–spectrum antibiotics. In the present chapter, *S. typhi*, *V. cholerae* and *B. mallei* were selected as representative sources of IspE enzymes for comparison on the basis of relative phylogenetic distances from *E. coli* IspE and *M. tuberculosis* IspE. In this chapter, *S. typhi* IspE, *V. cholerae* IspE, and *B. mallei* IspE were identified and newly developed *in vitro* HTS assay for *M. tuberculosis* IspE (chapter I–4) was applied and optimized for identify the activity of IspE orthologs. This assay is more facile and amenable to HTS assay than the radiochemical assay and NMR spectroscopy, previously employed for characterizing *E. coli* IspE (3).

II.3.B. Materials and Methods

PCR amplication and cloning of IspE orthologs from *S. typhi*, *V. cholerae*, and *B. mallei*. Putative *ispE* gene open reading frames from *S. typhi*, *V. cholerae* and *B. mallei* chromosomes were amplified by using oligonucleotide primers designed for amplifying the truncated versions removing 6–amino acids at C–terminal end based on the sequences available in Kyoto Encyclopedia of Genes and Genomes (KEGG) (http://www.genome.jp/kegg/). The primers were synthesized by Macromolecular Resources (Colorado State University) and are summarized in Table II.3.1. All the primers contain *Nde*I and *Hin*dIII restriction enzyme sites in the forward and reverse primers, respectively (underlined). Reverse primers were designed to amplify the *ispE* orthologs truncating six amino acids at C–terminal end. The truncated PCR products

TABLE II.3.1. **PCR primers used in this study**. The sequences recognized by restriction enzymes are underlined

Organism	Primer	Sequence	Enzyme
S. typhi	Forward	CATATGAACAACATGACAGCGATTGT	*Nde*I
	Reverse	AAGCTTTCTGATCATGATTTTCCTTATTACG	*Hin*dIII
V. cholerae	Forward	CATATGGCAGCCACTTTATTGGA	*Nde*I
	Reverse	AAGCTTTCGCATTATGCTTTCTCCTG	*Hin*dIII
B. mallei	Forward	CATATGACCTCCCGACTTTTTGCC	*Nde*I
	Reverse	AAGCTTTCAGGAAGCGCGCGCCGGTT	*Hin*dIII

were digested with *Nde*I and *Hin*dIII, and ligated into the pET28a(+) vector (EMD Biosciences, Inc., San Diego, CA). Transformation of DH5α subcloning cells (Life Technologies, Rockville, MD) with ligation mixtures afforded the recombinant strains: DH5α [pET28a(+)::mutant *S. typhi ispE*], DH5α [pET28a(+)::mutant *V. cholerae ispE*] and DH5α [pET28a(+)::mutant *B. mallei ispE*]. The expression constructs were isolated using Qiagen Plasmid Miniprep Kits. All expression constructs were purified and sequences confirmed by Marcomolecular Resources, Colorado State University.

Expression and purification of the recombinant mutant IspE orthologs. BL21(DE3) (Novagen, Madison, WI) was used as the expression host. Transformation of BL21(DE3) with the expression constructs harboring C–terminal end truncated *ispE* genes created the BL21(DE3) [pET28a(+)::mutant *S. typhi ispE*], BL21(DE3) [pET28a(+)::mutant *V. cholerae ispE*] and BL21(DE3) [pET28a(+)::mutant *B. mallei ispE*]. We used the same strategy for purifying the recombinant mutant IspE orthologs as described in chapter I–4.

Development of *in vitro* IspE assay using the ADP Quest HS Kinase Assay Kit. The ADP Quest HS Kinase Assay Kit was employed to measure the activities of three IspE orthologs. The same mixture as that of *M. tuberculosis* IspE (chapter I–4) was used. The amounts of enzymes used were 99.3 pmols for mutant *S. typhi* IspE, 95.8 pmols for mutant *V. cholerae* IspE, and 81.1 pmols for mutant *B. mallei* IspE. Overall catalytic mechanisms for generating measurable fluorescent signal are described in the Fig. I.4.4. Fluorescence was measured by Synergy™ HT Multi–Detection Microplate Reader (BioTek instruments) at excitation wavelength 530 nm and emission wavelength 590 nm.

Determination of optimal reaction conditions for the *in vitro* HTS enzyme assay using mutant IspE orthologs and kinetic properties of mutant IspE orthologs. We employed the same strategy as those used for mutant *M. tuberculosis* IspE (chapter I–4).

II.3.C. Results

Identification of IspE orthologs in Category B agents: *S. typhi*, *V. cholerae*, and *B. mallei*. A multiple alignment of five IspE orthologs of *E. coli* (3), *M. tuberculosis* (chapter I–4), *S. typhi*, *V. cholerae*, and *B. mallei* was performed (Fig.II.3.1) and indicated that the putative IspE orthologs of *S. typhi*, *V. cholerae* and *B. mallei* contain the conserved domains involving glycine–rich motifs and ATP–binding motifs (Fig.II.3.1), suggesting that the putative proteins have IspE orthologous functions. *S. typhi*, *V. cholerae* and *B. mallei* were selected as IspE enzyme sources for comparison because of their relative phylogenetic distances from *E. coli* IspE and *M. tuberculosis* IspE (Fig.II.3.2). All IspE open reading frames were predicted to encode cytosolic proteins with molecular masses of approximately 32 kDa.

Optimal reaction conditions for the *in vitro* HTS assays using recombinant mutant IspE orthologs of *S. typhi*, *V. cholerae* and *B. mallei*. At first, we tried to express and purify intact forms of IspE orthologs of *S. typhi*, *V. cholerae*, and *B. mallei* in *E. coli*. However, the expressed proteins were insoluble as was that of *M. tuberculosis* IspE (chapter I–4). Therefore, the same strategy as used for *M. tuberculosis* IspE was applied

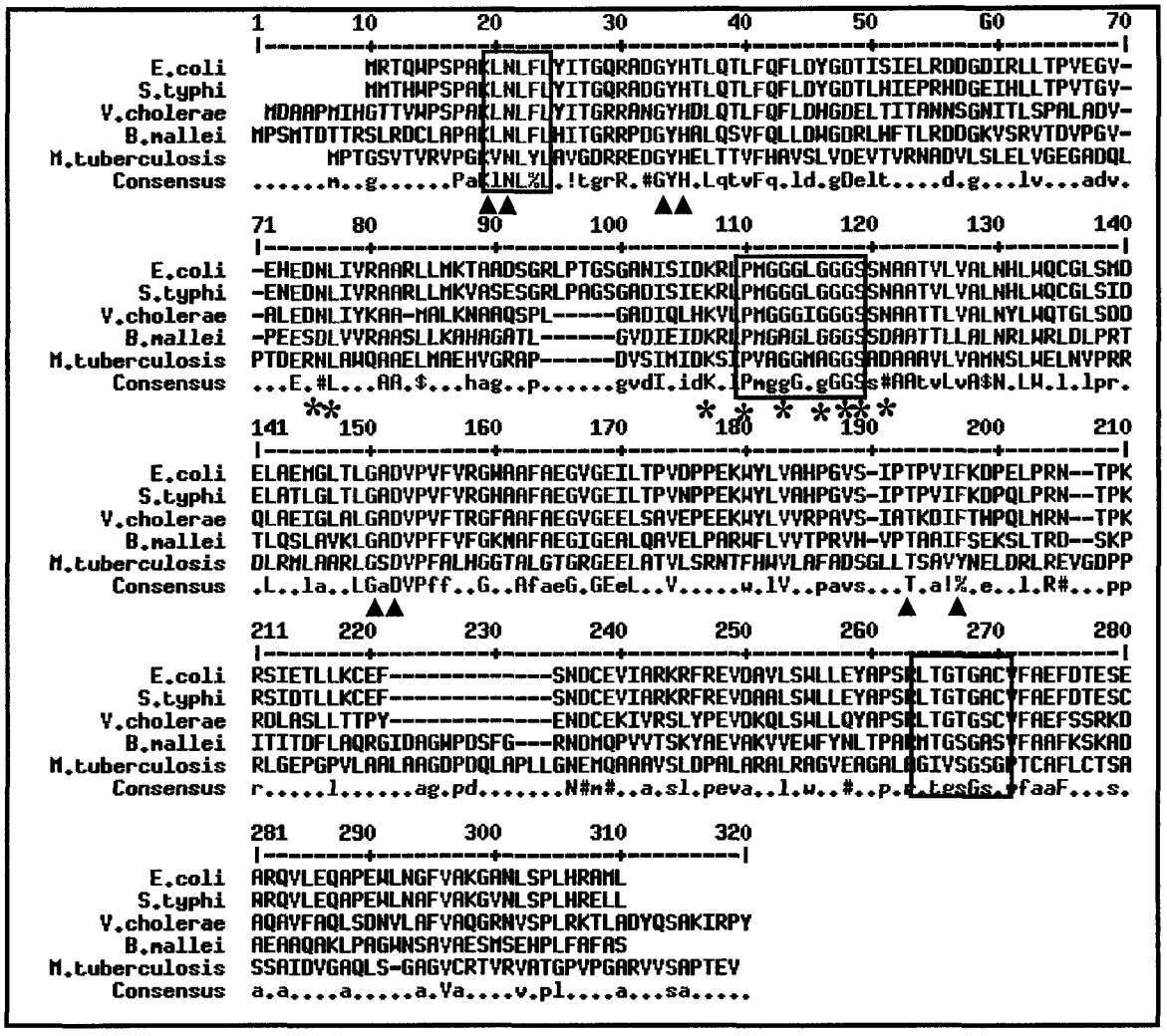

FIGURE II.3.1. **Multiple alignment of IspE amino acid sequences of five different bacterial pathogens: *E. coli*, *M. tuberculosis*, *S. typhi*, *V. cholerae* and *B. mallei*.** Identities are indicated by red and similarities are indicated by blue. The identities of the IspE orthologs of *S. typhi*, *V. cholerae*, *B. mallei*, and *M. tuberculosis* with *E. coli* IspE were 90%, 60%, 44% and 22%, respectively. The conserved amino acids involved in the ATP binding were highlighted with (*) and CDP–ME binding were highlighted with (▲). Three blue boxes indicate the conserved amino acids related with IspE catalytic activity. Second box is conserved glycine–rich domain (3, 4).

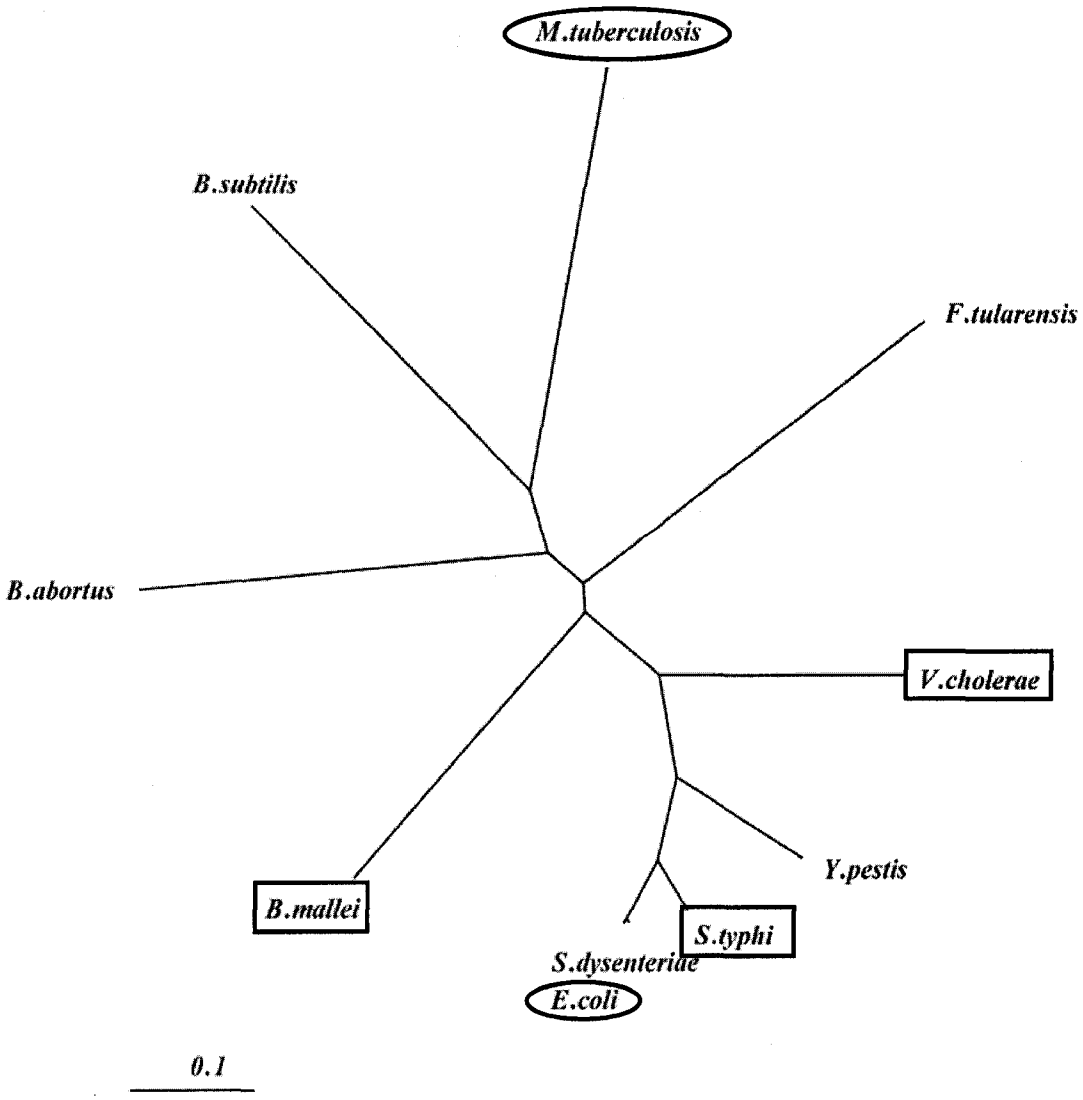

FIGURE II.3.2. **Unrooted dendrogram of IspE orthologs identified from ten representative bacterial pathogens.** *Bacillus* sp. *Yersinia pestis* and *Fransicella tularensis* are Category A agents. *Brucella abortus*, *Escherichia coli*, *Shigella dysenteriae*, *S. typhi*, *V. cholerae*, and *B. mallei* are Category B agents. Multidrug–resistant *M. tuberculosis* is a Category C agent according to the NIAID classification. The organisms studied here are depicted with solid square boxes and *E. coli* and *M. tuberculosis* were depicted with solid ellipse.

to optimize the expression levels for three IspE orthologs. 6–amino acid at C–terminal end of IspE orthologs were removed by PCR and expressed and purified through IMAC (Fig.II.3.3). Recombinant mutant IspE orthologs truncating 6–amino acid at C–terminal end were highly induced and expressed under the culture conditions tested. Expression was confirmed by Western blot analysis (Fig.II.3.3). All recombinant mutant IspE orthologs showed ATP–dependent kinase activity. The *in vitro* HTS assays using the mutant IspE orthologs were performed for finding the optimal pH and specificity of divalent cation. Plots of the *in vitro* HTS assays in terms of pH showed bell shaped with the highest florescent signals between pH 7.5 – pH 8.5 (Fig.II.3.4A). The highest florescent signal of the *in vitro* HTS assay using mutant *S. typhi* IspE was obtained at pH 8.5, whereas that of mutant *V. cholerae* IspE was at pH 8.0. In case of using the mutant *B. mallei* IspE, the signals were maintained between pH 7.5 and pH 9.0. The *in vitro* HTS assays showed optimal activity in the presence of approximately 10 mM Mg^{2+}. However, Mn^{2+} was ineffective at supporting the *in vitro* HTS assays at all concentrations tested (Fig.II.3.4B).

Kinetic properties of *S. typhi*, *V. cholerae* and *B. mallei* truncated IspE orthologs. All three IspE orthologs displayed linear relationship between enzymatic activity and purified enzyme concentrations (up to 198.5 pmols for mutant *S. typhi* IspE, 197.6 pmols for mutant *V. cholerae* IspE, and 162.2 pmols for mutant *B. mallei* IspE). The effects of CDP–ME or ATP concentration on reaction rates were determined by varying the concentration of one substrate while maintaining a fixed concentration of the other substrate. The K_m^{CDP-ME} values of IspE orthologs of *S. typhi*, *V. cholerae* and *B. mallei*

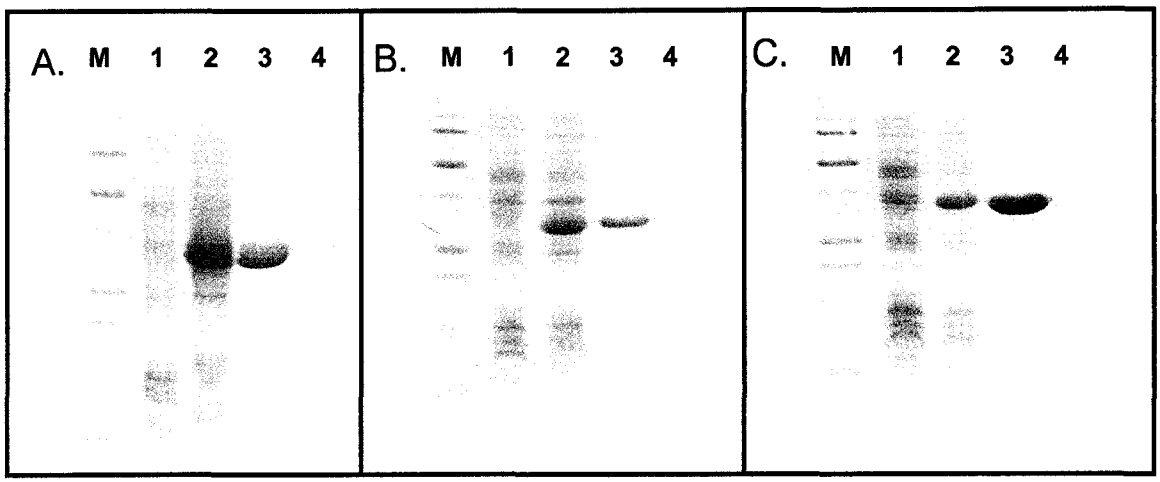

FIGURE II.3.3. **Expression and purification of histidine tagged truncated IspE orthologs of three human pathogens:** *S. typhi* (Panel A), *V. cholerae* (Panel B) and *B. mallei* (Panel C). Truncated IspE orthologs were cloned into pET28a(+) and transformed into the *E. coli* BL21(DE3) for expression of the hexa–histidine fusion proteins. Lanes 1 – 3 are SDS–PAGE gels visualized with Coomassie Brilliant Blue 250R. Lane 1: transformed BL21(DE3) cell lysates prior to IPTG treatment. Lane 2: transformed BL21(DE3) cell lysates after IPTG treatment. Lane 3: purified hexa–histidine tagged truncated IspE ortholog elutes from an IMAC column. Lane 4, Western blot analysis of purified hexa–histidine tagged truncated IspE orthologs using an anti–Histidine antibody. M: Molecular weight standards.

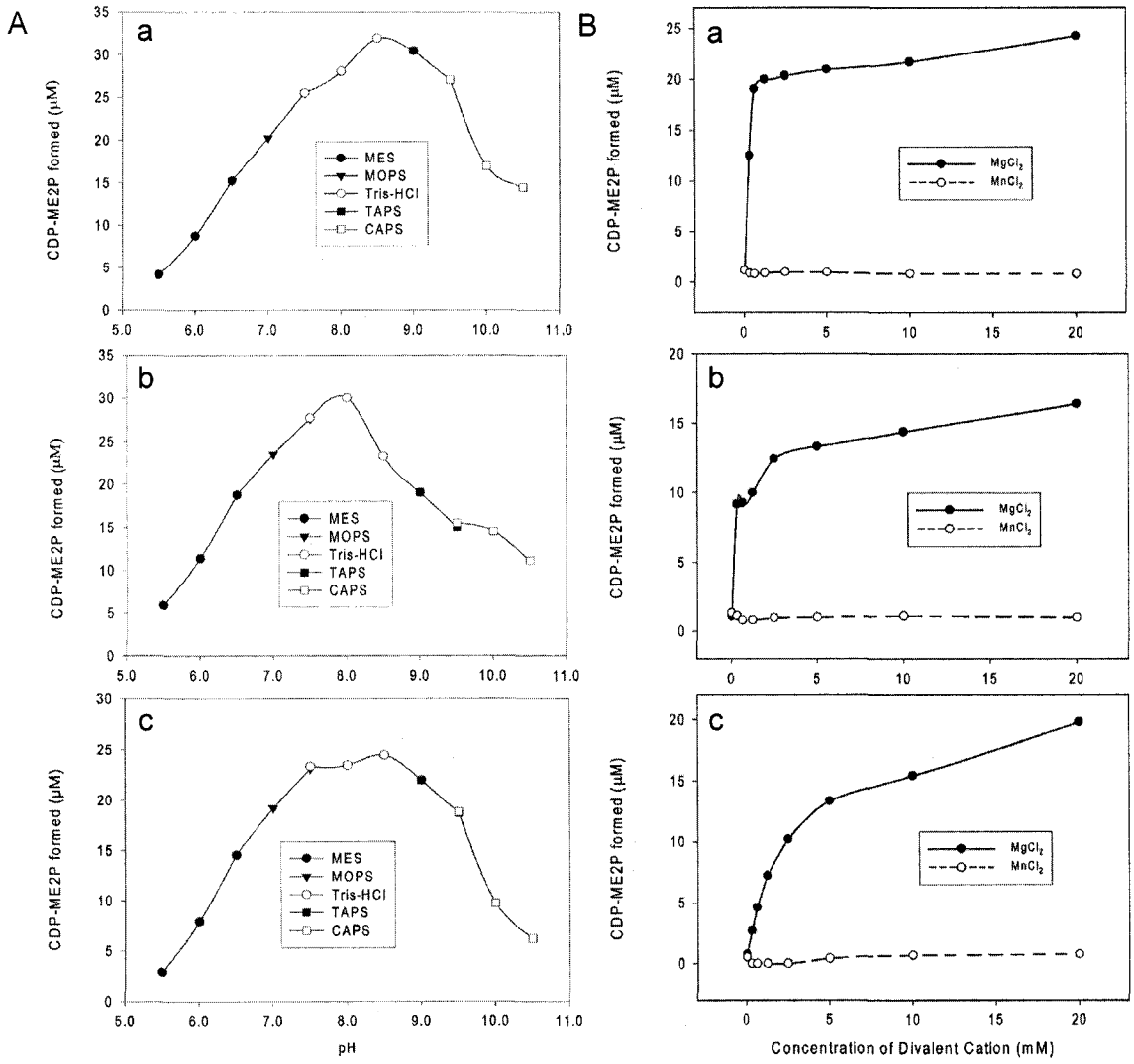

FIGURE II.3.4. **The effect of pH and divalent cation concentration on the *in vitro* HTS assays using mutant *S. typhi* (a), *V. cholerae* (b), and *B. mallei* (c) IspE orthologs**. A. The different buffer systems used to achieve the indicated pH values were: MES (pH 5.5 – pH 7.0), MOPS (pH 7.0 – pH 7.5), Tris (pH 7.5 – pH 8.5), TAPS (pH 8.5 – pH 9.0), and CAPS (pH 9.0 – pH 10.5). B. Divalent cation concentrations ranged from 0 – 20 mM. Reactions were performed as described in Materials and Methods.

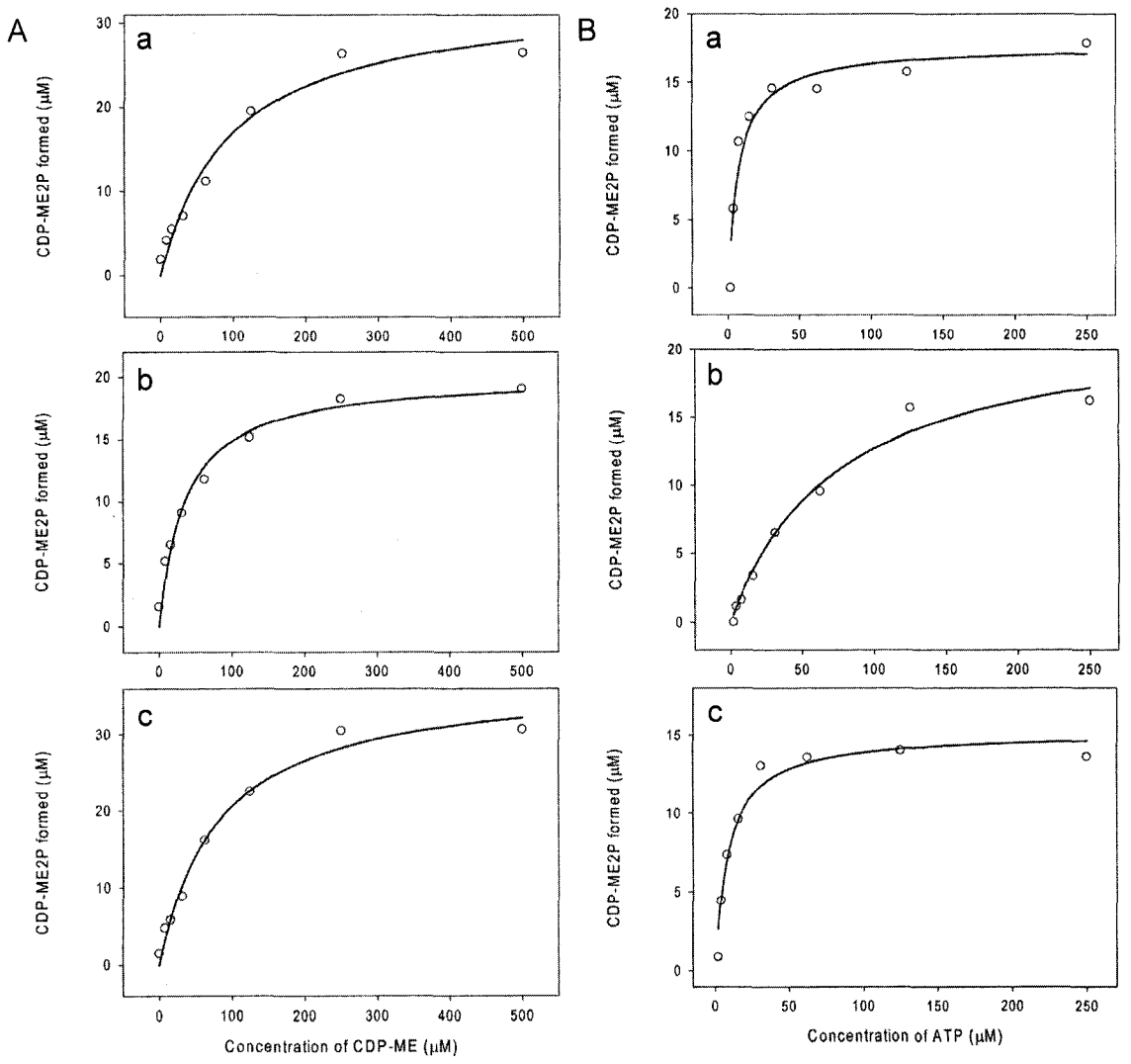

FIGURE II.3.5. **The effect of CDP–ME and ATP concentrations on mutant *S. typhi* (a), *V. cholerae* (b), and *B. mallei* (c) IspE ortholog catalytic activities**. A. To determine the effect of CDP–ME concentration, ATP concentration was held at 200 μM and the concentration of CDP–ME was varied from 0 to 640 μM. B. To determine the effect of ATP concentration, CDP–ME concentration was held at 100 μM and the concentration of ATP was varied from 0 to 250 μM.

were 97.2 μM 36.0 μM and 81.9 μM, respectively. The K_m^{ATP} values of mutant IspE orthologs of *S. typhi*, *V. cholerae* and *B. mallei* were 7.8 μM, 76.6 μM, and 9.1 μM, respectively. Calculated kinetic parameters were summarized in Table.II.3.2. Although K_m values for their substrates were significantly different according to the species of IspE origins, the IspE specificity constants (K_{cat}/K_m) values were very similar, suggesting that three IspE orthologs analyzed here have similar enzymatic properties.

II.3.D. Discussion

We have identified the IspE orthologs of *S. typhi*, *V. cholerae*, and *B. mallei* and developed the *in vitro* HTS assay targeting IspE orthologs of various human pathogens. For optimal expression of IspE orthologs tested, we have truncated 6–amino acids at the C–terminal end of three IspE orthologs, a similar strategy to that used to express *M. tuberculosis* IspE (chapter I–4). All mutant IspE orthologs of *S. typhi*, *V. cholerae*, and *B. mallei* were all well induced, expressed, and active. All recombinant mutant IspE orthologs were capable of phosphorylating CDP–ME to produce CDP–ME2P in an ATP–dependent manner. Therefore, we assumed that C–terminal end of three IspE orthologs have little functional contribution to their activities.

As mentioned in chapter I–4, the ADP Quest HS Kinase Assay Kit used for the *in vitro* HTS assay contains coupling enzymes for producing the measurable fluorescent signal (Fig.I.4.4). Therefore, radiochemical assay using [γ–^{32}P]ATP is needed to monitor the IspE activity in a direct way. The radiochemical assay would give the biochemical properties of IspE orthologs. The highest fluorescent signals of the *in vitro* HTS assay

TABLE II.3.2. **Calculated kinetic parameters for mutant IspE orthologs of *S. typhi*, *V. cholerae* and *B. mallei***

IspE origin/ Substrates		Calculated parameters			
		K_m (μM)	V_{max} (μmol/min)	K_{cat} (min^{-1})	K_{cat}/K_m ($\mu M^{-1}min^{-1}$)
S. typhi	ATP	7.8	1.2	1.2×10^4	1.5×10^3
	CDP–ME	97.2	2.2	2.2×10^4	2.3×10^2
V. cholerae	ATP	76.6	1.5	1.4×10^4	2.0×10^2
	CDP–ME	36.0	1.3	1.3×10^4	3.9×10^2
B. mallei	ATP	9.1	1.0	8.1×10^3	1.4×10^3
	CDP–ME	81.9	2.5	2.0×10^4	3.8×10^2

The amounts of recombinant enzymes used were 99.27 pmols for *S. typhi* truncated IspE, 95.81 pmols for *V. cholerae* truncated IspE, and 81.13 pmols for *B. mallei* truncated IspE. The data were calculated from the experiments shown in Fig.II.3.5. using non–linear regression analysis (Sigma Plot V.8.02A)

using mutant IspE orthologs were obtained in the presence of 10 mM of divalent cation (Mg^{2+}) and at pH 8.0. Their usage of divalent cation is very similar to that of the *in vitro* HTS assay using mutant *M. tuberculosis* IspE (chapter I–4). The *in vitro* HTS assays using mutant *S. typhi* IspE and mutant *B. mallei* IspE produced optimal florescent signals under the relatively broader pH range than that of the *in vitro* HTS assay using mutant *V. cholerae* IspE. The K_m^{ATP} values of the mutant IspE orthologs of *S. typhi*, *V. cholerae*, and *B. mallei* were 7.8 μM, 76.6 μM, and 9.1 μM, respectively. The K_m^{CDP-ME} values of the mutant IspE orthologs of *S. typhi*, *V. cholerae*, and *B. mallei* were 97.2 μM, 36.0 μM, and 81.9 μM, respectively. Although, the affinities for substrates were different depending on the IspE ortholog sources, their specificity constants (K_{cat}/K_m) and biochemical properties were comparable, including that of *M. tuberculosis* IspE (chapter I–4).

The technology associated with the manufacture of biological weapons is relatively inexpensive and easy to obtain (1). However, existing counter–bioterrorism strategies are insufficient to guarantee that biological weapons will not be used. Furthermore, it is obvious that biological weapons are proliferating. Therefore, new drug targets for broad–spectrum antimicrobials are urgently investigated. In this context, IspE can be exploited as an attractive target. IspE orthologs were well conserved over the broad–range of bacterial pathogens and expected to be essential for the bacilli viability based on the results obtained from previous experiments using *E. coli* IspE and *M. tuberculosis* IspE (8, 9). For screening lead compounds, we developed the *in vitro* HTS assays by coupling to the ADP Quest HS Kinase Assay Kit which produces a positive fluorescent signal directly proportional to the ADP concentration produced in the IspE reaction. This *in vitro* HTS assay is non–radioactive, more facile and inexpensive than

radiochemical assays using [2–^{14}C]CDP–ME as substrate (3, 10) or reverse–phase HPLC (7). Kinetic data indicates that inhibitors of IspE will likely be broad–spectrum.

II.3.E. References

1. **Inglesby, T. V., T. O'Toole, and D. A. Henderson.** 2000. Preventing the use of biological weapons: improving response should prevention fail. Clin Infect Dis **30:**926-9.
2. **Jacobs, M. K.** 2004. The history of biologic warfare and bioterrorism. Dermatol Clin **22:**231-46, v.
3. **Luttgen, H., F. Rohdich, S. Herz, J. Wungsintaweekul, S. Hecht, C. A. Schuhr, M. Fellermeier, S. Sagner, M. H. Zenk, A. Bacher, and W. Eisenreich.** 2000. Biosynthesis of terpenoids: YchB protein of *Escherichia coli* phosphorylates the 2-hydroxy group of 4-diphosphocytidyl-2C-methyl-D-erythritol. Proc Natl Acad Sci U S A **97:**1062-7.
4. **Miallau, L., M. S. Alphey, L. E. Kemp, G. A. Leonard, S. M. McSweeney, S. Hecht, A. Bacher, W. Eisenreich, F. Rohdich, and W. N. Hunter.** 2003. Biosynthesis of isoprenoids: crystal structure of 4-diphosphocytidyl-2C-methyl-D-erythritol kinase. Proc Natl Acad Sci U S A **100:**9173-8.
5. **Roffey, R., K. Lantorp, A. Tegnell, and F. Elgh.** 2002. Biological weapons and bioterrorism preparedness: importance of public-health awareness and international cooperation. Clin Microbiol Infect **8:**522-8.
6. **Roffey, R., A. Tegnell, and F. Elgh.** 2002. Biological warfare in a historical perspective. Clin Microbiol Infect **8:**450-4.
7. **Rohdich, F., J. Wungsintaweekul, H. Luttgen, M. Fischer, W. Eisenreich, C. A. Schuhr, M. Fellermeier, N. Schramek, M. H. Zenk, and A. Bacher.** 2000. Biosynthesis of terpenoids: 4-diphosphocytidyl-2-C-methyl-D-erythritol kinase from tomato. Proc Natl Acad Sci U S A **97:**8251-6.
8. **Sassetti, C. M., D. H. Boyd, and E. J. Rubin.** 2003. Genes required for

mycobacterial growth defined by high density mutagenesis. Mol Microbiol **48:**77-84.

9. **Sauret-Gueto, S., A. Ramos-Valdivia, E. Ibanez, A. Boronat, and M. Rodriguez-Concepcion.** 2003. Identification of lethal mutations in *Escherichia coli* genes encoding enzymes of the methylerythritol phosphate pathway. Biochem Biophys Res Commun **307:**408-15.

10. **Wada, T., T. Kuzuyama, S. Satoh, S. Kuramitsu, S. Yokoyama, S. Unzai, J. R. Tame, and S. Y. Park.** 2003. Crystal structure of 4-(cytidine 5'-diphospho)-2-C-methyl-D-erythritol kinase, an enzyme in the non-mevalonate pathway of isoprenoid synthesis. J Biol Chem **278:**30022-7.

Chapter III.

Summary & Conclusions

III.A. Summary & Conclusions

The early steps of isoprenoid biosynthesis in eubacteria can be exploited as sources of broad–spectrum anti–bacterial drugs including anti–mycobacterial agents. Although isoprenoids are structurally and functionally diverse, they derive from two simple precursors, IPP and its isomer DMAPP, which represent the five–carbon basic building blocks of all isoprenoids. For the biosynthesis of IPP and DMAPP, two separate pathways were discovered to date. One is the well–known MVA pathway and the other is the newly discovered MEP pathway. The MEP pathway has been demonstrated to be essential in most eubacteria, like *E. coli*, algae and plants. Due to its essentiality and absence in mammalian cells, the enzymes involved in the MEP pathway may provide excellent molecular targets for the development of new generations of anti–bacterial drugs. Furthermore, in–depth knowledge of the characteristics of individual biosynthetic steps of intermediates could refine the search for new drugs aiming at the inhibition of each intermediate of the corresponding pathways. Although this pathway was shown by NMR spectrometry experiments in many bacterial systems, it had not yet been fully elucidated in *M. tuberculosis* or other pathogens. In this dissertation, we have identified and characterized individual enzymes in the MEP pathway of four human pathogens: *Mycobacterium tuberculosis*, *Salmonella typhi*, *Vibrio cholerae*, and *Burkholderia mallei*.

In the *M. tuberculosis* MEP pathway, the initial step involves the formation of DXP through condensing pyruvate and GAP as shown in chapter I–5. This reaction is catalyzed by the DXS, which is encoded by *Rv2682c* in *M. tuberculosis*. The enzyme was identified by homology search with *E. coli* DXS and other members of the transketolase

superfamily identified in previous studies. The *in vitro* DXS assays were optimized to generate the HTS assay to screen the specific inhibitors from small compound libraries generated by Dr. Scott Franzblau's laboratory, UIC. Among the compounds screened, #39 (chapter I–5) showed the highest inhibitory effect. Unfortunately, the inhibitors screened here showed little inhibitory effects on *M. tuberculosis* viability, *in vivo* and a certain degree of mammalian cell toxicity, suggesting that the compounds need to be modified further. As mentioned in chapter I–5, *M. tuberculosis* DXS belongs to mammalian GHMP kinase superfamily, which would be major reasons for mammalian cell toxicity. However, there are several significant differences between bacterial DXS and GHMP kinase superfamily as mentioned in discussion of chapter I–5. The further modifications for reducing cytotoxicity or increasing killing effects on *M. tuberculosis* viability have been ongoing in UIC.

Four pathogens (*M. tuberculosis*, *S. typhi*, *V. cholerae*, and *B. mallei*) were selected according to the relative genetic distances from *E. coli* orthologs of the MEP pathway as representative sources of IspD and IspE. All pathogens possess the putative IspD and the IspE orthologs, suggesting they utilize the MEP pathway. The orthologs of distinct origins showed the similar catalytic activities and biochemical properties.

In the third step in the MEP pathway, MEP provides the substrate of IspD. In this step, IspD catalyzes transfer of the CMP moiety of CTP to MEP producing CDP–ME, with the corresponding release of PP*i*, a reaction characterized in chapter I–3 and chapter II–2. *M. tuberculosis* IspD is encoded by *Rv3582c*. The open reading frame *Rv3582c* of the *M. tuberculosis* H_{37}Rv genome was identified through comparison with the previously characterized *E. coli* IspD. The enzyme's function was identified by

comparing the IspD intrinsic activity of an *E. coli* control strain extract with that of a recombinant *E. coli* strain overexpressing Rv3582c. Increased IspD activity was observed in the cytosolic fraction. Previously, Rv3582c was predicted to be an essential gene by the Himar1–based transposon mutagenesis experiments performed by Sassetti et al (2). We confirmed Rv3582c essentiality for *M. tuberculosis* viability by providing direct evidence that the inability to isolate a non–functional mutant using a two step disruption strategy. Recombinant *M. tuberculosis* IspD was active over a broad pH range with highest activity at pH 8.0. Divalent cations are absolutely required for its cytidylyltransferase activity, with Mg^{2+} and Mn^{2+} supporting optimal activity. However, Zn^{2+} could also support the *M. tuberculosis* IspD activity at low concentrations. *M. tuberculosis* IspD showed a high degree of specificity for CTP. The *S. typhi* IspD, the *V. cholerae* IspD, and *B. mallei* IspD also showed similar biochemical properties, as shown in chapter II–2. The PP*i* released from the IspD catalytic reaction was utilized to generate the spectrophotometry based *in vitro* assays for monitoring the IspD activity. The spectrophotometry based *in vitro* assay proved to be facile, direct, and relatively inexpensive, facilitating high throughput screening for finding novel inhibitors against the IspD of four bacterial pathogens. As part of future directions, the spectrophotometry based *in vitro* HTS assay will be applied to screen the specific inhibitors against IspD from the compound libraries of the National screening laboratory for the regional centers of excellence in biodefense and emerging infectious diseases (NSRB).

The open reading frame *Rv1011* encodes the fourth enzyme in the *M. tuberculosis* MEP pathway (IspE). The *in vitro* HTS assay targeting *M. tuberculosis* IspE was developed, in chapter I–4. *M. tuberculosis* IspE catalyzes the transfer of the γ–

phosphate moiety of ATP to CDP–ME, forming CDP–ME2P and releasing ADP, in an ATP–dependent manner. The open reading frame of *Rv1011* of the $H_{37}Rv$ genome was identified by the alignment searches with *E. coli* IspE. The IspE catalytic function was identified as a result of comparing the IspE intrinsic activity of *M. smegmatis* mc^2155 control strain extract with that of Rv1011 overexpressing recombinant *M. smegmatis* mc^2155 strain. Increased IspE activity was observed in the cytosolic fraction. Previous Himar1–based transposon mutagenesis experiments (2) predicted that the *Rv1011* gene product is essential for *M. tuberculosis* viability. Unfortunately, intact form of Rv1011 proved to be difficult to express in a soluble form. For optimization of expression of recombinant Rv1011, 6–amino acids at the C–terminal end were truncated by PCR amplification. The recombinant mutant *M. tuberculosis* Rv1011 was highly expressed and showed the IspE catalytic activity as the intrinsic activity obtained from the cytosolic protein of *M. smegmatis* mc^2155. The newly developed *in vitro* HTS assays using the mutant *M. tuberculosis* IspE were dependent on the divalent cation, Mg^{2+}. However, Mn^{2+} was not able to support the *in vitro* HTS assay, at all. Optimal fluorescent signals of the *in vitro* HTS assays were obtained at relatively broad pH range. The K_m^{ATP} and $K_m^{CDP\text{–}ME}$ for the mutant *M. tuberculosis* IspE are 75.2 μM and 515.1 μM, respectively. Although the affinities of mutant *M. tuberculosis* IspE for the substrates (ATP and CDP–ME) are different from those obtained using mutant IspE orthologs of *S. typhi*, *V. cholerae*, and *B. mallei*, shown in chapter II–3, the specificity constants (K_{cat}/K_m) of all mutant IspE orthologs were similar, suggesting IspE can be exploited as a potential drug target for broad–spectrum antibiotics. Moreover, newly generated *in vitro* HTS assay is non–radioactive and amenable to screen the specific inhibitors. As part of future

directions, firstly, a radiochemical IspE assay using [γ–P^{32}]ATP needs to be developed for characterizing the mutant IspE orthologs of *M. tuberculosis*, *S. typhi*, *V. cholerae*, and *B. mallei*. Secondly, the K_m and V_{max} values obtained using the mutant *M. tuberculosis* IspE need to be compared with those of cytosolic fractions of wild *M. tuberculosis* strain. Thirdly, the Z–factor values for the *in vitro* HTS assays are determined to prove the reliability for screening inhibitors.

As proposed earlier, the great impact of discovering new drug targets for improving TB control will contribute to combat persistent TB and MDR–TB, resulting in shortening the duration of the DOTS programs. The non–replicating persistent state of *M. tuberculosis* is well known to be resistant to most of the current drugs (1, 3). More seriously, true representative *in vivo* or *vitro* models of persistent state of *M. tuberculosis* are not available, yet. As mentioned in the discussion of chapter I–3, the F_1F_0–ATP synthase and NADH type II dehydrogenase in the respiratory chain is required for mycobacterial growth as suppliers of ATP for the survival. Thus, inhibition of menaquinone synthesis, which would be achieved by inhibition of the enzymes in the MEP pathway, may well be lethal to *M. tuberculosis* in non–replicating persistence, a state thought to be prevalent in persistent infections with *M. tuberculosis*. In addition, it has not been reported that the enzymes in the MEP pathway are the targets for current anti–tuberculosis drugs. Therefore, the lead compounds inhibiting the MEP pathway may be used to combat MDR–TB infection.

In closing, the first enzyme (DXS) in *M. tuberculosis* was applied to screen for specific inhibitors. The third and fourth enzymes (IspD and IspE) in the MEP pathway were identified from four human bacterial pathogens (*M. tuberculosis*, *S. typhi*, *V.*

cholerae, and *B. mallei*) each of which are conserved over all organisms tested. Formally, it is necessary to determine their essentiality before the enzymes can be exploited for antimicrobial drug targeting. The results and knowledge obtained from this dissertation, hopefully, can be used to aid the development of a new generation of broad spectrum–antimicrobials including anti–tuberculosis drugs and contribute to improvement of the DOTS programs for TB control.

III.B.References

1. **Chopra, P., L. S. Meena, and Y. Singh.** 2003. New drug targets for *Mycobacterium tuberculosis*. Indian J Med Res **117:**1-9.
2. **Sassetti, C. M., D. H. Boyd, and E. J. Rubin.** 2003. Genes required for mycobacterial growth defined by high density mutagenesis. Mol Microbiol **48:**77-84.
3. **Sharma, K., P. Chopra, and Y. Singh.** 2004. Recent advances towards identification of new drug targets for *Mycobacterium tuberculosis*. Expert Opin Ther Targets **8:**79-93.